Brain-spine interface for the volitional control of trans-spinal magnetic stimulation to rehabilitate movement in paralyzed patients

Dissertation

zur Erlangung des Grades eines

Doktors der Naturwissenschaften

der Mathematisch-Naturwissenschaftlichen Fakultät

und

der Medizinischen Fakultät

der Eberhard-Karls-Universität Tübingen

vorgelegt

von

Ainhoa Insausti Delgado

aus Donostia-San Sebastián, Spanien

Dezember - 2021

Tag der mündlichen Prüfung:	3. Dezember 2021
Dekan der Math.-Nat. Fakultät:	Prof. Dr. Thilo Stehle
Dekan der Medizinischen Fakultät:	Prof. Dr. Bernd Pichler
1. Berichterstatter:	Prof. Dr. Ulf Ziemann
2. Berichterstatter:	Prof. Dr. Christoph Braun
Prüfungskommission:	Prof. Dr. Ulf Ziemann
	Prof. Dr. Christoph Braun
	Dr. Ander Ramos-Murguialday
	Dr. Daniel Häufle

Erklärung / Declaration:

Ich erkläre, dass ich die zur Promotion eingereichte Arbeit mit dem Titel: „Brain-spine interface for the volitional control of trans-spinal magnetic stimulation to rehabilitate movement in paralyzed patients“ selbständig verfasst, nur die angegebenen Quellen und Hilfsmittel benutzt und wörtlich oder inhaltlich übernommene Stellen als solche gekennzeichnet habe. Ich versichere an Eides statt, dass diese Angaben wahr sind und dass ich nichts verschwiegen habe. Mir ist bekannt, dass die falsche Abgabe einer Versicherung an Eides statt mit Freiheitsstrafe bis zu drei Jahren oder mit Geldstrafe bestraft wird.

I hereby declare that I have produced the work entitled: "Brain-spine interface for the volitional control of trans-spinal magnetic stimulation to rehabilitate movement in paralyzed patients", submitted for the award of a doctorate, on my own (without external help), have used only the sources and aids indicated and have marked passages included from other works, whether verbatim or in content, as such. I swear upon oath that these statements are true and that I have not concealed anything. I am aware that making a false declaration under oath is punishable by a term of imprisonment of up to three years or by a fine.

Tübingen, den

Datum / Date

Unterschrift / Signature

To my family, my friends and all my adventure colleagues in Tübingen.

Acknowledgements

I would like to begin by acknowledging the participation of volunteers and, especially, of the most motivated stroke patients (and their families) in the world. I will always be grateful to all of them for transmitting to me their determination for self-improvement and being a source of inspiration and motivation. I personally believe that it has been a unique life experience and that this project has been worthwhile because of them.

I would also like to express my sincere gratitude to Dr. Ander Ramos-Murguialday and Prof. Niels Birbaumer for bringing me the opportunity to join their research group and to introduce me to the amazing world of science. Thank you very much for sharing your experience and knowledge with me, for encouraging me to face every challenge, and for guiding me through this exciting adventure. I would also like to thank Prof. Ulf Ziemann for his valuable advice and support and for contributing to the success of the project.

Of course, I would like to thank Edu, my closest friend and colleague, because this work would not have been possible without him. He showed me to be meticulous and demanding with my work, and to have self-confidence. I will always be thankful for his encouragement and unconditional support, and for being there in the good and not so good times. Thanks for all those special, funny and crazy experiences we have lived together.

I also want to thank my colleagues, with whom I have shared so many memorable moments inside, but especially outside the lab (conferences, weekend trips, the Indian…). Thanks to Wala' (my darling), Carlos, Andreas, Florian, Pilar, Iñaki and Pascal for helping me and for suffering my shocks. I believe they are especially relieved by the finalization of this project. I also appreciate the assistance of the students: Delphine, Malte, Jagoba, Karolina and Carlo; and the support of other researchers at the institute.

I would also like to thank all the friends I have made through this long PhD way and to my little family in Kronenstrasse. Thanks for all those Friday nights at the Blauer Salon, the Latino parties, the barbecues and many other unforgettable moments. And

thanks to my lifelong friends that have always been ready to listen to me, advise and support me in every step of the way. You have helped me a lot and I really appreciate it.

Finally, very special gratitude to Ama, Aita, Aritz, Tamara and Laia for their endless love and support; and to other relatives (some of them in our thoughts) for their encouragement. Despite the distance, they have always been by my side and I could not be more grateful to all of them. It has been a long way, but...We made it!

List of abbreviations

ANOVA	Analysis of variance
AR	Autoregressive
BMI	Brain-machine interface
BSI	Brain-spine interface
CAR	Common average reference
CMCT	Central motor conduction time
CNS	Central nervous system
CPG	Central pattern generator
EEG	Electroencephalography
EMG	Electromyography
EOG	Electrooculography
ERD/ERS	Event-related (de)synchronization
FDR	False discovery rate (FDR)
FMA	Fugl-Meyer Assessment
fMRI	Functional magnetic resonance imaging
FTh	Functional threshold
Hmax	Maximum amplitude of the H-reflex
H-reflex	Hoffmann reflex
ICA	Independent component analysis

IMU	Inertial measurement units
LDA	Linear discriminant analysis
LRR	Linear regression reference
MANOVA	Multivariate analysis of variance
MAS	Modified Ashworth scale
MEP	Motor evoked potential
MI	Motor imagery
Mmax	Maximum amplitude of the M-wave
MRCP	Movement-related cortical potential
MSO	Maximum stimulator output
MTh	Motor threshold
NIRS	Near-infrared spectroscopy
NMES	Neuromuscular electrical stimulation
OSF	Optimal spatial filter
PNS	Peripheral nervous system
SCI	Spinal cord injury
SCS	Spinal cord stimulation
SD	Standard deviation
SMR	Sensorimotor rhythm
SEP	Somatosensory evoked potential

Sol	Soleus muscle
STh	Sensory threshold
SVM	Support vector machine
TA	Tibialis anterior muscle
TMS	Transcranial magnetic stimulation
TNR	True negative rate
TPR	True positive rate
ts-MS	Trans-spinal magnetic stimulation
ts-MEP	Trans-spinal motor evoked potential
ts-SEP	Trans-spinal somatosensory evoked potential
TUG	Timed up and go test
WL	Waveform length
WSO	World Stroke Organization
2mWT	2-minute walk test
10MWT	10-meter walk test

Abstract

Neurological pathologies damaging communication between central nervous system (CNS) and peripheral nervous system (PNS), such as stroke, can result in permanent motor impairment. Around 20% of stroke patients making a partial recovery remain with foot drop, which is expressed as weakness of ankle joint and abnormal muscle activations and movement coordination during locomotion. For these patients, the accident has an enormous impact in their life quality, social integration and economic situation. Currently, there is no effective treatment for this pathology and, given the rising worldwide prevalence of stroke during the upcoming years, there is a great need of improving existing rehabilitative interventions.

In this line, much research has focused on developing technology to improve rehabilitation and motor restoration of paralyzed patients. Advances in technology have considerably contributed to the capacity of acquiring, decoding and manipulating neural activity, and has been applied in clinical environments demonstrating its rehabilitative efficacy. Spinal cord stimulation (SCS) has emerged as a powerful tool for manipulation the spinal circuitry to generate walking-like patterns and to regain partial motor control of paralyzed limbs. Comparing to passive SCS, using brain activity to activate the stimulation is a more natural approach and allows volitional control of it. Brain-spine interfaces (BSI) have appeared as a technology to acquire, process and transform neural signals into commands to control SCS. BSIs enable associative connection between brain neural activity encoding motor intentions and activation of spinal pools and muscles, which may trigger Hebbian mechanisms that favor neuroplasticity boosting rehabilitative effects. To date, only implantable BSIs have been devised and tested in animals. Developing non-invasive BSIs would broaden the field of applicability of this rehabilitative technology on patients with motor disorders.

This thesis works on the development of a non-invasive BSI, based on continuous control of trans-spinal magnetic stimulation (ts-MS) using electroencephalographic activity (EEG), for motor rehabilitation of patients with lower limb paralysis. To this end, a set of 6 studies is presented, addressing the challenges and questions from three lines of work: *(1)* relevance of artifact removal methods, *(2)* neuromodulation by

electromagnetic stimulation, and *(3)* conception of a brain-spine interface for motor rehabilitation.

Firstly, towards integrating neurostimulators in closed-loop systems, we characterize how artifacts of electromagnetic and neurophysiological origin interfere with electrophysiological recordings reflecting active participation of the patient and simulate their impact in closed-loop control. Contamination of electrophysiological recordings hampers the estimation of neural activity of interest and directly affects the performance of rehabilitative systems. Particularly for brain-controlled neural interfaces, we propose a median filter to minimize stimulation artifacts and statistical thresholding to eliminate neurophysiological artifacts. We demonstrate the need of adequate artifact removal methods that avoid bias in the quantification of task-related motor activity allowing contingent peripheral feedback.

Secondly, we investigate the modulatory effects of electromagnetic stimulators on the nervous system at different levels and discuss its implications in neurorehabilitation. Two studies are proposed: one evaluates the influence of neuromuscular electrical stimulation (NMES) on sensorimotor excitability, and one investigates the influence of ts-MS on cortico-spino-muscular excitability. We evidence that intensity and dose of NMES can produce immediate and cumulative effects on sensorimotor excitability measured with EEG. Our exploratory study shows that lumbar ts-MS strengthens the corticomuscular efficacy. Understanding how passive stimulation interacts with the nervous system could help us to improve interventions based on closed-loop stimulation.

The third line of work composing this thesis focuses on the development and validation of a BSI for lower-limb motor rehabilitation. Given the knowledge acquired from the other two lines of work, we aim at engineering the first non-invasive BSI that integrates ts-MS controlled by EEG activity. We prove the effectiveness and robustness of the system to work in real-time eliminating stimulation artifacts and engaging motor and sensory nervous system. We test and validate the BSI system in healthy participants and stroke patients and measure the neurophysiological, clinical and behavioral changes induced by an intervention based on our system. Our results show that the BSI increases

the excitability of corticomuscular pathways, improves sensorimotor function, enhances balance and walking speed, and decreases spasticity.

In summary, this thesis proposes a novel non-invasive BSI that enables contingent connection between CNS and PNS, and evaluates its feasibility for rehabilitation of patients with motor paralysis. The here presented system provide relevant insights towards designing and developing of this innovative technology and may set the basis for future new investigations.

Keywords: brain-spine interface, trans-spinal magnetic stimulation, stroke, motor rehabilitation, artifact removal, neurostimulation, neuromodulation.

Contents

1. Synopsis

1.1 Introduction

1.1.1 Motor paralysis after stroke

Stroke is the second leading cause of mortality and disability around the world with an incidence of over 13.5 million new cases every year, according to the World Stroke Organization (WSO) (Lindsay et al., 2019). Stroke is a global health-care problem that derives from an interruption of blood flow in the brain due to an obstruction (ischemic) or rupture (hemorrhagic) of a blood vessel. Consequently, the lack of nutrients and oxygen into the brain leads to cell death.

Most stroke patients survive the cerebrovascular accident, however depending on the dimension and the location of the brain lesion, many of them remain with permanent motor dysfunctions (Dimyan and Cohen, 2011; Langhorne et al., 2011). Following the cortical damage, disturbances in the connections between central nervous system (CNS) and peripheral nervous system (PNS) arise, resulting in abnormal muscle activations and movement coordination. Subsequently, stroke patients might experience other after-effects related to these motor deficits, such as spasticity and muscle atrophy, that lead to the “claw hand” or “foot drop”.

Around 20% of stroke patients that experience partial recovery remain with foot drop (Burridge et al., 1997). The foot drop is characterized by weakness of the ankle articulation, which compromises locomotion and equilibrium of stroke patients, and presents reduced plantarflexion prior to the onset of the swing phase followed by limited dorsiflexion during swing phase (Lamontagne et al., 2002). The primary muscles contributing to foot drop are tibialis anterior and posterior, soleus and gastrocnemius (Thibaut et al., 2013). Along with this impairment, stroke patients also present other deficiencies in knee and hip joints that might result in compensatory movements, limited mobility, inefficient walking, and increased falling risk (Kottink et al., 2004; Kluding et al., 2013).

This episode directly affects the quality of lives of the patients requiring support and assistance of caregivers or relatives to undergo daily life tasks and restricts their social integration. Furthermore, the treatment of this disease has an enormous economic impact for the patients and the health care system (Kolominsky-Rabas et al., 2006). Given that the worldwide prevalence of stroke will increase in the next years, efforts to reduce the stroke burden are of great need (Lindsay et al., 2019). Currently there is no effective treatment for this disease, and thus, advances in medicine and in the rehabilitative interventions are required to achieve higher degree of functional recovery that could promote the autonomy of these patients.

Assistive systems for foot drop

The conventional treatment of foot drop includes an ankle-foot orthosis that maintains the articulation in a neutral position (Burridge et al., 1997). However, this technique has numerous disadvantages, being uncomfortable and unaesthetic, and limiting ankle mobility that can lead to muscle contracture (Kluding et al., 2013). Alternative approaches based on electrical stimulation assistance have been proposed (Kottink et al., 2004). These systems electrically stimulate the muscles or peripheral nerves through surface or implanted electrodes to produce tetanic muscle contractions that allow dorsiflexion during the swing phase of gait (Gil-Castillo et al., 2020). In order to trigger the stimulation in the precise phase of the swing, gait events are accurately detected by force, inertial and/or biological sensors, and control algorithms calculate the kinematic parameters (Gil-Castillo et al., 2020).

Although significant advances have been achieved in terms of portability of the system, and efficiency and robustness of control algorithms, there are still several limitations that have to be addressed for the widespread application of this technology as a therapeutic tool. These systems require more effective stimulation engaging different muscles and activating muscle synergies, optimized combination of sensors for gait detection including electroencephalographic (EEG) and electromyographic (EMG) guidance, and customization of the system to the needs of each patient. Apart from that, muscle fatigue due to repetitive stimulation needs to be reduced by optimizing stimulation protocols. More importantly, this therapeutic tool should involve the CNS

and PNS to support neuroplastic mechanisms, and should consider not only instantaneous assistance, but also long-term therapeutic effects. Therefore, an alternative and more efficient tool is required to boost these key features.

1.1.2 Neuroplasticity and neurorehabilitation

Neuroplasticity is the capacity of the nervous system to reorganize itself resulting in structural and functional changes by potentiating the generation of new connections or reinforcing existing ones (Dimyan and Cohen, 2011). One of the key mechanisms that plays a fundamental role in generation of neuroplastic changes was firstly introduced by Donald Hebb in 1949. He proposed that two neural populations exhibiting persistent and coincident activities could result in strengthening of the connectivity among them. The Hebbian theory could be summarized as "cells that fire together wire together" (Hebb, 1949). This strengthening in synaptic connectivity can be artificially induced using three stimulation paradigms: repetitive stimulation, paired stimulation, and closed-loop stimulation (Jackson and Zimmermann, 2012).

During the last decades, technology has evolved and considerably contributed to the improvement of rehabilitation of paralyzed patients (Pons et al., 2016). Owing to the advances in acquisition, decoding and manipulation of neural activity, technology has emerged as a potential tool to activate neuroplastic mechanisms that enable repair and regeneration of injured neural networks, which is essential in functional rehabilitation. In the context of manipulation of neural activity for the restoration of motor functions, recent advancements utilize spinal cord stimulation (SCS) that activate spinal neuronal pools to produce smooth movements and natural muscle activation compared to the direct stimulation of the muscles that results in jerky movements and increased muscle fatigue (Alam et al., 2016).

Neuromodulation of spinal networks

The spinal cord is a complex structure where embedded neural networks in the lumbar region are responsible for producing and modulating locomotor function in absence of brain commands (Hultborn and Nielsen, 2007; Edgerton and Roy, 2012).

Several neuromodulation approaches have been developed to target these self-regulated circuits, also known as central pattern generators (CPGs) (Minassian et al., 2017; Taccola et al., 2018). Decades of research in spinal physiology have demonstrated that invasive electrical stimulation of spinal neuronal pools leads to restoration of lower-limb motor control in animals (Edgerton et al., 2008; Gerasimenko et al., 2008; Alam et al., 2017) and individuals with spinal cord injury (Grahn et al., 2017; Angeli et al., 2018; Formento et al., 2018; Gill et al., 2018).

In this line, non-invasive stimulation of the spinal cord has also been proposed as an alternative tool to neuromodulate the spinal circuitry. Transcutaneous electrical stimulation of the spinal cord has been shown to generate stepping-like activation regaining certain degree of volitional control of paralyzed limbs (Minassian et al., 2016a; Gad et al., 2017; Hofstoetter et al., 2018; Alam et al., 2020). Magnetic stimulation of the motor axons at their exit from the spinal cord can also evoke motor potentials in leg muscles (Ugawa et al., 1989; Knikou, 2013; Matsumoto et al., 2013). Taking advantage of this property, repetitive trans-spinal magnetic stimulation (ts-MS) produces locomotor-like patterns and has been applied either in open-loop (Gerasimenko et al., 2010; Gorodnichev et al., 2010) or EMG-triggered (Sasada et al., 2014; Nakao et al., 2015). However, all these methods for spinal neuromodulation lack intentional brain control of the stimulation.

1.1.3 Brain-spine interfaces

Controlling the stimulation using brain activity results in a more natural strategy than activating the spinal neuronal pools through passive stimulation, since it mimics the descending flow of neural information from the brain to the spine (Jackson and Zimmermann, 2012; McPherson et al., 2015). Consequently, brain-spine interfaces (BSIs) have been developed to extract neural activity reflecting motor intentions and translate it into commands to volitionally control SCS that activates lower-limb muscles (Alam et al., 2016; Capogrosso et al., 2016, 2018). These neural correlates encoding motor execution or motor attempt can be detectable even in paralyzed patients (López-Larraz et al., 2015, 2018a), which makes them convenient to govern BSIs. A timely linked peripheral afferent activation that is contingent on the volitional activity recorded

in the brain can exploit Hebbian mechanisms that favor neuroplasticity and functional recovery (Nishimura et al., 2013a; Ramos-Murguialday et al., 2013; Mrachacz-Kersting et al., 2016; Kato et al., 2019). Spinal stimulation provides peripheral afferent feedback by modulating excitability of spinal networks (Hubli et al., 2013; Hofstoetter et al., 2018) and by contracting lower-limb muscles (Gerasimenko et al., 2018). The BSIs rely on this principle of activity-dependent association between brain and spinal neural activation to recover functional control of lower-limb and alleviate gait deficits (Borton et al., 2014; Zimmermann and Jackson, 2014; Bonizzato et al., 2018).

Up to now, only implantable BSIs have been engineered and validated in animal research (Nishimura et al., 2013b; McPherson et al., 2015; Bonizzato et al., 2018). Invasive cortical recordings with microelectrode arrays can provide better and more stable signal quality, allowing optimal control of neural interfaces. Similarly, intraspinal or epidural stimulation of the spinal cord through invasive electrodes enables accurate activation of motoneurons that results in fine movements. However, the acceptance rate of invasive neural interfaces among the patients is still low, mainly due to the possible risks that the surgery may entail (e.g., surgical intervention, biological incompatibility of the implant, etc.) (Waldert, 2016). Developing non-invasive approaches would expand the framework of BSIs, making them more accessible for experimentation with healthy individuals and paralyzed patients. EEG is a commonly used neuroimaging tool that allows acquiring brain signals non-invasively. Due to its good temporal resolution, EEG has been widely integrated in brain-controlled neural interfaces. However, its low signal-to-noise ratio and proneness to get contaminated limit the application of EEG recordings.

Challenges of brain-controlled neural interfaces

Towards the improvement of brain-controlled neural interfaces integrating neurostimulators, there are two main challenges that need to be overcome: (1) dealing with stimulation artifacts, and (2) discriminating between the physiological activity of interest and the one that is not.

Simultaneous EEG control of neurostimulation techniques has not been achieved due to the artifacts produced by the stimulation that hinder the quantification of brain

activity biasing the performance of continuous closed-loop systems. This fact has limited the development of brain-controlled real-time neural interfaces, since to avoid stimulation-induced distortions, these systems have only been used to trigger the onset of pre-programmed stimulation protocols without providing a continuous control or contingency (Pfurtscheller et al., 2005; Osuagwu et al., 2016; Trincado-Alonso et al., 2017; Biasiucci et al., 2018). Hence, different strategies have been proposed to deal with electromagnetic interferences in brain activity recordings, such as blanking, interpolation or linear regression reference (Walter et al., 2012a; Iturrate et al., 2018; Young et al., 2018). Nevertheless, because of signal discontinuities and instability of recording electrode impedance, none of these methodologies has shown effectiveness to eliminate artifacts and to quantify cortical activation measured with EEG.

Physiological artifacts (e.g., eye movements, motion artifacts and compensatory movements) can also interfere with brain recordings (Schlögl et al., 2007a; Muthukumaraswamy, 2013; Castermans et al., 2014), hampering the dissociation of the neural correlate of interest from other signals. This type of artifacts can be considerably reduced by good instructing of the participants, although their appearance is occasionally unavoidable. In addition, due to the dynamic nature of the nervous system, changes in neural excitability derived from activation of motor network and/or somatosensory feedback are constantly happening. Stimulation of the PNS and CNS is a manner of interacting with neural networks to modulate their response, which directly depends on the stimulation parameters. To date, few studies have addressed how oscillatory activity measured with EEG is regulated by peripheral stimulation (Tu-Chan et al., 2017; Corbet et al., 2018). Given the relevance of EEG and neurostimulation for neurorehabilitation, especially for EEG-based neural interfaces, understanding the cortical modulation driven by stimulation is of great importance.

Altogether, there are several aspects that have to be considered towards developing an EEG-based neural interface. In order to avoid a bias in the estimation of cortical activity, BSIs need to adapt to dynamic neural excitability fluctuations caused by neurostimulation and to integrate robust and effective artifact removal methods, both for electromagnetic and physiological artifacts, which should not be computationally demanding and should allow real-time operation.

Brain-spine interfaces for motor rehabilitation

Dozens of studies have investigated the influence of transcutaneous electrical stimulation (Cogiamanian et al., 2012; Priori et al., 2014; Megía García et al., 2019; Murray and Knikou, 2019) and ts-MS on regulating neural excitability (Nielsen and Sinkjaer, 1997; Krause et al., 2004). Furthermore, it has been reported the beneficial effects of transcutaneous spinal stimulation on motor control recovery (Inanici et al., 2018; Alam et al., 2020) and attenuation of spasticity (Minassian et al., 2016b; Hofstoetter et al., 2020) in patients with spinal cord injury. Research in animal models has demonstrated that, compared to passive stimulation, brain-controlled stimulation has the capability to accelerate and enhance gait recovery (McPherson et al., 2015; Capogrosso et al., 2016; Bonizzato et al., 2018). However, development and validation of non-invasive BSIs for rehabilitation of patients with motor deficits, such as stroke, are yet to be done. And more importantly, how brain-controlled stimulation could regulate the human nervous system and its effects on synaptic efficacy and sensorimotor impairment remain unknown.

BSIs encourage the voluntary motor activation to control spinal stimulation exploiting activity-dependent neural plasticity. This modulation of the nervous system can happen at different neural levels including supraspinal and spinal networks, where efferent, afferent and propriospinal segments are embedded. Thus, considering the disruptive connections between CNS and PNS in patients with motor disorders, an exhaustive evaluation of every neural component involved during the operation of a BSI is essential. Characterizing and determining the neural mechanisms regulated by BSIs are of great relevance for the design of optimal rehabilitation therapies based on this technology in order to boost functional recovery of lower-limb paralysis.

1.2 Objectives

The main objective of this thesis was to develop a BSI that allows continuous control of the spinal circuit activation via ts-MS using brain activity and to validate this system as a neurorehabilitative tool for restoration of motor function in patients with lower-limb paralysis. Towards the development and validation of the BSI, we conducted

6 different studies that constitute this thesis. Each of these studies contributed to the conception of the neurorehabilitative system and had a specific aim, as following:

1. Study 1: Influence of trans-spinal magnetic stimulation in electrophysiological recordings for closed-loop rehabilitative systems (Insausti-Delgado et al., 2017)

   Due to the potential of SCS for motor rehabilitation and the growing interest of integrating this technology in neural interfaces, we needed to characterize how electromagnetic stimulation interacts with the recording of neurophysiological signals. In this study, we recorded EEG and EMG activity of a participant who was magnetically stimulated at different intensities. The main goal of this study was to investigate how trans-spinal magnetic stimulation can affect EEG and EMG recordings, and to evidence the necessity of artifact removal methods for the implementation of closed-loop systems.

2. Study 2: Event-related desynchronization during movement attempt and execution in severely paralyzed stroke patients: an artifact removal relevance analysis (López-Larraz et al., 2018a)

   The EEG constitutes the most used neuroimaging tool to acquire non-invasive brain activity. Due to its low signal-to-noise ratio and susceptibility to get contaminated, interferences of neurophysiological origin can corrupt EEG signals limiting its applications. The increasing interest of using EEG to control neural interfaces requires of adequate cleaning methods that allow accurate estimation of cortical activity. Thus, the aim of this study was to evaluate the impact of neurophysiological artifacts in EEG recordings of stroke patients on the quantification of brain activity. We also aimed at proving the effect of different rejection procedures on the performance of brain-controlled neural interfaces.

3. Study 3: Intensity and dose of neuromuscular electrical stimulation influence sensorimotor cortical excitability (Insausti-Delgado et al., 2021)

Peripheral stimulation of neuromuscular systems has been largely used in neurorehabilitation due to its influence in afferent neural excitation. The regulation of neural processes directly depends on stimulation parameters, and to date, few studies have addressed the effects of peripheral electrical stimulation on sensorimotor oscillatory activity measured by EEG. Because of the relevance of this neuroimaging technique in the field of rehabilitative brain-controlled neural interfaces, the study objective was to investigate how the intensity and dose (i.e., number of pulses) of peripheral electrical stimulation can influence the instantaneous and cumulative sensorimotor excitability. We also aimed at demonstrating the effects of the stimulation artifacts on EEG signals and the need of removal methods for quantifying brain activity.

4. Study 4: Quantifying the effect of trans-spinal magnetic stimulation on spinal excitability (Insausti-Delgado et al., 2019)

SCS has prompt as a powerful tool to generate locomotor patterns and to modulate spinal circuits that could result in recovery of lower-limb function. Magnetic stimulation constitutes an alternative approach to electrical stimulation for spinal stimulation; however, little is known about how this modality of stimulation can interact with neural mechanisms. Filling this gap of knowledge would allow us to identify the neurophysiological changes induced by magnetic stimulation and to exploit them to optimize rehabilitative therapies for lower-limb impairment. Hence, the goal of this study was to evaluate and characterize the effects of ts-MS on the excitability of central and peripheral nervous system of healthy participants. We aimed at demonstrating the up-regulatory effects of trans-spinal stimulation on excitability of cortico-spino-muscular pathways.

5. Study 5: Non-invasive brain-spine interface: continuous brain control of trans-spinal magnetic stimulation using EEG (Insausti-Delgado et al., 2020)

The therapeutic benefits of SCS could be enhanced if integrated in brain-controlled neural interfaces that permit the volitional and natural control of the stimulation. In this line, BSIs aim at artificially connecting brain and spinal neural

networks and could be used for alleviating gait deficits in patients with motor disorders. However, the approach of developing a BSI for humans has never been explored before. To this end and with our previous knowledge from Study 1 and 4, the goal of this study was to devise and validate the first non-invasive BSI that enabled the contingent connection between cortical activation reflecting motor intentions and activation of spinal circuits and lower-limb muscles through ts-MS. Furthermore, we wanted to evidence the capacity of this neural interface to regulate the motor and sensory nervous system and its potential to be applied as a therapeutic tool.

6. Study 6: Brain-controlled trans-spinal magnetic stimulation to restore lower-limb paralysis: a proof-of-concept in stroke patients

We engineered the first non-invasive BSI that relies on extracting motor commands to timely trigger the activation of the spinal networks through ts-MS. However, how this neural interface could interact with the human nervous system remained unclear and understanding this process would allow us to design optimal interventions that could result in better rehabilitative benefits. Thus, continuing the work of Study 4 and 5, the purpose of this study was to evaluate and characterize how an intervention based on a BSI can neuromodulate the nervous system in healthy and stroke individuals. We firstly aim at assessing the neurophysiological changes in CNS and PNS of healthy subjects measured by an exhaustive battery of assessments of synaptic efficacy. Secondly, we wanted to validate the platform with paralyzed patients and to provide a detailed description of the neurophysiological and clinical changes after a BSI-based intervention.

1.3 Results and Discussion

The results of the studies that compose this thesis are arranged in 3 topics, where we discuss the implications of the main findings for the development of BSI technologies and for motor rehabilitation of paralyzed patients.

1.3.1 Artifact removal relevance

Stimulation of the spinal cord has arisen as a promising tool to activate neuronal pools generating functional recovery in patients with motor disorders (Taccola et al., 2018). Owing to its potential for motor rehabilitation, there is an increasing interest in integrating this technology in closed-loop neural interfaces. However, this step is not straightforward as it requires understanding, firstly, how stimulation interferes with electrophysiological recordings reflecting active participation of the patient and, secondly, how to dissociate this neurophysiological activity of interest from signals that are contaminated by other physiological activity.

In study 1 (Insausti-Delgado et al., 2017), we investigated the effects of lumbar ts-MS at different intensities (no stimulation, 10%, 30% and 50% of the maximum stimulator output) on EEG and EMG recordings, while a participant was required either to rest or to swing the right leg freely in the air like in a regular walking step. We firstly characterized the artifacts that ts-MS introduced in the neurophysiological recordings and found that these were high-amplitude peaks lasting around 10 ms. Accordingly, we proposed a median filter based on a sliding window of 20 ms to minimize the effects of the stimulation artifacts. Then, we evaluated the influence of the ts-MS in the power spectral density of cortical activity recorded in 2 representative channels (one highly and one less affected by stimulation). Our results showed that as the stimulation intensity incremented, an increasing artifact appeared at the stimulation frequency and its harmonics. Moreover, the whole power spectral density raised interfering with the alpha band (7–13) Hz of the sensorimotor rhythm (SMR), which is commonly used to control closed-loop devices. However, the median filter was able to attenuate the alterations of the power spectrum even in the most corrupted channel.

In addition, as an estimate of the performance of a closed-loop system controlled by EMG or EEG activity, we used the Bhattacharyya distance to measure the separability between data distributions corresponding to rest and movement periods. For EEG activity in the alpha band, as the intensity increased, the separability of the distributions reduced becoming closer to 0, or even reversing the sign of the distance between them. Nevertheless, the median filter improved the separability between distributions for both

highly and less affected EEG channels. Regarding the EMG activity, we divided the analysis between muscles innervated (i.e., *vastus medialis*) and not innervated (i.e., *biceps brachii*) by the stimulated neural pathways. We found that using muscle activity of *vastus medialis* to control a closed-loop system would result in increasing the distance between distributions, which would wrongly enhance the performance. The median filter could not prevent this bias in the classifier performance. Similarly, the Bhattacharyya distance was also enlarged when using *biceps brachii* activity, although the affectation of the stimulation was lower compared to lower-limb muscles, which could explain its use for controlling a neural interface, as presented in (Sasada et al., 2014). Altogether, our findings evidenced the necessity of artifact removal methods to clean neurophysiological signals from ts-MS contamination for their integration in closed-loop systems.

Given the easiness of EEG to get contaminated, study 2 (López-Larraz et al., 2018a) investigated the impact of physiological artifacts (i.e., eye movements, motion artifacts, muscle artifacts and compensatory movements) in EEG recordings of thirty-one stroke patients while trying to move their healthy and paretic arm. We quantified the cortical activation as the event-related desynchronization (ERD) of SMR and ran a pseudo-online simulation of a BMI control. To minimize the influence of artifacts we used a linear regression to eliminate ocular contaminations and a trial-based statistical thresholding to reject the other physiological artifacts. The effectiveness of each artifact removal method to deal with artifacts in EEG recordings of stroke patients was evaluated by means of ERD and BMI performance.

EEG recordings were mainly polluted by involuntary muscle activity and removing these artifacts helped to identify cortical signatures of interest during motor tasks resulting in an enhanced ERD or brain activation. This contamination was more pronounced during motor execution or motor attempt of paretic hand, probably due to the extra effort and compensatory movements, where other body parts were also involuntarily involved. Furthermore, we showed that lower BMI performances were achieved when cleaning brain activity from artifacts. This suggested that using contaminated brain activity led to a positive bias of the classifier output that improved the performance of the closed-loop system. However, this fact compromised the operant

functioning of BMIs that rely on the associative link between cortical activity and peripheral feedback. Altogether, this study evidenced the relevance of using appropriate methodologies to remove artifacts to accurately estimate the motor cortical activity from EEG datasets, especially those artifacts with ocular, motion and muscular contraction origin.

1.3.2 Neuromodulation by electromagnetic stimulation

Modulating the excitability of the nervous system using electromagnetic stimulation can support functional recovery and has several applications in neurorehabilitation (Carson and Buick, 2019; Megía García et al., 2019). Neuromuscular electrical stimulation (NMES) has been largely used to reduce muscle atrophy and to regulate afferent neural excitation (Knutson et al., 2015). Despite the influence of the stimulation in the neural excitation directly relies on stimulation parameters, little is known about how intensity and dose of NMES can modulate sensorimotor oscillatory activity measured with EEG. Given the importance of EEG and NMES for neurorehabilitation, with especial focus on EEG-driven neural interfaces, understanding the neuromodulatory effects of NMES on brain excitability is of paramount relevance. Therefore, in study 3 (Insausti-Delgado et al., 2021), we evaluated the sensorimotor activation, quantified as event-related (de)synchronization (ERD/ERS) of cortical oscillatory rhythms, in twelve healthy participants, whose wrist extensors were stimulated at three different intensities (two below and one above the individual motor threshold) during rest while wearing an EEG system.

First of all, following our prior knowledge from Study 1 (Insausti-Delgado et al., 2017) and Study 2 (López-Larraz et al., 2018a), we proposed a two-step artifact removal method composed by: *(1)* rejection method based on statistical thresholding of power-line noise to discard contaminated channels, and *(2)* median filtering for removal of NMES artifacts. We demonstrated the feasibility of the two-step procedure, which efficiently eliminated the stimulation artifacts induced by NMES and evidenced the relevance of artifact removal methods for accurate estimation of brain activity. After cleaning the EEG signals, we investigated the instantaneous and cumulative effects of NMES on sensorimotor oscillatory activity. On the one hand, a significant intensity-

dependent modulation of cortical oscillatory activity was observed. As the stimulation intensity increased, there was a proportional cortical response, presumably by recruiting larger number of afferent fibers that send ascending volleys to the sensory cortex. Noteworthy, our results revealed that stimulation below the motor threshold was not significantly different to not being stimulated. On the other hand, we found that the dose of NMES produced an intensity-dependent effect on sensorimotor activity modulation over time. While intensities below the motor threshold caused cortical inhibition, stimulation above the motor threshold caused cortical facilitation. We could speculate that above-motor-threshold NMES, in comparison to below-motor-threshold NMES, provided functionally "relevant" feedback (as an additive effect of *(1)* direct afference by recruitment of sensory fibers and cutaneous mechanoreceptors and *(2)* indirect secondary reafference by activation of proprioceptive receptors due to muscle contraction and joint movements) that boosted neural excitability. Overall, our findings highlighted the neuromodulatory effects of intensity and dose of NMES on afferent pathways from the muscle to the brain, which should be carefully considered for the design of neurorehabilitative systems integrating NMES and EEG, such as brain-controlled neural interfaces.

In contrast to jerky movements elicited by direct muscle stimulation, spinal cord stimulation can activate neural centers that generate smooth and natural muscle contractions (Alam et al., 2016). In the domain of lower-limb rehabilitation, SCS has been shown not only to produce walking-like rhythms, but also to induce changes in the spinal neural networks, leading to functional recovery (Gill et al., 2018). Although electrical stimulation of the spinal cord constitutes the most commonly used modality, magnetic stimulation could also be used to modulate the spinal circuits. However, the influence of this stimulation approach on neural excitability has been scarcely investigated.

Study 4 (Insausti-Delgado et al., 2019) evaluated whether passive lumbar ts-MS at the motor threshold could regulate the cortico-spino-muscular efficacy of seven healthy participants. We analyzed *(1)* the efficacy of cortical projections to the muscle by means of the peak-to-peak amplitude and latency of motor evoked potentials (MEP), *(2)* the efficacy of spino-muscular pathways by means of the peak-to-peak amplitude and

latency of trans-spinal motor evoked potentials (ts-MEP), and *(3)* the efficacy of cortico-spinal pathways by means of central motor conduction time. These neurophysiological assessments were measured three times over the experiment, one before the intervention, one right after finishing the intervention and one 30 min afterwards. We observed that the strength of the descending volleys from the cortex to the *soleus* muscle (i.e., target muscle of the intervention), quantified as MEP amplitude, increased almost 30% after the intervention and was kept up to 30 min later. This finding indicated that cortico-muscular excitability might have been enhanced by ts-MS, although no changes were found in the MEP latency. Regarding the efficacy of spino-muscular and cortico-spinal segments, we did not observe any differences in either ts-MEPs or central motor conduction time. Nevertheless, this exploratory study had a small sample size and no control group. In spite of these results not being conclusive (due to the lack of statistical power), they provide a hint about the possible up-regulatory effects of ts-MS on neural excitability that could be exploited in neurorehabilitation.

1.3.3 Brain-spine interfaces for motor rehabilitation

The neuromodulatory effects of SCS could be boosted if integrated in brain-controlled neural interfaces (Jackson and Zimmermann, 2012), which would allow volitional and more natural control of the stimulation as it resembles the neural transmission from supraspinal neural networks to the spine. BSIs enable this convergence of monitoring cortical signals encoding volitional activity and stimulating spinal pools in a closed-loop manner, which can prompt activity-dependent neural mechanisms. Towards developing a non-invasive neural interface for rehabilitation of lower-limb paralysis, in Study 5 (Insausti-Delgado et al., 2020) we engineered and investigated the feasibility of the first non-invasive BSI for humans that relied on the continuous control of lumbar ts-MS using EEG activity. Ten healthy participants validated this platform while being stimulated at different intensities (sham, 20%, 30% and 40% of the maximum stimulator output). As expected, the ts-MS was introduced in the EEG recordings as high-amplitude peaks and its influence affected the sensorimotor oscillatory activity used to govern the platform, impeding the correct functioning of the system. Given the knowledge from Study 1 and Study 3, we implemented a median filter to deal with ts-

MS-induced artifacts and an adaptative decoder to handle with potential changes of cortical activation over time. We demonstrated the efficiency and robustness of the system to eliminate the stimulation artifacts in real-time regardless of ts-MS intensity used, which would allow the closed-loop implementation of different stimulation protocols. This is an important feature of our system since to date continuous online control of neurostimulators integrated in brain-controlled neural interfaces has not been developed due to the undesirable artifacts that hinder the extraction of neural correlates of interest, biasing the decoding accuracy of these systems.

Our BSI allowed the contingent connection of cortical activity reflecting motor intentions with the direct activation of motor (from the spine to leg muscles) and sensory (from the spine to the somatosensory cortex) pathways through ts-MS, which would satisfy the requirements for Hebbian plasticity. Although neurophysiological assessments for synaptic efficacy were not included in this preliminary analysis, we showed the potential of our BSI to activate central and peripheral neural pathways. The ts-MS induced an intensity-dependent modulation of the motor and sensory circuits, measured as trans-spinal motor evoked potentials (ts-MEP) and trans-spinal somatosensory evoked potentials (ts-SEP), respectively. Furthermore, all participants agreed on a reduced usability of the system as the stimulation intensity increased (i.e., more pain and discomfort, and less ability to concentrate on the task), although their subjective perception did not affect the accuracy controlling the BSI. Overall, the here presented results shed some light on the designing and development of non-invasive BSIs as an innovative neuroscientific tool.

The next step following Study 5 (Insausti-Delgado et al., 2020) was to investigate the effectiveness of the non-invasive BSI to induce neuroplastic changes in human nervous system and to validate this platform as a neurorehabilitative tool of patients with lower-limb paralysis. With this aim, in Study 6, we recruited twenty-one healthy participants, who underwent a single-session experiment, and seven stroke patients, who tested the system and were evaluated after an 8-session intervention. Because of the structural complexity of the spinal cord, where ascendant and descendant tracts connecting central and peripheral nervous system are embedded, we proposed an exhaustive battery of assessments for the characterization of changes in synaptic efficacy

induced by a BSI-based intervention. Additionally, clinical and behavioral assessments were also conducted in stroke patients.

In healthy participants, we found that the BSI-intervention led to a significant increase of corticomuscular synaptic efficacy, measured as peak-to-peak amplitude of MEPs in the *tibialis anterior* and *soleus* muscles. This enhancement of cortical projections was observed right after finishing the brain-controlled lumbar ts-MS and, for the *tibialis anterior* muscle (i.e., target muscle of the intervention), was prolonged until 30 minutes after. Although we could not isolate the effect of the stimulation alone from the closed-loop stimulation, our results showed that those subjects with higher decoding accuracies had significantly bigger MEPs right after finishing the intervention. This finding supported the key feature of BSIs that enable timely-linked activation of brain and spinal pools resulting in greater excitability changes in the entire corticomuscular network. With respect to the other neurophysiological assessments, we could not find significant differences in the excitability of spino-muscular motor pathways, spinal reflexes, somatosensory pathways and motor cortex activation through the session. This implied that if the neural response of spino-muscular tracts did not change, the significant reinforcement of corticomuscular efficacy might have lain in an enhancement of cortico-spinal connections and/or supraspinal structures. Due to the lack of a control group, every assumption has to be carefully considered and it could not be concluded whether the observed changes in synaptic efficacy were caused by the BSI intervention. Nevertheless, we presume the associative activation of cortical and spinal neural networks might have contributed to these changes.

Study 6 also reported on the first validation on stroke patients of a non-invasive BSI, based on continuous lumbar ts-MS controlled by EEG, and explored neurophysiological and clinical changes induced by an intervention based on this system. Our descriptive analysis revealed that some patients experienced significant enhancement of synaptic efficacy of corticomuscular pathways over days and within session, quantified as peak-to-peak amplitude of MEPs in *tibialis anterior* muscle. We observed a progressive increase of the MEP size, being this more pronounced in the assessments of last sessions. This suggested that the BSI intervention might have induced immediate effects on the entire corticomuscular network, although it might have needed certain

amount of sessions to induce statistical significant cumulative effects. As in healthy subjects, the patients also showed no significant changes in the excitability of spino-muscular motor pathways, spinal reflexes, somatosensory pathways or motor cortex activation after the 8-day intervention. Regarding the behavioral assessments, all patients overall gained walking speed and ambulatory capacity. Furthermore, the scores of the Fugl-Meyer assessment (FMA) decreased showing an improvement of lower-limb motor control after the treatment. In addition, we found that the spastic tone was also reduced following the treatment and, more interestingly, a patient suffering from ankle clonus was recovered from this pathology. Because of the nature of our study with no control group, we cannot draw any further nor definitive conclusions from the neurophysiological and clinical changes observed after the 8-day intervention.

The applicability of the system also required evaluating the degree of usability according to the user experience. All patients reported good tolerability (e.g., low discomfort and pain) to the lumbar stimulation, good concentration in the control of the system and low fatigability. Despite the wide heterogeneity of brain lesions caused by stroke and their consequences in abnormal cortical activation, all patients satisfactorily controlled the BSI system using their EEG activity. Overall, the here presented system could constitute a relevant neurorehabilitative tool for the treatment of lower-limb paralysis.

1.4 Conclusions

These are the conclusions and implications for the development of BSIs to rehabilitate lower-limb motor dysfunction that can be extracted from this thesis:

- Electrophysiological recordings, such as signals acquired from brain and muscles, that reflect movement intention can be used to control rehabilitative neural interfaces. However, the applicability of these neurophysiological signals in closed-loop systems is drastically affected when combined with ts-MS. We evidenced the need of artifact removal methods and proposed the median filter as an effective methodology to deal with stimulation contaminations from EEG and EMG signals.

- Apart from artifacts of electromagnetic origin, EEG recordings are also contaminated by artifacts of biological origin (e.g., eye blinking, motion artifacts, compensatory movements). In the context of rehabilitative neural interfaces, polluted EEG activity leads to unreliable estimation of brain activity, that in turn, biases the interface control limiting the therapeutic effectiveness of the system. We demonstrated the necessity of adequate methodologies that remove biological-origin contamination allowing accurate estimation of sensorimotor task-related brain activity to provide contingent peripheral feedback, which is key to promote motor recovery.

- We found that intensity and dose of NMES can induce immediate and cumulative effects on the excitability of the sensorimotor cortex measured by EEG. This is of great relevance for NMES-based interventions, since intensity and dose are usually tuned, while other stimulation parameters are fixed. Understanding how NMES parameters can modulate the excitability of the cortex could help us to boost the benefits of rehabilitative therapies, for instance, in passive NMES and closed-loop neural interfaces like EEG-guided NMES.

- Ts-MS has the capacity to interact with the spinal cord generating afferent volleys to the cortex and efferent volleys to muscles, resulting in an increase of excitability of the entire cortico-spino-muscular network tracts. Nevertheless, the neuromodulatory effects of passive ts-MS need to be further investigated in order to optimize brain-driven neurostimulation protocols.

- We devised the first non-invasive BSI that relies on the continuous control of the ts-MS guided by EEG. Our BSI enables the simultaneous association of cortical activity reflecting motor intentions with the activation of spinal circuits triggering afferent and efferent neural pathways. We proved the effectiveness and robustness of the median filter to minimize ts-MS-induced artifacts allowing a precise estimation of brain activation and its implementation in real-time closed-loop systems. This innovative system was designed and developed to exploit

neuromodulatory mechanisms and constitutes the first steps towards developing a relevant tool for lower-limb motor rehabilitation.

- We evaluated and characterized for the first time the neurophysiological and clinical effects of an intervention based on our novel non-invasive BSI. Our study demonstrated that using the BSI system enhanced the synaptic efficacy of corticomuscular pathways of healthy participants in a single session and that this improvement was positively correlated with the BSI performance. Furthermore, we tested and studied the feasibility of this system for the first time in stroke patients. After 8-day BSI intervention, stroke patients showed positive changes in synaptic efficacy of corticomuscular projections, increased motor function and reduced spastic tone. Overall, our findings shed light on the applicability of BSI technology and proposes the latter as a rehabilitative tool for lower-limb paralysis.

1.5 Outlook

Neural interfaces have emerged as a potential tool to interact with the nervous system, allowing monitoring and manipulation of neural activity to invoke activity-dependent plastic mechanisms that can lead to functional recovery. Scientific research of last decades has brought brain-controlled interfaces that enable contingent link between cortical activity and activation of paretic limb resulting in therapeutic benefits. However, rehabilitative neural interfaces have not yet demonstrated to be effective enough to be adopted as a treatment to induce significant motor recovery in paralyzed patients. These systems are still in an early stage of development and need to overcome substantial challenges to gain relevance in the clinical environment.

Stroke causes a wide heterogeneity of brain lesions that, together with the singularity of individual cortical activity, leads to diverse cortical patterns among patients performing the same task (Stępień et al., 2011; Park et al., 2016). Customization of neural interfaces according to the abnormal neural patterns and the specific needs of each patient might be a key factor to maximize the outcomes of these interventions. Despite the acceptable performance of our BSI system, the control of EEG-guided neural interfaces

is restrained by the decoding accuracy that non-invasive acquisition techniques offer. EEG has low signal-to-noise ratio and poor spatial resolution, which implies that it is not only more prone to get contaminated by undesired noise, but also less effective to detect brain activity originated in deeper neural structures. Consequently, while brain activation reflecting hand movements is easily discriminated because of the large and superficial cortical representation of the hand, activation of foot cortex is more difficult to identify due to the cortical representation of this limb in the mesial wall (Pfurtscheller et al., 2006). Invasive recordings can provide better and more stable signal quality, which makes them potential candidates for high accuracy control of neural interfaces. Similarly, invasive stimulation of the spinal cord can yield precise activation of motoneurons resulting in fine movements. However, the risks associated with electrode implantation (e.g., surgical intervention, biological incompatibility of the implant, etc.) generate reluctance among the patients. Subsequently, non-invasive neural interfaces should consider incorporating advanced classification algorithms or techniques of feature extraction that could enhance the estimation of brain activity and optimizing specificity of non-implantable stimulation systems.

The majority of studies performed on stroke patients only last a few weeks, which allows testing the potential of the technology but prevents producing long-term effects. Duration of therapies is another pivotal factor and further research should continue investigating the rehabilitative benefits of BSIs in a larger population of patients during longer periods. Indeed, longer therapies would permit to adapt the interventions according to patients' evolution, which might have a direct impact in their functional recovery and, in turn, in their life quality. Towards the prolongation of the treatment duration, in the future rehabilitative interventions will not be restricted to the clinical environment and home-rehabilitation will gain importance. Incorporating neural interfaces to day-to-day lives of the patients will offer continued (i.e., daily sessions) and intensive (i.e., more hours per day) training that will probably enhance neurorehabilitative outcomes. New technologies will need to face the challenge of adapting to daily life of patients becoming portable and wearable systems. In the context of BSIs, this implies that both brain recording and spinal stimulation systems require further development in order to become home-rehabilitation a reality.

It should be also considered that, although this thesis has mainly focused on lower-limb rehabilitation of stroke patients, the framework of clinical BSIs is not restricted and could be extended to treat other diseases causing paralysis, such as spinal cord injury, and/or to restore upper-limb movement. This requires characterizing motor deficits of other diseases and broadening the knowledge about spinal circuits involved in afferent and efferent neural transmission of the upper limb. However, it should be noted that, in comparison to the neural circuits of the brain, the spinal cord circuitry exhibits a less clear spatial organization that hinders the functional characterization of network elements (Rybak et al., 2015). The diverse spinal reflexes (e.g., recurrent inhibition, reciprocal inhibition), with their connections and their influence in neural transmission unravel the complexity of this structure (Hultborn, 2006). Although the battery of assessments for synaptic efficacy we used aimed at identifying the role of different elements within this complex structure, this might not be specific enough and complementary electrophysiological measures might be needed to provide relevant insights of spinal excitability.

The results presented in this thesis are limited to the selected stimulation parameters and neural features used to govern the system. On the one hand, it has not been exhaustively explored the influence of passive ts-MS on neuroplasticity and future research requires a better characterization of the stimulation parameters (e.g., intensity, frequency, dose). On the other hand, we restricted the functioning of the system to a certain number of channels and frequencies, although the control strategy should aim at adapting the BSI system to patients' pathological profile trying to promote neural reorganization and to reestablish balance between hemispheres. In addition to the experimental findings and complementary electrophysiological measures, computational neuroscience and bioelectromagnetic modeling could also serve as complementary tools to provide a more complete understanding of the neural connections and mechanisms interacting with the stimulation.

Finally, this thesis has brought technological progress to the field of neural interfaces for the rehabilitation of patients with motor dysfunction. Although considerable advances are yet to be done for the widespread application of brain-controlled interfaces as a therapeutic tool, its clinical impact on the patient population

that could benefit from its use is enormous. Moreover, the here presented findings have shed light on the development of BSIs and have discussed challenges and questions that future research should focus efforts on. As the technology advances over the next few years, new generation devices optimized to generate neuroplasticity and functional recovery will be engineered and, consequently, the quality of life of paralyzed patients will be improved.

1.6 List of publications

- A. Insausti-Delgado, E. López-Larraz, C. Bibián, Y. Nishimura, N. Birbaumer, A. Ramos-Murguialday. **Influence of trans-spinal magnetic stimulation in electrophysiological recordings for closed-loop rehabilitative systems.** *39th Annual International Conference of the IEEE Engineering in Medicine and Biology Society (EMBC)*, 2017.

- E. López-Larraz, T. C. Figueiredo, A. Insausti-Delgado, U. Ziemann, N. Birbaumer, A. Ramos-Murguialday. **Event-related desynchronization during movement attempt and execution in severely paralyzed stroke patients: an artifact removal relevance analysis.** *NeuroImage: Clinical,* 2018.

- A. Insausti-Delgado, E. López-Larraz, J. Omedes, A. Ramos-Murguialday. **Intensity and dose of neuromuscular electrical stimulation influence sensorimotor cortical excitability.** *Frontiers in Neuroscience,* 2021.

- A. Insausti-Delgado, E. López-Larraz, Y. Nishimura, N. Birbaumer, U. Ziemann, A. Ramos-Murguialday. **Quantifying the effect of trans-spinal magnetic stimulation on spinal excitability.** *9th International IEEE EMBS Conference on Neural Engineering (NER),* 2019.

- A. Insausti-Delgado, E. López-Larraz, Y. Nishimura, U. Ziemann, A. Ramos-Murguialday. **Non-invasive brain-spine interface: continuous brain control of trans-spinal magnetic stimulation using EEG.** *BioRxiv*, 2020.

- A. Insausti-Delgado, E. López-Larraz, W. Mahmoud, D. Muller, Y. Nishimura, U. Ziemann, A. Ramos-Murguialday. **Brain-controlled trans-spinal magnetic stimulation to restore lower-limb paralysis: a proof-of-concept in stroke patients.** *Under preparation*.

1.7 Statement of contributions

1.7.1 Influence of trans-spinal magnetic stimulation in electrophysiological recordings for closed-loop rehabilitative systems

Ainhoa Insausti-Delgado	Protocol design
	Setup and experiment preparation
	Data collection and analysis
	Results discussion
	Manuscript drafting and review
Eduardo López-Larraz	Protocol design
	Setup and experiment preparation
	Data collection and analysis
	Results discussion
	Manuscript drafting and review
Carlos Bibián	Data analysis
	Results discussion
	Manuscript review

Yukio Nishimura	Protocol design
	Results discussion
	Manuscript review
Niels Birbaumer	Results discussion
	Manuscript review
Ander Ramos-Murguialday	Protocol design
	Data analysis
	Results discussion
	Manuscript review

1.7.2 Event-related desynchronization during movement attempt and execution in severely paralyzed stroke patients: an artifact removal relevance analysis

Eduardo López-Larraz	Protocol design
	Setup and experiment preparation
	Data collection and analysis
	Results discussion
	Manuscript drafting and review
Thiago C. Figueiredo	Protocol design
	Setup and experiment preparation
	Data collection and analysis

	Results discussion
	Manuscript review
Ainhoa Insausti-Delgado	Data analysis
	Results discussion
	Manuscript review
Ulf Ziemann	Results discussion
	Manuscript review
Niels Birbaumer	Protocol design
	Data analysis
	Results discussion
	Manuscript review
Ander Ramos-Murguialday	Protocol design
	Setup and experiment preparation
	Data collection and analysis
	Results discussion
	Manuscript review

1.7.3 Intensity and dose of neuromuscular electrical stimulation influence sensorimotor cortical excitability

Ainhoa Insausti-Delgado	Protocol design

	Setup and experiment preparation
	Data collection and analysis
	Results discussion
	Manuscript drafting and review
Eduardo López-Larraz	Protocol design
	Setup and experiment preparation
	Data analysis
	Results discussion
	Manuscript drafting and review
Jason Omedes	Protocol design
	Setup and experiment preparation
	Data collection
	Manuscript review
Ander Ramos-Murguialday	Protocol design
	Data analysis
	Results discussion
	Manuscript review

1.7.4 Quantifying the effect of trans-spinal magnetic stimulation on spinal excitability

Ainhoa Insausti-Delgado	Protocol design

	Setup and experiment preparation
	Data collection and analysis
	Results discussion
	Manuscript drafting and review
Eduardo López-Larraz	Protocol design
	Setup and experiment preparation
	Data collection and analysis
	Results discussion
	Manuscript drafting and review
Yukio Nishimura	Protocol design
	Manuscript review
Niels Birbaumer	Protocol design
	Manuscript review
Ulf Ziemann	Protocol design
	Results discussion
	Manuscript review
Ander Ramos-Murguialday	Protocol design
	Data analysis
	Results discussion
	Manuscript review

1.7.5 Non-invasive brain-spine interface: continuous brain control of trans-spinal magnetic stimulation using EEG

Ainhoa Insausti-Delgado	Protocol design Setup and experiment preparation Data collection and analysis Results discussion Manuscript drafting and review
Eduardo López-Larraz	Protocol design Setup and experiment preparation Data collection and analysis Results discussion Manuscript drafting and review
Yukio Nishimura	Results discussion Manuscript review
Ulf Ziemann	Results discussion Manuscript review
Ander Ramos-Murguialday	Protocol design Data analysis Results discussion Manuscript review

1.7.6 Brain-controlled trans-spinal magnetic stimulation to restore lower-limb paralysis: a proof-of-concept in stroke patients

Ainhoa Insausti-Delgado	Protocol design
	Setup and experiment preparation
	Data collection and analysis
	Results discussion
	Manuscript drafting and review
Eduardo López-Larraz	Protocol design
	Setup and experiment preparation
	Data collection and analysis
	Results discussion
	Manuscript drafting and review
Wala Mahmoud	Protocol design
	Data collection and analysis
	Results discussion
Delphine Muller	Protocol design
	Data collection
Yukio Nishimura	Protocol design
	Results discussion
Ulf Ziemann	Protocol design

	Results discussion
Ander Ramos-Murguialday	Protocol design
	Data analysis
	Results discussion
	Manuscript review

1.8 References

Alam, M., Garcia-alias, G., Jin, B., Keyes, J., Zhong, H., Roy, R. R., et al. (2017). Electrical neuromodulation of the cervical spinal cord facilitates forelimb skilled function recovery in spinal cord injured rats. *Exp. Neurol.* 291, 141–150. doi:10.1016/j.expneurol.2017.02.006.

Alam, M., Ling, Y. T., Wong, A. Y. L., Zhong, H., Edgerton, V. R., and Zheng, Y. P. (2020). Reversing 21 years of chronic paralysis via non-invasive spinal cord neuromodulation: a case study. *Ann. Clin. Transl. Neurol.* 7, 829–838. doi:10.1002/acn3.51051.

Alam, M., Rodrigues, W., Ngoc, B., and Thakor, N. V (2016). Brain-machine interface facilitated neurorehabilitation via spinal stimulation after spinal cord injury : Recent progress and future perspectives. *Brain Res.* 1646, 25–33. doi:10.1016/j.brainres.2016.05.039.

Angeli, C. A., Boakye, M., Morton, R. A., Vogt, J., Benton, K., Chen, Y., et al. (2018). Recovery of Over-Ground Walking after Chronic Motor Complete Spinal Cord Injury. *N. Engl. J. Med.*, NEJMoa1803588. doi:10.1056/NEJMoa1803588.

Biasiucci, A., Leeb, R., Iturrate, I., Perdikis, S., Al-Khodairy, A., Corbet, T., et al. (2018). Brain-actuated functional electrical stimulation elicits lasting arm motor recovery after stroke. *Nat. Commun.* 9, 2421. doi:10.1038/s41467-018-04673-z.

Bonizzato, M., Pidpruzhnykova, G., DiGiovanna, J., Shkorbatova, P., Pavlova, N., Micera, S., et al. (2018). Brain-controlled modulation of spinal circuits improves recovery from spinal cord injury. *Nat. Commun.* 9, 1–14. doi:10.1038/s41467-018-05282-6.

Borton, D., Bonizzato, M., Beauparlant, J., Digiovanna, J., Moraud, E. M., Wenger, N., et al. (2014). Corticospinal neuroprostheses to restore locomotion after spinal cord injury. *Neurosci. Res.* 78, 21–29. doi:10.1016/j.neures.2013.10.001.

Burridge, J. H., Taylor, P. N., Hagan, S. A., Wood, D. E., and Swain, I. D. (1997). The effects of common peroneal stimulation on the effort and speed of walking. A randomized controlled trial with chronic hemiplegic patients. *Clin. Rehabil.* 11, 201–210.

Capogrosso, M., Milekovic, T., Borton, D., Wagner, F., Martin Moraud, E., Mignardot, J.-B., et al. (2016). A brain–spine interface alleviating gait deficits after spinal cord injury in primates. *Nature* 539, 284–288. doi:10.1038/nature20118.

Capogrosso, M., Wagner, F. B., Gandar, J., Moraud, E. M., Wenger, N., Milekovic, T., et al. (2018). Configuration of electrical spinal cord stimulation through real-time processing of gait kinematics. *Nat. Protoc.* 13, 2031–2061. doi:10.1038/s41596-018-0030-9.

Carson, R. G., and Buick, A. R. (2019). Neuromuscular electrical stimulation promoted plasticity of the human brain. *J. Physiol.* doi:10.1113/jp278298.

Castermans, T., Duvinage, M., Cheron, G., and Dutoit, T. (2014). About the cortical origin of the low-delta and high-gamma rhythms observed in EEG signals during treadmill walking. *Neurosci. Lett.* 561, 166–170.

Cogiamanian, F., Ardolino, G., Vergari, M., Ferrucci, R., Ciocca, M., Scelzo, E., et al. (2012). Transcutaneous spinal direct current stimulation. *Front. psychiatry* 3, 63. doi:10.3389/fpsyt.2012.00063.

Corbet, T., Iturrate, I., Pereira, M., Perdikis, S., and Millán, J. del R. (2018). Sensory

threshold neuromuscular electrical stimulation fosters motor imagery performance. *Neuroimage* 176, 268–276. doi:10.1016/j.neuroimage.2018.04.005.

Dimyan, M. A., and Cohen, L. G. (2011). Neuroplasticity in the context of motor rehabilitation after stroke. *Nat. Rev. Neurol.* 7, 76–85. doi:10.1038/nrneurol.2010.200.

Edgerton, V. R., Courtine, G. G., Gerasimenko, Y. P., Lavrov, I., Ichiyama, R. M., Fong, A. J., et al. (2008). Training locomotor networks. *Brain Res. Rev.* 57, 241–254. doi:10.1016/j.brainresrev.2007.09.002.

Edgerton, V. R., and Roy, R. R. (2012). A new age for rehabilitation. *Eur. J. Phys. Rehabil. Med.* 48, 99–109.

Formento, E., Minassian, K., Wagner, F., Mignardot, J. B., Camille G. Le Goff-Mignardot, A. R., Bloch, J., et al. (2018). Electrical spinal cord stimulation must preserve proprioception to enable locomotion in humans with spinal cord injury. *Nat. Neurosci.* 6, 153–158. doi:10.1038/s41593-018-0262-6.

Gad, P., Gerasimenko, Y., Zdunowski, S., Turner, A., Sayenko, D., Lu, D. C., et al. (2017). Weight bearing over-ground stepping in an exoskeleton with non-invasive spinal cord neuromodulation after motor complete paraplegia. *Front. Neurosci.* 11, 1–8. doi:10.3389/fnins.2017.00333.

Gerasimenko, Y., Gorodnichev, R., Machueva, E., Pivovarova, E., Semyenov, D., Savochin, A., et al. (2010). Novel and direct access to the human locomotor spinal circuitry. *J. Neurosci.* 30, 3700–3708. doi:10.1523/JNEUROSCI.4751-09.2010.

Gerasimenko, Y., Roy, R. R., and Edgerton, V. R. (2008). Epidural stimulation : Comparison of the spinal circuits that generate and control locomotion in rats , cats and humans. 209, 417–425. doi:10.1016/j.expneurol.2007.07.015.

Gerasimenko, Y., Sayenko, D., Gad, P., Kozesnik, J., Moshonkina, T., Grishin, A., et al. (2018). Electrical spinal stimulation, and imagining of lower limb movements to modulate brain-spinal connectomes that control locomotor-like behavior. *Front.*

Physiol. 9, 1–13. doi:10.3389/fphys.2018.01196.

Gil-Castillo, J., Alnajjar, F., Koutsou, A., Torricelli, D., and Moreno, J. C. (2020). Advances in neuroprosthetic management of foot drop: A review. *J. Neuroeng. Rehabil.* 17, 1–19. doi:10.1186/s12984-020-00668-4.

Gill, M. L., Grahn, P. J., Calvert, J. S., Linde, M. B., Lavrov, I. A., Strommen, J. A., et al. (2018). Neuromodulation of lumbosacral spinal networks enables independent stepping after complete paraplegia. *Nat. Med.* 24, 1677–1682. doi:10.1038/s41591-018-0175-7.

Gorodnichev, R. M., Machueva, E. N., Pivovarova, E. A., Semenov, D. V, Ivanov, S. M., Savokhin, A. A., et al. (2010). A New Method for the Activation of the Locomotor Circuitry in Humans. *Fiziol. Cheloveka* 36, 95–103. doi:10.1134/S0362119710060113.

Grahn, P. J., Lavrov, I. A., Sayenko, D. G., Straaten, M. G. Van, Gill, M. L., Strommen, J. A., et al. (2017). Enabling Task-Specific Volitional Motor Functions via Spinal Cord Neuromodulation in a Human With Paraplegia. *Mayo Clin. Proc.* 92, 544–554. doi:10.1016/j.mayocp.2017.02.014.

Hebb, D. O. (1949). *The organization of behavior: a neuropsychological theory*. doi:10.2307/1418888.

Hofstoetter, U., Freundl, B., Danner, S., Krenn, M., Mayr, W., Binder, H., et al. (2020). Transcutaneous spinal cord stimulation induces temporary attenuation of spasticity in individuals with spinal cord injury. *J. Neurotrauma* 37, 481–493. doi:10.1089/neu.2019.6588.

Hofstoetter, U. S., Freundl, B., Binder, H., and Minassian, K. (2018). Common neural structures activated by epidural and transcutaneous lumbar spinal cord stimulation: Elicitation of posterior root-muscle reflexes. *PLoS One* 13, 1–22. doi:10.1371/journal.pone.0192013.

Hubli, M., Dietz, V., Bolliger, M., Schrafl-Altermatt, M., and Bolliger, M. (2013).

Modulation of spinal neuronal excitability by spinal direct currents and locomotion after spinal cord injury. *Clin. Neurophysiol.* 124, 1187–1195. doi:10.1016/j.clinph.2012.11.021.

Hultborn, H. (2006). Spinal reflexes, mechanisms and concepts: From Eccles to Lundberg and beyond. *Prog. Neurobiol.* 78, 215–232. doi:10.1016/j.pneurobio.2006.04.001.

Hultborn, H., and Nielsen, J. B. (2007). Spinal control of locomotion - From cat to man. *Acta Physiol.* 189, 111–121. doi:10.1111/j.1748-1716.2006.01651.x.

Inanici, F., Samejima, S., Gad, P., Edgerton, V. R., Hofstetter, C. P., and Moritz, C. T. (2018). Transcutaneous electrical spinal stimulation promotes long-term recovery of upper extremity function in chronic tetraplegia. *IEEE Trans. Neural Syst. Rehabil. Eng.* 26, 1272–1278. doi:10.1109/TNSRE.2018.2834339.

Insausti-Delgado, A., López-Larraz, E., Bibián, C., Nishimura, Y., Birbaumer, N., and Ramos-Murguialday, A. (2017). Influence of trans-spinal magnetic stimulation in electrophysiological recordings for closed-loop rehabilitative systems. in *39th Annual International Conference of the IEEE Engineering in Medicine and Biology Society (EMBC)*, 2518–2521. doi:10.1109/EMBC.2017.8037369.

Insausti-Delgado, A., López-Larraz, E., Nishimura, Y., Birbaumer, N., Ziemann, U., and Ramos-Murguialday, A. (2019). Quantifying the effect of trans-spinal magnetic stimulation on spinal excitability. *9th Int. IEEE EMBS Conf. Neural Eng.* doi:10.1109/NER.2019.8717016.

Insausti-Delgado, A., López-Larraz, E., Nishimura, Y., Ziemann, U., and Ramos-Murguialday, A. (2020). Non-invasive brain-spine interface: continuous brain control of trans-spinal magnetic stimulation using EEG. *bioRxiv*.

Insausti-Delgado, A., López-Larraz, E., Omedes, J., and Ramos-Murguialday, A. (2021). Intensity and dose of neuromuscular electrical stimulation influence sensorimotor cortical excitability. *Front. Neurosci.* 14, 1359. doi:10.3389/fnins.2020.593360.

Iturrate, I., Pereira, M., and Millán, J. del R. (2018). Closed-loop electrical neurostimulation: challenges and opportunities. *Curr. Opin. Biomed. Eng.* 8, 28–37. doi:10.1016/j.cobme.2018.09.007.

Jackson, A., and Zimmermann, J. B. (2012). Neural interfaces for the brain and spinal cord—restoring motor function. *Nat. Rev. Neurol.* 8, 690–699. doi:10.1038/nrneurol.2012.219.

Kato, K., Sawada, M., and Nishimura, Y. (2019). Bypassing stroke-damaged neural pathways via a neural interface induces targeted cortical adaptation. *Nat. Commun.* 10, 1–13. doi:10.1038/s41467-019-12647-y.

Kluding, P. M., Dunning, K., O'Dell, M. W., Wu, S. S., Ginosian, J., Feld, J., et al. (2013). Foot drop stimulation versus ankle foot orthosis after stroke: 30-week outcomes. *Stroke* 44, 1660–1669. doi:10.1161/STROKEAHA.111.000334.

Knikou, M. (2013). Neurophysiological characteristics of human leg muscle action potentials evoked by transcutaneous magnetic stimulation of the spine. *Bioelectromagnetics* 34, 200–210. doi:10.1002/bem.21768.

Knutson, J. S., Fu, M. J., Sheffler, L. R., and Chae, J. (2015). Neuromuscular electrical stimulation for motor restoration in hemiplegia. *Phys. Med. Rehabil. Clin. N. Am.* 26, 729–745. doi:10.1016/j.pmr.2015.06.002.

Kolominsky-Rabas, P. L., Heuschmann, P. U., Marschall, D., Emmert, M., Baltzer, N., Neundörfer, B., et al. (2006). Lifetime cost of ischemic stroke in Germany: Results and national projections from a population-based stroke registry - The Erlangen Stroke Project. *Stroke* 37, 1179–1183. doi:10.1161/01.STR.0000217450.21310.90.

Kottink, A. I., Oostendorp, L. J., Buurke, J. H., Nene, A. V, Hermens, H. J., and IJzerman, M. J. (2004). The orthotic effect of functional electrical stimulation on the improvement of walking in stroke patients with a dropped foot: a systematic review. *Artif. Organs* 28, 577--586. doi:10.1111/j.1525-1594.2004.07310.x.

Krause, P., Edrich, T., and Straube, A. (2004). Lumbar repetitive magnetic stimulation

reduces spastic tone increase of the lower limbs. *Spinal Cord* 42, 67–72. doi:10.1038/sj.sc.3101564.

Lamontagne, A., Malouin, F., Richards, C. L., and Dumas, F. (2002). Mechanisms of disturbed motor control in ankle weakness during gait after stroke. *Gait Posture* 15, 244–255. doi:10.1016/S0966-6362(01)00190-4.

Langhorne, P., Bernhardt, J., and Kwakkel, G. (2011). Stroke rehabilitation. *Lancet* 377, 1693–1702. doi:10.1016/S0140-6736(11)60325-5.

Lindsay, M. P., Norrving, B., Sacco, R. L., Brainin, M., Hacke, W., Martins, S., et al. (2019). World Stroke Organization (WSO): Global Stroke Fact Sheet 2019. *Int. J. Stroke* 14, 806–817. doi:10.1177/1747493019881353.

López-Larraz, E., Figueiredo, T. C., Insausti-Delgado, A., Ziemann, U., Birbaumer, N., and Ramos-Murguialday, A. (2018). Event-related desynchronization during movement attempt and execution in severely paralyzed stroke patients: an artifact removal relevance analysis. *NeuroImage Clin.* 20, 972–986. doi:10.1016/j.nicl.2018.09.035.

López-Larraz, E., Montesano, L., Gil-Agudo, Á., Minguez, J., and Oliviero, A. (2015). Evolution of EEG motor rhythms after spinal cord injury: A longitudinal study. *PLoS One* 10, e0131759. doi:10.1371/journal.pone.0131759.

Matsumoto, H., Hanajima, R., Terao, Y., and Ugawa, Y. (2013). Magnetic-motor-root stimulation: Review. *Clin. Neurophysiol.* 124, 1055–1067. doi:10.1016/j.clinph.2012.12.049.

McPherson, J. G., Miller, R. R., Perlmutter, S. I., and Jacob G. McPherson, Robert R. Miller, and S. I. P. (2015). Targeted, activity-dependent spinal stimulation produces long-lasting motor recovery in chronic cervical spinal cord injury. *Neurosurgery* 78, N18–N19. doi:10.1073/pnas.1505383112.

Megía García, A., Serrano-Muñoz, D., Taylor, J., Avendaño-Coy, J., and Gómez-Soriano, J. (2019). Transcutaneous Spinal Cord Stimulation and Motor

Rehabilitation in Spinal Cord Injury: A Systematic Review. *Neurorehabil. Neural Repair*, 1545968319893298. doi:10.1177/1545968319893298.

Minassian, K., Hofstoetter, U. S., Danner, S. M., Mayr, W., Bruce, J. A., Mckay, W. B., et al. (2016a). Spinal Rhythm Generation by Step-Induced Feedback and Transcutaneous Posterior Root Stimulation in Complete Spinal Cord – Injured Individuals. *Neurorehabil. Neural Repair* 30, 233–243. doi:10.1177/1545968315591706.

Minassian, K., Hofstoetter, U. S., Dzeladini, F., Guertin, P. A., and Ijspeert, A. (2017). The Human Central Pattern Generator for Locomotion: Does It Exist and Contribute to Walking? *Neurosci.* 3, 107385841769979. doi:10.1177/1073858417699790.

Minassian, K., Mckay, W. B., Binder, H., and Hofstoetter, U. S. (2016b). Targeting Lumbar Spinal Neural Circuitry by Epidural Stimulation to Restore Motor Function After Spinal Cord Injury. *Neurotherapeutics* 13, 284–294. doi:10.1007/s13311-016-0421-y.

Mrachacz-Kersting, N., Jiang, N., Stevenson, A. J. T., Niazi, I. K., Kostic, V., Pavlovic, A., et al. (2016). Efficient neuroplasticity induction in chronic stroke patients by an associative brain-computer interface. *J. Neurophysiol.* 115, 1410–1421. doi:10.1152/jn.00918.2015.

Murray, L. M., and Knikou, M. (2019). Transspinal stimulation increases motoneuron output of multiple segments in human spinal cord injury. *PLoS One* 14.

Muthukumaraswamy, S. (2013). High-frequency brain activity and muscle artifacts in MEG/EEG: a review and recommendations. *Front. Hum. Neurosci.* 7, 138.

Nakao, Y., Sasada, S., Kato, K., Murayama, T., Kadowaki, S., S, Y., et al. (2015). Restoring walking ability in individuals with severe spinal cord injury using a closed-loop spinal magnetic stimulation. in *Proceedings of the 45th Annual Meeting of Society for Neuroscience* Available at: https://www.abstractsonline.com/Plan/ViewAbstract.aspx?sKey=70d620e9-53bf-4bef-858d-e79452be5b51&cKey=5f31c5f3-9c0c-4873-8cd1-

2fab3b718c7d&mKey=d0ff4555-8574-4fbb-b9d4-04eec8ba0c84.

Nielsen, J. F., and Sinkjaer, T. (1997). Long-lasting depression of soleus motoneurons excitability following repetitive magnetic stimuli of the spinal cord in multiple sclerosis patients. *Mult. Scler. J.* 3, 18–30. doi:10.1177/135245859700300103.

Nishimura, Y., Perlmutter, S. I., Eaton, R. W., and Fetz, E. E. (2013a). Spike-timing-dependent plasticity in primate corticospinal connections induced during free behavior. *Neuron* 80, 1301–1309. doi:10.1016/j.neuron.2013.08.028.

Nishimura, Y., Perlmutter, S. I., and Fetz, E. E. (2013b). Restoration of upper limb movement via artificial corticospinal and musculospinal connections in a monkey with spinal cord injury. *Front. Neural Circuits* 7, 57. doi:10.3389/fncir.2013.00057.

Osuagwu, B. C. A., Wallace, L., Fraser, M., and Vuckovic, A. (2016). Rehabilitation of hand in subacute tetraplegic patients based on brain computer interface and functional electrical stimulation: A randomised pilot study. *J. Neural Eng.* 13, 065002. doi:10.1088/1741-2560/13/6/065002.

Park, W., Kwon, G. H., Kim, Y., Lee, J., and Kim, L. (2016). EEG response varies with lesion location in patients with chronic stroke. *J. Neuroeng. Rehabil.* 13, 21. doi:10.1186/s12984-016-0120-2.

Pfurtscheller, G., Brunner, C., Schlögl, A., and Lopes da Silva, F. H. (2006). Mu rhythm (de)synchronization and EEG single-trial classification of different motor imagery tasks. *Neuroimage* 31, 153–159. doi:10.1016/j.neuroimage.2005.12.003.

Pfurtscheller, G., Müller-Putz, G. R., Pfurtscheller, J., and Rupp, R. (2005). EEG-based asynchronous BCI controls functional electrical stimulation in a tetraplegic patient. *EURASIP J. Appl. Signal Processing* 2005, 3152–3155. doi:10.1155/ASP.2005.3152.

Pons, J. L., Raya, R., and González, J. (2016). *Emerging Therapies in Neurorehabilitation II*. Springer.

Priori, A., Ciocca, M., Parazzini, M., Vergari, M., and Ferrucci, R. (2014). Transcranial

cerebellar direct current stimulation and transcutaneous spinal cord direct current stimulation as innovative tools for neuroscientists. *J. Physiol.* 592, 3345–3369. doi:10.1113/jphysiol.2013.270280.

Ramos-Murguialday, A., Broetz, D., Rea, M., Läer, L., Yilmaz, Ö., Brasil, F. L., et al. (2013). Brain-machine interface in chronic stroke rehabilitation: A controlled study. *Ann. Neurol.* 74, 100–108. doi:10.1002/ana.23879.

Rybak, I. A., Dougherty, K. J., and Shevtsova, N. A. (2015). Organization of the Mammalian Locomotor CPG: Review of Computational Model and Circuit Architectures Based on Genetically Identified Spinal Interneurons. *eNeuro* 2. doi:10.1523/ENEURO.0069-15.2015.

Sasada, S., Kato, K., Kadowaki, S., Groiss, S. J., Ugawa, Y., Komiyama, T., et al. (2014). Volitional walking via upper limb muscle-controlled stimulation of the lumbar locomotor center in man. *J. Neurosci.* 34, 11131–11142. doi:10.1523/JNEUROSCI.4674-13.2014.

Schlögl, A., Keinrath, C., Zimmermann, D., Scherer, R., Leeb, R., and Pfurtscheller, G. (2007). A fully automated correction method of EOG artifacts in EEG recordings. *Clin. Neurophysiol.* 118, 98–114.

Stępień, M., Conradi, J., Waterstraat, G., Hohlefeld, F. U., Curio, G., and Nikulin, V. V (2011). Event-related desynchronization of sensorimotor EEG rhythms in hemiparetic patients with acute stroke. *Neurosci. Lett.* 488, 17–21.

Taccola, G., Sayenko, D., Gad, P., Gerasimenko, Y., and Edgerton, V. R. (2018). And yet it moves: Recovery of volitional control after spinal cord injury. *Prog. Neurobiol.* 160, 64–81. doi:10.1016/j.pneurobio.2017.10.004.

Thibaut, A., Chatelle, C., Ziegler, E., Bruno, M. A., Laureys, S., and Gosseries, O. (2013). Spasticity after stroke: Physiology, assessment and treatment. *Brain Inj.* 27, 1093–1105. doi:10.3109/02699052.2013.804202.

Trincado-Alonso, F., López-Larraz, E., Resquín, F., Ardanza, A., Pérez-Nombela, S.,

Pons, J. L., et al. (2017). A Pilot Study of Brain-Triggered Electrical Stimulation with Visual Feedback in Patients with Incomplete Spinal Cord Injury. *J. Med. Biol. Eng.* 38, 790–803. doi:10.1007/s40846-017-0343-0.

Tu-Chan, A. P., Natraj, N., Godlove, J., Abrams, G., and Ganguly, K. (2017). Effects of somatosensory electrical stimulation on motor function and cortical oscillations. *J. Neuroeng. Rehabil.* 14, 1–9. doi:10.1186/s12984-017-0323-1.

Ugawa, Y., Rothwell, J. C., Day, B. L., Thompson, P. D., and Marsden, C. D. (1989). Magnetic stimulation over the spinal enlargements. *J. Neurol. Neurosurg. Psychiatry* 52, 1025–1032. doi:10.1136/jnnp.52.9.1025.

Waldert, S. (2016). Invasive vs. non-invasive neuronal signals for brain-machine interfaces: Will one prevail? *Front. Neurosci.* 10, 295. doi:10.3389/fnins.2016.00295.

Walter, A., Ramos-Murguialday, A., Rosenstiel, W., Birbaumer, N., and Bogdan, M. (2012). Coupling BCI and cortical stimulation for brain-state-dependent stimulation: methods for spectral estimation in the presence of stimulation after-effects. *Front. Neural Circuits* 6, 87. doi:10.3389/fncir.2012.00087.

Young, D., Willett, F., Memberg, W. D., Murphy, B., Walter, B., Sweet, J., et al. (2018). Signal processing methods for reducing artifacts in microelectrode brain recordings caused by functional electrical stimulation. *J. Neural Eng.* 15, 026014. doi:10.1088/1741-2552/aa9ee8.

Zimmermann, J. B., and Jackson, A. (2014). Closed-loop control of spinal cord stimulation to restore hand function after paralysis. *Front. Neurosci.* 8, 1–8. doi:10.3389/fnins.2014.00087.

2. Chapter 2: Influence of trans-spinal magnetic stimulation in electrophysiological recordings for closed-loop rehabilitative systems

This manuscript has been published as (Insausti-Delgado et al., 2017).

2.1 Abstract

Recent studies have shown the feasibility of spinal cord stimulation (SCS) for motor rehabilitation. Currently, there is an increasing interest in developing closed-loop systems employing SCS for lower-limb recovery. These closed-loop systems are based on the use of neurophysiological signals to modulate the stimulation. It is known that electromagnetic stimulation can introduce undesirable noise to the electrophysiological recordings. However, there is little evidence about how electroencephalographic (EEG) or electromyographic (EMG) activities are corrupted when a trans-spinal magnetic stimulation is applied. This paper studies the effects of magnetic SCS in EEG and EMG activity. Furthermore, a median filter is proposed to ameliorate the effects of the artifacts, and to preserve the neural activity. Our results show that SCS can affect both EEG and EMG, and that, while the median filter works well to clean the EEG activity, it did not improve the contaminations of the EMG activity. The obtained results underline the need of cleaning EMG and EEG signals contaminated by SCS, which is essential for optimal closed-loop rehabilitation.

2.2 Introduction

Spinal cord stimulation (SCS) has emerged as a promising technique for motor rehabilitation of patients with motor disorders, such as spinal cord injury (SCI). SCS has been studied with non-invasive (i.e., magnetic stimulation, transcutaneous electrical stimulation) and invasive (i.e., intraspinal electrical stimulation) approaches with the aim of exploring the intrinsic motor capabilities of the spinal cord (Jackson and Zimmermann, 2012). So far, SCS has been largely evaluated in animals (Rossignol and Frigon, 2011;

Jackson and Zimmermann, 2012; Capogrosso et al., 2016) and also in humans (Minassian et al., 2007; Angeli et al., 2014). Several studies have evidenced that SCS can induce the activation of spinal neural pools resulting in smooth and natural movements (Alam et al., 2016; Capogrosso et al., 2016); and even in neuroplastic modifications (Angeli et al., 2014).

However, in the majority of the cited studies, there is an absence of intentional control of the SCS by the subject. It has been shown that an active participation of the subject is essential for a better recovery (Ramos-Murguialday et al., 2013). Closed-loop systems take advantage of this intentionality of the subject and have been widely used in rehabilitation. The key point of closed-loop rehabilitation is that it induces activity-dependent plasticity mechanisms due to a coherent and associative activation of two neural populations (Jackson and Zimmermann, 2012). Hence, there is a growing interest in developing closed-loop systems based on SCS for rehabilitation (Sasada et al., 2014). SCS could be volitionally controlled by non-invasive neural activity (i.e., electroencephalography–EEG, or electromyography–EMG). In this line, promising results have been shown using trans-spinal magnetic stimulation controlled by EMG in healthy subjects (Sasada et al., 2014) and in SCI patients (Nakao et al., 2015). Furthermore, invasive interventions have been successfully tested in animals: e.g., intraspinal electrical stimulation driven by neural spikes (Nishimura et al., 2013b; Capogrosso et al., 2016).

Despite closed-loop neural interfaces have been widely used combined with other technologies (e.g., exoskeletons) (Ramos-Murguialday et al., 2013; López-Larraz et al., 2016; Sarasola-Sanz et al., 2017), magnetic SCS in closed-loop approaches is not so frequent. Indeed, the concurrent use of electromagnetic stimulation and neurophysiological recordings is a challenge, since undesirable components (i.e., artifacts) could be introduced and contaminate the electrophysiological activity. These artifacts may represent a problem to control the SCS in closed-loop, since noise affecting the signal may blur the activity representing subject's volition (Rogasch et al., 2016). The use of magnetic fields for brain stimulation (i.e., transcranial magnetic stimulation–TMS) has been widely characterized. It is known that TMS pulses introduce a peak of several orders of magnitude larger than the ongoing EEG (Rogasch et al., 2016). Therefore, it is

important to characterize how neurophysiological signals are affected when a magnetic stimulation is applied over the spinal cord in order to develop an optimal closed-loop system based either on EEG or EMG.

This study focuses on the analysis of EEG and EMG recordings when magnetic SCS is applied. Different stimulation intensities (10%, 30% and 50% of the maximum output of a transcranial magnetic stimulator) were used to stimulate the lumbar spinal cord. We investigated the effect of the electromagnetic stimulation in the neural recordings. Moreover, an approach based on median filtering is proposed to remove the artifacts.

2.3 Methods

2.3.1 Experimental procedure

One male healthy subject (age 29) with no neurological disorders and full leg mobility was recruited for one session. The experiment was performed at the University of Tübingen (Germany) and approved by the ethics committee of the Faculty of Medicine of the University of Tübingen. The subject lay comfortably in a semiprone position on a physiotherapy bed with the right side of his body facing upwards. The right leg was suspended to ensure free mobility of the limb (hanging in the air without friction), as in Figure 2.1 (Sasada et al., 2014). During the session, brain and muscle activity was recorded while the subject was resting or moving his right leg in four different conditions: (1) no stimulation, (2) 10% of the maximum stimulator output, (3) 30% of the maximum stimulator output and (4) 50% of the maximum stimulator output. The session consisted of 8 blocks (2 blocks per condition) and each block included 20 trials. Each of these trials consisted of two different states: rest and movement, guided by auditory cues. Rest periods lasted randomly between 5-7 seconds, where the subject was asked to be completely relaxed. Movement periods had a duration of 3 seconds, and the subject was asked to swing his leg freely in the air like in a regular walking step. The magnetic stimulation was only applied during the movement periods in random intervals, mimicking a non-ideal closed-loop system.

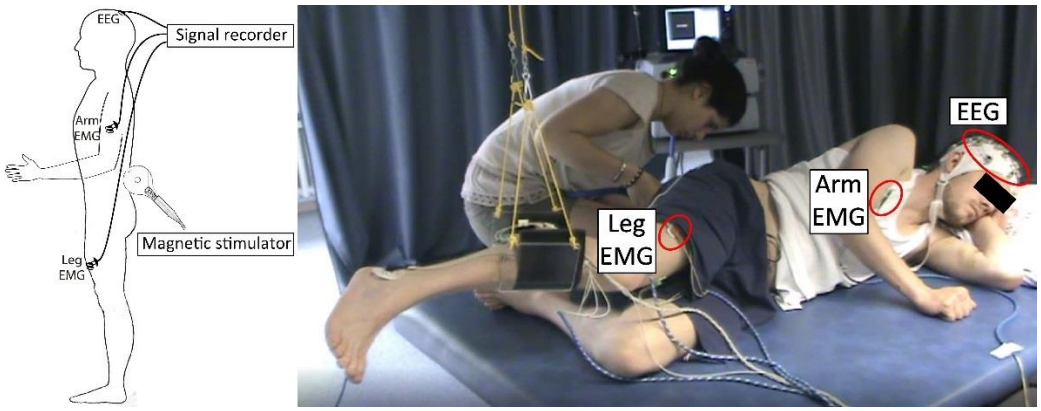

Figure 2.1: (Left) Magnetic SCS and signal recording (EEG, arm EMG and leg EMG) setup. (Right) Subject lying in a semiprone position on the physiotherapy bed with his leg suspended by a ceiling-mounted pulleys system.

2.3.2 Data acquisition

Electroencephalographic (EEG) activity was recorded using a 32-channel Acticap system including an MRcompatible amplifier (BrainProducts GmbH, Germany). The channels were distributed in the following locations FP1, FP2, F7, F3, Fz, F4, F8, FC3, FC1, FC2, FC4, C5, C3, C1, Cz, C2, C4, C6, CP5, CP3, CP1, CPz, CP2, CP4, CP6, P7, P3, Pz, P4, P8, O1, and O2; having the ground channel in AFz and the reference in FCz (according to the international 10/10 system). Surface electromyographic (EMG) activity was recorded using Ag/AgCl bipolar electrodes (Myotronics-Noromed, Tukwila, Wa, USA) with an inter-electrode space of 2 cm. An MR-compatible bipolar amplifier (BrainProducts GmbH, Germany) was also used for this acquisition. Eight muscles from the right leg (*tibialis anterior, soleus, gastrocnemius medialis, gastrocnemius lateralis, vastus medialis, vastus lateralis, semitendinosus and biceps femoris*) and one from the right arm (*biceps brachii*) were monitored. The *peroneal malleolus* was used as ground. Both brain and muscle activity were measured and synchronized at a sampling rate of 1 kHz.

2.3.3 Magnetic stimulation

Stimulation of the spinal cord over the lumbar area was applied using a Rapid2 magnetic stimulator (MagStim, UK) with a circular (90 mm diameter) coil. The experimenter localized the intervertebral lumbar region L4-L5 following anatomical

landmarks and placed the coil tangentially to the vertebra during the session, following (Sasada et al., 2014). In order to apply the stimulation over the same spot, this target point was marked in the back of the subject. The stimulation intensity was performed for 10%, 30% and 50% of the maximum output of the magnetic stimulator with a fixed frequency of 20 Hz (Sasada et al., 2014). For every stimulation output, the subject was asked first if stimulation produced pain before continuing.

2.3.4 Data processing

1) Preprocessing: The EEG signal was filtered with a 4th order Butterworth band-pass filter between 1-50 Hz; and then, it was subsampled to 100 Hz. The EMG signal was filtered with a high-pass filter of 5 Hz.

2) Epoching: Each block was divided into trials including the rest and movement periods. Each trial went from -4 seconds to +3 seconds, being 0 the moment where the auditory cue was presented.

3) Power estimation: Trials belonging to the same stimulation condition were pooled together. The power spectral density of the signals was calculated using a periodogram with 1 s hamming windows, 50% of overlapping, and a frequency resolution of 0.25 Hz. Then, power distributions were calculated for both states: rest and movement. In the EEG power spectrum, frequencies between 7-13 Hz (i.e., sensorimotor rhythms–SMR) were selected. According to (Pfurtscheller and Lopes da Silva, 1999), during a motor execution, a desynchronization, or power decrease, occurs in this specific frequency range. Hence, power distributions during rest were expected to be higher than during movement. On the other hand, higher power of EMG activity was expected at frequencies between 20-500 Hz, when the movement was executed.

The magnetic stimulation can introduce a large peak to the signal of interest (Rogasch et al., 2016). In order to measure the scale and latency of this peak, examples of stimulation artifacts at different intensities were aligned and plotted in Figure 2.2. The artifact peak has a larger magnitude compared to the EEG signal, lasting around 10 ms. According to the characteristics of this peak, a median filter could be used as a removal method, since it is suited for removing peaks of large scale. A sliding window of 20 ms

was applied to the signal, and the filter output was computed as the median value of the analyzed window. The efficacy of the median filter was compared for both EEG and EMG signals.

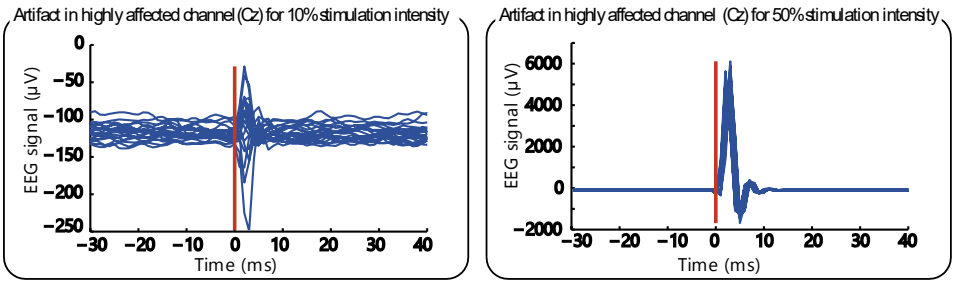

Figure 2.2: Single trials of EEG activity aligned to the stimulus in a highly affected channel (Cz). Artifact induced by 10% (left) and 50% (right) of the maximum intensity output of the magnetic stimulator.

2.3.5 Data evaluation

The main purpose of this study was to assess the feasibility of using neurophysiological signals under magnetic stimulation. Therefore, the influence of the stimulation in the power distributions of rest and movement states was evaluated. The magnetic stimulation could modify the distribution of the data in two different ways: (1) reducing their separability or separating the distributions in the wrong direction (i.e., if the power of SMR during movement execution in EEG activity becomes closer or even higher than in resting state); (2) increasing the distance between distributions, which could result in a biased performance of a classifier (i.e., if the EMG activity during movement augments, resulting in a sharper difference). As an estimate of classifier performance, Bhattacharyya distance was used to measure the separability between data distributions corresponding to rest and movement epochs. The sign of the distance was considered in order to account to the positive or negative difference between distributions,

$$D(m,r) = \left(\frac{1}{4}\ln\left(\frac{1}{4}\left(\frac{\sigma_r^2}{\sigma_m^2} + \frac{\sigma_m^2}{\sigma_r^2} + 2\right)\right) + \frac{1}{4}\left(\frac{(\mu_m - \mu_r)^2}{\sigma_r^2 + \sigma_m^2}\right)\right) \times sign(\mu_m - \mu_r)$$

where D is the Bhattacharyya distance, r represents the activity of the rest intervals, and m of the movement intervals.

2.4 Results

2.4.1 Magnetic SCS influence in EEG activity

Figure 2.3a-b present the power spectral density of brain activity for 2 representative channels: one highly affected by the stimulation and one less affected. These differences might be caused by variations in electrode impedances, or bad contact due to the posture of the subject. The effect of different magnetic stimulator intensities during movement are plotted in comparison to the power in rest periods. For the highly affected channel (Cz, Figure 2.3a), when the magnetic stimulation intensity increased, an augmenting artifact appeared at 20 Hz and its harmonics. Moreover, the whole spectrum also raised with the stimulation intensity, leading to a signal distortion and disappearance of the desynchronization in SMR. For the less affected channel (Pz, Figure 2.3b), the SMR was slightly better preserved under magnetic stimulation. However, the artifacts were still present in the signal. In Figure 2.3c the artifact attenuation of the median filter in the more corrupted channel is shown. The influence of the artifacts and the median filtering can be seen by analyzing the Bhattacharyya distances between rest and movement distributions. In raw EEG activity of the highly affected channel, as the stimulator output intensity increased (Figure 2.4a), the distances became closer to 0, or even positive for the 50% of the stimulation intensity. The use of the median filter always improved the distance between the distributions. Regarding the less affected channel (Figure 2.4b), a smaller influence of artifacts was observed as the stimulation intensity augmented. The median filter also improved the separability in comparison to the raw signal.

2.4.2 Magnetic SCS influence in EMG activity

Separate analyses were done in order to assess the influence of the magnetic stimulation in (1) a muscle innervated by the magnetically stimulated nerves, and (2) a muscle innervated by nerves rostral to the magnetic stimulation.

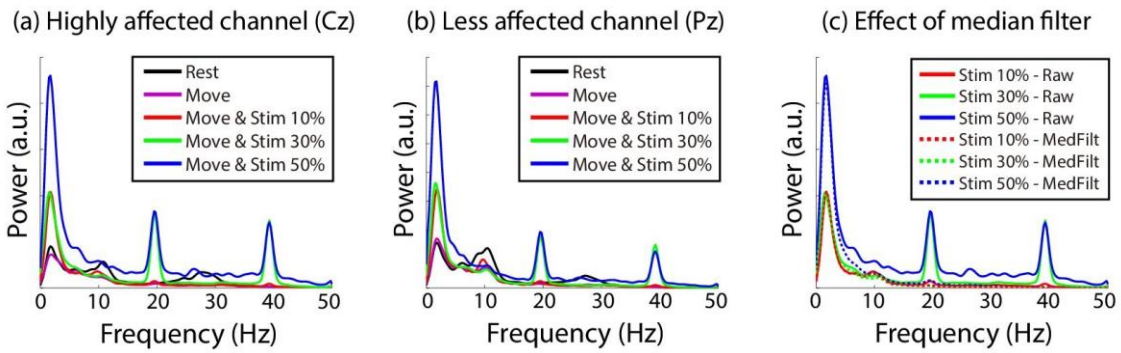

Figure 2.3: Power spectral density of EEG activity for (a) a highly affected EEG channel (Cz) and (b) a less affected EEG channel (Pz) in rest and movement intervals for different stimulation conditions. (c) Power spectral density of EEG activity of raw and median filtered signals in the highly affected channel for different stimulation conditions.

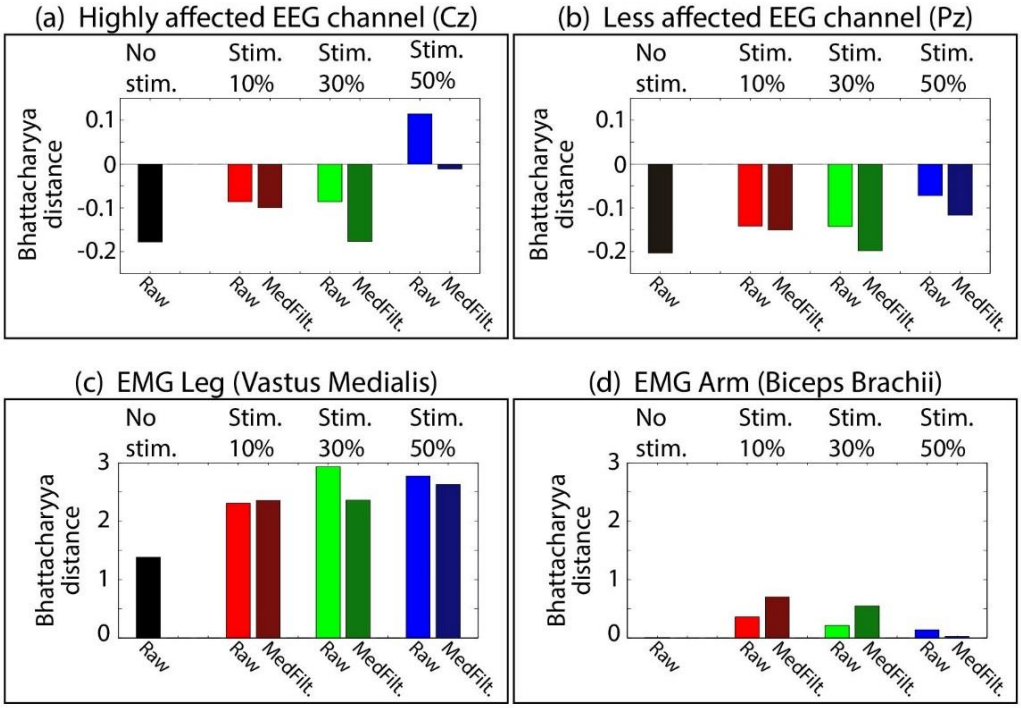

Figure 2.4: Separability between rest and movement distributions for different stimulation conditions given by Bhattacharyya distances. The distances between raw signals (light colored bars) and median filtered signals (dark colored bars) distributions are shown in (a) highly affected EEG channel, Cz; (b) less affected EEG channel, Pz; (c) leg muscular activity; and (d) arm muscular activity.

1) Lower-limb EMG activity: The analysis focused on the vastus medialis (although the rest of the leg muscles presented similar effects), since it is an extensor muscle highly involved in walking. Figure 2.4c shows the increase of Bhattacharyya distances as the stimulator intensity augmented, which would incorrectly enhance the

performance of a classifier distinguishing between rest and movement. However, in this case, the median filter was not always able to improve this negative effect.

2) Upper limb EMG activity: Figure 2.4d presents the Bhattacharyya distance of power distributions in the *biceps brachii*. Note that the subject was not asked to move his arm while walking, thus no difference between rest and movement was expected (distance during no stimulation condition is almost zero). As the magnetic field increased, the distances slightly raised. However, the distortions were notably smaller than in the leg EMG. Applying the median filter did not improve the effect either. Nevertheless, the affectation of the stimulation to the arm EMG was relatively small, which explains the feasibility of this method for closed-loop control, as shown in (Sasada et al., 2014).

2.5 Discussion and conclusions

Motor rehabilitation based on closed-loop neural interfaces is of great interest, since an active participation of the patient is required to promote neuroplasticity for a better recovery (Ramos-Murguialday et al., 2013). Electrophysiological recordings (e.g., EEG and EMG) can provide a reliable estimation of voluntary movement, and therefore can be used to drive the rehabilitative interventions. This paper reported how EEG and EMG are affected by magnetic spinal cord stimulation (SCS), which might negatively influence the performance of the rehabilitative systems. Thus, this paper evidences the need of processing the neural signals to deal with undesired components induced by electromagnetic contaminations and improve the applicability of rehabilitative systems based on this technology.

The power spectra of two representative EEG channels were analyzed. An increase of artifact peaks and distortion of background power spectrum associated to the stimulation intensity was found. A median filter was applied to diminish the influence of the stimulation. Bhattacharyya distances revealed that the median filter improved the discrimination between two classes, not only in the less affected channel, but also in the highly affected one.

Regarding the EMG activity, different results were obtained depending on the location of the muscle. Muscles innervated by the stimulated nerves presented a high distortion (resulting in an increase of Bhattacharyya distances), which could not be ameliorated by the use of a median filter. Consequently, a closed-loop system controlled by leg EMG would have a biased performance. On the other hand, EMG activity in a muscle that was not innervated by the stimulated nerves presented less contamination. Bhattacharyya distances were notably smaller than for the leg muscle and similar between the different stimulation intensities. Thus, lumbar stimulation controlled by EMG activity of the arm can be a suitable configuration, as shown in (Sasada et al., 2014).

While the median filter worked well with EEG signals, it did not improve the contaminations of EMG activity. Therefore, more advanced artifact removal methods should be implemented for closed-loop systems controlled by muscular activity. Finally, remark that, since this study was performed on a single subject, further research is needed to confirm the obtained results. In addition, extending these analyses to other stimulation approaches, such as functional electrical stimulation (FES), will be relevant for the development of rehabilitative strategies based on these technologies.

2.6 Acknowledgements

This study was funded by the Baden-Württemberg Stiftung (GRUENS ROB-1), the Deutsche Forschungsgemeinschaft (DFG, Koselleck), the Fortüne-Program of the University of Tübingen (2422-0-0), and the Bundesministerium für Bildung und Forschung BMBF MOTORBIC (FKZ 13GW0053) and AMORSA (FKZ 16SV7754). The work of A. Insausti-Delgado was supported by the Basque Government's scholarship for predoctoral students.

2.7 References

Engineering in Medicine and Biology Society (EMBC), 2518–2521. doi:10.1109/EMBC.2017.8037369.

Alam, M., Rodrigues, W., Ngoc, B., and Thakor, N. V (2016). Brain-machine interface facilitated neurorehabilitation via spinal stimulation after spinal cord injury : Recent progress and future perspectives. *Brain Res.* 1646, 25–33. doi:10.1016/j.brainres.2016.05.039.

Angeli, C. A., Edgerton, V. R., Gerasimenko, Y. P., and Harkema, S. J. (2014). Altering spinal cord excitability enables voluntary movements after chronic complete paralysis in humans. *Brain* 137, 1394–1409. doi:10.1093/brain/awu038.

Capogrosso, M., Milekovic, T., Borton, D., Wagner, F., Martin Moraud, E., Mignardot, J.-B., et al. (2016). A brain–spine interface alleviating gait deficits after spinal cord injury in primates. *Nature* 539, 284–288. doi:10.1038/nature20118.

Jackson, A., and Zimmermann, J. B. (2012). Neural interfaces for the brain and spinal cord—restoring motor function. *Nat. Rev. Neurol.* 8, 690–699. doi:10.1038/nrneurol.2012.219.

López-Larraz, E., Trincado-Alonso, F., Rajasekaran, V., Pérez-Nombela, S., Del-Ama, A. J., Aranda, J., et al. (2016). Control of an ambulatory exoskeleton with a brain-machine interface for spinal cord injury gait rehabilitation. *Front. Neurosci.* 10. doi:10.3389/fnins.2016.00359.

Minassian, K., Persy, I., Rattay, F., Pinter, M. M., Kern, H., and Dimitrijevic, M. R. (2007). Human lumbar cord circuitries can be activated by extrinsic tonic input to generate locomotor-like activity. *Hum. Mov. Sci.* 26, 275–295. doi:10.1016/j.humov.2007.01.005.

Nakao, Y., Sasada, S., Kato, K., Murayama, T., Kadowaki, S., S, Y., et al. (2015). Restoring walking ability in individuals with severe spinal cord injury using a closed-loop spinal magnetic stimulation. in *Proceedings of the 45th Annual Meeting of Society for Neuroscience* Available at: https://www.abstractsonline.com/Plan/ViewAbstract.aspx?sKey=70d620e9-53bf-

4bef-858d-e79452be5b51&cKey=5f31c5f3-9c0c-4873-8cd1-2fab3b718c7d&mKey=d0ff4555-8574-4fbb-b9d4-04eec8ba0c84.

Nishimura, Y., Perlmutter, S. I., and Fetz, E. E. (2013). Restoration of upper limb movement via artificial corticospinal and musculospinal connections in a monkey with spinal cord injury. *Front. Neural Circuits* 7, 57. doi:10.3389/fncir.2013.00057.

Pfurtscheller, G., and Lopes da Silva, F. H. (1999). Event-related EEG/MEG synchronization and desynchronization: basic principles. *Clin. Neurophysiol.* 110, 1842–1857. doi:10.1016/S1388-2457(99)00141-8.

Ramos-Murguialday, A., Broetz, D., Rea, M., Läer, L., Yilmaz, Ö., Brasil, F. L., et al. (2013). Brain-machine interface in chronic stroke rehabilitation: A controlled study. *Ann. Neurol.* 74, 100–108. doi:10.1002/ana.23879.

Rogasch, N. C., Sullivan, C., Thomson, R. H., Rose, N. S., Bailey, N. W., Fitzgerald, P. B., et al. (2016). Analysing concurrent transcranial magnetic stimulation and electroencephalographic data : A review and introduction to the open-source TESA software. *Neuroimage* 147, 934–951. doi:10.1016/j.neuroimage.2016.10.031.

Rossignol, S., and Frigon, A. (2011). Recovery of Locomotion After Spinal Cord Injury : Some Facts and Mechanisms. doi:10.1146/annurev-neuro-061010-113746.

Sarasola-Sanz, A., Irastorza-Landa, N., López-Larraz, E., Bibián, C., Helmhold, F., Broetz, D., et al. (2017). A Hybrid Brain-Machine Interface based on EEG and EMG activity for the Motor Rehabilitation of Stroke Patients. in *15th International Conference on Rehabilitation Robotics (ICORR)*.

Sasada, S., Kato, K., Kadowaki, S., Groiss, S. J., Ugawa, Y., Komiyama, T., et al. (2014). Volitional walking via upper limb muscle-controlled stimulation of the lumbar locomotor center in man. *J. Neurosci.* 34, 11131–11142. doi:10.1523/JNEUROSCI.4674-13.2014.

3. Chapter 3: Event-related desynchronization during movement attempt and execution in severely paralyzed stroke patients: an artifact removal relevance analysis

This manuscript has been published as (López-Larraz et al., 2018a).

3.1 Abstract

The electroencephalogram (EEG) constitutes a relevant tool to study neural dynamics and to develop brain-machine interfaces (BMI) for rehabilitation of patients with paralysis due to stroke. However, the EEG is easily contaminated by artifacts of physiological origin, which can pollute the measured cortical activity and bias the interpretations of such data. This is especially relevant when recording EEG of stroke patients while they try to move their paretic limbs, since they generate more artifacts due to compensatory activity. In this paper, we study how physiological artifacts (i.e., eye movements, motion artifacts, muscle artifacts and compensatory movements with the other limb) can affect EEG activity of stroke patients. Data from 31 severely paralyzed stroke patients performing/attempting grasping movements with their healthy/paralyzed hand were analyzed offline. We estimated the cortical activation as the event-related desynchronization (ERD) of sensorimotor rhythms and used it to detect the movements with a pseudo-online simulated BMI. Automated state-of-the-art methods (linear regression to remove ocular contaminations and statistical thresholding to reject the other types of artifacts) were used to minimize the influence of artifacts. The effect of artifact reduction was quantified in terms of ERD and BMI performance. The results reveal a significant contamination affecting the EEG, being involuntary muscle activity the main source of artifacts. Artifact reduction helped extracting the oscillatory signatures of motor tasks, isolating relevant information from noise and revealing a more prominent ERD activity. Lower BMI performances were obtained when artifacts were eliminated from the training datasets. This suggests that artifacts produce an optimistic bias that improves

theoretical accuracy but may result in a poor link between task-related oscillatory activity and BMI peripheral feedback. With a clinically relevant dataset of stroke patients, we evidence the need of appropriate methodologies to remove artifacts from EEG datasets to obtain accurate estimations of the motor brain activity.

3.2 Introduction

The electroencephalogram (EEG) allows studying the oscillatory activity associated to voluntary movement, which is a major area of interest within the fields of neurology and neurophysiology (Ramos-Murguialday and Birbaumer, 2015). The degree of motor cortex involvement during motor tasks has been largely studied and quantified by means of the event-related desynchronization of the alpha and beta rhythms (Pfurtscheller and Lopes da Silva, 1999). The existence of a tool to assess and quantify cortical involvement during motor tasks has served, for instance, to characterize the pathological patterns of cortical activation of patients with motor disorders, such as stroke or spinal cord injury (Kaiser et al., 2012; López-Larraz et al., 2015; Park et al., 2016). It has also allowed to discover differences in oscillatory activity between stroke patients suffering subcortical and cortical lesions (Stępień et al., 2011; Park et al., 2016; Ray et al., 2017) and to study their cortical reorganization over time (Tangwiriyasakul et al., 2014b).

Measuring the cortical signatures of movement with EEG has also allowed the development of non-invasive systems that interpret those signals in real-time to create brain-machine interfaces (BMI) with rehabilitative or assistive purpose (Chaudhary et al., 2016; Lebedev and Nicolelis, 2017; López-Larraz et al., 2018c). Different devices, including robotics and prosthetics, have been controlled by patients using brain activity only, to facilitate the movement of their paralyzed arms and legs (Hortal et al., 2015; López-Larraz et al., 2016; Ibáñez et al., 2017). The use of these systems to provide a contingent proprioceptive feedback has been demonstrated to promote neural plasticity and motor learning in healthy individuals and patients (Mrachacz-Kersting et al., 2012, 2016; Ramos-Murguialday et al., 2012). Further, BMI-based rehabilitation interventions have proven their success in promoting clinical improvements after stroke and spinal cord injury (Ramos-Murguialday et al., 2013; Ono et al., 2014; Ang et al., 2015; Pichiorri et

al., 2015; Donati et al., 2016; Trincado-Alonso et al., 2017; Biasiucci et al., 2018). The key point of these interventions is to establish a link that associates the neural activity related to voluntary movement and the peripheral feedback to facilitate plasticity by Hebbian mechanisms (Jackson and Zimmermann, 2012).

The main limitation of EEG recordings, either for neurophysiological assessment or for BMI development, is its low signal to noise ratio and easiness to get contaminated. Generally, several tens of repetitions (i.e., trials) of the same task have to be recorded and averaged to derive an accurate estimate of the brain process of interest, or to calibrate the classification algorithm for the BMI (Graimann and Pfurtscheller, 2006a). Interferences of electrical or physiological origin (i.e., artifacts) contaminate the EEG signals, potentially biasing the information and interpretations that can be extracted from these data. Electrical artifacts can be avoided by following good practices, such as recording the EEG data in an electrically shielded room, using battery-powered devices, and minimizing electrode impedances (Hammond and Gunkelman, 2001; Nunez and Srinivasan, 2006). When these artifacts are produced by the sources of stimulation used by a BMI (e.g., closed-loop electric or magnetic stimulation), they can induce a bias in the estimation of EEG power. Different methods have been proposed to avoid this phenomenon, such as ignoring or interpolating the contaminated portions of signal (Hoffmann et al., 2011; Walter et al., 2012b) or using median filtering to minimize the peaks (Insausti-Delgado et al., 2017). Physiological artifacts can be largely reduced by instructing the subjects on how to avoid them; however, sometimes their occurrence is unavoidable. The most common physiological contaminations of EEG recordings are caused by: (1) electrooculographic (EOG) activity, which generates electrical currents due to eyelid movements and movements of the retinal dipoles (Schlögl et al., 2007b); (2) motion artifacts, with low-frequency, high-amplitude oscillations as a result of (involuntary) head or body movements during the execution or attempt of other movements (Castermans et al., 2014); and (3) muscular artifacts, which produce power increases in high-frequencies of the EEG due to the overlap with the spectral bandwidth of muscle activity (Muthukumaraswamy, 2013).

Dozens of methods are currently available to try to minimize the influence of each type of artifact in EEG recordings (Croft and Barry, 2000; Muthukumaraswamy, 2013;

Urigüen and Garcia-Zapirain, 2015). However, there are four important problems missing in the literature that can be of crucial importance, especially when working with EEG of patients with motor paralysis (e.g., due to stroke). Firstly, most of the works study the effects of "cleaning" the artifacts on the resulting signals only; not quantifying, for instance, the differences in the estimation of cortical activation or in BMI performance (Urigüen and Garcia-Zapirain, 2015). Secondly, they generally measure the influence of artifacts in healthy individuals, although there might be differences in how these contaminations affect data of healthy vs. paralyzed subjects (López-Larraz et al., 2017), since patients generate more compensatory activity during attempts of movement. Thirdly, assuming that artifacts are just additive noise that lowers the signal-to-noise ratio can be problematic; if the artifacts are somehow correlated with the studied task (e.g., muscular contamination of the EEG due to excessive contraction during movement attempt), they can be learned by the BMI classifier, leading to an optimistic bias in its performance (Castermans et al., 2014). Fourthly, in addition to the EEG artifacts, compensatory movements of limbs not related to the task are commonly ignored, although they can also bias the measurement of cortical activity (Ramos-Murguialday et al., 2010).

Given the growing interest in the use of EEG and EEG-based BMIs to improve the assessment and motor rehabilitation of patients with paralysis due to stroke, the appropriate cleaning of these signals might be of paramount importance to obtain accurate estimations of brain activation. This work aims at measuring the influence of physiological artifacts in EEG recordings of stroke patients on the quantification of cortical activity and for the use of rehabilitative BMI systems. We expect that more restrictive artifact rejection procedures will lead to a more accurate estimation of the cortical activity during a motor task, which should also result in a better link between the brain and the paralyzed muscles in a BMI therapy. We analyzed a clinically relevant dataset of 31 severely paralyzed stroke patients to study the effects of rejecting EEG and EMG artifacts from an electrophysiological and from a neurotechnological point of view.

3.3 Materials and methods

3.3.1 Patients

Thirty-one chronic stroke patients (19 males, mean age 54.0±11.7 years, range 29–73, time since stroke 60.3±58.2 months, range 10–232) were recruited for this study. Inclusion criteria were: (1) hand paralysis with no finger extension; (2) minimum time since stroke 10 months; (3) age between 18 and 80 years; (4) no psychiatric or neurological condition other than stroke; (5) no cerebellar lesion or bilateral motor deficit; (6) no pregnancy; (7) no epilepsy or medication for epilepsy during the last 6 months; (8) eligibility to undergo magnetic resonance imaging (MRI); and (9) ability to understand and follow instructions. Demographic and clinical data of the patients can be found in Table 3.1. Further details about the lesion location and the brain areas affected by the stroke in each patient can be found in Supplementary Table 3.1 and Supplementary Figure 3.1. The experiments were conducted at the University of Tübingen, Germany. The experimental procedure was approved by the ethics committee of the Faculty of Medicine of the University of Tübingen, and all the patients provided written informed consent.

3.3.2 Experimental design and procedure

The patients were asked to perform an assessment task in which they had to move their healthy hand, or to attempt to move their paralyzed hand, while their electroencephalographic (EEG) and electromyographic (EMG) activity was recorded. Each patient performed between 4 and 6 blocks, each of which contained, in a random order, 17 trials of movement execution (healthy hand) and 17 trials of movement attempt (completely paralyzed hand). The number of blocks recorded depended on the tiredness of the patients, as in some cases they requested to stop the measurements before finishing

the 6 expected blocks[1].Audiovisual cues guided the patients regarding the phases of a trial: rest (random duration between 4 and 5 seconds), movement execution/attempt (4 seconds), and an inter-trial interval that was included every three trials (random duration between 8 and 9 seconds). The patients were asked to perform (or try to perform) openings and closings with their healthy (or paretic) hand at a comfortable personal pace during the 4 seconds of the movement execution/attempt interval (generally, it took them around 1.5 s to perform a complete open-close cycle). Before starting the first block, they were instructed to minimize compensatory movements and any other source of contamination for the EEG activity during the rest and movement intervals.

3.3.3 Data recording and preprocessing

EEG activity was recorded using a commercial Acticap system (BrainProducts GmbH, Germany), with 16 electrodes placed on Fp1, Fp2, F3, Fz, F4, T7, C3, Cz, C4, T8, CP3, CP4, P3, Pz, P4, and Oz (according to the international 10/20 system). The ground and reference electrodes were placed on AFz and FCz, respectively. Vertical and horizontal electrooculography (EOG) was also recorded to capture eye movements. Electromyographic activity was recorded using bipolar Ag/AgCl electrodes (Myotronics-Noromed, USA) from four muscle groups of each arm: *extensor carpi ulnaris*, *extensor digitorum*, external head of the *biceps* and external head of the *triceps*. All signals were synchronously recorded at 500 Hz.

The EEG data were filtered between 0.1 and 48 Hz with a 4-th order causal Butterworth filter. The signals were trimmed down to 7-second trials, from -3 to +4 seconds with respect to the movement cue. Although the shortest duration of the rest intervals was 4 seconds, we decided to consider only the last 3 seconds to ensure that the patients were in resting state.

[1] In a post-hoc analysis, we verified that there were no significant differences due to the distinct amount of trials for each patient in terms of estimated cortical activity and BMI accuracy.

ID	Gender	Age (years)	Time since stroke (months)	Lesion side	Lesion type	cFMA
1	M	60	14	R	C+S	13
2	F	52	156	L	C+S	5.5
3	F	66	23	L	C+S	16.5
4	F	54	10	L	C+S	8
5	M	58	28	R	C+S	8.5
6	M	62	10	R	C+S	1
7	F	73	23	R	C+S	1
8	M	60	130	L	S	9.5
9	F	36	16	L	C+S	11
10	M	57	122	R	S	17
11	M	47	80	R	S	12
12	M	51	16	L	C+S	3.5
13	M	69	89	R	C+S	26
14	F	35	28	R	C+S	11
15	F	72	44	L	S	2
16	F	55	17	R	S	0.5
17	M	66	48	R	C+S	7.5
18	M	69	72	L	S	5.5
19	F	55	45	L	S	16.5
20	F	53	30	L	S	5
21	F	35	60	R	S	25.5
22	M	58	28	R	C+S	8.5
23	M	29	25	R	C+S	15
24	M	47	232	R	C+S	13.5
25	M	50	215	L	S	33.5
26	M	48	45	R	S	7.5
27	F	53	20	L	S	17.5
28	M	40	53	R	C+S	3.5
29	M	70	23	L	C+S	8
30	M	40	46	L	S	30.5
31	M	54	121	R	C+S	16

Table 3.1: Patients demographic data. Lesion side indicates the damaged hemisphere. Lesion type indicates if the stroke affected subcortical areas only (S) or cortical and subcortical areas (C+S). cFMA stands for combined Fugl-Meyer assessment, which comprises hand and arm motor scores combined, excluding coordination, speed and reflexes (range 0 - 54 points, with 54 points indicating normal hand/arm function).

3.3.4 Artifact rejection procedures

The artifact rejection procedures were designed to identify and minimize the influence of four types of contaminations that can frequently occur when measuring EEG activity during movement executions or attempts: electrooculographic contaminations, motion artifacts, muscle artifacts, and compensatory movements with other limbs. For that, we relied on the recorded EEG and EMG activities. Three different methods were proposed and compared between them and with no artifact rejection: (1) artifact rejection based on EMG activity only; (2) artifact rejection based on EEG activity only; (3) artifact rejection based on EMG and EEG. The EMG activity was used to identify undesired compensatory movements with the arm that the patients should keep relaxed. The EEG (and EOG) activity was used to detect electrooculographic contaminations, motion artifacts and muscle artifacts. These artifact rejection procedures were applied to the available set of trials of each patient: i.e., to all the trials of the patient when applied for quantifying the brain activation, and only to the trials used to train the BMI for detecting the movement execution/attempts (see Sections 3.3.5 and 3.3.6). The processing of artifacts was done on a single trial basis: i.e., each trial was processed and marked as clean or as contaminated, and when marked as contaminated it was discarded.

Artifact rejection based on EMG

The EMG activity was used to identify trials with undesired movements of the arms, which might generate cortical activity that masks the activity of interest (more than physiologic artifacts, these trials correspond to an incorrect performance of the requested task). This method is referred to as "EMG rejection". We defined as artifacts those trials that had: (1) muscular activations in any of the recorded muscles during the rest intervals; or (2) muscular activations in the muscles of the opposite arm to the one requested to move (e.g., compensatory movements with the healthy arm during the attempt of movement of the paretic hand).

The processing of the EMG signals was as follows. First, the EMG of each trial was high-pass filtered at 20 Hz with a 4th-order non-causal Butterworth filter. The waveform length (WL) was computed in 200 ms windows with a sliding step of 20 ms,

as in (Ramos-Murguialday et al., 2010). The WL values of the rest interval (i.e., [-3, 0] s) of each trial were averaged, and the mean and standard deviation (SD) between trials were used to compute the rejection threshold: i.e., 3 SD above the mean. Those rest intervals presenting WL values higher than this threshold for a duration longer than 200 ms were considered artifacts and discarded. Subsequently, the mean and SD of the non-rejected trials were computed and used to re-calculate the rejection threshold (i.e., 3 SD above the new mean). Those trials in which this threshold was exceeded for more than 200 ms were considered as artifacts if: (1) the activation occurred in any muscle during the rest interval (i.e., [-3, 0] s); or (2) the activation occurred in any of the muscles of the opposite arm to the moving one during the movement interval (i.e., [0, 4] s).

Artifact rejection based on EEG

Our method to reject artifacts relying on EEG activity was first presented in (López-Larraz et al., 2017) and aims at eliminating the three main (physiological) sources of contamination: eye movements, motion artifacts, and muscle artifacts. This procedure is referred to as "EEG rejection" and involves one step of EOG removal (or correction) and two steps of rejection of trials with artifacts. The influence of eye movements on the EEG was corrected by using linear regression on the EOG data; a method that constitutes one of the state-of-the-art procedures to remove undesired ocular activity while keeping the relevant brain information (Urigüen and Garcia-Zapirain, 2015; Kobler et al., 2017). On the other hand, motion artifacts and muscle artifacts are more difficult to "clean" (i.e., to filter the contamination while maintaining the amount of trials), and there is disagreement in the literature about the effectiveness of techniques to correct these contaminations (Muthukumaraswamy, 2013; Kline et al., 2015; Urigüen and Garcia-Zapirain, 2015). Therefore, we implemented a statistical procedure to identify trials containing artifacts and to completely discard them. Note that not all the EEG channels were considered for the identification of artifacts, but only the ones that were involved in the corresponding analysis (see Sections 3.3.5 and 3.3.6). For instance, when detecting the attempts of movement using the contralateral EEG electrodes, only the contralateral electrodes and their neighbors (used to re-reference by Laplacian derivations) were considered.

Removal of ocular artifacts. The horizontal and vertical components of eye movements were removed from the EEG by using linear regression between the EEG and EOG activities, as proposed in (Schlögl et al., 2007b). This method assumes that the measured EEG signals are a linear combination between the brain activity and the contamination due to eye movements:

$$X_{c,t} = EEG_{c,t} + b_{c,d} \times EOG_{d,t} \qquad (1)$$

where $X_{c,t}$ represents the recorded EEG signals, measured in c electrodes during t time points; $EEG_{c,t}$ is the actual brain activity; $EOG_{d,t}$ are the derivations of electrooculographic activity (in our case d = 2, with horizontal and vertical EOG derivations); and $b_{c,d}$ are the coefficients that represent the weights of the EOG contamination of each EEG channel. The coefficients b are estimated as the product of the auto-covariance matrix of the EOG derivations and the cross-covariance between the EEG and EOG. After that, the brain activity clean of ocular contaminations is calculated by subtracting the weighted contaminations from the measured signals:

$$EEG = X - b \times EOG \qquad (2)$$

It is possible to estimate the coefficients b from a given segment of data and clean such data (i.e., offline analysis), or to apply these coefficients to new, unseen data (i.e., for online filtering). Therefore, this method corrects the artifacts (i.e., removes the contamination) but preserves the amount of trials.

Rejection of motion artifacts and muscle artifacts. The rejection of these two types of artifacts was done using a similar statistical method to the one used with the EMG activity (see 2.4.1). Motion artifacts are generally characterized by low frequency oscillations, while muscular artifacts can be observed in the EEG in high frequencies. To capture those artifacts, we computed the spectral power in delta ([1-4] Hz) and gamma ([30-48] Hz) for the rest and for the movement intervals of each trial (i.e., one value per frequency band and interval for each trial). The mean and SD of delta and gamma power during the rest intervals were used to define the first rejection threshold (3 SD above the mean of each band). All those trials exceeding this threshold in the rest interval were

discarded. We recalculated the rejection threshold for each band using the rest interval of the non-rejected trials only, and also discarded all the trials that exceeded this new threshold in any of the bands in the rest or in the movement intervals.

Artifact rejection based on EMG and EEG

The last method was the most restrictive and combined the use of both EMG and EEG activity to identify trials with undesired movements, eye movements, motion artifacts or muscle artifacts. This method is referred to as "EMG+EEG rejection". Firstly, trials with undesired movements (i.e., malperformance of the task) were rejected by using the method described in Subsection *Artifact rejection based on EMG*. Secondly, the remaining trials were processed with the methods detailed in Subsection *Artifact rejection based on EEG* to eliminate eye movements, motion artifacts, and muscle artifacts[2].

3.3.5 Quantification of cortical activity

The degree of cortical activation during motor execution and motor attempt was quantified by computing the event-related synchronization/desynchronization (ERS/ERD) of the central alpha ([7-13] Hz) and central beta ([14-30] Hz) rhythms (Pfurtscheller and Lopes da Silva, 1999). Figure 3.1a displays the flowchart with the processing steps to compute the ERS/ERD. First, the artifact rejection methods were applied to the trials of each patient separately. Afterwards, the data of all the patients were pooled together to study the average activation for each condition.

The EEG signals were re-referenced using small Laplacian derivations to reduce the effect of volume conduction (Hjorth, 1975). Time-frequency maps representing the cortical activity were computed using Morlet Wavelets (Tallon-Baudry et al., 1997) in

[2] The order of this sequential process (EMG rejection followed by EEG rejection) was chosen to first eliminate the trials in which the task was performed incorrectly, and then to compute the statistical parameters for rejection of motion and muscle artifacts from the trials in which the task was performed correctly. In a post-hoc analysis, we compared the effect of reversing this process (EEG rejection followed by EMG rejection), obtaining no significant differences between both approaches.

the frequency range [1-50] Hz, with a frequency resolution of 0.25 Hz. In these time-frequency maps, the percentage of relative power decrease with respect to a resting-state baseline ([-2.5, -1] s) was calculated to obtain the ERS/ERD patterns, and their statistical significance was estimated using a bootstrap resampling method (Graimann and Pfurtscheller, 2006a).

For each patient and artifact rejection method, the mean ERS/ERD percentage in alpha and beta frequencies was computed from the time-frequency maps of the channels C3 and C4 (i.e., as descriptors of the left- and right-hemispheric sensorimotor cortex, respectively). For that, the ERS/ERD values in the frequency ranges [7-13] Hz (alpha) and [14-30] Hz (beta) were averaged in the time interval [0, 4] s. Higher magnitude of ERD activity (i.e., more negative values) is related to higher cortical activation during motor tasks (Pfurtscheller and Lopes da Silva, 1999), while muscular contaminations tend to generate ERS activity. Therefore, we would expect that cleaner EEG datasets display ERD values of higher magnitude.

3.3.6 Movement execution/attempt detection

Design

We implemented a procedure to classify the brain activity corresponding to rest and movement execution, or to rest and movement attempt (the procedures were applied separately for the healthy and the paretic hand) following our previous developments (Eduardo et al., 2017; López-Larraz et al., 2017). Although the analysis was conducted offline, all the methodologies were applied in a pseudo-online manner (using sliding windows, causal filters and auto-regressive models), simulating a real-time setup. Figure 3.1b displays the flowchart with the steps of the movement execution/attempt detection algorithm.

We used a block-based *N*-fold cross validation strategy, where *N* corresponded to the number of blocks recorded for each patient (*N* varied across patients between 4 and 6 blocks). In each fold, one of the blocks was kept apart for testing, and the rest of the blocks were used as training dataset. When the artifact rejection methods were applied, they were only applied to the training datasets. For the EOG artifact removal, the

coefficients for the regression were computed using the training data only and applied posteriorly to the test trials, simulating an online execution.

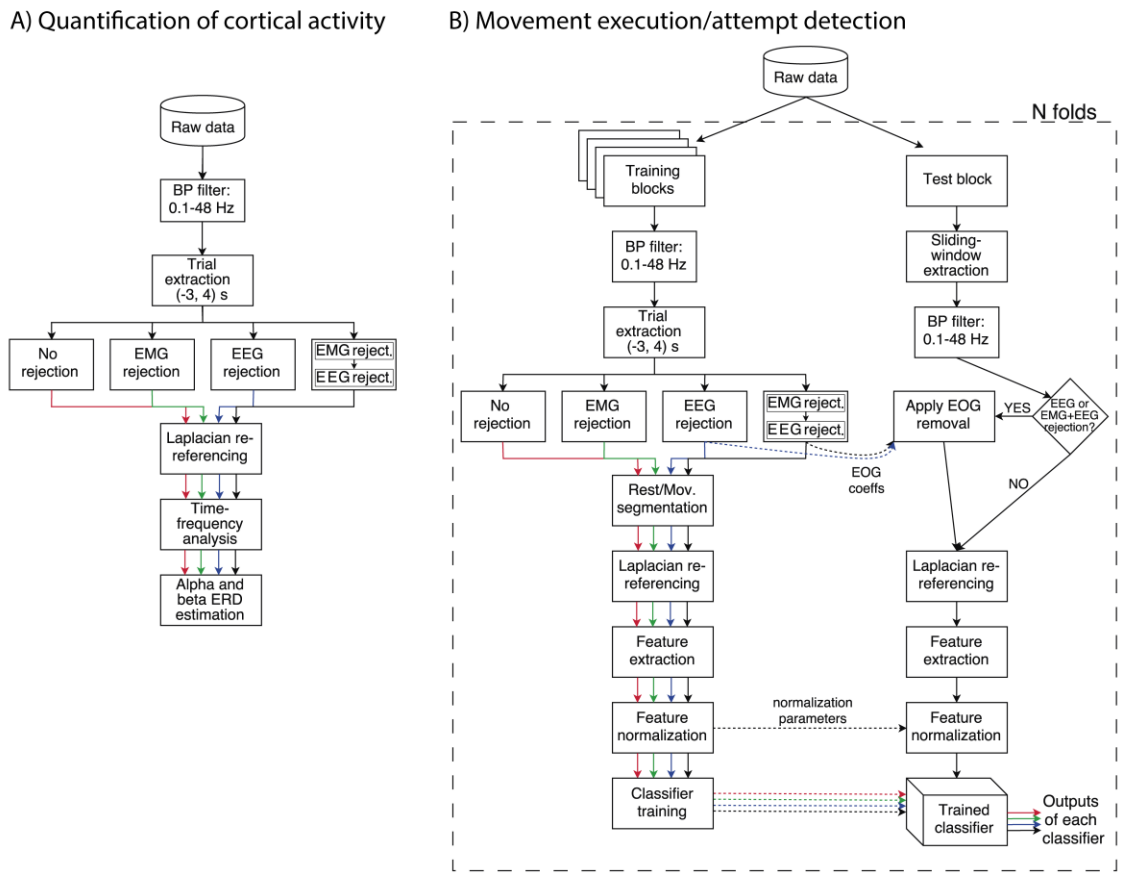

Figure 3.1: Flowchart with the steps of each analysis. A) Steps for the quantification of cortical activity during the movement execution/attempt. The whole set of trials is processed four times (i.e., with each of the artifact rejection methods and without artifact rejection) and the cortical activity is estimated for each of the four methods. Notice that this procedure is performed separately for the movement executions with the healthy hand and the movement attempts with the paretic hand. B) Steps for the pseudo-online classification of movement execution/attepmt. The set of trials considered for training is processed four times (i.e., with each of the artifact rejection methods and without artifact rejection) and the four resulting training datasets are used to calibrate four classifiers. The test data is validated simuling an online processing, where parameters calculated in the training dataset are applied to the test set (e.g., EOG coefficients and normalization parameters). This scheme is performed as a N-fold cross validation, where N is the number of blocks recorded for each patient. Notice that this procedure is performed separately for the movement executions with the healthy hand and the movement attempts with the paretic hand

With this procedure, we simulated different scenarios in which we process the data for training the BMI with different artifact rejection procedures and observe the effects on performance. The test trials with artifacts were not rejected; firstly, to simulate a real-time BMI use in which test artifacts cannot be predicted, and secondly, to have a

fixed and unbiased test dataset for all the artifact rejection methods. Notice that all the proposed methods can be applied in real-time during the BMI operation to detect the artifacts in the test trials and, for instance, stop the feedback if an artifact is detected. With our approach, we assume that training the BMI with clean data is sufficient to characterize the brain activity of interest, and that therefore, the presence of those artifacts in the test trials should not bias the performance.

Feature extraction

The 7-second trials (from -3 to +4 seconds with respect to the movement cue) were re-referenced using small Laplacian derivations (Hjorth, 1975). Unless otherwise specified, the BMI was trained with the activity of the electrodes placed on the contralateral hemisphere to the involved limb only: i.e., C3, CP3 and P3 if the right hand was involved; C4, CP4, P4 if the left hand was involved. Only those electrodes and their neighbors (used for the Laplacian) were considered for the artifact rejection.

We used one-second time windows to extract examples of EEG activity corresponding to resting state and to movement (execution or attempt). The examples of the rest class were extracted from the time interval [-2, 0] s, and for the movement class they were extracted from the interval [1, 3] s (since the reaction time in these patients may be slow (Yilmaz et al., 2015)), using a sliding step of 0.25 s in both cases (i.e., 5 windows of each class extracted from each trial). For each one-second window, the average power in the alpha ([7-13] Hz) and the beta ([14-30] Hz) frequency bands was computed for each of the three contralateral electrodes (i.e., the feature vector of each one-second window included 6 values). The power spectral density was computed using an order-20 autoregressive model, with a frequency resolution of 1 Hz, based on the Burg algorithm (Burg, 1975). The feature vectors of the training dataset were normalized to have zero mean and unit variance. The normalization parameters (i.e., distribution mean and variance) were stored and applied to the test set in the pseudo-online validation of the BMI.

We also aimed at understanding how the artifacts can affect the features (i.e., the frequency bands) and the electrodes (i.e., the cortical positions) used to configure the

BMI. Therefore, we repeated the process described above after varying the following parameters. Firstly, we evaluated the classification by using features of the alpha band only or the beta band only. In these cases, only 3 features were included in the feature vector: 1 frequency band for 3 electrodes. Secondly, we trained the classifier using the EEG electrodes from both hemispheres (i.e., contra- and ipsilateral to the moving limb). In this case, 12 features integrated the feature vectors (i.e., 2 frequency bands for 6 electrodes), and the six electrodes and their neighbors were taken into account for the artifact rejection.

A linear discriminant analysis (LDA) and a support vector machine (SVM) with a radial basis function kernel were evaluated as representative examples of linear and nonlinear classifiers (Lotte et al., 2007). The comparison between a linear and a non-linear classifier can provide relevant information to understand how they behave with data highly contaminated by artifacts. A linear classifier will trace the hyperplane that best separates between the data distributions of rest and movement. On the other hand, a non-linear classifier might be able to draw complex boundaries and learn both the artifacts (higher power with respect to rest) and the ERD activity (lower power with respect to rest), distinguishing them from the rest and providing higher accuracies.

Classification

The test blocks were classified simulating an online scenario. A one-second sliding window was applied from -3 to +4 seconds on each trial (notice that the first output was thus generated at t = -2 s), with the classifier generating an output every 20 ms.

The performance of the movement execution/attempt classifier was quantified in terms of average decoding accuracy, computed as the mean between the true positive rate (TPR) and the true negative rate (TNR). The TPR measures the success of the classifier during the movement period, which was considered the time interval [1, 4] s. The TNR measures the success of the classifier during the rest period, considered as the interval [-2, 0] s.

3.3.7 Statistical analysis

Statistical analyses were performed to test if the different artifact rejection methods had a significant influence on the electrophysiological activity and on the performance of the classifier. We used the Friedman's test for non-Gaussian data with repeated measures (i.e., within subject comparisons), considering the artifact rejection method as factor, and the cortical activity (i.e., ERD in C3 or C4) or the decoding accuracy as dependent variables. Paired post-hoc comparisons were performed using the Wilcoxon signed-rank test to analyze significant differences between pairs. False discovery rate (FDR) correction was applied to control for the multiple comparisons, and statistical significance was considered when corrected *p*-values were smaller than 0.05. Correlation between the percentage of discarded trials and other clinical/demographic/performance variables was studied using Spearman's correlation coefficient.

3.4 Results

The average number of trials discarded for each patient by each artifact rejection method varied significantly between the healthy and the paretic limb (Wilcoxon signed-rank test, $p < 0.05$ for the three methods after FDR correction). For the movements of the healthy hand, 29.7±21.7% of the trials were discarded if the EMG rejection was applied, 40.4±12.5% for the EEG rejection, and 59.2±15.9% for the EMG+EEG rejection. For the movement attempts of the paretic hand, the percentages of discarded trials were 39.2±20.3% for the EMG rejection, 49.2±20.6% for the EEG rejection, and 69.5±16.08% for the EMG+EEG rejection. The number of discarded trials did not correlate significantly with any of the demographic data of the patients: i.e., gender, age, time since stroke, lesion side, location of the stroke, lesion volume and Fugl-Meyer score (Spearman correlation, $p > 0.05$ for the three methods and all the variables after FDR correction).

3.4.1 Quantification of cortical activity

Effect of artifact rejection on ERS/ERD

To facilitate visualization, we rearranged the EEG data to simulate that all the patients had the stroke in the left hemisphere. The lateralized cortical positions of patients with the stroke in the right hemisphere were flipped about the midline. Therefore, in subsequent analyses and figures, the left arm is always considered the healthy one, while the right arm is always considered the paretic one. Likewise, the left hemisphere of the motor cortex (represented by C3 cortical position) was always the ipsilesional area, while the right hemisphere (represented by C4 cortical position) corresponded to the contralesional area.

Figure 3.2 compares the estimated brain activation after applying each of the artifact rejection methods. The time-frequency maps with the event-related (de)synchronization patterns are shown for the movement of the healthy hand (left) and for the movement attempt of the paretic hand (right). As can be seen, the most restrictive artifact rejection (based on EMG+EEG; bottom panels of the figure) clearly enhances the alpha and beta ERD in both hemispheres (i.e., ipsilesional or contralesional), regardless of the role they play with respect to the hand asked to move (i.e., contralateral or ipsilateral). On average for the group of patients, the contralesional electrodes showed stronger activation than the ipsilesional electrodes. Even when the patients attempted to move their paretic hand, the contralesional (i.e., ipsilateral) hemisphere was more active than the ipsilesional (i.e., contralateral) hemisphere. This may be explained by the fact that there were more patients with lesions involving the motor cortex, and these patients do not generally show a significant activation of the ipsilesional hemisphere during movement attempts but they activate the contralesional hemisphere (Luft et al., 2004; Park et al., 2016).

Figure 3.3 illustrates the differences in alpha and beta ERD according to the artifact rejection method applied, and a summary of the statistic comparisons performed. For the movements of the healthy hand (Figure 3.3, left panel), we first analyzed the ERD

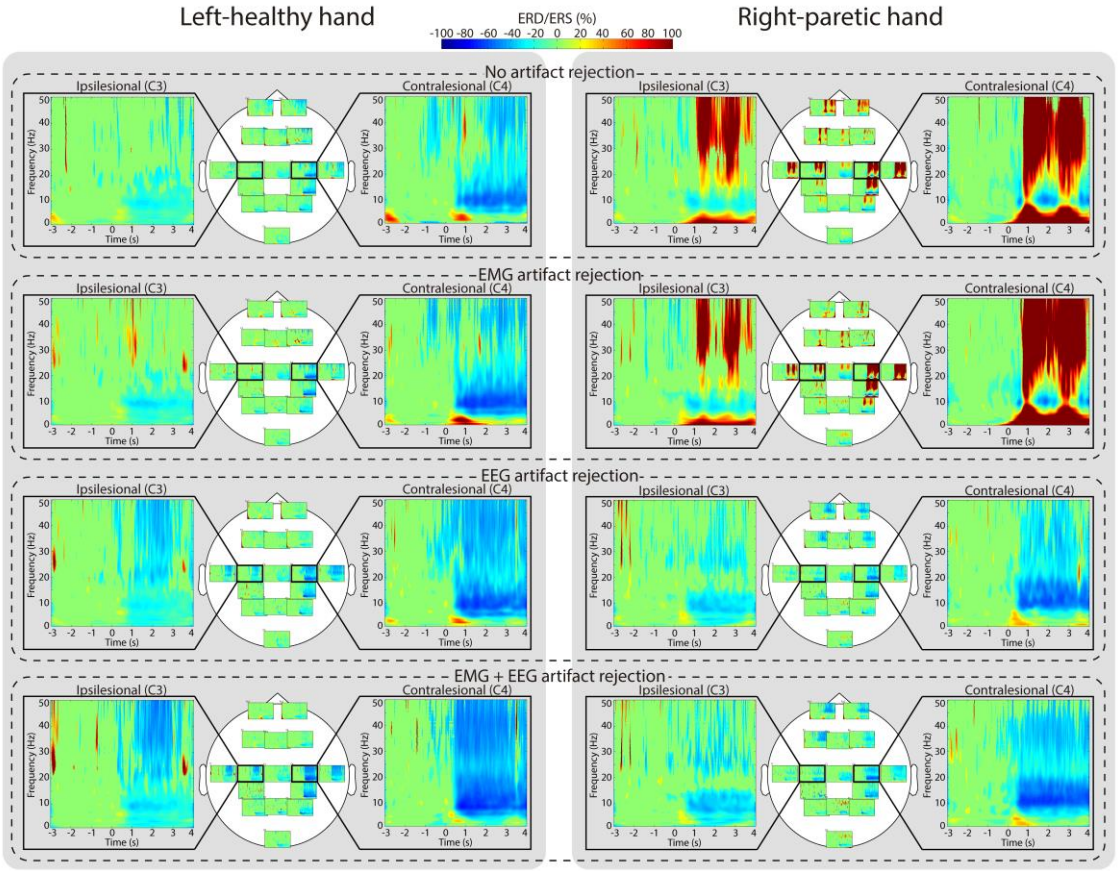

Figure 3.2: Estimated cortical activation with each of the artifact rejection methods. The time-frequency maps represent the event-related (de)synchronization (ERS/ERD), averaged for all the patients, for each of the artifact rejection methods. Notice that the lateralized cortical positions of patients with the stroke in the right hemisphere are swapped, simulating that all the patients have the stroke in the left hemisphere. The percentage of ERS/ERD is calculated with respect to the resting baseline [-2.5, -1] s. The left gray area corresponds to the movements of the healthy (left) hand, while the right gray area corresponds to the attempts of movement of the paretic (right) hand. Each of the four rows indicates one of the artifact rejection methods, encircled by dashed panels. The heads depict the ERD activity of each of the 16 EEG electrodes, averaged for all the patients. The activity of the left (i.e., ipsilesional) and right (i.e., contralesional) hemispheres is detailed by zooming the activity of C3 and C4 channels, respectively. Blue color indicates desynchronization, while red color represents synchronization with respect to the resting baseline. The artifact rejection methods, especially the ones based on EEG and EMG+EEG, reduce the influence of artifacts that cause the appearance of alpha and beta synchronization (i.e., ERS) during movement attempts, and enhance the ERD magnitude.

of the contralateral (i.e., contralesional; C4 electrode) hemisphere. There was a significant effect of the artifact rejection method on alpha ERD magnitude ($\chi^2(3) = 11.48$; $p = 0.009$), with a significant difference in the post-hoc comparisons between no artifact rejection and EMG+EEG rejection ($p = 0.048$); as well as an effect on the beta ERD magnitude ($\chi^2(3) = 19.06$; $p = 0.0003$), with significant differences in the post-hoc

comparisons between no artifact rejection and EMG+EEG rejection (p = 0.029) and between EMG rejection and EMG+EEG rejection (p = 0.004). For the ipsilateral hemisphere to the moved healthy hand (i.e., ipsilesional; C3 electrode), the effect on alpha ERD was not significant ($\chi^2(3) = 7.80$; $p = 0.0503$), although it was for beta ERD ($\chi^2(3) = 7.95$; $p = 0.047$), with significant differences in the post-hoc comparisons between EMG rejection and EEG rejection (p = 0.003) and between EMG rejection and EMG+EEG rejection (p = 0.014).

For the attempts of movement of the paretic hand (Figure 3.3, right panel), we followed the same procedure. In the contralateral (i.e., ipsilesional; C3 electrode) hemisphere, there was a significant effect of the artifact rejection method on alpha ERD magnitude ($\chi^2(3) = 14.52$; $p = 0.002$), with a significant difference in the post-hoc comparisons between no artifact rejection and EMG+EEG rejection (p = 0.0007) and between EMG rejection and EMG+EEG rejection (p = 0.007); similarly, there was a significant effect on the beta ERD magnitude ($\chi^2(3) = 11.92$; $p = 0.008$), with significant differences between no artifact rejection and EEG rejection (p = 0.028), between EMG rejection and EEG rejection (p = 0.004), and between EMG rejection and EMG+EEG rejection (p = 0.0009). For the ipsilateral hemisphere (i.e., contralesional; C4 electrode), the effect on alpha ERD was not significant ($\chi^2(3) = 5.00$; $p = 0.17$), despite the mean differences were higher than for the contralateral hemisphere (compare upper-left and -right plots of the right panel in Figure 3.3); whilst for the beta ERD it was significant ($\chi^2(3) = 8.60$; $p = 0.035$), although none of the post-hoc comparisons were significant after correction.

Influence of each component of the EEG artifact rejection

We also studied the influence of each of the three components of the EEG artifact rejection procedure on the ERD: i.e., EOG removal, motion artifact rejection (based on low frequencies—LowFreq), and muscle artifact rejection (based on high frequencies—HighFreq); and compared them with the combination of the three of them (i.e., EEG rejection). In Figure 3.4, we show the alpha and beta ERD elicited by the movement of the healthy hand and the movement attempt of the paretic hand in the contralateral hemisphere. For simplicity, the statistical results reported below correspond to the

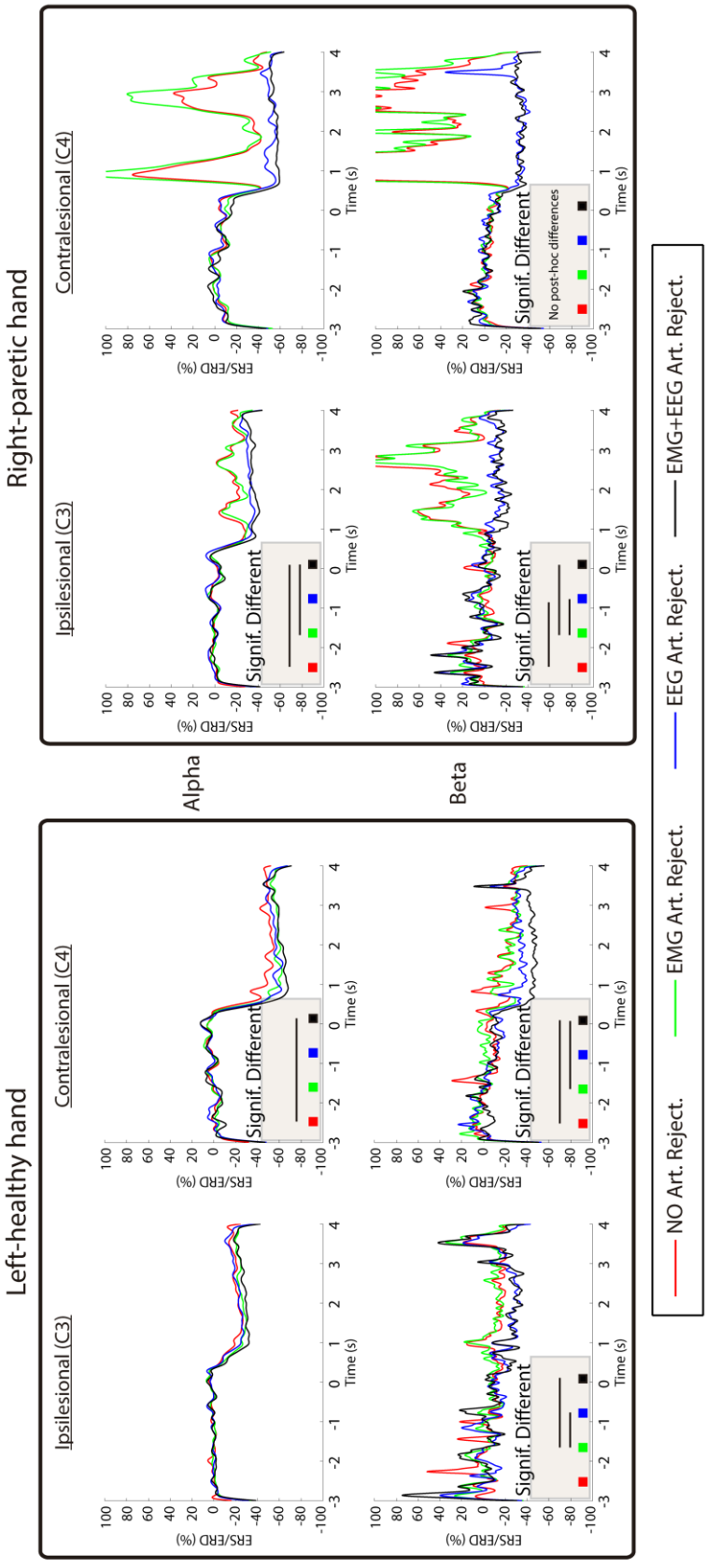

Figure 3.3: Temporal evolvement of ERS/ERD in alpha (i.e., [7-13] Hz) and beta (i.e., [14-30] Hz) frequencies for the four artifact processing methods. Notice that the lateralized cortical positions of patients with the stroke in the right hemisphere are swapped, simulating that all the patients have the stroke in the left hemisphere. The percentage of ERS/ERD is calculated with respect to the resting baseline [-2.5, -1] s. The left panel corresponds to the movements of the healthy (left) hand, while the right panel corresponds to the attempts of movement of the paretic (right) hand. Within each panel, plots corresponding to the ipsilesional (left column) and contralesional (right column) hemispheres, and to alpha (upper row) and beta (bottom row) frequencies are included. Each plot shows the average ERD for each of the four artifact processing methods, indicated by the different colors. The results of the statistical analyses are indicated by the colored squares and horizontal lines in the shaded panel at the bottom-left of the plots. The presence of the " Signif. Different" panel indicates a significant effect of artifact rejection method on ERD magnitude (in the interval [0, 4] s), while the horizontal lines between pairs indicate the pairs of methods with significantly different ERD after correction for multiple comparisons.

contralateral hemisphere to the involved limb. The results of the ipsilateral hemisphere are summarized in Supplementary Figure 3.2.

For the healthy hand (Figure 3.4, left panel), there were no differences between the four compared methods on alpha ERD ($\chi^2(3) = 7.36$; $p = 0.061$), but there were significant differences on beta ERD ($\chi^2(3) = 10.09$; $p = 0.018$), with significant differences between EEG rejection and EOG removal ($p = 0.046$), and between EOG removal and HighFreq rejection ($p = 0.017$). For the paretic hand (Figure 3.4, right panel), there were significant differences both on alpha ERD ($\chi^2(3) = 9.80$; $p = 0.020$), with significant differences between EEG rejection and EOG removal ($p = 0.043$), and between EOG removal and HighFreq rejection ($p = 0.004$); as well as on beta ERD ($\chi^2(3) = 14.16$; $p = 0.003$), with significant differences between EEG rejection and EOG removal ($p = 0.018$), between EEG rejection and LowFreq rejection ($p = 0.005$), between EOG removal and HighFreq rejection ($p = 0.032$), and between LowFreq rejection and HighFreq rejection ($p = 0.047$).

3.4.2 Movement detection

Effects of artifact rejection

Figure 3.5 shows the average results for the detection of movement execution and attempt based on the linear classifier (LDA) combining alpha and beta features extracted over the contralateral motor cortex. The figure displays the performance of the classifiers, indicating the percentage of outputs that are classified as movement (or movement attempt) on each time instant (i.e., this value should be low in the rest periods and high in the movement periods). We considered this configuration of classifier and feature extraction procedure as the reference for posterior comparisons. For the healthy hand (Figure 3.5 left), there were no significant differences in accuracy between the four methods to process the artifacts ($\chi^2(3) = 1.71$; $p = 0.63$). For the paretic hand (Figure 3.5 right), the different artifact rejection methods led to significantly different accuracies ($\chi^2(3) = 9.98$; $p = 0.019$). Post-hoc comparisons revealed that training the BMI without rejecting artifacts provided significantly higher decoding accuracies than rejecting artifacts based on EEG ($p = 0.022$) or based on EMG+EEG ($p = 0.044$).

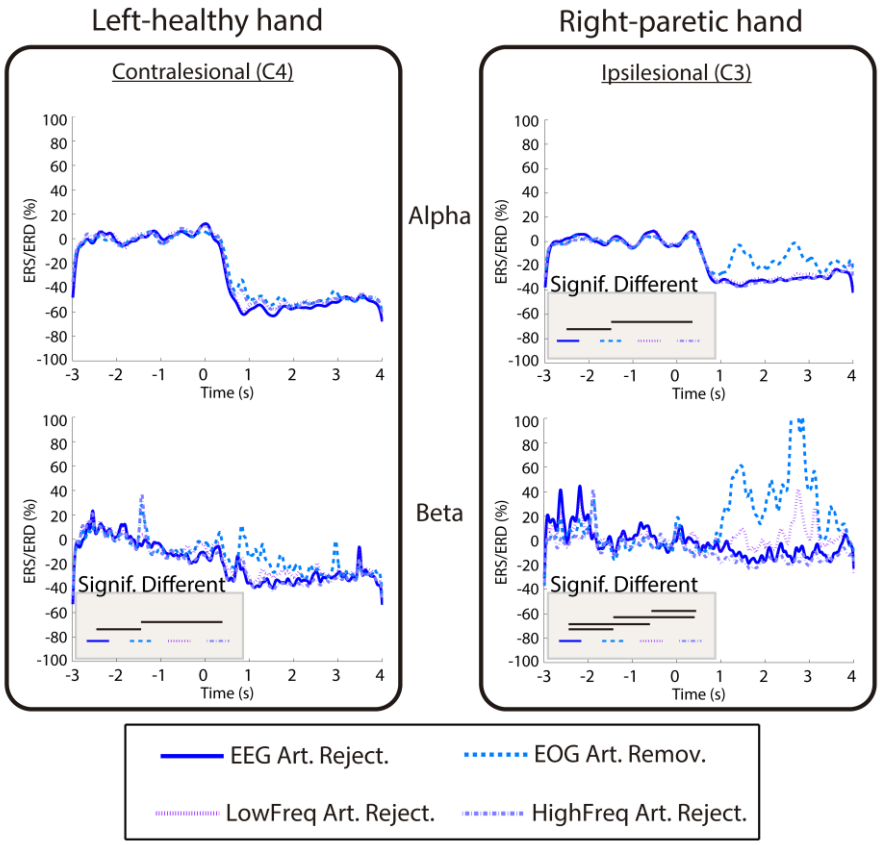

Figure 3.4: Temporal evolvement of ERS/ERD in alpha (i.e., [7-13] Hz) and beta (i.e., [14-30] Hz) frequencies for the EEG artifact rejection, and for each of its components separately. Notice that the lateralized cortical positions of patients with the stroke in the right hemisphere are swapped, simulating that all the patients have the stroke in the left hemisphere. The percentage of ERS/ERD is calculated with respect to the resting baseline [-2.5, -1] s. The left panel corresponds to the movements of the healthy (left) hand, while the right panel corresponds to the attempts of movement of the paretic (right) hand. Within each panel, the activity of the contralateral hemisphere (i.e., contralesional for the healthy hand, and ipsilesional for the paretic hand) for alpha (upper row) and beta (bottom row) frequencies is shown. Each plot shows the average ERD for each of the four methods, indicated by the different colors and types of line. The results of the statistical analyses are indicated in the shaded panel at the bottom-left of the plots. The presence of the "Signif. Different" panel indicates a significant effect of artifact rejection method on ERD magnitude (in the interval [0, 4] s), while the horizontal black lines between pairs indicate the pairs of methods with significantly different ERD after correction for multiple comparisons.

When using a non-linear SVM classifier, the results were very similar to the ones observed with the linear classifier (see Supplementary Figure 3.3). Paired comparisons between the four artifact processing methods for LDA and SVM were conducted (separately for each hand), showing no significant differences between the two classifiers in any case ($p > 0.05$). Therefore, all the subsequent analyses are based on an LDA-based classifier, since it is a simpler approach than the non-linear SVM.

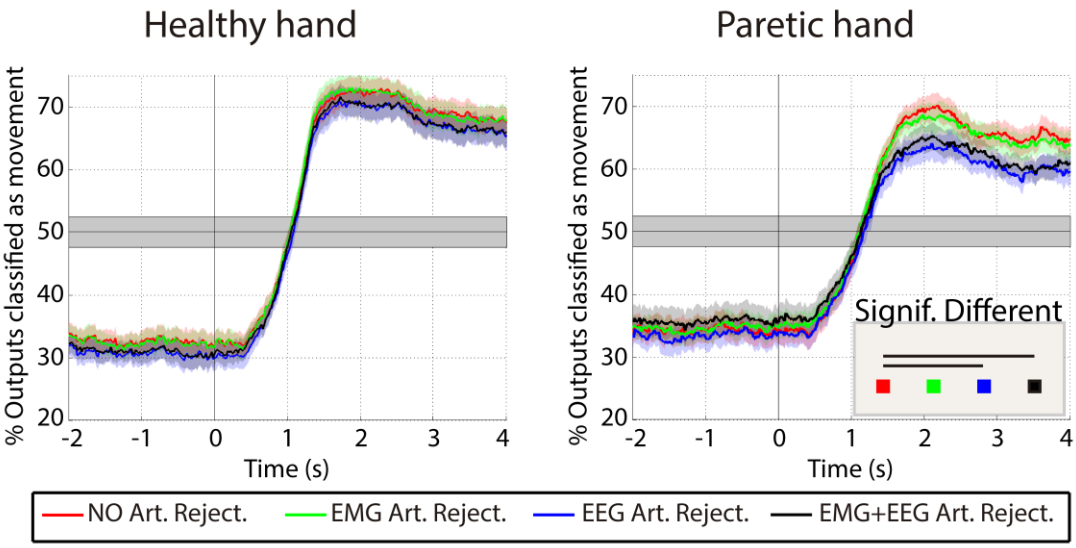

Figure 3.5: Average performance with a linear classifier (LDA-based) for the healthy (left) and the paretic (right) hands with each of the four artifact processing methods. On each panel, the lines represent the percentage of classifier outputs identified as movement, averaged for all the patients, and the shades indicate the standard error of the mean. Notice that the values before t = 0 correspond to false positives, while the values after t = 0 correspond to true positives. The shaded gray area indicates the confidence interval of the chance level (alpha = 0.01), computed on the basis of all the test trials, according to (Müller-Putz et al., 2008). The results of the statistical analyses are indicated by the colored squares and horizontal lines in the shaded panel at the bottom-right of the plots. The presence of the "Signif. Different" panel indicates a significant effect of artifact rejection method on the average BMI accuracy, while the horizontal lines between pairs indicate the pairs of methods with significantly different accuracy after correction for multiple comparisons.

Importance of the number and type of trials rejected

Discarding trials with artifacts from the training dataset led to average decreases in accuracy. One could think that this is due to the reduction of the number of observations used for training the classifier, and not to the fact that only the contaminated trials were rejected. To avoid this possible bias, we conducted two analyses.

Firstly, we measured if there is a significant correlation between the percentage of trials discarded by the different artifact rejection methods and the performance of the classifier. We used Spearman correlation with the data of all the subjects and artifact rejection methods and found no significant correlation neither for the healthy hand (r = -0.11; p = 0.25) nor for the paretic hand (r = -0.15; p = 0.20).

Secondly, we repeated the classification procedure but randomly eliminating from the training dataset the same number of trials that were rejected by the most restrictive method (i.e., based on EMG+EEG). This process was repeated 10 times for each fold of each patient. Figure 3.6 shows the average results for this procedure with the reduced training dataset, compared with the training datasets without artifact rejection and with EMG+EEG artifact rejection (as displayed in Figure 3.5). As for the analysis presented in the previous section, no significant differences in performance were found between the three procedures for the healthy hand ($\chi^2(2) = 2.20$; $p = 0.33$). For the paretic hand, the rejection method had a significant effect on decoding accuracy ($\chi^2(2) = 8.11$; $p = 0.017$). Post-hoc comparisons showed that the EMG+EEG artifact rejection led to significantly lower performances than if no trials were rejected ($p = 0.017$), or if random trials were rejected from the training data ($p = 0.0015$); while not rejecting or rejecting random trials from the training dataset led to not significantly different results ($p > 0.05$).

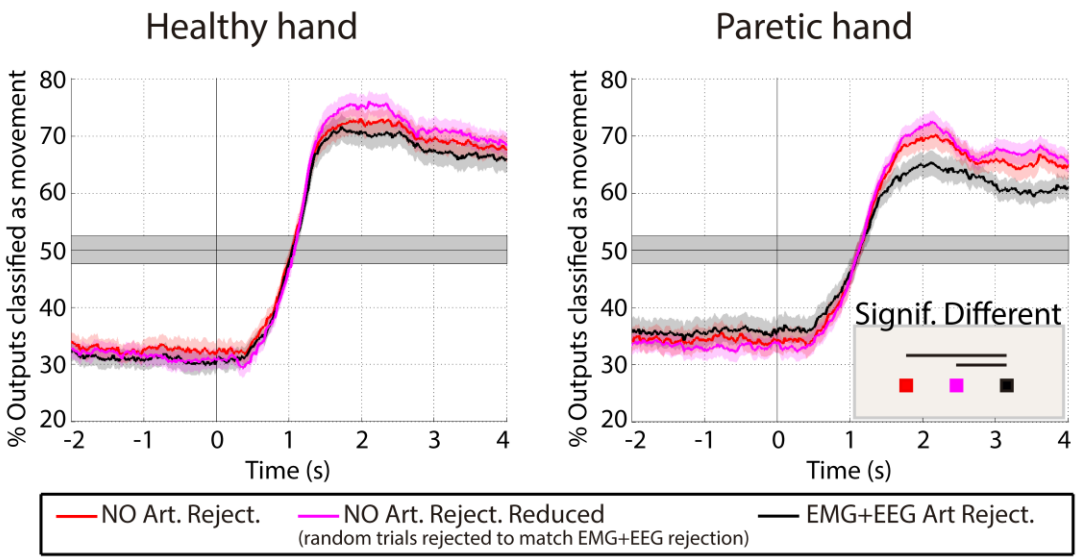

Figure 3.6: Average performance for the healthy (left) and the paretic (right) hands analyzing the influence of the number of trials rejected from the training dataset. On each panel, the lines represent the percentage of classifier outputs identified as movement, averaged for all the patients, and the shades indicate the standard error of the mean. Notice that the values before t = 0 correspond to false positives, while the values after t = 0 correspond to true positives. The shaded gray area indicates the confidence interval of the chance level (alpha = 0.01), computed on the basis of all the test trials, according to (Müller-Putz et al., 2008). The results of the statistical analyses are indicated in the shaded panel at the bottom-right of the plots. The presence of the "Signif. Different" panel indicates a significant effect of the method on the average BMI accuracy, while the horizontal lines between pairs indicate the pairs of methods with significantly different accuracy after correction for multiple comparisons.

Effects in the different frequency bands

When the linear classifier was trained with features of the alpha band only, the artifact rejection method had no significant influence on performance either for the healthy ($\chi^2(3) = 4.69$; $p = 0.20$) or for the paretic hand ($\chi^2(3) = 6.25$; $p = 0.10$). Similarly, for the classifier trained with the beta band only, no differences between artifact rejection methods in the healthy ($\chi^2(3) = 2.11$; $p = 0.55$) nor the paretic hand ($\chi^2(3) = 0.66$; $p = 0.88$) were found.

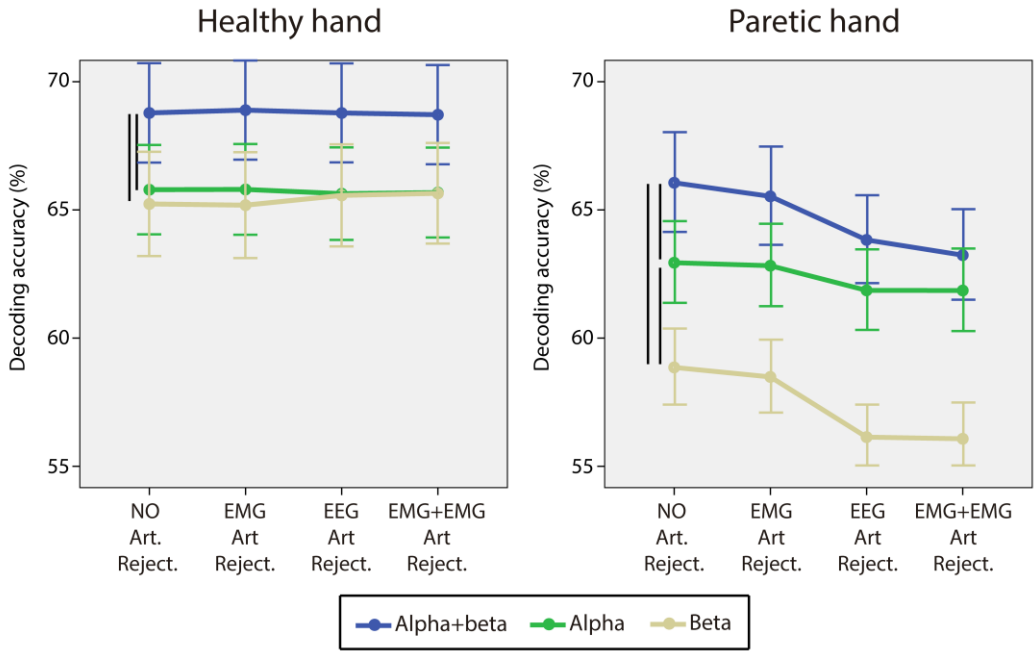

Figure 3.7: Interaction plots studying the effects on decoding accuracy of the artifact rejection methods and the frequency bands used to extract the features for the BMI classifier. Only the factor "type of feature" was significant for the linear model. The vertical black bars denote statistical significance between pairs of types of features after correction for multiple comparisons. The whiskers on each point show the standard error of the mean.

To measure possible interactions between these features and the artifact rejection method, we fitted a linear model, considering accuracy as dependent variable, and artifact rejection method (4 levels) and type of features (3 levels: alpha+beta, alpha, and beta) as factors. For the healthy hand, the type of features was a significant factor ($F_{2,11} = 3.84$, $p = 0.022$), with alpha+beta configuration providing significantly higher accuracies than alpha only ($p = 0.048$) and beta only ($p = 0.039$). For the paretic hand, again the type of features was a significant factor ($F_{2,11} = 21.15$, $p = 2.1\times10^{-9}$), with alpha+beta configuration providing significantly higher accuracies than alpha only ($p = 0.046$) and

beta only ($p = 1.83\times10^{-9}$), and alpha being also significantly higher than beta ($p = 3.40\times10^{-5}$). Figure 3.7 displays the performances of alpha, beta, and alpha+beta configurations for each of the four artifact processing methods when using the BMI for the healthy or paretic hand.

Influence of each EEG artifact rejection component

We also evaluated the effect that each of the three EEG artifact rejection components (namely EOG removal, motion artifacts rejection, and muscle artifacts rejection) had on decoding accuracy. Figure 3.8 shows the results for the healthy and the paretic hand, comparing five configurations: no artifact rejection, complete EEG artifact rejection (as reported in the previous results), EOG artifact removal only (EOG), motion artifact rejection only (based on low frequencies—LowFreq), muscle artifact rejection only (based on high frequencies—HighFreq). For the healthy hand, there were no significant differences in accuracy ($\chi^2(4) = 3.19$; $p = 0.52$). For the paretic hand, there was a significant effect on performance due to the EEG artifact rejection method ($\chi^2(4) = 16.24$; $p = 0.003$). Post-hoc comparisons revealed significant differences between no artifact rejection and the complete EEG artifact rejection (as already reported in 3.1.1; $p = 0.02$), between EEG rejection and EOG removal ($p = 0.0003$), between EEG and HighFreq rejection ($p = 0.004$), between EOG removal and LowFreq rejection ($p = 0.01$), and between EOG removal and HighFreq rejection ($p = 0.02$).

Effects when using both hemispheres

Providing contingent feedback associated to the activation of the contralateral (i.e., ipsilesional) hemisphere to the paralyzed limb during attempts of movement can lead to motor recovery in stroke patients (Ramos-Murguialday et al., 2013). Combining the activity of both hemispheres can lead to higher decoding accuracies than using only the ipsilesional one (Eduardo et al., 2017), despite there is no evidence supporting that this can also facilitate recovery.

We also investigated how the artifact rejection methods influenced the movement detection based on the activity of both hemispheres (Figure 3.9). For this, both the artifact rejection and the feature extraction considered the electrodes placed on the left and right

hemispheres. In this case, we found a significant effect of the artifact rejection method for the healthy hand ($\chi^2(3) = 22.85$; $p = 4.35\times10^{-5}$), with significant differences in performance between no artifact rejection and EMG+EEG artifact rejection ($p = 0.0007$), and between EMG and EMG+EEG artifact rejection ($p = 0.0015$). For the paretic hand, there were also significant differences in accuracy dependent on the rejection method ($\chi^2(3) = 33.00$; $p = 3.22\times10^{-7}$); paired comparisons showed significant differences in performance between no artifact rejection and EEG rejection ($p = 0.0001$), no artifact rejection and EMG+EEG rejection ($p = 0.0001$), EMG rejection and EEG rejection ($p = 0.011$), and EMG rejection and EMG+EEG rejection ($p = 0.0005$).

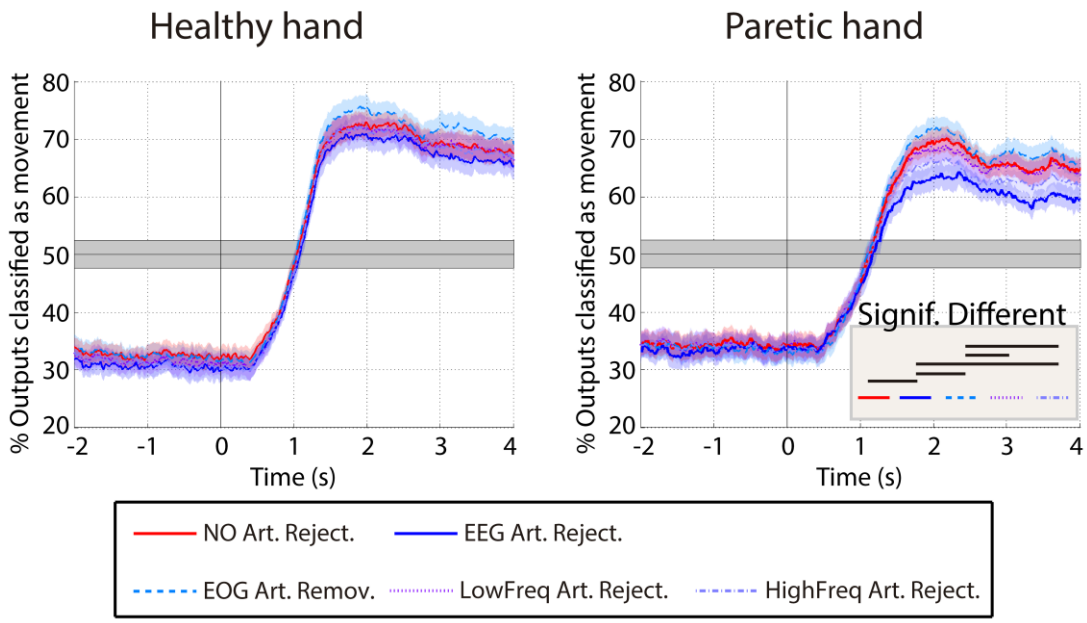

Figure 3.8: Average performance for the healthy (left) and the paretic (right) hands analyzing the influence of the different components of the EEG artifact rejection. On each panel, the lines represent the percentage of classifier outputs identified as movement, averaged for all the patients, and the shades indicate the standard error of the mean. Notice that the values before t = 0 correspond to false positives, while the values after t = 0 correspond to true positives. The shaded gray area indicates the confidence interval of the chance level (alpha = 0.01), computed on the basis of all the test trials, according to (Müller-Putz et al., 2008). The results of the statistical analyses are indicated in the shaded panel at the bottom-right of the plots. The presence of the "Signif. Different" panel indicates a significant effect of the method on the average BMI accuracy, while the horizontal black lines between pairs indicate the pairs of methods with significantly different accuracy after correction for multiple comparisons.

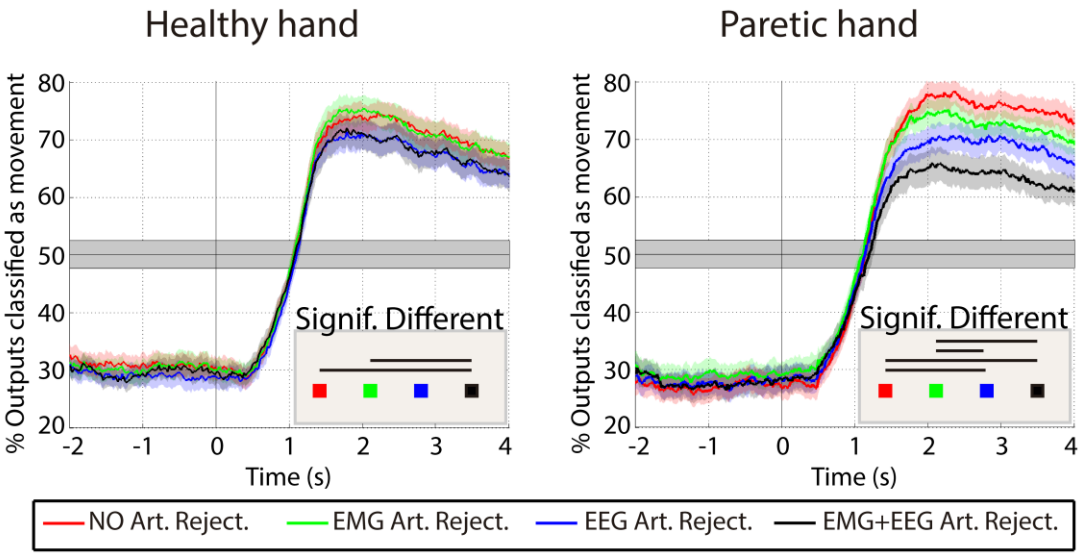

Figure 3.9: Average performance for the healthy (left) and the paretic (right) hands when the BMI was trained with the activity of both hemishperes. On each panel, the lines represent the percentage of classifier outputs identified as movement, averaged for all the patients, and the shades indicate the standard error of the mean. Notice that the values before t = 0 correspond to false positives, while the values after t = 0 correspond to true positives. The shaded gray area indicates the confidence interval of the chance level (alpha = 0.01), computed on the basis of all the test trials, according to (Müller-Putz et al., 2008). The results of the statistical analyses are indicated in the shaded panel at the bottom-right of the plots. The presence of the "Signif. Different" panel indicates a significant effect of the method on the average BMI accuracy, while the horizontal black lines between pairs indicate the pairs of methods with significantly different accuracy after correction for multiple comparisons.

3.5 Discussion

EEG recordings are a relevant tool to study neural dynamics and to develop brain-machine interfaces (BMI) for motor rehabilitation of severely paralyzed stroke patients. The present study evidences the importance of appropriate methodologies to remove artifacts in EEG recordings of stroke patients to obtain accurate estimations of the motor brain activity. Firstly, removing the contaminations improves the quantification of the EEG-cortical activation during motor tasks. Secondly, when this activity is classified by a BMI to detect movement (or movement attempt), artifacts can cause an optimistic bias in the performance. This implies that training a BMI with a dataset not properly cleaned from artifacts can weaken the link that associates brain activation and proprioceptive feedback, which is hypothesized to be key to promote motor recovery (Ramos-Murguialday et al., 2013).

3.5.1 Methods for identifying and rejecting the artifacts

A large variety of methodologies can be applied to try to minimize the influence of artifacts on EEG data (Croft and Barry, 2000; Muthukumaraswamy, 2013; Urigüen and Garcia-Zapirain, 2015). Several methods allow removing (i.e., correcting) certain types of artifacts and reconstructing the EEG signals after cleaning the undesired components. These methods are especially useful for removing eye contaminations, since they are easy to be characterized, captured and filtered (Urigüen and Garcia-Zapirain, 2015). Among these methods, linear regression and independent component analysis (ICA) have been proven as the most efficient ones to remove ocular artifacts (Schlögl et al., 2007b; Klados et al., 2009; Urigüen and Garcia-Zapirain, 2015; Kobler et al., 2017); although there is certain controversy about how the use of ICA may introduce additional sources of variance to the EEG and negatively impact the signals of interest (Pontifex et al., 2016). However, for muscle and motion artifacts, these techniques may not be so effective. On the one hand, linear regression and adaptive filtering require a reference signal (as for instance, the EOG activity), which is hardly available for body motions and for all the muscles that may contaminate the EEG (e.g., shoulder, neck and cranial muscles) (Urigüen and Garcia-Zapirain, 2015). On the other hand, despite ICA has also been used in offline analyses to clean artifactual components such as motion and muscle artifacts, it has two limitations that hinder their direct applicability to BMI-based rehabilitation therapies for patients with paralysis. Firstly, it is not trivial to decipher what components correspond to artifacts, and for this reason they are generally selected by visual inspection (Seeber et al., 2016; Wagner et al., 2016; Pereira et al., 2017), which makes it unpractical for a BMI therapy. Secondly, when patients try to move their paralyzed limb, these types of artifacts can be highly correlated with the brain activity of interest, which can reduce the capacity of the algorithm to remove the contaminations. For these reasons, statistical methods have been proposed as a simple way of rejecting outlier values with respect to a threshold on certain signal descriptors (e.g., amplitude, variance, power on a frequency band, etc.) (Nolan et al., 2010; López-Larraz et al., 2014). This allows analyzing the EEG signals after removing the influence of motion and muscle artifacts, among others.

We used automated state-of-the-art methods to minimize the influence of artifacts. The types of artifacts that we tried to detect and eliminate were: 1) undesired movements (monitoring EMG to avoid trials with movements during the baseline intervals or involving the limb that was asked to keep relaxed); 2) eye contaminations; 3) motion artifacts; and 4) muscle artifacts. Eye contaminations were removed with a linear regression (Schlögl et al., 2007b), while the other three types of artifacts were identified with a trial-based statistical thresholding and rejected. The rejection based on EMG activity identified the trials with inappropriate movements, which, if not discarded, might affect the quantification of the cortical activity (Ramos-Murguialday et al., 2010). The rejection based on EEG activity, and especially the one based on high frequencies (i.e., identification of muscle artifacts) was the one that contributed the most to enhance the estimated cortical activation, measured as the ERD. Although we cannot warrantee that the methods we used identified and rejected all the artifacts in the signals, they are sufficient to investigate if and to what extent the artifacts influenced the measured brain activity.

It is not trivial to determine what the optimal procedure is to eliminate artifacts from EEG activity. In environments where external interferences are introduced, for instance, by closed-loop electric or magnetic stimulation, ad-hoc studies should be conducted to find the best strategy that minimizes their influence (Hoffmann et al., 2011; Walter et al., 2012b; Insausti-Delgado et al., 2017). Physiological artifacts have different origins, and different procedures are required to minimize them. For instance, in the context of the present study with severely paralyzed stroke patients, muscle artifacts were the ones affecting to a higher extent both ERD magnitude and BMI performance. Therefore, the rejection based on high frequencies of the EEG had the strongest influence. Rejection based on low frequency EEG and electrooculographic activity had a smaller impact on ERD and BMI performance. This is probably due to the fact that we based our analyses on alpha and beta frequency bands (i.e., [7-30] Hz), but also because the patients performed a grasping task, which elicits less eye and head movements, in contrast to other movements such as reaching or walking (Velu and de Sa, 2013; Ibáñez et al., 2014; López-Larraz et al., 2016; Shiman et al., 2017). Therefore, the methodology employed to

remove contaminations from EEG activity should always be carefully designed according to the aim of the study and the particularities of the protocol to be conducted.

3.5.2 Influence on the quantification of cortical activity

We showed that rejecting trials with artifacts helps to capture more accurately the brain activation during motor execution and motor attempt. The values of the ERD were always higher in absolute value (since the ERD is measured with negative values (Graimann and Pfurtscheller, 2006a)) using the most restrictive artifact rejection method (i.e., based on EMG+EEG activity). The rejection of artifacts revealed a stronger contralesional activation during the attempt of movement of the hand, which could not be appreciated without removing artifacts (cf. Figure 3.2). This contralesional activation is a known phenomenon that has already been described in fMRI studies (Ward et al., 2003; Grefkes et al., 2008; Rehme et al., 2011). Proper cleaning of EEG contaminations is a crucial step for future analyses that aim at characterizing specific brain activation patterns after stroke. Further research could be conducted to investigate how EEG activity varies according to the location of the stroke, revealing which brain structures contribute most to the magnitude of the ERD, and complementing previous fMRI studies (Luft et al., 2004).

Although artifacts also influenced the brain activity related to the movements of the healthy hand, the effect was more evident for the activity elicited during the movement attempts of the paretic hand. This probably reflects the fact that the attempts of movement with a paralyzed limb require extra efforts that generate more frequent and larger artifacts (e.g., head and eye movements or contractions of neck and cranial muscles) and compensatory movements with other body parts. In general, the beta band was more affected than alpha, presumably due to its proximity to the spectral bandwidth of muscle activity (Muthukumaraswamy, 2013). This reveals why the EEG artifact rejection based on high frequencies contributed the most to cleaning these artifacts (cf. Figure 3.4).

The artifact rejection method based on EMG activity discarded almost 40% of the trials of the paretic hand and 30% of the healthy hand. Interestingly, it never improved

the measurements of cortical activity compared to not rejecting artifacts. This suggests that the undesired movement components detected by the EMG rejection may not significantly influence the estimated brain activity. However, this result should be interpreted with caution. The fact that the estimations of cortical activation did not change significantly after our EMG rejection does not imply that compensatory movements do not affect the activity. The subjects should always be carefully instructed to avoid compensatory activity with other limbs, and their compliance with the task should be monitored. Furthermore, certain tasks can be more prone to cause other limbs to move during the unsuccessful attempts; for instance, the task in this study (i.e., grasping) may require less compensation with the trunk or with the healthy arm than a reaching task. If those contaminated trials are not rejected, their processing can result in an inaccurate estimation of cortical activation, not corresponding to the task that is under investigation (Pineda et al., 2000), which can bias the conclusions or hamper the BMI-based rehabilitation therapy. Still, we observed that the combination of EMG and EEG rejection led to slightly higher values of brain activation, although the differences were not statistically significant (see, for instance, how in the right plots of the left panel of Figure 3.3, the black line is always more negative than the blue line during the movement period; or how in Figure 3.2, the fourth row displays a stronger activation than the third row). For these reasons, we would recommend researchers to carefully analyze their datasets and identify possible contaminations that may be cleaned by the proposed EMG rejection: i.e., discarding those trials with muscular activation during the rest intervals, or activation of the other limbs.

3.5.3 Implications for brain machine interfaces

The differences that we observed in the brain activity with the artifact rejection methods also translated into differences in BMI classification accuracy. We already demonstrated in a previous study that eliminating EOG, motion and muscle artifacts decreased, in general, the BMI performance (López-Larraz et al., 2017). We confirmed those results and observed that additionally rejecting the trials with undesired movements (based on the EMG activity) did not change significantly the performance of the BMI classifier trained with the electrodes of the contralateral hemisphere only. Interestingly,

when the BMI classifier relied on cortical information from both hemispheres, the differences between artifact rejection methods were larger, especially for the paretic limb. This is likely due to the higher degree of contamination that we found in the ipsilateral hemisphere during the attempts of movement. In addition, it has important implications for BMIs using the contralesional activity to detect movement attempts of stroke patients (Ono et al., 2014; Tangwiriyasakul et al., 2014a; Ang et al., 2015; Antelis et al., 2017; Eduardo et al., 2017; López-Larraz et al., 2018b), since the training data should be more carefully cleaned to avoid biasing the classifier with artifacts.

We did not find any evidence supporting that linear or non-linear classifiers are more prone to being contaminated with artifacts, and very similar performances were obtained when using LDA- or SVM-based classifiers. This result supports the idea that in this type of BMI for movement detection, the features and processing of the data have a stronger influence than the classifier itself (Bashashati et al., 2015). In fact, we could observe that combining features based on alpha and beta frequencies to train the BMI classifier had a significantly positive impact on performance.

3.5.4 Implications for clinical practice

Brain machine interfaces have demonstrated their efficacy for rehabilitation after paralysis (Ramos-Murguialday et al., 2013; Ono et al., 2014; Ang et al., 2015; Pichiorri et al., 2015; Donati et al., 2016; Trincado-Alonso et al., 2017; Biasiucci et al., 2018). However, this technology is still in a preliminary stage, and there is a great margin for investigation and improvement before it becomes one standard tool in the portfolio of clinical treatments for motor rehabilitation (Asín Prieto et al., 2014; López-Larraz et al., 2018c). The results presented in this study demonstrate, on the one hand, that rejecting trials with artifacts from the EEG datasets helps to better quantify the brain activity of stroke patients during motor tasks; and on the other hand, that after rejecting the artifacts from the training datasets, the obtained BMI performances are lower. However, it detects significantly better the brain activity related to the motor task, guaranteeing a better link between brain and muscles, shown to be key for motor rehabilitation (Ramos-Murguialday et al., 2013). Therefore, for an actual BMI intervention, we would recommend cleaning the training datasets with all the available information; meaning that

EEG rejection should necessarily be conducted, while EMG rejection could be included or not depending on the protocol and the availability of EMG signals.

We have shown in a previous study that drops in performance of EEG-based movement intention detection might be due to the presence of artifacts in the test data (López-Larraz et al., 2017). This suggests that when artifacts are removed from the training dataset, the classifier does not learn those patterns, and therefore avoids their possible bias in the BMI control, since it is not able to recognize them as relevant information. The important question that arises is: What is the influence that this drop in performance has in rehabilitation? To date, we can only speculate that it is not the general BMI performance (as measured in this or in previous papers) the responsible for the success of the therapy. More specifically, we conjecture that it is the accurate and contingent link between the activation of the neuronal populations in the motor network and the peripheral feedback in the paralyzed limbs what supports recovery (Jackson and Zimmermann, 2012). As shown in this paper, artifact rejection is an efficient way to improve the characterization of the brain activity responsible of motor commands. Therefore, it should be able to improve the contingent association between brain and muscles and intensify the neuroplastic and rehabilitative effects of BMI-based therapies.

3.5.5 Limitations and perspectives

In this study, we focused on quantifying the brain activation by means of the event-related desynchronization/synchronization (ERD/ERS) of the alpha and beta rhythms. These EEG correlates of movement are the most widely used in BMI rehabilitative therapies with stroke or SCI patients (Ramos-Murguialday et al., 2013; Ono et al., 2014; Ang et al., 2015; Pichiorri et al., 2015; Donati et al., 2016; Biasiucci et al., 2018). Other correlates, such as the movement-related cortical potentials (MRCP) have also been proposed for rehabilitative BMI systems, due to its good temporal precision (Mrachacz-Kersting et al., 2012, 2016), that can facilitate Hebbian plasticity, and their capacity to encode information about different movements (Schwarz et al., 2018). However, MRCPs require asynchronous paradigms (i.e., no visual/auditory cues are used to guide the patients), since the use of cues reduces their amplitude (Savić et al., 2014), and they are more easily contaminated by motion artifacts (Castermans et al., 2014).

Consequently, further research should evaluate the response of BMIs relying on these correlates in the presence of artifacts.

Despite we conducted the simulations of the BMI in a pseudo-online fashion, it was still an offline analysis that does not allow capturing the possible artifacts or influences that can appear during a real-time use of this type of systems. Our results help understanding how to process the EEG datasets before calibrating a BMI for being used in closed-loop rehabilitation. However, during the closed-loop operation, artifacts also occur. Some of them, such as the EOG contaminations, can be effectively filtered in real-time, while for other types of artifacts, automatized procedures for removal are not sufficiently precise. Our approach assumed that having a clean training dataset is enough to appropriately model the activity that we want to detect, so that in real-time, muscle and motion artifacts do not bias the BMI performance. However, notice that it may also be possible to implement an online system that detects the artifacts, based on the same procedures we presented here, and completely stops the feedback when contaminations are detected. For instance, a real-time detector of compensatory movements with other limbs may stop the movement of the rehabilitative device in a BMI therapy when the patient activates muscles that should remain relaxed (Wright et al., 2014).

The BMI design that we used was rather simple in terms of the feature extraction and the classification algorithms. We estimated the spectral power of the alpha and beta frequencies with an auto-regressive model and used a linear discriminant analysis as a classifier. There are several studies investigating how to optimize the feature processing and the classification algorithms (Bashashati et al., 2007, 2015; Lotte et al., 2007; Brunner et al., 2011; López-Larraz et al., 2018b), and therefore, our approach may not be the best available method in terms of classification accuracy. Our motivation for using this design was based on our previous work (Ramos-Murguialday et al., 2013), which proved the BMI rehabilitation efficacy (coupled with physiotherapy) of the contingent association between ipsilesional activity and peripheral feedback during movement attempts in stroke patients. We hypothesize that more advanced BMI methodologies (e.g., common-spatial patterns (Blankertz et al., 2008; Sannelli et al., 2016)) may lead to higher global performances, but still would be sensitive to the presence of artifacts in the training datasets, and this might result in a poorer rehabilitation efficacy. However,

further research should be conducted to verify the response of other BMI designs with the presence or absence of artifacts in the data.

3.6 Acknowledgments

The authors thank all the people involved in the data recording for their hard work. This study was funded by the *f*ortüne-Program of the University of Tübingen (2422-0-0 and 2452-0-0), the Bundesministerium für Bildung und Forschung BMBF MOTORBIC (FKZ 13GW0053) and AMORSA (FKZ 16SV7754), the Deutsche Forschungsgemeinschaft (DFG), the Basque Government Science Program (EXOTEK: KK 2016/00083). The work of A. Insausti-Delgado was supported by the Basque Government's scholarship for predoctoral students.

3.7 Supplementary material

ID	Lesion volume	Lesion type	Lesion location
1	57931	C+S	FL, PL; PrG, PoG, CR.
2	345498	C+S	FL, PL, TL; SFG, MeFG, MFG, IFG, PrG, PoG, SMG, AG; MTG, ITG; CR, HCd, CIa, CIg, CIp, Pu, Th, EC, TCC, INS.
3	112440	C+S	FL, PL; SFG, MeFG, MFG, IFG, PrG, PoG.
4	158213	C+S	FL, PL, TL; IFG, PrG, PoG, MTG; CR, CIa, CIg, CIp, EC, Pu, Th.
5	235219	C+S	FL, PL, TL; MFG, IFG, PrG, PoG, SMG, AG; TCC, CR, Cd, Pu, CIa, CIg, CIp, Th, EC, INS.
6	83794	C+S	FL, PL, TL; SMG, PoG; HCd, CR, Pu, EC, CIa, CIg, CIp, Th, TCC, INS.
7	103584	C+S	FL, PL, TL; SFG, MeFG, MFG, IFG, PrG, PoG; CR, Th, Pu, CIg, CIp, EC, TCC.
8	30980	S	PL; PrG; CR, CIa, Pu, EC, Th, INS.
9	97903	C+S	FL, PL; MFG, IFG, PoG; CR, Cd, EC CIa, CIg, CIp, Th Pu, INS.
10	10373	S	CR, EC, Pu, ICp, Th.
11	19010	S	Cia, CIg, CIp, EC, Pu, HCd, Th.
12	134434	C+S	FL, PL, MFG, IFG, PrG, PoG, MTG.
13		C+S	FL, PL, TL; MFG, IFG, PrG, PoG, SMG, MTG, ITG; CR, HCd, CIa, CIg, CIp, EC, Pu, TCC, INS, Th.
14	115592	C+S	FL, PL, TL; IFG, PrG, PoG; CR, HCd, CIa, CIg, CIp, EC, Th, Pu, INS.
15		S	FL, PL; IFG, PrG, PoG, SMG; TCC, HCd, CR, Pu, EC, CIa, CIg, CIp, Th.
16	51050	S	CR, Cd, EC, Pu, CIa, CIg, INS.
17	140212	C+S	FL, PL, TL; MFG, IFG, PrG, PoG; CR, EC, Pu, INS.
18		S	FL, PL; IFG, PrG, CR, HCd, CIa, CIg, CIp, EC, Pu, Th, INS.

ID	Lesion volume	Lesion type	Lesion location
19	17194	S	CR, HCd, EC, CIa, CIg, CIp, Pu, Th.
20	4019	S	CR, EC, Th, Pu, CIa, CIg, CIp.
21	63848	S	FL, PL, TL; PoG, MTG, AG; CIa, CIg, CIp, Th, EC, Cd.
22	187586	C+S	FL, PL; SFG, MeFG, MFG, IFG, PrG; EC, Pu, INS.
23	82473	C+S	FL, PL; IFG, PrG; EC, CIa, CIg, CIp, HCd, Pu, Th, INS.
24	79827	C+S	FL, PL; PrG; CR, Th, Pu, CIp, EC, INS.
25	31769	S	CR, CIa, CIg, CIp, Th, EC, Pu, INS.
26	27977	S	CIa, CIg, CIp, EC, Pu, Th, HCd, CR, INS.
27	8838	S	HCd, CIa, CIg, CIp, Pu, Th, CR, EC.
28	103191	C+S	FL, PL, TL; IFG, PrG, PoG, SMG; CR, HCd, CIa, CIg, CIp, Pu, EC, Th, TCC, INS.
29	70449	C+S	FL, PL; IFG, PrG; EC, Pu, Th, CIa, CIg, CIp, INS.
30	17121	S	Hcd, CIa, CIg, CIp, EC, Pu, CR.
31	166160	C+S	FL, PL; SFG, MeFG, MFG, IFG, PrG, PoG, SMG; CR, HCd.

Lobes: FL – Frontal Lobe, PL – Parietal Lobe, TL – Temporal Lobe;

Gyrus: SFG – superior frontal, MeFG – medial frontal, MFG – midle frontal, IFG – inferior frontal, PrG – precentral, SMG – supramarginal, PoG – postcentral, AG – angular, MTG – midle temporal, ITG – inferior temporal;

Subcortical areas: HCd - head of caudate nucleus, CR – corona radiata, Pu – putamen, EC – external capsule, Th – thalamus, TCC – trunk of corpus callosum, Cd – caudate nucleus, GP – globus pallidus, INS – Insula.

Supplementary Table 3.1: Patients' details about the location of the stroke. Lesion volume is measured in voxels. Lesion type indicates if the stroke affected subcortical areas only (S) or cortical and subcortical areas (C+S). Lesion location details the areas affected by the stroke (abbreviations legend below).

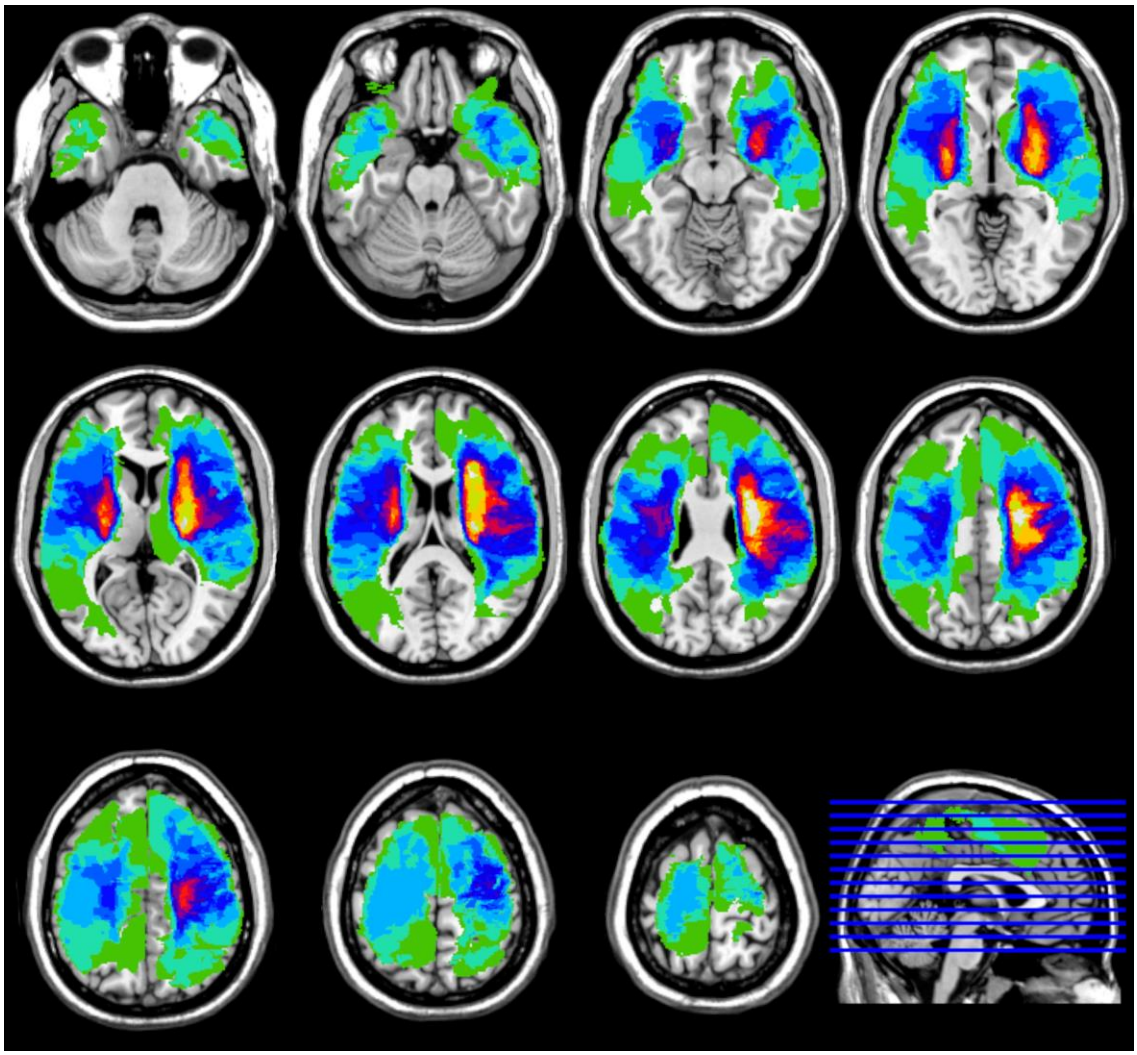

Supplementary Figure 3.1: MRI lesion masks showing the lesion location of the patients. Lesions are normalized and superimposed to the Collin Holmes 27 (ch2) template of the International Consortium for Brain Mapping (ICBM).

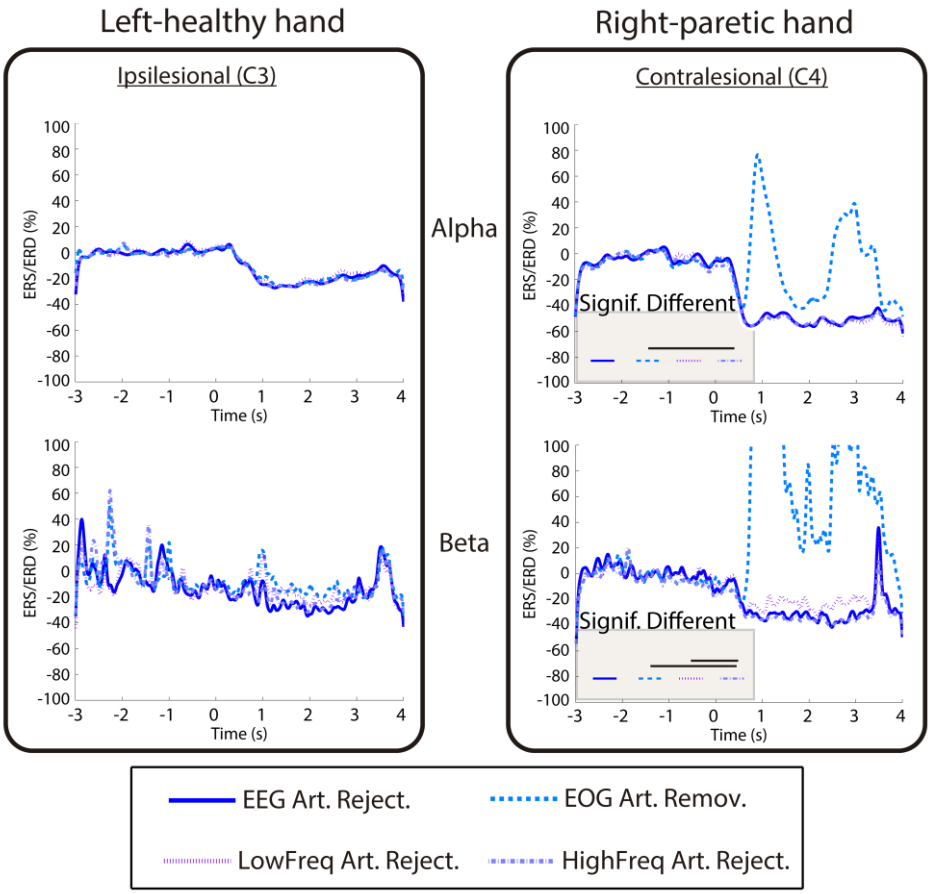

Supplementary Figure 3.2: Temporal evolvement of ERS/ERD in alpha (i.e., [7-13] Hz) and beta (i.e., [14-30] Hz) frequencies for the EEG artifact rejection, and for each of its components separately. Notice that the lateralized cortical positions of patients with the stroke in the right hemisphere are swapped, simulating that all the patients have the stroke in the left hemisphere. The percentage of ERS/ERD is calculated with respect to the resting baseline [-2.5, -1] s. The left panel corresponds to the movements of the healthy (left) hand, while the right panel corresponds to the attempts of movement of the paretic (right) hand. Within each panel, the activity of the ipsilateral hemisphere (i.e., ipsilesional for the healthy hand, and contralesional for the paretic hand) for alpha (upper row) and beta (bottom row) frequencies is included. Each plot shows the average ERD for each of the four methods, indicated by the different colors and types of line. The results of the statistical analyses are indicated in the shaded panel at the bottom-left of the plots. The presence of the "Signif. Different" panel indicates a significant effect of artifact rejection method on ERD magnitude (in the interval [0, 4] s), while the horizontal black lines between pairs indicate the pairs of methods with significantly different ERD after correction for multiple comparisons.

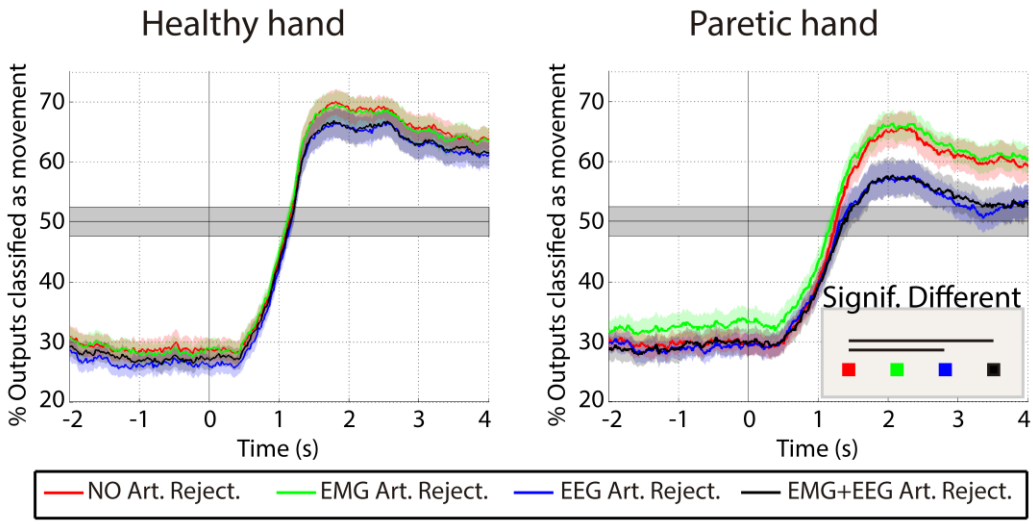

Supplementary Figure 3.3: Average performance with a non-linear classifier (SVM-based) for the healthy (left) and the paretic (right) hands with each of the four artifact processing methods. On each panel, the lines represent the percentage of classifier outputs identified as movement, averaged for all the patients, and the shades indicate the standard error of the mean. Notice that the values before t = 0 correspond to false positives, while the values after t = 0 correspond to true positives. The shaded gray area indicates the confidence interval of the chance level (alpha = 0.01), computed on the basis of all the test trials, according to (Müller-Putz et al., 2008). The results of the statistical analyses are indicated in the shaded panel at the bottom-right of the plots. The presence of the "Signif. Different" panel indicates a significant effect of artifact rejection method on the average BMI accuracy, while the horizontal black lines between pairs indicate the pairs of methods with significantly different accuracy after correction for multiple comparisons.

3.8 References

Ang, K. K., Chua, K. S. G., Phua, K. S., Wang, C., Chin, Z. Y., Kuah, C. W. K., et al. (2015). A randomized controlled trial of EEG-based motor imagery brain-computer interface robotic rehabilitation for stroke. *Clin. EEG Neurosci.* 46, 310–320. doi:10.1177/1550059414522229.

Antelis, J. M., Montesano, L., Ramos-Murguialday, A., Birbaumer, N., and Minguez, J. (2017). Decoding Upper Limb Movement Attempt from EEG Measurements of the Contralesional Motor Cortex in Chronic Stroke Patients. *IEEE Trans. Biomed. Eng.* 64, 99–111. doi:10.1109/TBME.2016.2541084.

Asín Prieto, G., Cano-de-la-Cuerda, R., López-Larraz, E., Metrot, J., Molinari, M., and van Dokkum, L. E. H. (2014). "Emerging perspectives in stroke rehabilitation," in

Emerging Therapies in Neurorehabilitation, eds. J. L. Pons and D. Torricelli (Berlin: Springer Berlin Heidelberg), 3–21. doi:10.1007/978-3-642-38556-8.

Bashashati, A., Fatourechi, M., Ward, R. K., and Birch, G. E. (2007). A survey of signal processing algorithms in brain-computer interfaces based on electrical brain signals. *J. Neural Eng.* 4, R32-57. doi:10.1088/1741-2560/4/2/R03.

Bashashati, H., Ward, R. K., Birch, G. E., and Bashashati, A. (2015). Comparing Different Classifiers in Sensory Motor Brain Computer Interfaces. *PLoS One* 10, e0129435. doi:10.1371/journal.pone.0129435.

Biasiucci, A., Leeb, R., Iturrate, I., Perdikis, S., Al-Khodairy, A., Corbet, T., et al. (2018). Brain-actuated functional electrical stimulation elicits lasting arm motor recovery after stroke. *Nat. Commun.* 9, 2421. doi:10.1038/s41467-018-04673-z.

Blankertz, B., Tomioka, R., and Lemm, S. (2008). Optimizing spatial filters for robust EEG single-trial analysis. *IEEE Signal Process. Mag.* 25, 41–56. doi:10.1109/MSP.2008.4408441.

Brunner, C., Billinger, M., Vidaurre, C., and Neuper, C. (2011). A comparison of univariate, vector, bilinear autoregressive, and band power features for brain-computer interfaces. *Med. Biol. Eng. Comput.* 49, 1337–46. doi:10.1007/s11517-011-0828-x.

Burg, J. P. (1975). Maximum Entropy Spectral Analysis. in *Proceedings of the 37th Annual International SEG Meeting*.

Castermans, T., Duvinage, M., Cheron, G., and Dutoit, T. (2014). About the cortical origin of the low-delta and high-gamma rhythms observed in EEG signals during treadmill walking. *Neurosci. Lett.* 561, 166–170.

Chaudhary, U., Birbaumer, N., and Ramos-Murguialday, A. (2016). Brain-computer interfaces for communication and rehabilitation. *Nat. Rev. Neurol.* 12, 513–525. doi:10.1038/nrneurol.2016.113.

Croft, R. J., and Barry, R. J. (2000). Removal of ocular artifact from the EEG: a review.

Neurophysiol. Clin. 30, 5–19. doi:10.1016/S0987-7053(00)00055-1.

Donati, A. R. C., Shokur, S., Morya, E., Campos, D. S. F., Moioli, R. C., Gitti, C. M., et al. (2016). Long-Term Training with a Brain-Machine Interface-Based Gait Protocol Induces Partial Neurological Recovery in Paraplegic Patients. *Sci. Rep.* 6, 1–16. doi:10.1038/srep30383.

Eduardo, L., Ray, A. M., Figueiredo, T. C., Bibi, C., Birbaumer, N., and Ramos-murguialday, A. (2017). Stroke lesion location influences the decoding of movement intention from EEG. 1–4.

Graimann, B., and Pfurtscheller, G. (2006). Chapter 6 Quantification and visualization of event-related changes in oscillatory brain activity in the time-frequency domain. *Prog. Brain Res.* 159, 79–97. doi:10.1016/S0079-6123(06)59006-5.

Grefkes, C., Nowak, D. A., Eickhoff, S. B., Dafotakis, M., Ku, J., Karbe, H., et al. (2008). Cortical connectivity after subcortical stroke assessed with functional magnetic resonance imaging. *Ann. Neurol.* 63, 236–246. doi:10.1002/ana.21228.

Hammond, D. C., and Gunkelman, J. (2001). *The art of artifacting*. Society for Neuronal Regulation.

Hjorth, B. (1975). An on-line transformation of EEG scalp potentials into orthogonal source derivations. *Electroencephalogr. Clin. Neurophysiol.* 39, 526–530. doi:10.1016/0013-4694(75)90056-5.

Hoffmann, U., Cho, W., Ramos-Murguialday, A., and Keller, T. (2011). Detection and removal of stimulation artifacts in electroencephalogram recordings. in *33rd Annual International Conference of the IEEE Engineering in Medicine and Biology Society*, 7159–7162. doi:10.1109/IEMBS.2011.6091809.

Hortal, E., Planelles, D., Resquin, F., Climent, J. M., Azorin, J. M., and Pons, J. L. (2015). Using a brain-machine interface to control a hybrid upper limb exoskeleton during rehabilitation of patients with neurological conditions. *J. Neuroeng. Rehabil.* 12, 92. doi:10.1186/s12984-015-0082-9.

Ibáñez, J., Monge-Pereira, E., Molina-Rueda, F., Serrano, J. I., del Castillo, M. D., Cuesta-Gómez, A., et al. (2017). Low latency estimation of motor intentions to assist reaching movements along multiple sessions in chronic stroke patients: A feasibility study. *Front. Neurosci.* 11, 1–12. doi:10.3389/fnins.2017.00126.

Ibáñez, J., Serrano, J. I., del Castillo, M. D., Monge-Pereira, E., Molina-Rueda, F., Alguacil-Diego, I., et al. (2014). Detection of the onset of upper-limb movements based on the combined analysis of changes in the sensorimotor rhythms and slow cortical potentials. *J. Neural Eng.* 11, 056009. doi:10.1088/1741-2560/11/5/056009.

Insausti-Delgado, A., López-Larraz, E., Bibián, C., Nishimura, Y., Birbaumer, N., and Ramos-Murguialday, A. (2017). Influence of trans-spinal magnetic stimulation in electrophysiological recordings for closed-loop rehabilitative systems. in *39th Annual International Conference of the IEEE Engineering in Medicine and Biology Society (EMBC)*, 2518–2521. doi:10.1109/EMBC.2017.8037369.

Jackson, A., and Zimmermann, J. B. (2012). Neural interfaces for the brain and spinal cord—restoring motor function. *Nat. Rev. Neurol.* 8, 690–699. doi:10.1038/nrneurol.2012.219.

Kaiser, V., Daly, I., Pichiorri, F., Mattia, D., Müller-Putz, G. R., and Neuper, C. (2012). Relationship between electrical brain responses to motor imagery and motor impairment in stroke. *Stroke* 43, 2735–2740. doi:10.1161/STROKEAHA.112.665489.

Klados, M. A., Papadelis, C. L., and Bamidis, P. D. (2009). REG-ICA: A new hybrid method for EOG artifact rejection. in *Final Program and Abstract Book - 9th International Conference on Information Technology and Applications in Biomedicine, ITAB 2009* doi:10.1109/ITAB.2009.5394295.

Kline, J. E., Huang, H. J., Snyder, K. L., and Ferris, D. P. (2015). Isolating gait-related movement artifacts in electroencephalography during human walking. *J. Neural Eng.* 12, 046022. doi:10.1088/1741-2560/12/4/046022.

Kobler, R. J., Sburlea, A. I., and Müller-Putz, G. R. (2017). A comparison of ocular

artifact removal methods for block design based electroencephalography experiments. in *Proceedings of the 7th Graz Brain-Computer Interface Conference*, 236–241. doi:10.3217/978-3-85125-533-1-44.

Lebedev, M. A., and Nicolelis, M. A. L. (2017). Brain-Machine Interfaces: From Basic Science to Neuroprostheses and Neurorehabilitation. *Physiol. Rev.* 97, 767–837. doi:10.1152/physrev.00027.2016.

López-Larraz, E., Bibián, C., Birbaumer, N., and Ramos-Murguialday, A. (2017). Influence of artifacts on movement intention decoding from EEG activity in severely paralyzed stroke patients. in *15th International Conference on Rehabilitation Robotics (ICORR)*, 901–906. doi:10.1109/ICORR.2017.8009363.

López-Larraz, E., Figueiredo, T. C., Insausti-Delgado, A., Ziemann, U., Birbaumer, N., and Ramos-Murguialday, A. (2018a). Event-related desynchronization during movement attempt and execution in severely paralyzed stroke patients: an artifact removal relevance analysis. *NeuroImage Clin.* 20, 972–986. doi:10.1016/j.nicl.2018.09.035.

López-Larraz, E., Ibáñez, J., Trincado-Alonso, F., Monge-Pereira, E., Pons, J. L., and Montesano, L. (2018b). Comparing Recalibration Strategies for Electroencephalography-Based Decoders of Movement Intention in Neurological Patients with Motor Disability. *Int. J. Neural Syst.* 28, 1750060. doi:10.1142/S0129065717500605.

López-Larraz, E., Montesano, L., Gil-Agudo, Á., and Minguez, J. (2014). Continuous decoding of movement intention of upper limb self-initiated analytic movements from pre-movement EEG correlates. *J. Neuroeng. Rehabil.* 11, 153. doi:10.1186/1743-0003-11-153.

López-Larraz, E., Montesano, L., Gil-Agudo, Á., Minguez, J., and Oliviero, A. (2015). Evolution of EEG motor rhythms after spinal cord injury: A longitudinal study. *PLoS One* 10, e0131759. doi:10.1371/journal.pone.0131759.

López-Larraz, E., Sarasola-Sanz, A., Irastorza-Landa, N., Birbaumer, N., and Ramos-

Murguialday, A. (2018c). Brain-machine interfaces for rehabilitation in stroke: A review. *NeuroRehabilitation* 43, 77–97. doi:10.3233/NRE-172394.

López-Larraz, E., Trincado-Alonso, F., Rajasekaran, V., Pérez-Nombela, S., Del-Ama, A. J., Aranda, J., et al. (2016). Control of an ambulatory exoskeleton with a brain-machine interface for spinal cord injury gait rehabilitation. *Front. Neurosci.* 10. doi:10.3389/fnins.2016.00359.

Lotte, F., Congedo, M., Lécuyer, A., Lamarche, F., and Arnaldi, B. (2007). A review of classification algorithms for EEG-based brain-computer interfaces. *J. Neural Eng.* 4, R1–R13. doi:10.1088/1741-2560/4/2/R01.

Luft, A. R., Waller, S., Forrester, L., Smith, G. V., Whitall, J., Macko, R. F., et al. (2004). Lesion location alters brain activation in chronically impaired stroke survivors. *Neuroimage* 21, 924–935. doi:10.1016/j.neuroimage.2003.10.026.

Mrachacz-Kersting, N., Jiang, N., Stevenson, A. J. T., Niazi, I. K., Kostic, V., Pavlovic, A., et al. (2016). Efficient neuroplasticity induction in chronic stroke patients by an associative brain-computer interface. *J. Neurophysiol.* 115, 1410–1421. doi:10.1152/jn.00918.2015.

Mrachacz-Kersting, N., Kristensen, S. R., Niazi, I. K., and Farina, D. (2012). Precise temporal association between cortical potentials evoked by motor imagination and afference induces cortical plasticity. *J. Physiol.* 590, 1669–82. doi:10.1113/jphysiol.2011.222851.

Müller-Putz, G., Scherer, R., Brunner, C., Leeb, R., and Pfurtscheller, G. (2008). Better than random: A closer look on BCI results. *Int. J. Bioelectromagn.* 10, 52–55.

Muthukumaraswamy, S. (2013). High-frequency brain activity and muscle artifacts in MEG/EEG: a review and recommendations. *Front. Hum. Neurosci.* 7, 138.

Nolan, H., Whelan, R., and Reilly, R. B. (2010). FASTER: Fully Automated Statistical Thresholding for EEG artifact Rejection. *J. Neurosci. Methods* 192, 152–162. doi:10.1016/j.jneumeth.2010.07.015.

Nunez, P. L., and Srinivasan, R. (2006). *Electric Fields of the Brain*. doi:10.1093/acprof:oso/9780195050387.001.0001.

Ono, T., Shindo, K., Kawashima, K., Ota, N., Ito, M., Ota, T., et al. (2014). Brain-computer interface with somatosensory feedback improves functional recovery from severe hemiplegia due to chronic stroke. *Front. Neuroeng.* 7, 19. doi:10.3389/fneng.2014.00019.

Park, W., Kwon, G. H., Kim, Y., Lee, J., and Kim, L. (2016). EEG response varies with lesion location in patients with chronic stroke. *J. Neuroeng. Rehabil.* 13, 21. doi:10.1186/s12984-016-0120-2.

Pereira, J., Ofner, P., Schwarz, A., Sburlea, A. I., and Müller-Putz, G. R. (2017). EEG neural correlates of goal-directed movement intention. *Neuroimage* 149, 129–140. doi:10.1016/j.neuroimage.2017.01.030.

Pfurtscheller, G., and Lopes da Silva, F. H. (1999). Event-related EEG/MEG synchronization and desynchronization: basic principles. *Clin. Neurophysiol.* 110, 1842–1857. doi:10.1016/S1388-2457(99)00141-8.

Pichiorri, F., Morone, G., Petti, M., Toppi, J., Pisotta, I., Molinari, M., et al. (2015). Brain-computer interface boosts motor imagery practice during stroke recovery. *Ann. Neurol.* 77, 851–865. doi:10.1002/ana.24390.

Pineda, J. A., Allison, B. Z., and Vankov, A. (2000). The effects of self-movement, observation, and imagination on μ rhythms and readiness potentials (RP's): Toward a brain-computer interface (BCI). *IEEE Trans. Rehabil. Eng.* 8, 219–222. doi:10.1109/86.847822.

Pontifex, M. B., Gwizdala, K. L., Parks, A. C., Billinger, M., and Brunner, C. (2016). Variability of ICA decomposition may impact EEG signals when used to remove eyeblink artifacts. *Psychophysiology* 54, 386–398. doi:10.1111/psyp.12804.

Ramos-Murguialday, A., and Birbaumer, N. (2015). Brain oscillatory signatures of motor tasks. *J. Neurophysiol.* 113, 3663–3682. doi:10.1152/jn.00467.2013.

Ramos-Murguialday, A., Broetz, D., Rea, M., Läer, L., Yilmaz, Ö., Brasil, F. L., et al. (2013). Brain-machine interface in chronic stroke rehabilitation: A controlled study. *Ann. Neurol.* 74, 100–108. doi:10.1002/ana.23879.

Ramos-Murguialday, A., Schürholz, M., Caggiano, V., Wildgruber, M., Caria, A., Hammer, E. M., et al. (2012). Proprioceptive Feedback and Brain Computer Interface (BCI) Based Neuroprostheses. *PLoS One* 7, e47048. doi:10.1371/journal.pone.0047048.

Ramos-Murguialday, A., Soares, E., and Birbaumer, N. (2010). Upper limb EMG artifact rejection in motor sensitive BCIs. in *32nd Annual International Conference of the IEEE Engineering in Medicine and Biology Society (EMBC)*, 1–6. doi:10.1109/IEMBS.2010.5735240.

Ray, A. M., López-Larraz, E., Figueiredo, T. C., Birbaumer, N., and Ramos-Murguialday, A. (2017). Movement-related brain oscillations vary with lesion location in severely paralyzed chronic stroke patients. in *39th Annual International Conference of the IEEE Engineering in Medicine and Biology Society (EMBC)*, 1664–1667. doi:10.1109/EMBC.2017.8037160.

Rehme, A. K., Eickhoff, S. B., Wang, L. E., Fink, G. R., and Grefkes, C. (2011). Dynamic causal modeling of cortical activity from the acute to the chronic stage after stroke. *Neuroimage* 55, 1147–1158. doi:10.1016/j.neuroimage.2011.01.014.

Sannelli, C., Vidaurre, C., Müller, K.-R., and Blankertz, B. (2016). Ensembles of adaptive spatial filters increase BCI performance: an online evaluation. *J. Neural Eng.* 13, 046003. doi:10.1088/1741-2560/13/4/046003.

Savić, A., Lontis, R., Jiang, N., Popović, M., Farina, D., Dremstrup, K., et al. (2014). "Movement related cortical potentials and sensory motor rhythms during self initiated and cued movements," in *Replace, Repair, Restore, Relieve-Bridging Clinical and Engineering Solutions in Neurorehabilitation* Biosystems & Biorobotics., eds. W. Jensen, O. K. Andersen, and M. Akay (Springer International Publishing), 701–707. doi:10.1007/978-3-319-08072-7.

Schlögl, A., Keinrath, C., Zimmermann, D., Scherer, R., Leeb, R., and Pfurtscheller, G. (2007). A fully automated correction method of EOG artifacts in EEG recordings. *Clin. Neurophysiol.* 118, 98–104. doi:10.1016/j.clinph.2006.09.003.

Schwarz, A., Ofner, P., Pereira, J., Sburlea, A. I., and Müller-Putz, G. R. (2018). Decoding natural reach-and-grasp actions from human EEG. *J. Neural Eng.* 15, 016005. doi:10.1088/1741-2552/aa8911.

Seeber, M., Scherer, R., and Muller-Putz, G. R. (2016). EEG Oscillations Are Modulated in Different Behavior-Related Networks during Rhythmic Finger Movements. *J. Neurosci.* 36, 11671–11681. doi:10.1523/JNEUROSCI.1739-16.2016.

Shiman, F., López-Larraz, E., Sarasola-Sanz, A., Irastorza-Landa, N., Spueler, M., Birbaumer, N., et al. (2017). Classification of different reaching movements from the same limb using EEG. *J. Neural Eng.* 14, 046018. doi:10.1088/1741-2552/aa70d2.

Stępień, M., Conradi, J., Waterstraat, G., Hohlefeld, F. U., Curio, G., and Nikulin, V. V (2011). Event-related desynchronization of sensorimotor EEG rhythms in hemiparetic patients with acute stroke. *Neurosci. Lett.* 488, 17–21.

Tallon-Baudry, C., Bertrand, O., Delpuech, C., and Permier, J. (1997). Oscillatory gamma-band (30-70 Hz) activity induced by a visual search task in humans. *J. Neurosci.* 17, 722–734. doi:10.1007/s11064-011-0538-7.

Tangwiriyasakul, C., Mocioiu, V., van Putten, M. J. a M., and Rutten, W. L. C. (2014a). Classification of motor imagery performance in acute stroke. *J. Neural Eng.* 11, 036001. doi:10.1088/1741-2560/11/3/036001.

Tangwiriyasakul, C., Verhagen, R., Rutten, W. L. C., and van Putten, M. J. A. M. (2014b). Temporal evolution of event-related desynchronization in acute stroke: A pilot study. *Clin. Neurophysiol.* 125, 1112–1120. doi:10.1016/j.clinph.2013.10.047.

Trincado-Alonso, F., López-Larraz, E., Resquín, F., Ardanza, A., Pérez-Nombela, S., Pons, J. L., et al. (2017). A Pilot Study of Brain-Triggered Electrical Stimulation

with Visual Feedback in Patients with Incomplete Spinal Cord Injury. *J. Med. Biol. Eng.* 38, 790–803. doi:10.1007/s40846-017-0343-0.

Urigüen, J. A., and Garcia-Zapirain, B. (2015). EEG artifact removal—state-of-the-art and guidelines. *J. Neural Eng.* 12, 031001. doi:10.1088/1741-2560/12/3/031001.

Velu, P. D., and de Sa, V. R. (2013). Single-trial classification of gait and point movement preparation from human EEG. *Front. Neurosci.* 7, 84. doi:10.3389/fnins.2013.00084.

Wagner, J., Makeig, S., Gola, M., Neuper, C., and Müller-Putz, G. (2016). Distinct beta band oscillatory networks subserving motor and cognitive control during gait adaptation. *J. Neurosci.* 36, 2212–2226. doi:10.1523/JNEUROSCI.3543-15.2016.

Walter, A., Ramos Murguialday, A., Spüler, M., Naros, G., Leão, M. T., Gharabaghi, A., et al. (2012). Coupling BCI and cortical stimulation for brain-state-dependent stimulation: methods for spectral estimation in the presence of stimulation after-effects. *Front. Neural Circuits* 6, 87. doi:10.3389/fncir.2012.00087.

Ward, N. S., Brown, M. M., Thompson, A. J., and Frackowiak, R. S. J. (2003). Neural correlates of outcome after stroke: A cross-sectional fMRI study. *Brain* 126, 1430–1448. doi:10.1093/brain/awg145.

Wright, Z. A., Rymer, W. Z., and Slutzky, M. W. (2014). Reducing abnormal muscle coactivation after stroke using a myoelectric-computer interface: A pilot study. *Neurorehabil. Neural Repair* 28, 443–451. doi:10.1177/1545968313517751.

Yilmaz, O., Birbaumer, N., and Ramos-Murguialday, A. (2015). Movement related slow cortical potentials in severely paralyzed chronic stroke patients. *Front. Hum. Neurosci.* 8, 1–8. doi:10.3389/fnhum.2014.01033.

4. Chapter 4: Intensity and dose of neuromuscular electrical stimulation influence sensorimotor cortical excitability

This manuscript has been published as (Insausti-Delgado et al., 2021).

4.1 Abstract

Neuromuscular electrical stimulation (NMES) of the nervous system has been extensively used in neurorehabilitation due to its capacity to engage the muscle fibers, improving muscle tone, and the neural pathways, sending afferent volleys towards the brain. Although different neuroimaging tools suggested the capability of NMES to regulate the excitability of sensorimotor cortex and corticospinal circuits, to date how intensity and dose of NMES can neuromodulate the brain oscillatory activity measured with electroencephalography (EEG) is unknown. We quantified the effect of NMES parameters on brain oscillatory activity of twelve healthy participants who underwent stimulation of wrist extensors during rest. Three different NMES intensities were included, two below and one above the individual motor threshold, fixing the stimulation frequency to 35 Hz and the pulse width to 300 μs. Firstly, we efficiently removed stimulation artifacts from the EEG recordings. Secondly, we analyzed the effect of amplitude and dose on the sensorimotor oscillatory activity. On the one hand, we observed a significant NMES intensity-dependent modulation of brain activity, demonstrating the direct effect of afferent receptors recruitment. On the other hand, we described a significant NMES intensity-dependent dose-effect on sensorimotor activity modulation over time, with below-motor-threshold intensities causing cortical inhibition and above-motor-threshold intensities causing cortical facilitation. Our results highlight the relevance of intensity and dose of NMES, and show that these parameters can influence the recruitment of the sensorimotor pathways from the muscle to the brain, which should be carefully considered for the design of novel neuromodulation interventions based on NMES.

4.2 Introduction

Neuromuscular electrical stimulation (NMES) is an electrophysiological technique that consists of applying electrical currents on the skin to depolarize motor and sensory nerves beneath the stimulating electrodes (Bergquist et al., 2011). NMES has been used as a neuroscientific tool to study sensorimotor neural mechanisms from the muscles or peripheral sensory receptors (mechanoreceptors, nociceptors, etc.) to the spine and brain (Collins, 2007; Carson and Buick, 2019). NMES has also been utilized as a neurorehabilitative tool to reduce muscle atrophy, and to improve muscle tone and motor function in patients with paralysis after stroke (Knutson et al., 2015; Yang et al., 2019) or spinal cord injury (SCI) (Patil et al., 2015). The working principle of rehabilitative NMES is based on: 1) the direct effect on muscle tone; and 2) the activation of receptors and sensory axons that send afferent volleys to the sensorimotor cortex, after being processed by spinal networks and subcortical structures.

Numerous studies using functional magnetic resonance imaging (fMRI) and near-infrared spectroscopy (NIRS) have investigated the activity produced by NMES in different brain structures (Kampe et al., 2000; Blickenstorfer et al., 2009; Iftime-Nielsen et al., 2012; Schürholz et al., 2012; Wegrzyk et al., 2017). These works demonstrated that the brain activity is proportionally increased with the applied stimulation intensity (Backes et al., 2000; Smith et al., 2003; Schürholz et al., 2012). Recent experiments have also shown that peripheral stimulation can modulate corticospinal excitability, measured by motor evoked potentials (MEP) (Chipchase et al., 2011; Veldman et al., 2014). As the stimulation intensity increases, there is a progressive recruitment of more afferent receptors (i.e., cutaneous mechanoreceptors, muscle spindles and Golgi tendon organs) that modulate spinal and cortical circuits to a different extent (Maffiuletti et al., 2008; Bergquist et al., 2011; Golaszewski et al., 2012). It has been proven that the afference provided by muscle spindles and Golgi tendon organs due to muscle contraction travels through the spinal cord to the somatosensory cortex and can directly project to the motor cortex (Carson and Buick, 2019). Therefore, the presence or absence of muscle contraction elicited by NMES has a direct impact on somatosensory cortex, and indirectly, on motor cortex excitability (Sasaki et al., 2017). The neural excitability

depends on the modulation of nervous structures, such as spinal networks, involved in the afferent transmission from the stimulated muscle to the brain.

Although the effect of intensity on cortical activation and corticospinal excitability has been investigated, the dose or energy of the stimulation has not attracted much attention and might play a pivotal role in modulating activity of sensory regions. There is evidence showing that the number of peripheral stimulation pulses (i.e., dose) over time and the inter-pulse interval influence ongoing neural oscillations and have a neuromodulatory effect on the somatosensory cortex affecting indirectly corticospinal connectivity (Nitsche and Paulus, 2000; Schaworonkow et al., 2018; Zrenner et al., 2018). The nervous system maintains its excitability within an equilibrium range through adjustments derived from the history of neuronal activity, preventing excessive inhibition or facilitation (Pozo and Goda, 2010). Prolonged periods of stimulation-induced excitability/inhibition have been shown to activate homeostatic plasticity mechanisms that drive the system towards a more inhibited/excited state, reducing the effects of the stimulation (Gamboa et al., 2010; Andrews et al., 2013). Further, a progressive perceptual adaptation (or reduction of sensory responsiveness) has been evidenced after prolonged intervals of peripheral vibrotactile and electrocutaneous stimulation (Leung et al., 2005; Buma et al., 2007; Graczyk et al., 2018), indicating a neural compensation after a perturbation of the oscillatory neural system. Therefore, it could be conceivable that prolonged periods of NMES result in changes of neural excitability, resulting in a rebalance of the cortical response along time.

Although most of the studies so far have used fMRI and NIRS to track slow brain correlates, or TMS-induced MEPs to asses corticospinal excitability, electroencephalography (EEG) is a powerful neuroimaging technique with high temporal resolution that has been used to study sensorimotor processes (including sensory evoked potentials and rhythms) (Birbaumer et al., 1990; Buzsaki, 2006; Shibasaki and Hallett, 2006; Leodori et al., 2019). The sensorimotor oscillations that mainly comprise the rolandic alpha [(7–13) Hz] and beta [(14–30) Hz] rhythms rhythms, have been thoroughly used to study cortical involvement during sensorimotor tasks (Ramos-Murguialday and Birbaumer, 2015; López-Larraz et al., 2018a), being quantified as the event-related (de)synchronization (ERD/ERS) (Pfurtscheller and Lopes da Silva, 1999). Furthermore,

it has also been used as a feature for neuromodulation of sensorimotor neural network via proprioception and haptics (Ray et al., 2020; Sebastián-Romagosa et al., 2020). To date, only a few studies have reported how oscillatory activity measured with EEG is modulated by NMES (Vidaurre et al., 2016, 2019; Tu-Chan et al., 2017; Corbet et al., 2018). Understanding this process is of great importance given the relevance of EEG and NMES for neurorehabilitation, especially for EEG-based neural interfaces. It is important to note that, although the neural response can be directly influenced by every stimulation parameter (e.g., frequency, pulse width, pulse waveform), we focused on investigating the influence of intensity and dose of stimulation, since these are the parameters that are usually personalized for each patient.

In this work, we acquired EEG activity from 12 healthy participants during NMES of the wrist extensor muscles at three different intensities (two below and one above the motor threshold) to investigate the neuromodulatory effect of peripheral stimulation on the ongoing cortical oscillatory activity, while the subjects rested in a comfortable sitting position. Firstly, we wanted to confirm that as the intensity increases, there is a proportional neural excitation, probably resulting from the recruitment of more afferent fibers, which provide a greater projection of afferent volleys to the sensory cortex. Secondly, we wanted to assess if the dose of stimulation has an effect on the magnitude of neural excitation over time, expecting that after the stimulation has been provided during a prolonged time, the cortical responsiveness is lower.

4.3 Materials and methods

4.3.1 Participants

Twelve right-handed healthy participants (four females, age = 27.5±3.0 years, height = 176.3±8.6 cm, weight = 69.8±9.8 kg) were recruited to participate in the study. All of them signed an informed consent form. The experimental procedure was approved by the Ethics Committee of the Faculty of Medicine of the University of Tübingen (Germany).

Participants were asked to stay comfortably seated on a chair with their right arm resting on a side table and the hand hanging with the palm facing downwards. Neuromuscular electrical stimulation (NMES) electrodes were placed on the right-hand extensors (more detailed description in section 4.3.4), as described in **¡Error! No se encuentra el origen de la referencia.**Figure 4.1a. Electroencephalography (EEG) and muscle activity of two sensors were recorded during the experiment. The electrical artifact recorded from the muscle sensors was used to align stimulation onset during the EEG signal processing.

4.3.2 Experimental design and procedure

The main purpose of the experiment was to investigate NMES neuromodulatory effects (instantaneous and cumulative) on brain oscillatory activity. With this aim, we compared the afferent cortical activity generated by 3 different NMES intensities. Participants were passively stimulated, meaning that they were resting, and no volitional motor command was generated during stimulation. Each participant underwent one session consisting of 9 blocks, each comprising 18 trials. One of the three NMES intensities was randomly assigned to each block (determination of the current intensities explained in the section 4.3.4), resulting in 3 blocks per intensity. A Ready cue was presented 2.6 to 3 seconds before the NMES interval, which had a random duration between 3.4 and 3.8 seconds. From the offset of the NMES to the next Ready cue, a 3-second inter-trial period was introduced (see Figure 4.1b). Auditory cues announced the beginning of each interval. The time between blocks was used as breaks, lasting around 150 s (i.e., two and a half minutes). The entire session including setup did not exceed 90 minutes.

4.3.3 Data acquisition

The electroencephalographic (EEG) activity was recorded with a commercial 32-channel Acticap system (BrainProducts GmbH, Germany) and a monopolar BrainAmp amplifier (BrainProducts GmbH, Germany). The recording electrodes were placed at FP1, FP2, F7, F3, Fz, F4, F8, FC3, FC1, FCz, FC2, FC4, C5, C3, C1, Cz, C2, C4, C6, CP5, CP3, CP1, CPz, CP2, CP4, CP6, P7, P3, P4, P8, O1, and O2, following the

international 10/20 system. Ground and reference electrodes were placed at AFz and Pz, respectively.

Muscle activity of the right forearm of the participants was recorded by an MR-compatible BrainAmp amplifier (BrainProducts GmbH, Germany) using two Ag/AgCl bipolar sensors (Myotronics-Noromed, Tukwila, Wa, USA). The sensors were placed laterally to the stimulation pads (see Figure 4.1a), using the right collarbone as ground. Both EEG and muscle activity were synchronously acquired at a sampling rate of 1000 Hz.

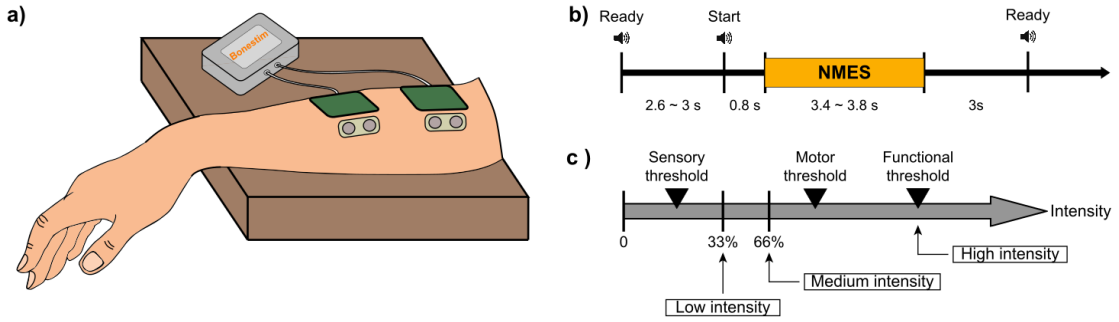

Figure 4.1: Experimental design and procedure. (a) Representation of the location of stimulation electrodes and sensors to measure muscle activity placed on right wrist extensors. (b) Timeline of the 3 phases included in each trial: preparation, NMES and inter-trial period. (c) Determination of NMES intensities: low intensity as one third between the sensory threshold and motor threshold, medium intensity as two thirds between the sensory threshold and motor threshold, and high intensity as functional motor threshold.

4.3.4 Neuromuscular electrical stimulation (NMES)

A programmable neuromuscular stimulator Bonestim (Tecnalia, Serbia) was used to deliver the stimulation. The cathode (3x3.5 cm, self-adhesive electrode) was placed over the muscles involved in wrist extension (*extensor digitorum* and *extensor carpi ulnaris)*, at one third of the distance between the lateral epicondyle of the humerus and the Lister's tubercle at the wrist. The anode (5x5 cm, self-adhesive electrode) was placed 5 cm distal to the cathode. To ensure the correct location of the electrodes, individually determined for each participant, stimulation above the motor threshold was applied until a complete wrist extension was induced.

The frequency of the NMES was set to 35 Hz, and the pulse width to 300 μs (Lynch and Popovic, 2008). The individual intensities for each subject were obtained by a scan of currents, starting at 1 mA and increasing in steps of 1 mA. The participants were asked to report the initiation of the following sensations: *(i)* tingling of the forearm (i.e., sensory threshold—STh), *(ii)* twitching of the fingers (i.e., motor threshold—MTh), and *(iii)* complete extension of the wrist (i.e., functional threshold—FTh). According to these thresholds, the three NMES intensities (two below and one above the motor threshold) were calculated, following the equations defined in the study of Smith and colleagues (Smith et al., 2003). Low intensity was defined as one third between the STh and MTh; medium intensity as two thirds between the STh and MTh; and high intensity as the FTh (see Equations 1, 2 and 3 and Figure 4.1c). These intensities were kept constant throughout the experiment and the complete extension of the wrist induced by functional stimulation was visually verified. None of the participants reported pain or any harmful effect due to the stimulation.

$$[Eq.1]\ Low\ intensity = (MTh - STh) \times 0.33 + STh$$
$$[Eq.2]\ Medium\ intensity = (MTh - STh) \times 0.66 + STh$$
$$[Eq.3]\ High\ intensity = FTh$$

4.3.5 Data preprocessing and analysis

Artifact removal procedures

One important limitation for the quantification of EEG activity during continuous stimulation is the contamination of the signals due to the electrical currents delivered to the body. The EEG is easily polluted by these currents, and artifact removal methodologies are essential to properly estimate cortical activation. With this aim, different techniques for contamination removal in invasive and non-invasive brain activity recordings have been proposed, such as interpolation, blanking or linear regression reference (LRR) (Walter et al., 2012a; Iturrate et al., 2018; Young et al., 2018). Blanking of the data is the most restrictive method as contaminated data are rejected and signals that could be of interest are neglected for further analysis. However, if the removal is implemented using hardware, the artifact has less influence on the recovery period of

the amplifier preventing it from being saturated and allows the use of other methods to compensate for the missing data (Kent and Grill, 2012). Another approach is to linearly interpolate the corrupted data, connecting the last point before the artifact and the first point after the artifact. However, interpolation induces a bias in the estimation of power spectrum of the signals (Walter et al., 2012a). LRR re-references the signals through weights that are assigned to each channel. The weights are calculated in a training block according to the noise of each channel generated by the electrical stimulation. This method effectively reduces artifacts, but it fixes the weights and assumes no changes in channel noise during the intervention. So far, the feasibility of this method has only been proven in invasive recordings (Young et al., 2018), in which impedances are less likely to change within sessions and are more similar among channels (Ball et al., 2009). Normally, impedances deteriorate and noise-influence increases throughout an EEG session complicating the implementation of LRR in non-invasive recordings of brain activity. Therefore, we implemented an alternative two-step artifact removal method and demonstrated its feasibility. The raw EEG signals were pre-processed using custom-developed scripts in Matlab (MathWorks, Natick, MA, USA).

Channel removal based on power-line noise

During an EEG session, particularly during setup and during periods between experimental blocks, special care is required to maintain EEG signal clean (i.e., raw data inspection and impedance check). However, our empirical experience shows that, sometimes, certain EEG electrodes present higher contamination due to the stimulation than others (see Figure 4.2a). These electrodes present broadband artifacts that impede further analyses even after applying the median filter preprocessing described below. We hypothesized that this effect might be due to degraded impedances, which occasionally deteriorate even when during the setup were set below 5 kOhm. Despite we did not store the impedances of each electrode to check this and discard the electrodes with high impedance, we ideated an automatized method to detect and discard them offline. This way, we could automatically eliminate contaminated channels without the human bias that would constitute a manual rejection.

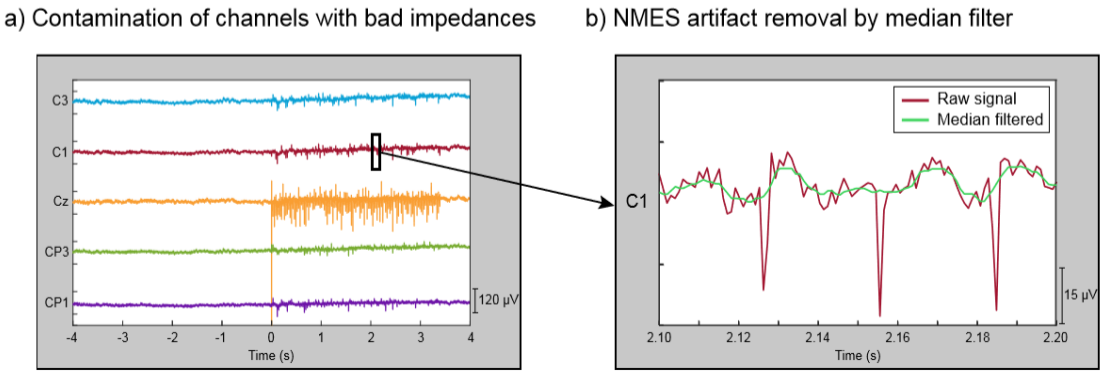

Figure 4.2: Characterization of contamination induced by NMES. (a) EEG of a representative trial showing non-contaminated channels (C3, C1, CP3, CP1) and one contaminated channel (Cz) during high intensity stimulation. Channels with bad impedances are more prone to be contaminated by electrical stimulation. (b) Zoom in 100 ms segment of a representative EEG trial in a non-contaminated channel that presents NMES artifacts (red line). The effect of stimulation artifacts is minimized by median filter (green line).

Having high impedance between the recording electrode and the skin resembles an open circuit, where the electrode behaves like an antenna and captures outside electric frequencies (like the power-line noise). Our method exploits this effect and identifies the EEG electrodes with unusually high power-line noise (50 Hz in Europe). Since all the electrodes should be approximately equally exposed to electromagnetic signals at 50 Hz, we assume that very high power at this frequency is an indirect indicator of high skin-electrode impedance. The procedure was applied block-wise, meaning that it was used to detect and remove contaminated channels within each individual EEG block. The EEG activity was high-pass filtered at 0.1 Hz with a 4th order Butterworth. The power spectral distribution at 48-52 Hz was estimated using Welch's method, averaging the periodogram of 1-second Hamming windows with 50% overlapping. The power mean and standard deviation (SD) of all the EEG channels were calculated from all trials in each block. Channels whose power was higher than 4 SD above the mean were discarded from that specific block. The remaining channels were used to re-compute the mean and SD. The procedure was iteratively repeated until no channels exceeded the rejection threshold (see Figure 4.3 dashed box, Supplementary Figure 4.1, Supplementary Figure 4.2 and Supplementary Table 4.1).

Median filtering for removal of electrical stimulation contamination

It is well known that applying electromagnetic currents to stimulate the neural system can introduce undesired noise to the recordings. The NMES configuration used

in this study introduces large peaks of short latency (~5 ms) to the recorded EEG signal. Therefore, median filtering was used to minimize the NMES induced artifacts (Insausti-Delgado et al., 2017). This filter is suited to eliminate high-amplitude peaks from a time series (Gallagher and Wise, 1981), and can remove the short-latency high-amplitude artifacts caused by the NMES. A sliding window of 10 ms was applied to the EEG signal in steps of one sample, providing as output the median value of each window. We selected a 10 ms window as it fully covers the electrical artifact. This filter produces a frequency-dependent attenuation that follows an exponential function from 0 to 100 Hz (i.e., the frequency with a period that completely fits within the 10 ms window), leading to low attenuation at low frequencies and a complete attenuation at 100 Hz (Supplementary Figure 4.3). With this window size, the attenuation of the signal at 10 Hz, 20 Hz and 30 Hz is 1.28%, 4.89% and 10.90%, respectively. The relatively low attenuation at low frequencies makes this method suitable for analyzing alpha and beta sensorimotor oscillations. Figure 4.2b displays a zoomed segment of 100 ms of activity, showing the effect of the median filter on the stimulation artifacts.

4.3.6 Quantification of brain oscillatory activity

A common average reference (CAR) was applied to the EEG signals. The re-referenced signals were band-pass filtered at 0.1-45 Hz using a 1st order Butterworth filter. Each block was trimmed down to (18 x) 8-second trials, from -4 seconds to +4 seconds, being 0 the beginning of the stimulation. The trials were down sampled at 100 Hz, and those belonging to the same level of NMES intensity were pooled together.

The quantification of cortical activity was performed by evaluating the spectrum differences of the sensorimotor rhythms, by means of the alpha and beta event-related (de)synchronization (ERD/ERS), i.e. decrease or increase in power generated by an event compared to a baseline (Pfurtscheller and Lopes da Silva, 1999). Large ERD values (i.e., more negative power values) represent stronger cortical activation compared to baseline time interval, as it represents disinhibition/excitation of neural population activity (Ritter et al., 2009). For the quantification of brain activity, we used the Fieldtrip toolbox (https://www.fieldtriptoolbox.org/) for Matlab. Time-frequency maps were calculated using Morlet wavelets in the frequency range from 1 to 45 Hz, with a resolution of 0.5

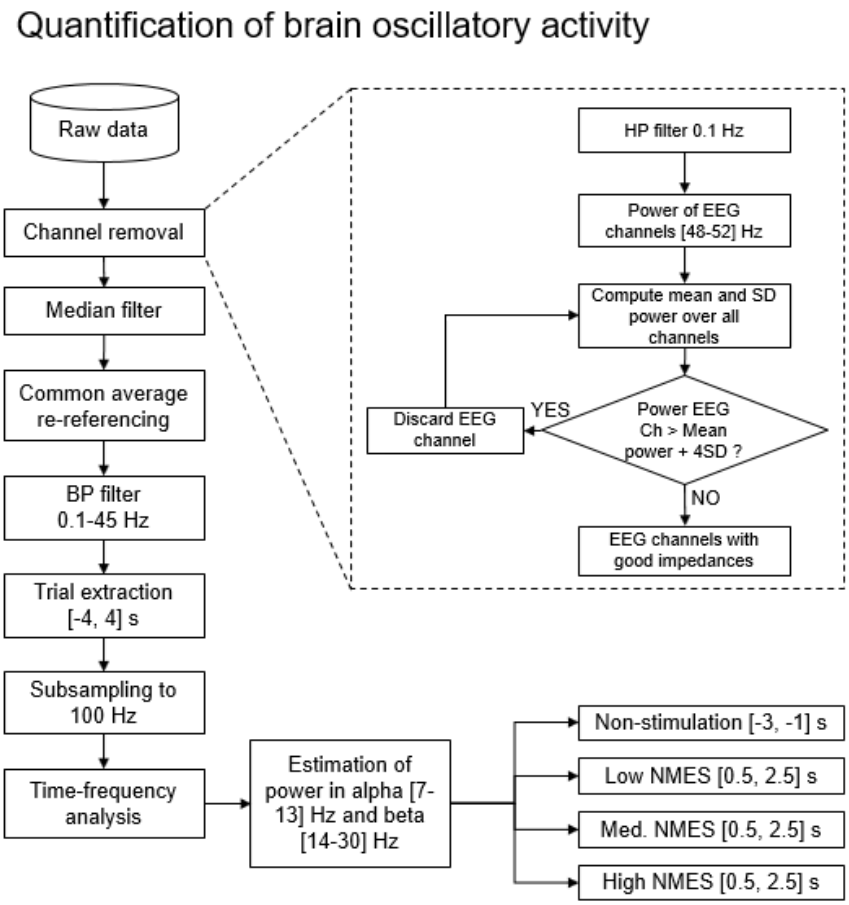

Figure 4.3: Flowchart with the steps for the quantification of brain oscillatory activity. The whole set of data is firstly preprocessed by a two-step procedure based on channel removal and median filtering. In this level, channels with bad impedances and artifacts due to electrical stimulation are removed. Then, the remaining clean data are filtered and divided into trials. Finally, power is estimated in alpha (7–13) Hz and beta (14–30) Hz bands for non-stimulation [(−3, −1) s] and NMES [(0.5, 2.5) s] intervals, being the baseline (−2.5, −1.5) s.

Hz. The power change was computed as the percentage of increase or decrease in power (i.e., ERS or ERD) with respect to the baseline ([-2.5, -1.5] s), where P_j represents the signal power at the j^{th} sample, as described in Equation 4.

$$[Eq.4]\ ERD/ERS_j(\%) = \frac{P_j - Baseline}{Baseline} \times 100$$

From the time-frequency maps, we calculated the sensorimotor averaged changes in power in alpha (7–13) Hz and beta (14– 30) Hz bands for non-stimulation [(−3, −1) s] and NMES [(0.5, 2.5) s] intervals, using as baseline the (−2.5, −1.5) s interval interval (see Figure 4.3). The NMES period was defined as starting at 0.5 s to avoid potential bias and influence of the stimulation onset like event-related brain potentials (e.g.,

somatosensory evoked potential) at t=0. For the topographical inspection and the descriptive analysis of the entire brain activity, all EEG channels were analyzed individually. For the quantitative analysis, we calculated the mean change in power of channels C1, C3, CP1 and CP3 (i.e., area over the sensorimotor cortex representing right forearm, contralateral hemisphere to the stimulated limb), since we considered that averaged values over these electrodes could better quantify the overall changes in the sensorimotor areas.

4.3.7 Statistical analysis

The statistical tests were performed in IBM SPSS 25.0 Statistics software (SPSS Inc., Chicago, IL, USA) and Matlab. We used the Shapiro-Wilk test to determine the normality of the data. Accordingly, a multivariate analysis of variance (MANOVA) for repeated measures was performed to find differences in the dependent variables, alpha and beta ERD/ERS, with NMES intensity (4 levels: no stimulation, low, medium and high intensity stimulation) as within-subject factor. In order to determine the origin of the significant effect, post-hoc tests with Bonferroni correction were performed.

In order to analyze whether NMES can induce a dose-effect, we studied the ERD/ERS changes over time. For that, we computed the alpha and beta ERD/ERS for each single trial (i.e., in Eq. 4, *Pj* was the alpha/beta power of each trial during the NMES period, and the baseline was calculated from the grand average of all the trials of each intensity). A linear regression was estimated for the ERD/ERS values over trials for the two frequency bands (i.e., alpha and beta) and the three NMES intensities (i.e., low, medium and high). Correlation between ERD/ERS and sequence of trials were calculated using Pearson's correlation coefficient to study stimulation effects over time.

4.4 Results

4.4.1 Effect of artifact removal

The pre-processing of the data eliminated satisfactorily the electrical noise contamination coming from the peripheral electrical stimulation. It reduced the effect of

the artifacts to an extent that allowed us to perform EEG spectral analysis of the brain oscillatory activity.

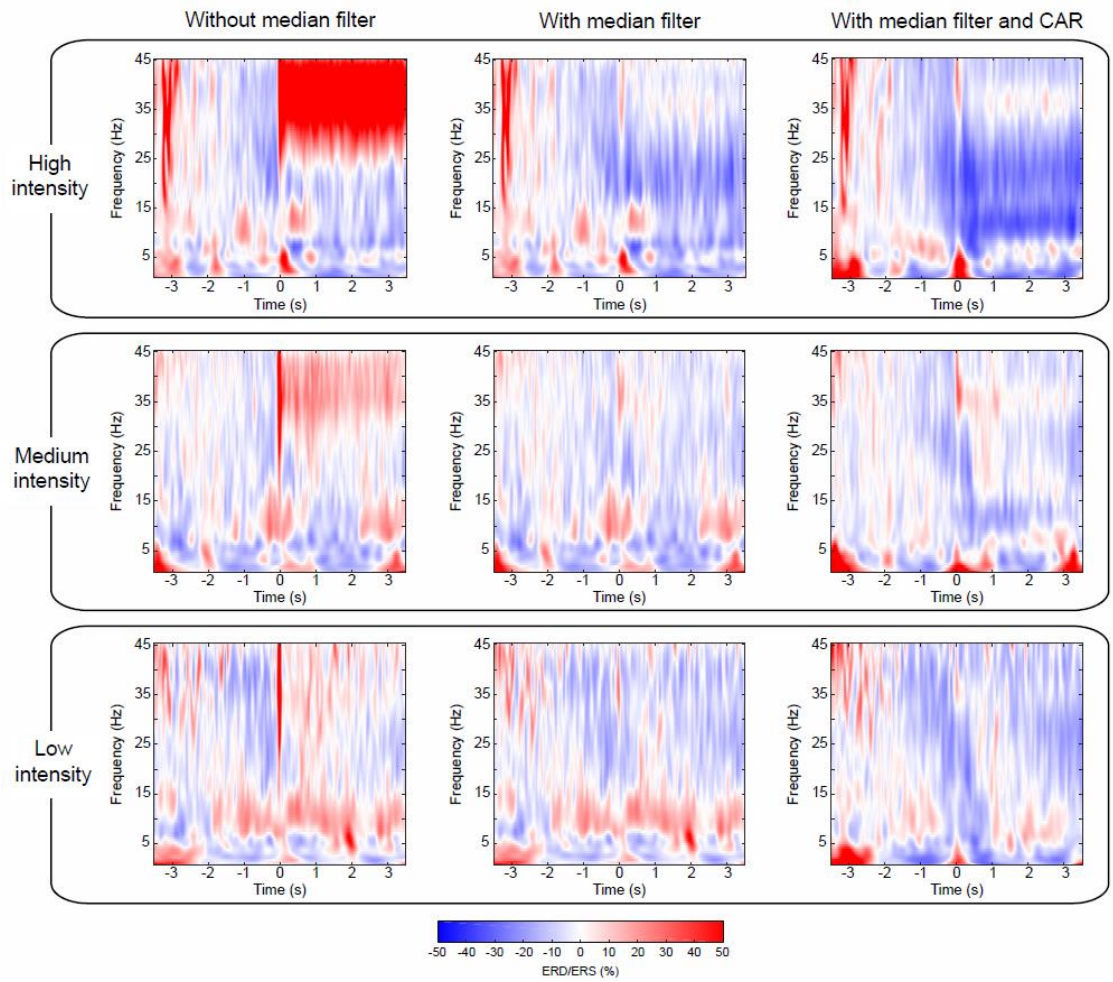

Figure 4.4: Comparison of cortical activation after median and spatial filtering. Time-frequency maps averaged over all participants, representing ERD/ERS, of the average of channels (C3, C1, CP3, and CP1) located over the contralateral sensorimotor cortex to the stimulated limb. Averaged time-frequency maps without median filter (left column), with median filter (center column), and with median and CAR filter (right column) after removal of contaminated channels. Rows show the different NMES intensities: high (upper row), medium (middle row), and low intensity (lower row). The percentage of ERD/ERS is computed according to the baseline (−2.5, −1.5) s. Time 0 s is aligned with the onset of the stimulation.

Channels with good impedances are also influenced by the electrical stimulation artifact that is introduced into the signal as large peaks. Figure 4.2b illustrates in a 100 ms segment of a representative trial how the median filter deals with these undesired artifacts. To prove the efficacy of the method, we focused on the worst-case scenario, as the contamination is larger for higher stimulation intensities. This effect can be observed

in Figure 4.4, which depicts the EEG time-frequency activity at the different NMES intensities including artifacts, and after the median and spatial filters are applied. The NMES generates an increase of power, or ERS, around 35 Hz (i.e., the stimulation frequency), which increases as the NMES intensity is incremented (Figure 4.4, left column). This power increase in high-beta/low-gamma band due to stimulation artifact was eliminated for all intensities after median filtering. Applying the median filter did not change the power in alpha and beta frequencies before the stimulation onset (t = 0 s), but eliminated the ERS during the stimulation period, minimizing the artifacts and revealing the alpha and beta modulation. The common average re-reference (CAR) after median filtering enhanced the power decrease of the bands of interest for every NMES intensity, as it does with non-contaminated EEG (Wolpaw et al., 2002b). Regardless of the intensity delivered, the initiation of the stimulation generated time- and phase-locked activity (i.e., event-related potentials-ERP), presumably due to the sensory processing of the NMES (Reynolds et al., 2015). This can be seen as power increase at low frequencies (1-5 Hz).

4.4.2 Influence of stimulation intensity on cortical activation

To analyze the influence of stimulation intensity on cortical activation, we compared the changes in brain oscillatory activity in four conditions: non-stimulation, low, medium and high intensity stimulation (see topoplots of alpha and beta rhythms in Figure 4.5). Topographic maps of non-stimulation condition were calculated using the interval $(-3, -1)$ s prior to the stimulation, while the other conditions were extracted from the interval (0.5, 2.5) s after stimulation onset. An increment of the stimulation intensity resulted in an increasing ERD (i.e., larger decrease in power) in both frequency bands over the sensorimotor cortex as expected (Backes et al., 2000; Smith et al., 2003; Schürholz et al., 2012), while occipital areas showed idling activity. At high intensity stimulation, the sensorimotor cortex of both hemispheres presented a decrease of power, being more pronounced in the contralateral hemisphere, as demonstrated in previous work studying brain oscillatory signatures of motor tasks (Ramos-Murguialday and Birbaumer, 2015).

Our MANOVA analysis reflected a significant effect of intensity on alpha and beta ERD ($F(6, 86) = 4.356$, $p = 0.001$). Rightmost panels in Figure 4.5 display the results of the post-hoc comparisons. For both alpha and beta, there was a significantly higher ERD (i.e., more negative power values) induced by high intensity NMES compared to rest ($p = 0.004$ for alpha, $p < 0.001$ for beta), to low intensity NMES ($p = 0.013$ for alpha, $p = 0.004$ for beta) and to medium intensity ($p = 0.045$ for alpha, $p < 0.001$ for beta).

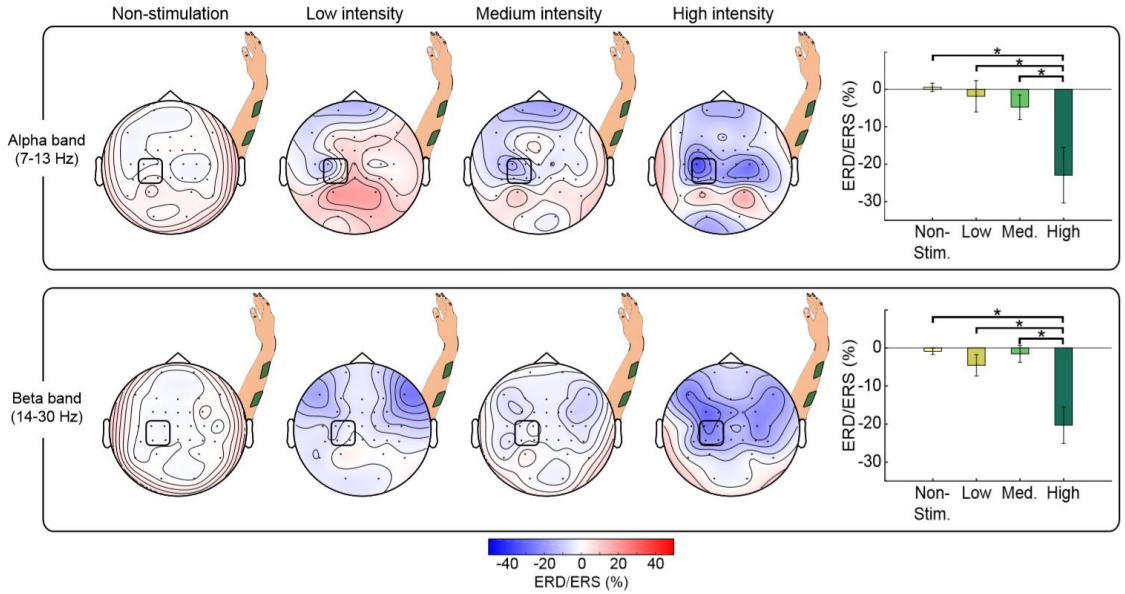

Figure 4.5: Comparison of cortical activation for different stimulation intensities for alpha and beta band EEG activity. Topographic maps, averaged over all participants, showing ERD/ERS of non-stimulation periods (−3, −1) s and NMES periods (0.5, 2.5) s belonging to each intensity (i.e., low, medium, and high) for alpha (upper row) and beta (lower row) frequency bands. Bar graphs show the mean percentage of ERD/ERS averaged from channels (C3, C1, CP3, and CP1) for each intensity and frequency band. The statistically significant differences between pairs are expressed with horizontal lines and stars. The percentage of ERD/ERS is calculated with respect to the baseline (−2.5, −1.5) s. The signals are processed using the two-step procedure (i.e., removal of contaminated channels and median filter) and a CAR.

4.4.3 Stimulation dose-effect

To study the influence of stimulation dose on cortical activity, we computed the ERD/ERS of each single trial and performed a regression in time within session appending same stimulation intensity blocks in order of appearance (blocks of different intensities were presented randomly). Figure 4.6 shows the average ERD/ERS for all participants in both frequency bands during the 54 trials (3 blocks x 18 trials, see vertical

yellow lines) for each intensity and a linear regression to fit them. We also performed regressions over time within each block with consecutive trials (see Supplementary Figure 4.4).

The first thing we observed is a clear modulation based on stimulation, reducing its variability with stimulation amplitude. Low and medium intensities caused a significant reduction of alpha ERD over time (p = 7.8e-4 for low; p = 0.0053 for medium). In contrast, high intensity caused a significant enhancement of beta ERD over time (p = 5.12e-5). Furthermore, as can be seen in Figure 4.6, we observed that in every block (separated by yellow vertical lines) there is a reduction of the ERD (increase of power plotted as linear regression in Supplementary Figure 4.4) progressively induced per trial from the first to the last trial. The first trial of the new block presented a larger ERD (decrease of power) in comparison to the ERD of the last trial of the previous block (irrespective of the stimulation intensity and order of the block within the session).

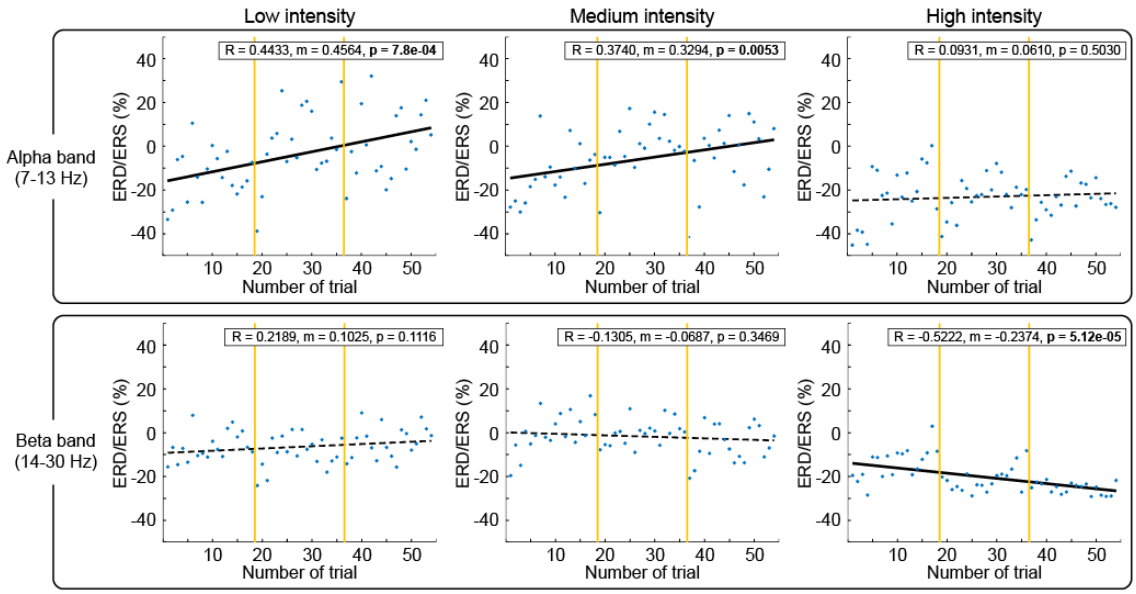

Figure 4.6: Comparison of cortical activation over trials for alpha and beta bands. The cortical activity during NMES period [(0.5, 2.5) s] quantified as ERD/ERS over the 54 trials for each stimulation intensity, divided into blocks by vertical yellow lines, and averaged for all the participants. The percentage of ERD/ERS is calculated according to the baseline (−2.5, −1.5) s. Different intensities are compared in columns: low (left), medium (middle), and high (right). Alpha (upper row) and beta (lower row) frequency bands are described. Significant correlations between ERD/ERS and sequence of trials over session are represented with black solid linear regressions.

4.5 Discussion

This study demonstrated the significant effects of artifacts, intensity and dose of neuromuscular electrical stimulation (NMES) of the upper limb on the ongoing brain oscillatory activity recorded using EEG. First of all, we dealt with the issue of artifact removal to allow accurately estimating the cortical oscillatory activity. Recordings of brain activity are easily polluted, especially when electrical stimulation interacting with the nervous system is concurrently used. This contamination can negatively affect the signal to noise ratio, covering the brain activity. Our findings evidenced that the median filter enhanced the detection of sensorimotor oscillatory activity after removing stimulation artifacts.

After the EEG data was cleaned, especially of NMES-induced artifacts, we analyzed the modulation of alpha and beta oscillations produced by the stimulation. Power suppression, or desynchronization, of these frequencies has been associated with cortical excitation, whereas synchronization reflects a state of inhibition (Klimesch et al., 2007). During high intensity NMES, the induced desynchronization in alpha and beta was significantly larger than during stimulation at low or medium intensities or no stimulation. While below-motor-threshold stimulation intensities only activate cutaneous mechanoreceptors (e.g., Pacinian corpuscles and Merkel disks) and sensory axons, stimulation above the motor threshold also recruits proprioceptive receptors (e.g., muscle spindles, Golgi tendon organs and joint afferents) (Maffiuletti et al., 2008; Bergquist et al., 2011; Golaszewski et al., 2012). It has been proposed that muscle spindles transmit inputs to the spinal cord and can directly influence the motor cortex (M1) through the area 3a, while the projections from area 3b activated by cutaneous feedback to M1 are less likely to happen (Carson and Buick, 2019). We can therefore assume that high intensity NMES leads to higher neural excitation, probably by recruiting a larger number of receptors derived from muscle contractions, in addition to the cutaneous and sensory fiber afference that is also engaged in sensory-threshold stimulation, and that the recruitment of muscle spindles results in activation of M1 via area 3a of the somatosensory cortex (S1) (Schabrun et al., 2012; Carson and Buick, 2019). These results of intensity-dependent brain activation are in line with corticomuscular responses (Sasaki

et al., 2017), metabolic responses recorded by functional magnetic resonance imaging (fMRI) (Backes et al., 2000; Smith et al., 2003) and near-infrared spectroscopy (NIRS) (Schürholz et al., 2012), which demonstrated a direct quantitative association with stimulation intensity. Noteworthy, our results showed that the cortical activity measured with EEG, quantified as event-related (de)synchronization (ERD/ERS), during low and medium intensities was not significantly different to no stimulation. This suggests that below motor-threshold NMES might not recruit enough afferent fibers to induce significant cortical modulation, and that more afference (probably through muscle contraction, proprioception due to the movement and a larger number of sensory fibers recruited) is required to transmit more information that reaches the brain and is measurable in the EEG at the analyzed frequencies.

It is well known that during voluntary movement, a stronger cortical activation is seen in alpha than in beta (López-Larraz et al., 2014; Ramos-Murguialday and Birbaumer, 2015). Such modulation in alpha and beta cortical activity has been related to the control of top-down and bottom-up neural processes, suggesting its role in the integration of motor tasks preparation and execution with movement-related sensory feedback. However, this balance between alpha and beta rhythms is altered in absence of top-down regulation. Passive mobilizations (e.g., bottom-up transmission) exhibit stronger beta band activity compared with active movements, indicating the relationship of this frequency band with proprioception without volitional muscle contraction (Alegre et al., 2002; Ramos-Murguialday and Birbaumer, 2015), and thus the inhibitory effect of top-down neural control in this frequency. In this study, the peripheral electrical stimulation at the functional intensity level not only generated passive movement of the limb, but also non-volitional contraction of the forearm muscles. This stimulation intensity induced a significant brain activation in beta frequency band, suggesting that this change might be comprised by two components: proprioception and afference of muscle contraction (without volition) through Golgi tendons and muscle spindles. Therefore, our results give a hint of the relevance of beta rhythm on bottom-up neuromodulation (i.e., afferent neural excitation). In agreement with previous studies, we can speculate that there might be differences in the afferent modulation between passive movements and functional electrical stimulation (Francis et al., 2009; Iftime-Nielsen et

al., 2012). Whereas NMES over the motor threshold recruits afferent axons from muscle spindles, Golgi tendon organs and cutaneous receptors (Maffiuletti et al., 2008; Bergquist et al., 2011; Golaszewski et al., 2012), Golgi tendon organs are less sensitive to passive movements and discharge less (Paillard and Brouchon, 1968; Purves et al., 2004), and the firing rate of the muscle spindles is muscle lengthening dependent (Chye et al., 2010). However, it cannot be concluded whether our functional NMES induces stronger beta activity than passive movements since we did not include the latter condition in our experimental protocol.

We tracked changes of the EEG sensorimotor oscillatory activity and evidenced that NMES induced a dose-effect on the activation patterns over time. To minimize the muscle fatigue due to NMES, we defined a low stimulation frequency as described in the literature (Gregory et al., 2007; Barss et al., 2018) and let non-stimulation periods to the muscle tissue to recover. However, we are aware that our results might be limited by muscle fatigue and that the stimulation parameters (e.g., pulse width) could be optimized to recruit central pathways and reduce fatigability (Collins, 2007). Regardless of the stimulation intensity applied, both alpha and beta bands presented a short-term reduction of ERD (reduction of brain excitatory effect of NMES) between consecutive trials within a block, showing that the ERD response of a specific trial depended on the previous stimulation. This reduction of ERD vanished at the beginning of every new block, demonstrating the ability of the sensorimotor oscillations to reset its excitability after the ~2-minute inter-block period. However, the overall activity throughout the session depicts that long-term effects survive temporary resets and exhibits a dose-effect over time, suggesting a conditioning effect. Despite the discontinuities due to inter-block pauses that could limit the significance of our results, we observed different long-term modulatory responses between sensorimotor oscillations in alpha and beta bands conditioned by the stimulation intensity.

For sensory-threshold intensities (i.e., low and medium), the power in alpha band was significantly reduced throughout the session, suggesting a habituation effect (Leung et al., 2005). NMES at sensory-threshold recruits cutaneous receptors and sensory axons (without eliciting any muscle contraction or movement) that activate spinal pathways and provide sensory afference to the brain (Maffiuletti et al., 2008). It has been evidenced

that alpha band is relevant for information processing of attention and awareness (Händel et al., 2011; Klimesch, 2012), and we speculate that the repeated activation of functionally irrelevant sensory afference (i.e., cutaneous and sensory axons afference in absence of movement) results in inhibition of the sensorimotor oscillations in alpha. A progressive habituation or desensitization (i.e., reduction of perceived sensation) of sensory perception is also presented after prolonged vibrotactile and electrocutaneous stimulation (Graczyk et al., 2018), which is slower at high stimulation intensities (Buma et al., 2007). This desensitization might be caused by a hyperpolarization of axon membranes (i.e., increasing membrane inhibition) controlled by the activity of Na-K pump that prevents the membrane from excessive excitation due to the repetitive electrical stimulation (Kiernan et al., 2004; Nodera and Kaji, 2006). One can hypothesize that the desensitization of sensory perception and habituation of alpha band might be connected somehow. However, we cannot conclude whether attention shifts over time could also induce the habituation in alpha oscillations, although non-significant fMRI responses have been reported in S1 when comparing different attention levels combined with sensory-threshold stimulation (Backes et al., 2000).

The modulation of beta power due to stimulation at functional-threshold intensity incremented with time, indicating an excitatory effect on the sensorimotor neural network. This result contrasts with what we initially expected, that is a lower cortical responsiveness after prolonged stimulation. Beta oscillations have been related to the neural transmission from the primary motor cortex to the muscles and back to the motor cortex, via afferent sensory pathways, spinal cord and somatosensory cortex (Aumann and Prut, 2015; Khademi et al., 2018). This closed-loop neural network provides the sensorimotor cortex with information of movements, comprising the muscles and joints. NMES at functional intensity recruits proprioceptive receptors (e.g., muscle spindles, Golgi tendon organs and joint afferents) in addition to cutaneous mechanoreceptors (Maffiuletti et al., 2008; Golaszewski et al., 2012). One plausible explanation of our results is that the activation of this larger number of receptors keeps the aforementioned loop working and results in higher excitability of the network over time. Humans are constantly performing motor tasks, and movement drives our behavior and has driven our nervous system development. We can speculate that functionally relevant afferent

information excites the sensorimotor cortex, while afferent information not related to movement (i.e., sensory axons activation and mechanoreception due to low and medium NMES) might not be considered "relevant" and therefore is omitted, suppressing neural excitability (Schabrun et al., 2012). Consequently, stimulation above the motor threshold has been proposed to result in improvements of motor function due to the secondary afference coming from muscle contractions and joints feedback, in addition to the primary sensory afference by NMES (de Kroon et al., 2005). All this highlights the different effect when muscle contraction and proprioception together with afference of sensory receptors enrich afferent activity (probably due to their ecologically relevant role in sensorimotor function), indicating that habituation or attention shift during a movement is less likely to occur due to its functional role in sensorimotor function.

To the best of our knowledge, this is the first time a sensorimotor cortical facilitation and inhibition effect due to NMES has been measured using EEG and characterized as presenting significant intensity- and dose-effects, which occurred in a short period of time. We particularly focused on these stimulation parameters because in NMES-based rehabilitative interventions other parameters are usually fixed, while intensity and dose are modified. EEG is a widely used neuroimaging tool and, thanks to its good temporal resolution, has a great potential in the context of neurorehabilitation, especially in EEG-guided neural interfaces. Understanding how NMES parameters, such as intensity and dose, can modulate the excitability of cortical oscillations measured by EEG could be clinically relevant. For instance, NMES could be used for regulating rolandic alpha since motor recovery has been related to an enhancement of this activity (Tangwiriyasakul et al., 2014b; Ray et al., 2020), or could be integrated in rehabilitative neural interfaces that are controlled by sensorimotor oscillations.

We are aware that to be able to deepen into the neural mechanisms involved in the transmission of volleys from the muscle to the brain, we would need additional and more complex measurements to characterize the afferent pathways (including different reflexes, cortical and subcortical motor evoked potentials, or sensory evoked potentials). Investigating how intensity and dose of NMES can affect other EEG features, such as phase, connectivity or low-frequency oscillations, could also complement the here presented results. Further work should disclose whether more functional afferent activity

(including proprioception and muscle contraction) is needed to increase functional plasticity and modulate sensorimotor function (e.g., corticomuscular synaptic efficacy, cortico-cortico functional connectivity, etc.). The effect of ongoing activity and other stimulation parameters (i.e., pulse width, pulse form, frequency and energy) need to be carefully studied (Kampe et al., 2000; Wegrzyk et al., 2017), probably based on computational neuroscience and bioelectromagnetic modeling, to understand their effect in excitatory and inhibitory mechanisms. Nevertheless, the presented results shed some light onto the neuromodulatory effects that can be investigated and exploited using NMES.

4.5.1 Study limitations

First, the main limitation of the current study is that the utilized neuroimaging tool only allowed us to characterize excitatory changes of the sensorimotor cortex. However, we cannot conclude that other subcortical structures, such as the spinal cord, might also be modulated by the stimulation (Mang et al., 2011), and in turn, affect the inputs arriving to the cortex. Nevertheless, we assume that our experimental paradigm ensured a constant state. Second, among the wide range of stimulation parameters (i.e., current intensity, frequency, pulse with, waveform, etc.) that could be tuned to modulate the neural excitability, we focused on the effect of current intensity and the results of this study are limited by the stimulation parameters selected. Although there is evidence showing that using larger pulse widths and higher frequencies to recruit central pathways through sensory axons might have a greater neural impact (Collins, 2007; Lagerquist and Collins, 2010), we defined our stimulation parameters within the ranges that have already been used for rehabilitation of motor function in paralyzed patients (Quandt and Hummel, 2014; Knutson et al., 2015; Carson and Buick, 2019). Third, despite following the experimental protocols of Backes and colleagues (Backes et al., 2000) and Smith and colleagues (Smith et al., 2003), the absence of arm fixation and objective measurements of wrist extension makes difficult to ensure that the different trials had the same effect on the neuromuscular system over time, especially as muscle fatigue progresses. However, we assumed that our experimental protocol regarding electrode size, careful electrode placement, and visual inspection for clean and consistent wrist extension over time

minimized the variability of the results. Fourth, not including the conditions of passive wrist extension (without simulation) and high-intensity NMES with the arm fixed in our experimental design also limits our results. Since we cannot isolate the afference contribution of the joint movement, muscle contraction, and sensory axon activation, it is not possible to disclose which components contributed more to the regulation of brain activity during NMES. Finally, due to the differences in the afferent projections to the cortex from distinct muscle groups (Mang et al., 2011), we cannot assume that the interpretations taken from our results could be generalized to other muscles. Altogether, further research should address these issues to better understand the neuromodulatory effects of NMES.

4.6 Acknowledgements

This study was funded by the Bundesministerium für Bildung und Forschung BMBF MOTORBIC (FKZ 13GW0053), AMORSA (FKZ 16SV7754), and the Fortüne-Program of the University of Tübingen (2422-0-1 and 2556-0-0 to EL-L and 2452-0-0 to AR-M). The work of AI-D was funded by the Basque Government's scholarship for predoctoral students.

4.7 Supplementary material

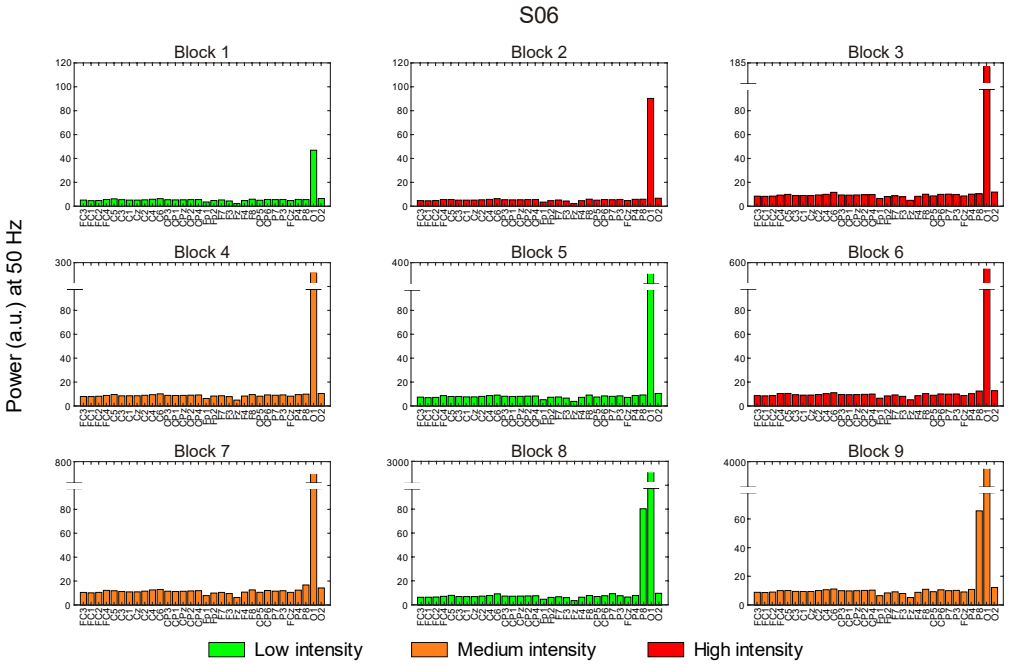

Supplementary Figure 4.1: Estimation of power-line noise for channel removal. The barplots represent the power-line noise in each EEG channel for every block of a representative subject. The green, orange and red color of the bars is associated with low, medium and high NMES intensity, respectively. High power-line noise was as an indicator of bad impedance and bad electrode-skin conductivity. We proposed a method based on the removal of the channels that exceeded the mean EEG power + 4 standard deviations. In this particular subject, O1 was rejected from all the blocks, and P8 from block 8 and block 9.

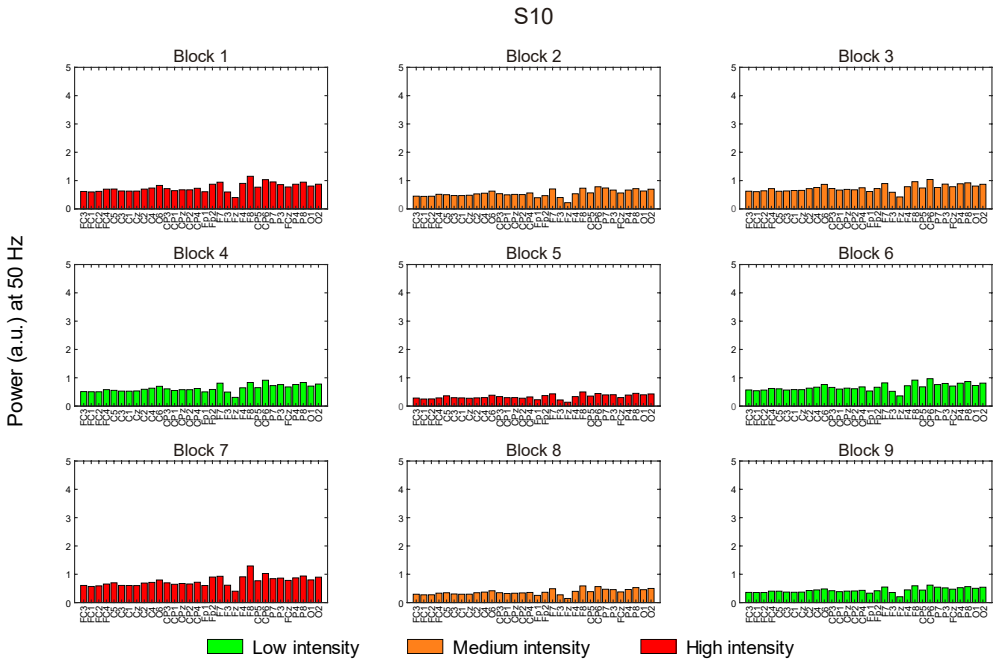

Supplementary Figure 4.2: Estimation of power-line noise for channel removal. The barplots represent the power-line noise in each EEG channel for every block of a representative subject. The green, orange and red color of the bars is associated with low, medium and high NMES intensity, respectively. High power-line noise was as an indicator of bad impedance and bad electrode-skin conductivity. We proposed a method based on the removal of the channels that exceeded the mean EEG power + 4 standard deviations. In this particular subject, all the channels in every block satisfied the inclusion criteria.

	Block 1	Block 2	Block 3	Block 4	Block 5	Block 6	Block 7	Block 8	Block 9
Subject 1	FP1, FC3	FP1	FP1	FP1	FP1	FP1	FP1	FP1, F7	FP1, C5
Subject 2	FC1	FC1	FC1, FC2	FC2	F4, FC2	FP2, F4, FC2	FP2, FC2	FP2, F4, FC2	FP1, FP2, F4, FC2
Subject 3									FP1, FP2
Subject 4			Cz	Cz	Cz	Cz	Cz	Cz	Cz
Subject 5		Fz	Fz	Fz	Fz	Fz		Fz	
Subject 6	O1	O1	O1	O1	O1	O1	O1	P8, O1	P8, O1
Subject 7									
Subject 8									
Subject 9									
Subject 10									
Subject 11					Fz	Fz	Fz	FP1, FP2, Fz	
Subject 12		Fz	Fz	Fz				Fz	

Supplementary Table 4.1: Channel removal according to the power-line noise. We proposed a method based on the removal of the channels that exceeded the mean EEG power + 4 standard deviations. The table shows the list of the channels that exceeded the rejecting threshold for every subject in each block.

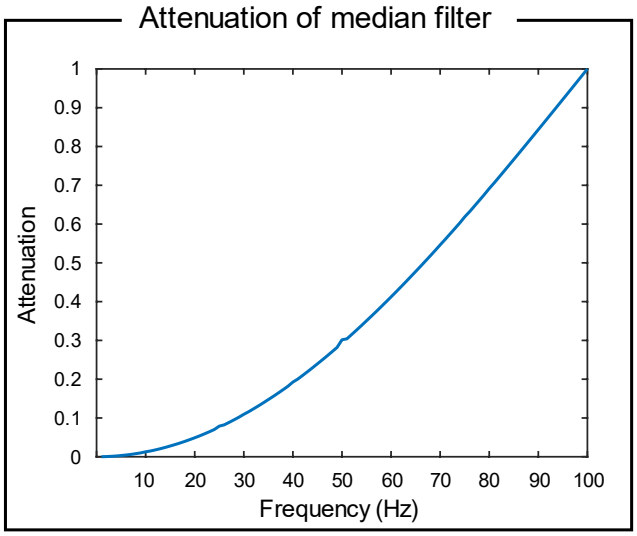

Supplementary Figure 4.3: Attenuation of median filter. The median filter induces an exponential attenuation of the signal, which is frequency dependent. This filter attenuates from 0 (no attenuation) to the inverse of the selected window length of the filter; in our case the window of 10 ms produces a total attenuation at 100 Hz. As an example, the attenuation at 10 Hz, 20 Hz and 30 Hz is 1.28%, 4.89% and 10.90%, respectively

.

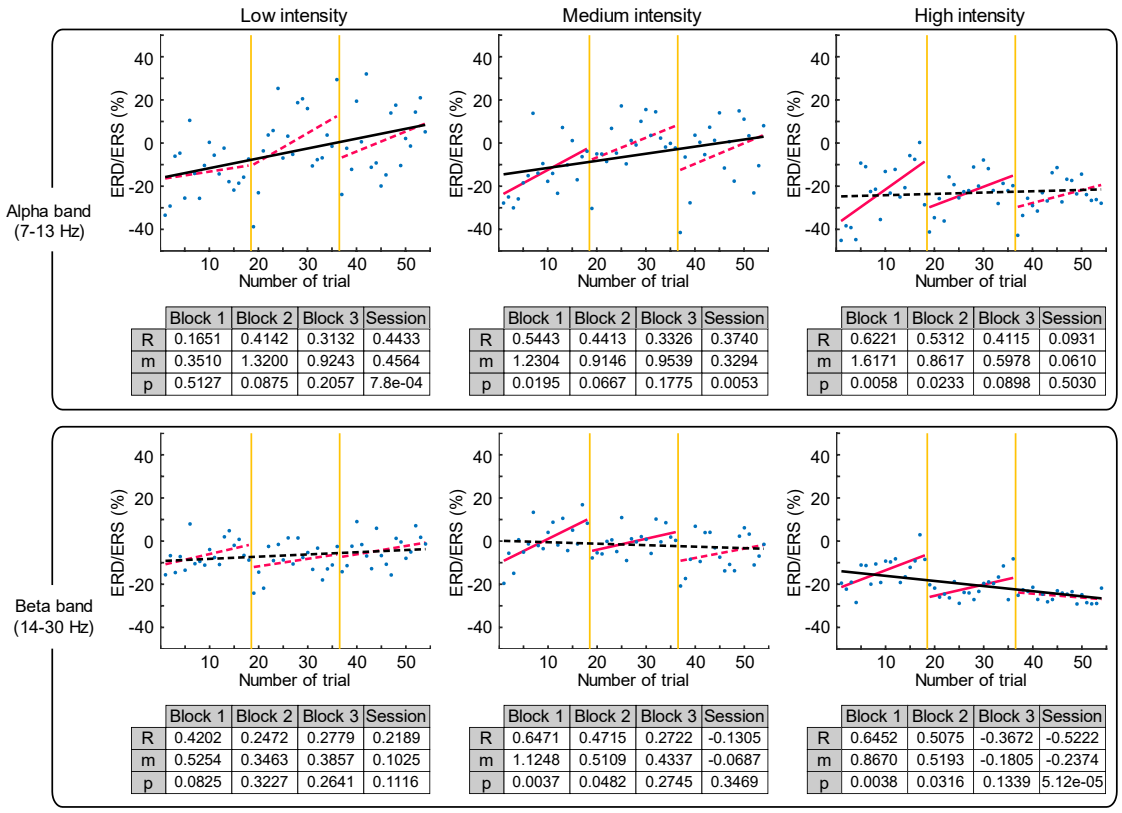

Alpha band	Block 1	Block 2	Block 3	Session
R	0.1651	0.4142	0.3132	0.4433
m	0.3510	1.3200	0.9243	0.4564
p	0.5127	0.0875	0.2057	7.8e-04

Alpha band	Block 1	Block 2	Block 3	Session
R	0.5443	0.4413	0.3326	0.3740
m	1.2304	0.9146	0.9539	0.3294
p	0.0195	0.0667	0.1775	0.0053

Alpha band	Block 1	Block 2	Block 3	Session
R	0.6221	0.5312	0.4115	0.0931
m	1.6171	0.8617	0.5978	0.0610
p	0.0058	0.0233	0.0898	0.5030

Beta band	Block 1	Block 2	Block 3	Session
R	0.4202	0.2472	0.2779	0.2189
m	0.5254	0.3463	0.3857	0.1025
p	0.0825	0.3227	0.2641	0.1116

Beta band	Block 1	Block 2	Block 3	Session
R	0.6471	0.4715	0.2722	-0.1305
m	1.1248	0.5109	0.4337	-0.0687
p	0.0037	0.0482	0.2745	0.3469

Beta band	Block 1	Block 2	Block 3	Session
R	0.6452	0.5075	-0.3672	-0.5222
m	0.8670	0.5193	-0.1805	-0.2374
p	0.0038	0.0316	0.1339	5.12e-05

Supplementary Figure 4.4: Comparison of cortical activation over trials for alpha and beta band. The cortical activity during NMES period [(0.5, 2.5) s] quantified as ERD/ERS over the 54 trials divided into blocks by vertical yellow lines of each stimulation intensity, averaged for all the participants. The percentage of ERD/ERS is calculated according to the baseline (-2.5, -1.5) s. Different intensities are compared in columns: low (left), medium (middle) and high (right). Alpha (upper row) and beta (lower row) frequency bands are described. Significant correlations between ERD/ERS and sequence of trials over session are represented with black solid linear regressions. Within block significant correlations are displayed by magenta solid linear regressions. Tables show the correlation (R), slope (m) and p-value (p) for every block and session.

4.8 References

Alegre, M., Labarga, A., Gurtubay, I. G., Iriarte, J., Malanda, A., and Artieda, J. (2002). Beta electroencephalograph changes during passive movements: Sensory afferences contribute to beta event-related desynchronization in humans. *Neurosci. Lett.* 331, 29–32. doi:10.1016/S0304-3940(02)00825-X.

Andrews, R. K., Schabrun, S. M., Ridding, M. C., Galea, M. P., Hodges, P. W., and Chipchase, L. S. (2013). The effect of electrical stimulation on corticospinal excitability is dependent on application duration: A same subject pre-post test

design. *J. Neuroeng. Rehabil.* 10, 51. doi:10.1186/1743-0003-10-51.

Aumann, T. D., and Prut, Y. (2015). Do sensorimotor β-oscillations maintain muscle synergy representations in primary motor cortex? *Trends Neurosci.* 38, 77–85. doi:10.1016/j.tins.2014.12.002.

Backes, W. H., Mess, W. H., van Kranen-Mastenbroek, V., and Reulen, J. P. H. (2000). Somatosensory cortex responses to median nerve stimulation: fMRI effects of current amplitude and selective attention. *Clin. Neurophysiol.* 111, 1738–1744. doi:10.1016/S1388-2457(00)00420-X.

Ball, T., Kern, M., Mutschler, I., Aertsen, A., and Schulze-Bonhage, A. (2009). Signal quality of simultaneously recorded invasive and non-invasive EEG. *Neuroimage* 46, 708–716. doi:10.1016/j.neuroimage.2009.02.028.

Barss, T. S., Ainsley, E. N., Claveria-Gonzalez, F. C., Luu, M. J., Miller, D. J., Wiest, M. J., et al. (2018). *Utilizing Physiological Principles of Motor Unit Recruitment to Reduce Fatigability of Electrically-Evoked Contractions: A Narrative Review*. The American Congress of Rehabilitation Medicine doi:10.1016/j.apmr.2017.08.478.

Bergquist, A. J., Clair, J. M., Lagerquist, O., Mang, C. S., Okuma, Y., and Collins, D. F. (2011). Neuromuscular electrical stimulation: implications of the electrically evoked sensory volley. *Eur. J. Appl. Physiol.* 111, 2409–2426. doi:10.1007/s00421-011-2087-9.

Birbaumer, N., Elbert, T., Canavan, A. G., and Rockstroh, B. (1990). Slow potentials of the cerebral cortex and behavior. *Physiol. Rev.* 70, 1–41. doi:10.1152/physrev.1990.70.1.1.

Blickenstorfer, A., Kleiser, R., Keller, T., Keisker, B., Meyer, M., Riener, R., et al. (2009). Cortical and subcortical correlates of functional electrical stimulation of wrist extensor and flexor muscles revealed by fMRI. *Hum. Brain Mapp.* 30, 963–975. doi:10.1002/hbm.20559.

Buma, D. G., Buitenweg, J. R., and Veltink, P. H. (2007). Intermittent stimulation delays

adaptation to electrocutaneous sensory feedback. *IEEE Trans. Neural Syst. Rehabil. Eng.* 15, 435–441. doi:10.1109/TNSRE.2007.903942.

Buzsaki, G. (2006). *Rhythms of the Brain*. Oxford University Press.

Carson, R. G., and Buick, A. R. (2019). Neuromuscular electrical stimulation promoted plasticity of the human brain. *J. Physiol.* doi:10.1113/jp278298.

Chipchase, L. S., Schabrun, S. M., and Hodges, P. W. (2011). Peripheral electrical stimulation to induce cortical plasticity: A systematic review of stimulus parameters. *Clin. Neurophysiol.* 122, 456–463. doi:10.1016/j.clinph.2010.07.025.

Chye, L., Nosaka, K., Murray, L., Edwards, D., and Thickbroom, G. (2010). Corticomotor excitability of wrist flexor and extensor muscles during active and passive movement. *Hum. Mov. Sci.* 29, 494–501. doi:10.1016/j.humov.2010.03.003.

Collins, D. F. (2007). Central contributions to contractions evoked by tetanic neuromuscular electrical stimulation. *Exerc. Sport Sci. Rev.* 35, 102–109. doi:10.1097/jes.0b013e3180a0321b.

Corbet, T., Iturrate, I., Pereira, M., Perdikis, S., and Millán, J. del R. (2018). Sensory threshold neuromuscular electrical stimulation fosters motor imagery performance. *Neuroimage* 176, 268–276. doi:10.1016/j.neuroimage.2018.04.005.

de Kroon, J. R., IJzerman, M. J., Chae, J., Lankhorst, G. J., and Zilvold, G. (2005). Relation between stimulation characteristics and clinical outcome in studies using electrical stimulation to improve motor control of the upper extremity in stroke. *J. Rehabil. Med.* 37, 65–74. doi:10.1080/16501970410024190.

Francis, S., Lin, X., Aboushoushah, S., White, T. P., Phillips, M., Bowtell, R., et al. (2009). fMRI analysis of active, passive and electrically stimulated ankle dorsiflexion. *Neuroimage* 44, 469–479. doi:10.1016/j.neuroimage.2008.09.017.

Gallagher, N. C., and Wise, G. L. (1981). A Theoretical Analysis of the Properties of Median Filters. *IEEE Trans. Acoust.* 29, 1136–1141. doi:10.1109/TASSP.1981.1163708.

Gamboa, O. L., Antal, A., Moliadze, V., and Paulus, W. (2010). Simply longer is not better: Reversal of theta burst after-effect with prolonged stimulation. *Exp. Brain Res.* 204, 181–187. doi:10.1007/s00221-010-2293-4.

Golaszewski, S. M., Bergmann, J., Christova, M., Kunz, A. B., Kronbichler, M., Rafolt, D., et al. (2012). Modulation of motor cortex excitability by different levels of whole-hand afferent electrical stimulation. *Clin. Neurophysiol.* 123, 193–199. doi:10.1016/j.clinph.2011.06.010.

Graczyk, E. L., Delhaye, B. P., Schiefer, M. A., Bensmaia, S. J., and Tyler, D. J. (2018). Sensory adaptation to electrical stimulation of the somatosensory nerves. *J. Neural Eng.* 15, 046002. doi:10.1088/1741-2552/aab790.

Gregory, C. M., Dixon, W., and Bickel, C. S. (2007). Impact of varying pulse frequency and duration on muscle torque production and fatigue. *Muscle and Nerve* 35, 504–509. doi:10.1002/mus.20710.

Händel, B. F., Haarmeier, T., and Jensen, O. (2011). Alpha oscillations correlate with the successful inhibition of unattended stimuli. *J. Cogn. Neurosci.* 23, 2494–2502. doi:10.1162/jocn.2010.21557.

Iftime-Nielsen, S. D., Christensen, M. S., Vingborg, R. J., Sinkjær, T., Roepstorff, A., and Grey, M. J. (2012). Interaction of electrical stimulation and voluntary hand movement in SII and the cerebellum during simulated therapeutic functional electrical stimulation in healthy adults. *Hum. Brain Mapp.* 33, 40–49. doi:10.1002/hbm.21191.

Insausti-Delgado, A., López-Larraz, E., Bibián, C., Nishimura, Y., Birbaumer, N., and Ramos-Murguialday, A. (2017). Influence of trans-spinal magnetic stimulation in electrophysiological recordings for closed-loop rehabilitative systems. in *39th Annual International Conference of the IEEE Engineering in Medicine and Biology Society (EMBC)*, 2518–2521. doi:10.1109/EMBC.2017.8037369.

Insausti-Delgado, A., López-Larraz, E., Omedes, J., and Ramos-Murguialday, A. (2021). Intensity and dose of neuromuscular electrical stimulation influence sensorimotor

cortical excitability. *Front. Neurosci.* 14, 1359. doi:10.3389/fnins.2020.593360.

Iturrate, I., Pereira, M., and Millán, J. del R. (2018). Closed-loop electrical neurostimulation: challenges and opportunities. *Curr. Opin. Biomed. Eng.* 8, 28–37. doi:10.1016/j.cobme.2018.09.007.

Kampe, K. K. W., Jones, R. A., and Auer, D. P. (2000). Frequency dependence of the functional MRI response after electrical median nerve stimulation. *Hum. Brain Mapp.* 9, 106–114. doi:10.1002/(SICI)1097-0193(200002)9:2<106::AID-HBM5>3.0.CO;2-Y.

Kent, A. R., and Grill, W. M. (2012). Recording evoked potentials during deep brain stimulation: development and validation of instrumentation to suppress the stimulus artefact. *J. Neural Eng.* 9. doi:10.1088/1741-2560/9/3/036004.

Khademi, F., Royter, V., and Gharabaghi, A. (2018). Distinct beta-band oscillatory circuits underlie corticospinal gain modulation. *Cereb. Cortex* 28, 1502–1515. doi:10.1093/cercor/bhy016.

Kiernan, M. C., Lin, C. S.-Y., and Burke, D. (2004). Differences in activity-dependent hyperpolarization in human sensory and motor axons. *J. Physiol.* 558, 341–349. doi:10.1113/jphysiol.2004.063966.

Klimesch, W. (2012). Alpha-band oscillations, attention, and controlled access to stored information. *Trends Cogn. Sci.* 16, 606–617. doi:10.1016/j.tics.2012.10.007.

Klimesch, W., Sauseng, P., and Hanslmayr, S. (2007). EEG alpha oscillations: The inhibition-timing hypothesis. *Brain Res. Rev.* 53, 63–88. doi:10.1016/j.brainresrev.2006.06.003.

Knutson, J. S., Fu, M. J., Sheffler, L. R., and Chae, J. (2015). Neuromuscular electrical stimulation for motor restoration in hemiplegia. *Phys. Med. Rehabil. Clin. N. Am.* 26, 729–745. doi:10.1016/j.pmr.2015.06.002.

Lagerquist, O., and Collins, D. F. (2010). Influence of stimulus pulse width on M-waves, H-reflexes, and torque during tetanic low-intensity neuromuscular stimulation.

Muscle and Nerve 42, 886–893. doi:10.1002/mus.21762.

Leodori, G., Thirugnanasambandam, N., Conn, H., Popa, T., Berardelli, A., and Hallett, M. (2019). Intracortical inhibition and surround inhibition in the motor cortex: A tms-EEG study. *Front. Neurosci.* 13, 612. doi:10.3389/fnins.2019.00612.

Leung, Y. Y., Bensmaïa, S. J., Hsiao, S. S., and Johnson, K. O. (2005). Time-Course of Vibratory Adaptation and Recovery in Cutaneous Mechanoreceptive Afferents. *J. Neurophysiol.* 94, 3037–3045. doi:10.1152/jn.00001.2005.

López-Larraz, E., Figueiredo, T. C., Insausti-Delgado, A., Ziemann, U., Birbaumer, N., and Ramos-Murguialday, A. (2018). Event-related desynchronization during movement attempt and execution in severely paralyzed stroke patients: an artifact removal relevance analysis. *NeuroImage Clin.* 20, 972–986. doi:10.1016/j.nicl.2018.09.035.

López-Larraz, E., Montesano, L., Gil-Agudo, Á., and Minguez, J. (2014). Continuous decoding of movement intention of upper limb self-initiated analytic movements from pre-movement EEG correlates. *J. Neuroeng. Rehabil.* 11, 153. doi:10.1186/1743-0003-11-153.

Lynch, C. L., and Popovic, M. R. (2008). Functional electrical stimulation. *IEEE Control Syst. Mag.* 28, 40–50. doi:10.1109/MCS.2007.914689.

Maffiuletti, N. A., Herrero, A. J., Jubeau, M., Impellizzeri, F. M., and Bizzini, M. (2008). Differences in electrical stimulation thresholds between men and women. *Ann. Neurol.* 63, 507–512. doi:10.1002/ana.21346.

Mang, C. S., Clair, J. M., and Collins, D. F. (2011). Neuromuscular electrical stimulation has a global effect on corticospinal excitability for leg muscles and a focused effect for hand muscles. *Exp. Brain Res.* 209, 355–363. doi:10.1007/s00221-011-2556-8.

Nitsche, M. A., and Paulus, W. (2000). Excitability changes induced in the human motor cortex by weak transcranial direct current stimulation. *J. Physiol.* 527, 633–639. doi:10.1111/j.1469-7793.2000.t01-1-00633.x.

Nodera, H., and Kaji, R. (2006). Nerve excitability testing and its clinical application to neuromuscular diseases. *Clin. Neurophysiol.* 117, 1902–1916. doi:10.1016/j.clinph.2006.01.018.

Paillard, J., and Brouchon, M. (1968). Active and passive movements in the calibration of position sense. *Neuropsychol. Spat. oriented Behav.* 11, 37–55.

Patil, S., Raza, W. A., Jamil, F., Caley, R., and O'connor, R. J. (2015). Functional electrical stimulation for the upper limb in tetraplegic spinal cord injury: A systematic review. *J. Med. Eng. Technol.* 39, 419–423. doi:10.3109/03091902.2015.1088095.

Pfurtscheller, G., and Lopes da Silva, F. H. (1999). Event-related EEG/MEG synchronization and desynchronization: basic principles. *Clin. Neurophysiol.* 110, 1842–1857. doi:10.1016/S1388-2457(99)00141-8.

Pozo, K., and Goda, Y. (2010). Unraveling mechanisms of homeostatic synaptic plasticity. *Neuron* 66, 337–351. doi:10.1016/j.neuron.2010.04.028.

Purves, D., Augustine, G. J., Fitzpatrick, D., Hall, W. C., LaMantia, A. S., McNamara, J. O., et al. (2004). *Neuroscience*. 3rd ed. Sunderland, Massachusetts U.S.A.: Sinauer Associates. Inc. doi:10.1111/j.1365-2486.2006.01288.x.

Quandt, F., and Hummel, F. C. (2014). The influence of functional electrical stimulation on hand motor recovery in stroke patients: A review. *Exp. Transl. Stroke Med.* 6, 1–7. doi:10.1186/2040-7378-6-9.

Ramos-Murguialday, A., and Birbaumer, N. (2015). Brain oscillatory signatures of motor tasks. *J. Neurophysiol.* 113, 3663–3682. doi:10.1152/jn.00467.2013.

Ray, A. M., Figueiredo, T. D., López-Larraz, E., Birbaumer, N., and Ramos-Murguialday, A. (2020). Brain oscillatory activity as a biomarker of motor recovery in chronic stroke. *Hum. Brain Mapp.* 41, 1296–1308. doi:doi:10.1002/hbm.24876.

Reynolds, C., Osuagwu, B. A., and Vuckovic, A. (2015). Influence of motor imagination on cortical activation during functional electrical stimulation. *Clin. Neurophysiol.*

126, 1360–1369. doi:10.1016/j.clinph.2014.10.007.

Ritter, P., Moosmann, M., and Villringer, A. (2009). Rolandic alpha and beta EEG rhythms' strengths are inversely related to fMRI-BOLD signal in primary somatosensory and motor cortex. *Hum. Brain Mapp.* 30, 1168–1187. doi:10.1002/hbm.20585.

Sasaki, R., Kotan, S., Nakagawa, M., Miyaguchi, S., Kojima, S., Saito, K., et al. (2017). Presence and absence of muscle contraction elicited by peripheral nerve electrical stimulation differentially modulate primary motor cortex excitability. *Front. Hum. Neurosci.* 11, 1–9. doi:10.3389/fnhum.2017.00146.

Schabrun, S. M., Ridding, M. C., Galea, M. P., Hodges, P. W., and Chipchase, L. S. (2012). Primary Sensory and Motor Cortex Excitability Are Co-Modulated in Response to Peripheral Electrical Nerve Stimulation. *PLoS One* 7, 1–7. doi:10.1371/journal.pone.0051298.

Schaworonkow, N., Caldana Gordon, P., Belardinelli, P., Ziemann, U., Bergmann, T. O., and Zrenner, C. (2018). μ-Rhythm Extracted With Personalized EEG Filters Correlates With Corticospinal Excitability in Real-Time Phase-Triggered EEG-TMS. *Front. Neurosci.* 12, 1–6. doi:10.3389/fnins.2018.00954.

Schürholz, M., Rana, M., Robinson, N., Ramos-Murguialday, A., Cho, W., Rohm, M., et al. (2012). Differences in hemodynamic activations between motor imagery and upper limb FES with NIRS. in *2012 Annual International Conference of the IEEE Engineering in Medicine and Biology Society*, 4728–4731. doi:10.1109/EMBC.2012.6347023.

Sebastián-Romagosa, M., Udina, E., Ortner, R., Dinarès-Ferran, J., Cho, W., Murovec, N., et al. (2020). EEG Biomarkers Related With the Functional State of Stroke Patients. *Front. Neurosci.* 14, 1–16. doi:10.3389/fnins.2020.00582.

Shibasaki, H., and Hallett, M. (2006). What is the Bereitschaftspotential? *Clin. Neurophysiol.* 117, 2341–2356. doi:10.1016/j.clinph.2006.04.025.

Smith, G. V., Alon, G., Roys, S. R., and Gullapalli, R. P. (2003). Functional MRI determination of a dose-response relationship to lower extremity neuromuscular electrical stimulation in healthy subjects. *Exp. Brain Res.* 150, 33–39. doi:10.1007/s00221-003-1405-9.

Tangwiriyasakul, C., Verhagen, R., Rutten, W. L. C., and van Putten, M. J. A. M. (2014). Temporal evolution of event-related desynchronization in acute stroke: A pilot study. *Clin. Neurophysiol.* 125, 1112–1120. doi:10.1016/j.clinph.2013.10.047.

Tu-Chan, A. P., Natraj, N., Godlove, J., Abrams, G., and Ganguly, K. (2017). Effects of somatosensory electrical stimulation on motor function and cortical oscillations. *J. Neuroeng. Rehabil.* 14, 1–9. doi:10.1186/s12984-017-0323-1.

Veldman, M. P., Maffiuletti, N. A., Hallett, M., Zijdewind, I., and Hortobágyi, T. (2014). Direct and crossed effects of somatosensory stimulation on neuronal excitability and motor performance in humans. *Neurosci. Biobehav. Rev.* 47, 22–35. doi:10.1016/j.neubiorev.2014.07.013.

Vidaurre, C., Klauer, C., Schauer, T., Ramos-Murguialday, A., and Müller, K.-R. (2016). EEG-based BCI for the linear control of an upper-limb neuroprosthesis. *Med. Eng. Phys.* 38, 1195–1204. doi:10.1016/j.medengphy.2016.06.010.

Vidaurre, C., Ramos-Murguialday, A., Haufe, S., Gómez-Fernández, M., Müller, K. R., and Nikulin, V. V. (2019). Enhancing sensorimotor BCI performance with assistive afferent activity: An online evaluation. *Neuroimage* 199, 375–386. doi:10.1016/j.neuroimage.2019.05.074.

Walter, A., Ramos-Murguialday, A., Rosenstiel, W., Birbaumer, N., and Bogdan, M. (2012). Coupling BCI and cortical stimulation for brain-state-dependent stimulation: methods for spectral estimation in the presence of stimulation after-effects. *Front. Neural Circuits* 6, 87. doi:10.3389/fncir.2012.00087.

Wegrzyk, J., Ranjeva, J. P., Fouré, A., Kavounoudias, A., Vilmen, C., Mattei, J. P., et al. (2017). Specific brain activation patterns associated with two neuromuscular electrical stimulation protocols. *Sci. Rep.* 7, 1–13. doi:10.1038/s41598-017-03188.

Wolpaw, J. R., Birbaumer, N., McFarland, D. J., Pfurtscheller, G., and Vaughan, T. M. (2002). Brain-computer interfaces for communication and control. *Clin. Neurophysiol.* 113, 767–91. doi:10.1016/S1388-2457(02)00057-3.

Yang, J.-D., Liao, C.-D., Huang, S.-W., Tam, K.-W., Liou, T.-H., Lee, Y.-H., et al. (2019). Effectiveness of electrical stimulation therapy in improving arm function after stroke: a systematic review and a meta-analysis of randomised controlled trials. *Clin. Rehabil.*, 0269215519839165. doi:10.1177/0269215519839165.

Young, D., Willett, F., Memberg, W. D., Murphy, B., Walter, B., Sweet, J., et al. (2018). Signal processing methods for reducing artifacts in microelectrode brain recordings caused by functional electrical stimulation. *J. Neural Eng.* 15, 026014. doi:10.1088/1741-2552/aa9ee8.

Zrenner, C., Desideri, D., Belardinelli, P., and Ziemann, U. (2018). Real-time EEG-defined excitability states determine efficacy of TMS-induced plasticity in human motor cortex. *Brain Stimul.* 11, 374–389. doi:10.1016/j.brs.2017.11.016.

5. Chapter 5: Quantifying the effect of trans-spinal magnetic stimulation on spinal excitability

This manuscript has been published as (Insausti-Delgado et al., 2019).

5.1 Abstract

During the last decades, spinal cord stimulation (SCS) has attracted much attention due to its capability to modulate the motor and sensory networks. The potential of this technique has been proved, and several investigations have focused on applying it for restoring lower-limb function. The majority of SCS approaches are based on electrical stimulation, and few studies have explored magnetic fields for non-invasive SCS. This paper presents a trans-spinal magnetic stimulation (ts-MS) protocol and studies its effects on spinal circuits with seven healthy subjects, considering central and peripheral nervous systems. Motor evoked potentials (MEP) and trans-spinal motor evoked potentials (ts-MEP) were assessed before and after the ts-MS intervention to characterize excitatory responses. After the intervention, we found an increase of almost 30% (not statistically significant) in MEP amplitude, but no changes in ts-MEP amplitude. Further research is required to confirm, in a larger population of subjects, the potential of this technology, which could be used to improve rehabilitation therapies for patients with motor disabilities.

5.2 Introduction

Much research in last decades has focused on the neuromodulation of the excitability of spinal cord neural circuits for rehabilitation of patients with motor disabilities, such as spinal cord injury (SCI) (Hofstoetter et al., 2014; Minassian and Hofstoetter, 2016a). Spinal cord stimulation (SCS) has appeared as a powerful technology to induce changes in the spinal circuits (Zimmermann and Jackson, 2014; Alam et al., 2017), which could result in motor recovery of patients with motor impairments (Angeli et al., 2014; Grahn et al., 2017). Therefore, there is a considerable

increasing interest in understanding how the stimulation interacts not only with spinal networks, but also with cortico-muscular circuits, in order to design optimal SCS interventions for rehabilitation after paralysis.

Numerous investigations based on electrical stimulation, both invasive (i.e., epidural) (Angeli et al., 2014; Grahn et al., 2017) and non-invasive (i.e., transcutaneous) (Hubli et al., 2013; Hofstoetter et al., 2014; Powell et al., 2018), have evidenced the capability of SCS to neuromodulate the spinal networks. Magnetic stimulation has also been presented as a non-invasive approach to stimulate the spinal circuits (Matsumoto et al., 2013) and an adequate protocol design of repetitive trans-spinal magnetic stimulation (ts-MS) demonstrated facilitation of locomotion (Gerasimenko et al., 2010; Sasada et al., 2014).

However, little is still known about how the ts-MS affects spinal circuits and interacts with the central and peripheral nervous system. So far, few studies have addressed this question, and they mostly investigated the effects of stimulation on peripheral reflexes (Nielsen and Sinkjaer, 1997; Knikou, 2013). Filling this gap of knowledge is of great relevance since it would help us to understand the effects of electromagnetic stimulation on sensorimotor neural networks and lead us to design better rehabilitation therapies based on ts-MS for lower-limb impairment.

In the present study, we aim at evaluating the effect of ts-MS on the excitability of spinal neural networks and its influence in cortico-spino-muscular tracts. For this purpose, we recruited 7 healthy subjects who underwent one session of ts-MS. In order to characterize the neurophysiological effects of the stimulation on central and peripheral nervous system, motor evoked potentials (MEPs) and trans-spinal motor evoked potentials (ts-MEPs) were recorded before and after the intervention (0 min and 30 min after finishing the stimulation).

5.3 Methods

5.3.1 Subjects

Seven healthy subjects with no neurological disorders and full leg mobility were involved in one experimental session. The study was conducted at the University of Tübingen (Germany), and ethical approval for the experimental procedure was provided by the ethics committee of the Faculty of Medicine of the University of Tübingen. All subjects gave written informed consent before participating in the study.

5.3.2 Experimental design and procedure

The subjects were asked to sit comfortably on a chair with their back straight, and their knee and ankle joint angles at 120º and 90º, respectively. Maintaining the body posture during all the session, especially during the measurements, is essential for the robustness of the measurements, and the subjects were requested to keep it.

The subjects underwent an intervention of trans-spinal magnetic stimulation (ts-MS), and electrophysiological assessments were conducted before and after to measure the effects of the stimulation on the excitability of the motor networks. The intervention consisted of 20 trials, which started with 7 seconds without stimulation followed by 5 seconds with stimulation. In total, the intervention lasted 4 minutes, from which 1 min 40 sec corresponded to stimulation (2000 pulses delivered in total). The subjects were instructed to be relaxed during the whole intervention, without performing any motor command. For the electrophysiological assessments, motor evoked potentials (MEP) and trans-spinal motor evoked potentials (ts-MEP) were recorded. These assessments were conducted three times, one before the intervention (Pre), one right after concluding the intervention (Post0) and one 30 min afterwards (Post30).

5.3.3 Trans-spinal magnetic stimulation (ts-MS)

Given the unnatural (and sometimes unpleasant) feeling that ts-MS can induce, and to ensure that all the subjects could bear the stimulation, all of them performed a

familiarization session of ts-MS one day before the experiment. The stimulation setup consisted of a circular coil (90 mm diameter powered by a Rapid2 magnetic stimulator (MagStim, UK). Before starting the session, the experimenter localized and marked the vertebrae from T12 to L5 following anatomical landmarks. The coil was centrally placed over the midline of T12 and moved downwards in steps of one vertebra. Single pulses above the motor threshold were applied in each location, and the spot eliciting largest evoked potentials in the right soleus muscle was selected and marked as hotspot for the experiment. The motor threshold (Mth) for each participant was defined as the minimum stimulator output intensity required for inducing at least 5 evoked potentials of at least 50 mV out of 10 consecutive stimuli on the selected stimulation spot. During the intervention, continuous magnetic stimulation was delivered at 20 Hz (following (Sasada et al., 2014)) on the hot-spot at the motor threshold intensity.

5.3.4 Data acquisition

Electromyographic (EMG) activity of both legs was registered using Ag/AgCl bipolar electrodes (Myotronics- Noromed, Tukwila, WA, USA) with 2 cm inter-electrode space. The EMG of four muscles (*vastus medialis, tibialis anterior, soleus and gastrocnemius medialis*) was acquired at a sampling rate of 5 kHz using an MR-compatible bipolar amplifier (BrainProducts GmbH, Germany). Ground electrode was placed on the right *peroneal malleolus*.

5.3.5 Assessments of excitability

1) Motor evoked potentials (MEP): The strength of the descending volleys from the cortex to the target muscle along the cortico-muscular pathway can be assessed through MEPs. The Rapid2 magnetic stimulator with a double cone coil (110mm diameter) was employed to stimulate the area projecting to the right soleus muscle on the left primary motor cortex. The scalp of each subject was registered and used in a neuronavigation system (Localite, GmbH, Germany) in order to plan and control the stimulation spot during the entire session. The standardized procedure described in (Groppa et al., 2012) was followed to determine the cortical motor threshold (CMth) as the minimum stimulation intensity needed to elicit 5 evoked potentials of at least 50 mV

out 10 stimuli. In pre- and postintervention assessments, 10 MEP repetitions at 120% of CMth were applied at a rate of one pulse every 5 to 5.5 seconds.

2) Trans-spinal motor evoked potentials (ts-MEP): The assessment of peripheral neural networks was conducted eliciting volleys from the spinal cord to the target muscle using the Rapid2 magnetic stimulator and the 90 mmcircular coil. The determination of the stimulation spot at the lumbar level and the calculation of the Mth were realized as explained in section 5.3.3. A permanent marker was used to draw reference lines on the skin to reduce variability during coil positioning. Ten trials of ts-MEPs were delivered at 120% of the spinal Mth in pre- and post-intervention assessments every 5 to 5.5 seconds.

5.3.6 Data analysis

The EMG activity of the soleus muscle was band-pass filtered between 10 and 1000 Hz with a 2nd order Butterworth filter. MEP and ts-MEP trials from pre- and post-assessments were separately averaged for each subject. We measured the efficacy of cortico-spino-muscular tracts by analyzing the amplitude of the MEPs, as the peak-to-peak difference from the most negative to the most positive deflection, and the latency of the MEPs applying the cumulative sum technique on the rectified signal (Brinkworth and Türker, 2003). Similarly, we assessed the efficacy of spino-muscular tracts by analyzing the amplitude and latency of the ts-MEPs. In addition, subtracting the onset of ts-MEPs from the onset of MEPs, we obtained the central motor conduction time (CMCT), which reflects the processing time of the cortico-spinal segment (Groppa et al., 2012).

We conducted statistical analyses (Friedman’s test for related samples) to assess the effects before (Pre) and after the intervention (Post0 and Post30) for the five outcome measurements: peak-to-peak amplitude and latency of MEPs and ts-MEPs, and the CMCT.

5.4 Results

The optimal stimulation spot was found in L4-L5 intervertebral spaces for all the subjects, resulting in spinal-roots stimulation as presented in (Matsumoto et al., 2013).

5.4.1 Influence of ts-MS in cortico-spino-muscular tracts

Figure 5.1a shows the mean±std of the MEPs in the soleus muscle from an illustrative subject before and after the intervention. The mean peak-to-peak amplitude of the MEPs across all participants increased 29.42% for Post0 and 28.97% for Post30 with respect to the baseline (preintervention). The boxplots in Figure 5.2a display the distribution of the MEP amplitudes for all the subjects in the three performed assessments. The changes in amplitude between the three assessments were not statistically significant (χ^2 (2) = 2.0; p = 0.37). The latencies of the MEPs remained more stable after the intervention (0.17% decrease for Post0 and 1.26% decrease for Post30, see Figure 5.2b). These latencies were not significantly different between the three assessments (χ^2 (2) = 3.12; p = 0.21).

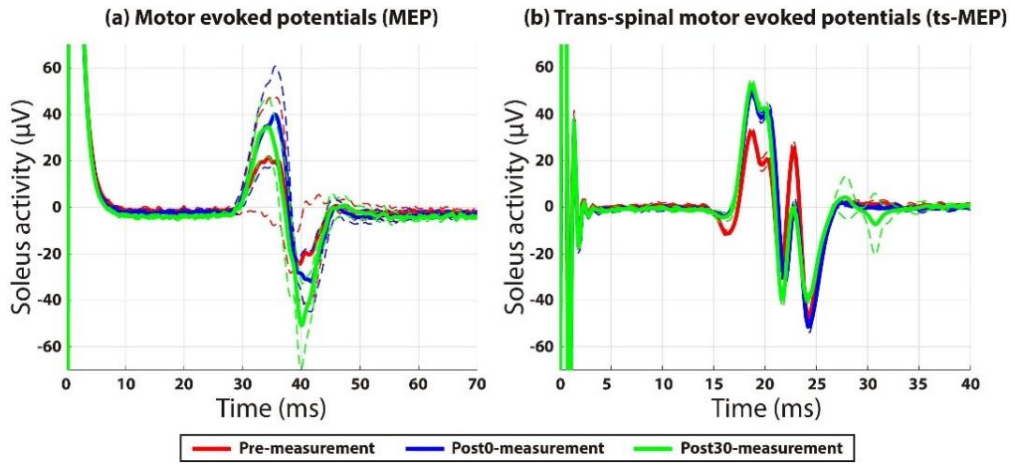

Figure 5.1: Mean (solid line) ± std (dashed line) of the (a) MEPs and of the (b) ts-MEPs from an illustrative subject in the right soleus muscle. Pre-, Post0- and Post30-assessments are represented in red, blue and green, respectively. Note the stimulation artifact at 0 ms.

5.4.2 Influence of ts-MS in spino-muscular tracts

The mean±std of the ts-MEPs in the soleus muscle before and after intervention from an illustrative subject is presented in Figure 5.1b. The changes in ts-MEP amplitude across all participants were lower than for the MEPs. In Post0, there was an increase of 3.20% in ts-MEP amplitude, while in Post30 it increased to 10.71% with respect to Pre (see Figure 5.2c). The amplitudes of the ts-MEPs were not significantly different between the three assessments (χ^2 (2) = 1.14; p = 0.56). The latencies of the ts-MEP were also

stable after the intervention (0.69% increase for Post0 and 3.65% increase for Post30, see Figure 5.2d). The ts-MEPs latencies were not significantly different between the three assessments (χ^2 (2) = 2.27; p = 0.32).

5.4.3 Influence of ts-MS in cortico-spinal tracts

For the assessment of cortico-spinal tracts, we determined the conduction time. The CMCT, as the other latency assessments, remained stable with respect to before the intervention: 0.97% decrease in Post0 and 5.77% decrease in Post30 (see Figure 5.2e). The CMCT was not significantly different between the three assessments (χ^2 (2) = 3.43; p = 0.18).

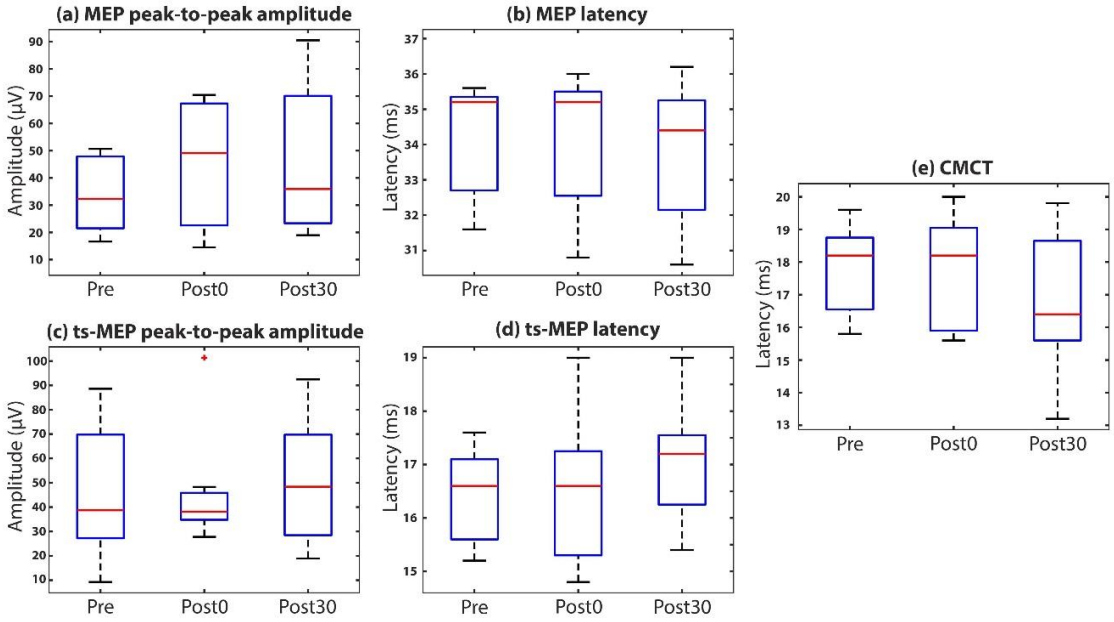

Figure 5.2: Changes in (a) MEP amplitude, (b) MEP latency, (c) ts-MEP amplitude, (d) ts-MEP latency and (e) CMCT for right soleus across all participants displayed in boxplots. The red lines represent the median of the distribution, and the blue boxes represent the 25th and 75th-percentiles, respectively.

5.5 Discussion and conclusions

The objective of the present study was to investigate whether cortico-spino-muscular neural networks can be modulated by trans-spinal magnetic stimulation (ts-MS) in healthy subjects. With this aim, we proposed a ts-MS intervention and evaluated its effects on synaptic efficacy in healthy subjects.

There is not much evidence in the literature about detailed quantification of electrophysiological effects induced by magnetic spinal cord stimulation. In general, studies propose setups that are specific to certain applications, which hinders results comparison. A study by Nielsen and Sinkjær proposed thoracic (T8) stimulation with a train of 16 stimuli at 25Hz with an intensity of 60% of maximum stimulator output (Nielsen and Sinkjaer, 1997). They measured the effects on MEP amplitude at different intervals (10 to 25000 ms) following the intervention in three healthy subjects, and only one out of the three subjects showed an increase in soleus MEP amplitude. Further, they proposed another stimulation protocol, in which repetitive magnetic stimulation was delivered for 5 min at 25 Hz in sequences of 5 seconds of stimulation and 5 seconds of rest. They did not use MEPs, but H-reflexes to characterize the effect of the magnetic stimulation, observing an initial amplitude increase, followed by an amplitude decrease 8 min after the intervention that remained even 30 min later (Nielsen and Sinkjaer, 1997). A more recent study by Knikou recorded single pulses of ts-MS over thoracic (T10) and assessed the neurophysiological changes by amplitude of soleus H-reflex in intervals of milliseconds before and after the stimulation (Knikou, 2013). Their results are in line with the ones of Nielsen and Sinkjær, confirming that ts-MS can decrease amplitude or inhibit spinal reflexes. These studies could be complementary to our results as long as the differences in ts-MS protocols and neurophysiological assessments (i.e., reflexive responses instead of motor pathways) are considered.

We observed that MEP peak-to-peak amplitudes increased almost 30% after the intervention, while the changes in the other metrics were less pronounced. However, none of these changes was statistically significant. Therefore, this study does not provide conclusive evidence about the potential of ts-MS to enhance the excitability of the motor networks. It should be further disclosed with new experiments whether the lack of statistical significance in our results is due to a real absence of an effect after the ts-MS, or to the lack of statistical power due to the low number of recruited subjects. Nevertheless, the potential of spinal cord stimulation is undeniable, with increasing evidence showing that it can be used to restore movement after complete paralysis (Angeli et al., 2014; Minassian and Hofstoetter, 2016b). The integration of this technology in closed-loop systems has already been successfully applied in animal

(Capogrosso et al., 2016) and human models (Wagner et al., 2018). Developments for improving the integration of spinal stimulation with non-invasive brain-controlled systems (Insausti-Delgado et al., 2017) is also an attractive field of research that may serve to improve future motor rehabilitation therapies (Alam et al., 2016). Future research continuing this work should focus on investigating in a larger number of subjects the effects of ts-MS on excitatory and inhibitory mechanisms. A more detailed assessment, including reflexes and sensory processing could also provide a better characterization of the whole sensorimotor network (Insausti-Delgado et al., 2018) in response to ts-MS. Finally, the influence of the protocol parameters such as the duration, intensity and frequency of stimulation or the number of pulses administered need to be investigated in order to have a clear understanding of the effects of spinal cord stimulation and expedite their application to rehabilitation.

5.6 Acknowledgments

This study was funded by the Bundesministerium für Bildung und Forschung BMBF MOTORBIC (FKZ 13GW0053) and AMORSA (FKZ 16SV7754), the Deutsche Forschungsgemeinschaft (DFG), the fortüne-Program of the University of Tübingen (2422-0-1 and 2452-0-0), and the Basque Government Science Program (EXOTEK: KK 2016/00083). The work of A. Insausti-Delgado was funded by the Basque Government's scholarship for predoctoral students.

5.7 References

Alam, M., Garcia-alias, G., Jin, B., Keyes, J., Zhong, H., Roy, R. R., et al. (2017). Electrical neuromodulation of the cervical spinal cord facilitates forelimb skilled function recovery in spinal cord injured rats. *Exp. Neurol.* 291, 141–150. doi:10.1016/j.expneurol.2017.02.006.

Alam, M., Rodrigues, W., Ngoc, B., and Thakor, N. V (2016). Brain-machine interface facilitated neurorehabilitation via spinal stimulation after spinal cord injury : Recent progress and future perspectives. *Brain Res.* 1646, 25–33. doi:10.1016/j.brainres.2016.05.039.

Angeli, C. A., Edgerton, V. R., Gerasimenko, Y. P., and Harkema, S. J. (2014). Altering spinal cord excitability enables voluntary movements after chronic complete paralysis in humans. *Brain* 137, 1394–1409. doi:10.1093/brain/awu038.

Brinkworth, R. S. A., and Türker, K. S. (2003). A method for quantifying reflex responses from intra-muscular and surface electromyogram. *J. Neurosci. Methods* 122, 179–193. doi:10.1016/S0165-0270(02)00321-7.

Capogrosso, M., Milekovic, T., Borton, D., Wagner, F., Martin Moraud, E., Mignardot, J.-B., et al. (2016). A brain–spine interface alleviating gait deficits after spinal cord injury in primates. *Nature* 539, 284–288. doi:10.1038/nature20118.

Gerasimenko, Y., Gorodnichev, R., Machueva, E., Pivovarova, E., Semyenov, D., Savochin, A., et al. (2010). Novel and direct access to the human locomotor spinal circuitry. *J. Neurosci.* 30, 3700–3708. doi:10.1523/JNEUROSCI.4751-09.2010.

Grahn, P. J., Lavrov, I. A., Sayenko, D. G., Straaten, M. G. Van, Gill, M. L., Strommen, J. A., et al. (2017). Enabling Task-Specific Volitional Motor Functions via Spinal Cord Neuromodulation in a Human With Paraplegia. *Mayo Clin. Proc.* 92, 544–554. doi:10.1016/j.mayocp.2017.02.014.

Groppa, S., Oliviero, A., Eisen, A., Quartarone, A., Cohen, L. G., Mall, V., et al. (2012). A practical guide to diagnostic transcranial magnetic stimulation: Report of an IFCN committee. *Clin. Neurophysiol.* 123, 858–882. doi:10.1016/j.clinph.2012.01.010.

Hofstoetter, U. S., McKay, W. B., Tansey, K. E., Mayr, W., Kern, H., and Minassian, K. (2014). Modification of spasticity by transcutaneous spinal cord stimulation in individuals with incomplete spinal cord injury. *J. Spinal Cord Med.* 37, 202–11. doi:10.1179/2045772313Y.0000000149.

Hubli, M., Dietz, V., Bolliger, M., Schrafl-Altermatt, M., and Bolliger, M. (2013). Modulation of spinal neuronal excitability by spinal direct currents and locomotion after spinal cord injury. *Clin. Neurophysiol.* 124, 1187–1195. doi:10.1016/j.clinph.2012.11.021.

Insausti-Delgado, A., López-Larraz, E., Bibián, C., Nishimura, Y., Birbaumer, N., and Ramos-Murguialday, A. (2017). Influence of trans-spinal magnetic stimulation in electrophysiological recordings for closed-loop rehabilitative systems. in *39th Annual International Conference of the IEEE Engineering in Medicine and Biology Society (EMBC)*, 2518–2521. doi:10.1109/EMBC.2017.8037369.

Insausti-Delgado, A., López-Larraz, E., Birbaumer, N., and Ramos-Murguialday, A. (2018). An exhaustive assessment to quantify changes in spinal excitability after spinal-cord stimulation. in *11th FENS Forum of Neuroscience*.

Knikou, M. (2013). Neurophysiological characteristics of human leg muscle action potentials evoked by transcutaneous magnetic stimulation of the spine. *Bioelectromagnetics* 34, 200–210. doi:10.1002/bem.21768.

Matsumoto, H., Hanajima, R., Terao, Y., and Ugawa, Y. (2013). Magnetic-motor-root stimulation: Review. *Clin. Neurophysiol.* 124, 1055–1067. doi:10.1016/j.clinph.2012.12.049.

Minassian, K., and Hofstoetter, U. S. (2016a). Spinal Cord Stimulation and Augmentative Control Strategies for Leg Movement after Spinal Paralysis in Humans. *CNS Neurosci. \& Ther.* 22, 262–270. doi:10.1111/cns.12530.

Minassian, K., and Hofstoetter, U. S. (2016b). Spinal Cord Stimulation and Augmentative Control Strategies for Leg Movement after Spinal Paralysis in Humans. 22, 262–270. doi:10.1111/cns.12530.

Nielsen, J. F., and Sinkjaer, T. (1997). Long-lasting depression of soleus motoneurons excitability following repetitive magnetic stimuli of the spinal cord in multiple sclerosis patients. *Mult. Scler. J.* 3, 18–30. doi:10.1177/135245859700300103.

Powell, E. S., Carrico, C., Salyers, E., Westgate, P. M., and Sawaki, L. (2018). The effect of transcutaneous spinal direct current stimulation on corticospinal excitability in chronic incompletespinal cord injury. *NeuroRehabilitation*, 1–10. doi:10.3233/NRE-172369.

Sasada, S., Kato, K., Kadowaki, S., Groiss, S. J., Ugawa, Y., Komiyama, T., et al. (2014). Volitional walking via upper limb muscle-controlled stimulation of the lumbar locomotor center in man. *J. Neurosci.* 34, 11131–11142. doi:10.1523/JNEUROSCI.4674-13.2014.

Wagner, F. B., Mignardot, J. B., Le Goff-Mignardot, C. G., Demesmaeker, R., Komi, S., Capogrosso, M., et al. (2018). Targeted neurotechnology restores walking in humans with spinal cord injury. *Nature* 563, 65–71. doi:10.1038/s41586-018-0649-2.

Zimmermann, J. B., and Jackson, A. (2014). Closed-loop control of spinal cord stimulation to restore hand function after paralysis. *Front. Neurosci.* 8, 1–8. doi:10.3389/fnins.2014.00087.

6. Chapter 6: Non-invasive brain-spine interface: continuous brain control of trans-spinal magnetic stimulation using EEG

This manuscript has been published as (Insausti-Delgado et al., 2020).

6.1 Abstract

Brain-controlled neuromodulation therapies have emerged as a promising tool to promote functional recovery in patients with motor disabilities. This neuromodulatory strategy is exploited by brain-machine interfaces and could be used for restoring lower-limb muscle activity or alleviating gait deficits. Towards a non-invasive approach for leg neurorehabilitation, we present a set-up that combines acquisition of electroencephalographic (EEG) activity to volitionally control trans-spinal magnetic stimulation (ts-MS). We engineered, for the first time, a non-invasive brain-spine interface (BSI) to contingently connect motor cortical activation during leg motor imagery with the activation of leg muscles via ts-MS. This novel brain-controlled stimulation was validated with 10 healthy participants who underwent one session including different ts-MS conditions. After a short screening of their cortical activation during lower-limb motor imagery, the participants used the closed-loop system at different stimulation intensities and scored system usability and comfort. We demonstrate the efficiency and robustness of the developed system to remove online stimulation artifacts from EEG regardless of ts-MS intensity used. All the participants reported absence of pain due to ts-MS and good usability. Our results also revealed that ts-MS controlled afferent and efferent intensity-dependent modulation of the nervous system. The here presented system represents a novel non-invasive means to neuromodulate peripheral nerve activity of lower limb using brain-controlled spinal stimulation.

6.2 Introduction

Spinal neural networks are in charge of generating locomotor patterns and have the capacity to modulate them even in the absence of brain control (Dimitrijevic et al., 1998; Hultborn and Nielsen, 2007; Edgerton and Roy, 2012). Targeting these self-regulated circuits, also known as central pattern generators (CPGs), for restoring lower-limb impairments is the goal of spinal neuromodulation approaches (Minassian et al., 2017; Taccola et al., 2018). During the last decades, invasive electrical stimulation of spinal neuronal pools has been investigated in animals (Ichiyama et al., 2005; Gerasimenko et al., 2008; Alam et al., 2017) and spinal cord injury (SCI) patients (Harkema et al., 2011; Grahn et al., 2017; Formento et al., 2018; Gill et al., 2018) to restore gait patterns.

In this line, magnetic stimulation of the spinal cord presents an alternative modality to neuromodulate the spinal networks non-invasively (Nardone et al., 2015b). In clinical environments, non-invasive magnetic stimulation has been widely used to investigate the central and peripheral nervous systems (Groppa et al., 2012; Nardone et al., 2015a; Rossini et al., 2015). Magnetic stimulation at the spinal level can activate peripheral motor axons at their exit from the spinal cord, evoking muscle action potentials (Ugawa et al., 1989; Knikou, 2013; Matsumoto et al., 2013). Given this knowledge, several studies evidenced the feasibility of repetitive trans-spinal magnetic stimulation (ts-MS) to induce locomotor rhythms using open-loop (Gerasimenko et al., 2010) or EMG-triggered protocols (Sasada et al., 2014; Nakao et al., 2015). However, these procedures lacked volitional and natural brain control.

Neural interfaces allow transferring volitional neural commands between different neuronal populations, bypassing the damaged pathways (Jackson and Zimmermann, 2012). Using brain activity to control the direct stimulation of the spinal cord below the injury level is a natural manner of mimicking the flow of the descending commands from the brain to the spine. This phenomenon has motivated the development of brain-spine interfaces (BSIs) that aim at artificially connecting brain and spinal neural networks to recover motor function (Borton et al., 2014; Zimmermann and Jackson, 2014; Bonizzato et al., 2018). The BSIs record neural activity of the brain reflecting

motor intentions and transform this activity into commands for spinal stimulation (Alam et al., 2016; Capogrosso et al., 2016, 2018; Yadav et al., 2020). These neural signatures associated with motor execution or motor attempt can be also detected even in patients with motor deficits (López-Larraz et al., 2015, 2018a), which makes them suitable for BSI control. In order to favor Hebbian plasticity and promote functional recovery, a timely linked brain activity encoding motor intention and peripheral afferent neural activation is essential (Nishimura et al., 2013a; Ramos-Murguialday et al., 2013; Mrachacz-Kersting et al., 2016; López-Larraz et al., 2018d; Kato et al., 2019). In BSIs, peripheral neural activity is generated by the spinal stimulation, modulating the excitability of spinal networks (Hubli et al., 2013; Hofstoetter et al., 2018) and generating muscular contractions of the limbs (Gerasimenko et al., 2018).

To date, BSIs have only been developed as implantable systems, and tested in animal experiments. Non-invasive BSIs would allow broadening this field of research, facilitating experimentation in healthy subjects and patients with motor disorders. Electroencephalography (EEG) constitutes the most common technique for non-invasive acquisition of brain signals. However, the low signal to noise ratio and artifacts often limit EEG applications. This problem aggravates when EEG is concurrently used with electromagnetic stimulation because it can contaminate the EEG signals and impede the estimation of cortical activity (Insausti-Delgado et al., 2021).

In the current study, we propose an innovative design for a non-invasive BSI, relying on the continuous EEG monitoring of brain activity, removal of stimulation artifacts by median filtering, and control of the trans-spinal magnetic stimulation (ts-MS) to volitionally (but artificially) contract lower-limb muscles. The system was tested and validated in 10 healthy participants, with 4 different stimulation conditions. As a proof of the feasibility of this interface, we report the evaluation of different indicators: *(i)* the performance, robustness and decoding accuracy of the BSI, *(ii)* the usability and perception of all the users, and *(iii)* the neurophysiological effects of the system.

6.3 Materials and methods

6.3.1 Participants

Ten healthy participants (4 females, age = 29.5 ± 4.67 years) with no neurological disorders and complete mobility of lower limbs were recruited for the study. All the participants provided written informed consent before starting the experiment, which was approved by the Ethics Committee of the Faculty of Medicine of the University of Tübingen (Germany).

The participants were comfortably seated on a chair, with their back straight and their right leg slightly extended, having the knee and ankle joint angles around 120° and 90°, respectively. A wedge-shaped structure was used to place the foot and ensure the angle of the leg was kept constant (Figure 6.1a). Neurophysiological activity was recorded by electroencephalography (EEG) and electromyography (EMG).

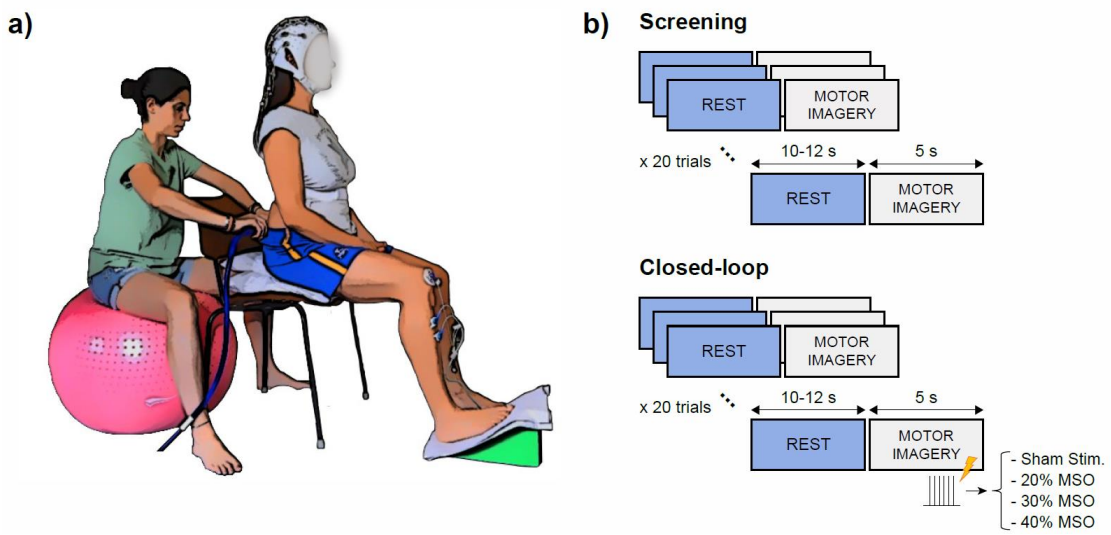

Figure 6.1: Experimental procedure. (a) Participant with the EEG system and EMG sensor on the right tibialis anterior (TA) muscle, and experimenter placing the coil for spinal stimulation. The experimenter in the picture is the first author of the paper and gives consent for publication of her image. (b) Block diagram of the two experiment phases: screening and closed-loop stimulation. Each phase included blocks of 20 trials, consisting of rest and motor imagery periods announced by an auditory cue of "Rest" and "Move", respectively. During the closed-loop phase, contingent ts-MS was applied at 20 Hz when the motor imagery was detected from the EEG of the participant. Each closed-loop block was executed with a fixed intensity: 20% of the maximum stimulator output (MSO), 30% of the MSO, 40% of the MSO, or sham stimulation.

6.3.2 Experimental design and procedure

Each participant performed one session, including a screening phase and a closed-loop stimulation phase (Figure 6.1b). The screening consisted of 2 blocks of 20 trials each, which included rest (10-12 s) and motor imagery (5 s) periods, each announced by an auditory cue of "Rest" and "Move", respectively. During rest, the participants were asked to relax and stay still without executing or imagining any movement. During motor imagery (MI), the participants were asked to perform kinesthetic motor imagery of the plantar dorsiflexion of the right leg (Neuper et al., 2005). The EEG data recorded during the screening was used to train a classifier to differentiate between the "rest" and "motor imagery" brain states.

The closed-loop stimulation phase consisted of 12 blocks of 20 trials each. We evaluated 4 stimulation conditions: 3 different ts-MS intensities and sham stimulation (further details in section 6.3.4). We recorded 3 blocks of each condition, randomizing the sequence of intensities across subjects, resulting in 60 trials of each intensity. The timing of the stimulation trials was identical to the screening trials. Closed-loop feedback was given according to the decoded brain patterns during the MI periods (note that the stimulation was off during resting periods).

6.3.3 Data acquisition

EEG activity was recorded with a commercial Acticap system (BrainProducts GmbH, Germany), with 32 channels placed on FP1, FP2, F7, F3, F4, F8, FC3, FC1, FCz, FC2, FC4, C5, C3, C1, Cz, C2, C4, C6, CP3, CP1, CPz, CP2, CP4, T7, T8, P7, P3, Pz, P4, P8, O1, and O2, following the international 10/20 system (Seeck et al., 2017). The ground and reference electrodes were located at FPz and Fz, respectively. The recording electrodes were connected to a monopolar BrainAmp amplifier (BrainProducts GmbH, Germany).

EMG activity from the right tibialis anterior (TA) muscle was recorded using Ag/AgCl bipolar electrodes (Myotronics-Noromed, Tukwila, Wa, USA) combined with an MR-compatible BrainAmp amplifier (BrainProducts GmbH, Germany). The

recording electrodes had an inter-electrode space of 4 cm. The ground electrode was placed on the right patella. All the signals were synchronously acquired at 1 kHz sampling rate.

6.3.4 Trans-spinal magnetic stimulation (ts-MS)

Due to the unnatural (and occasionally uncomfortable) sensation that the participants can experience with ts-MS, and to ensure that they were able to bear the stimulation, a familiarization session was conducted with all of them on a separate day before the experiment. We used a magnetic stimulator (Magstim Rapid2, Magstim Ltd, UK) with a circular coil (Magstim 90 mm Coil, Magstim Ltd, UK) to provide the ts-MS (biphasic single cosine cycle pulses of 400 μs).

Before starting the recording, we localized and marked the vertebrae from T12 to L5 according to anatomical landmarks. The circular coil was initially centered over the midline of the intervertebral space of T12 and shifted towards L5, advancing one vertebra in each step (coil currents directed clockwise). Single pulse stimulation was delivered above the motor threshold to locate the hot-spot of the TA muscle (i.e., the spot that led to the largest trans-spinal motor evoked potentials in 10 trials). This spot was marked for the closed-loop stimulation phase.

During the closed-loop phase, continuous brain-controlled ts-MS was applied at 20 Hz (Sasada et al., 2014). According to our previous experimental evidence, the spinal motor threshold (i.e., the minimum intensity needed for eliciting at least 5 motor evoked potentials out of 10 trials with at least 50 μV of peak-to-peak amplitude) lays between 25% and 40% of the maximum stimulator output (MSO) (Insausti-Delgado et al., 2018, 2019). According to these values, we defined 4 conditions for the closed-loop stimulation: *(i)* ts-MS at 20% of the MSO, *(ii)* ts-MS at 30% of the MSO, *(iii)* ts-MS at 40% of the MSO, and *(iv)* sham stimulation. For the sham stimulation, the experimenter held the coil 1 m away from the participant, so that the stimulation took place and the participants had auditory but no sensory feedback. In this sham condition, the stimulation was set to 30% of the MSO. For the three real ts-MS conditions, the coil was placed on the hot-spot.

6.3.5 Detection of movement intention

After the 2 screening blocks, a classifier was trained to discriminate between the brain states of rest and MI.

Data preprocessing

The EEG data were band-pass filtered with a 4th order Butterworth filter between 1 and 50 Hz. The signals were trimmed down to 15-second trials (from -10 s to +5 s with respect to the MI cue) and subsampled to 100 Hz. Optimized spatial filtering (OSF) was applied to improve the estimation of the task-related motor cortex activation. We considered 17 electrodes (from the 32 recorded) to measure this activation: FC3, FC1, FCz, FC2, FC4, C5, C3, C1, Cz, C2, C4, C6, CP3, CP1, CPz, CP2 and, CP4. The signal of these electrodes was band-pass filtered between 7 and 15 Hz (4th order Butterworth), to isolate the modulation of the alpha rhythm (López-Larraz et al., 2014). The OSF calibration consists of a gradient-descent optimization to find weights for the linear combination of electrodes that minimizes alpha power during MI and maximizes it during rest. This has been validated as an effective automated method to improve the measurement of event-related desynchronization (ERD) of sensorimotor activity during motor tasks (Graimann and Pfurtscheller, 2006b). The result of this process is a virtual channel that synthesizes the activation over the motor cortex. The OSF weights were computed using the trials of the screening phase and kept fixed during the closed-loop phase.

Feature extraction

A one-second sliding window, with 200 ms sliding-step, was applied to each 15-second trial of the OSF virtual channel in the interval [-3, -1] s for the rest class and [1, 3] s for the MI class (i.e., 6 windows per class and trial). The power spectrum between 1 Hz and 50 Hz was calculated for each of these windows using a 20th-order autoregressive (AR) model with 1 Hz resolution, based on the Burg algorithm (Burg, 1967). The most discriminant range of frequencies to separate between rest and MI classes was selected by visually inspecting the signed r-squared values (point-biserial correlation coefficients). Despite alpha ([7-15] Hz) and beta ([15-30] Hz) being generally the most

reactive frequency bands during MI, we restricted the selection of features to the alpha range only, to avoid the repetitive ts-MS at 20 Hz interfering with our brain features of interest. The power values within the selected frequency range were averaged, resulting in one unique feature.

All the extracted windows from the screening trials, transformed into one feature per window, were z-score normalized and fed to a linear discriminant analysis (LDA) classifier to distinguish between both classes.

Classification

During the closed-loop blocks, the classifier analyzed the EEG activity in real-time and activated the stimulator when the MI brain states were detected. A new block of EEG data arrived every 200 ms. This block was median-filtered (see details in 2.5.3.1), band-pass filtered between 1 and 50 Hz, OSF filtered (using the coefficients computed from the screening data), and appended to a one-second ring-buffer to compute the newest power output (following 2.5.2). The classifier determined whether this power output corresponded to rest or MI class and triggered ts-MS as long as MI was detected, providing continuous feedback. Note that the stimulation was deactivated during the rest periods, avoiding stimulation due to false positives.

To deal with EEG-nonstationarities and potential changes of cortical activation patterns due to ts-MS, we continuously updated the normalization coefficients of the features (initially, the mean and standard deviation of the training dataset). We kept two 48-second buffers, one for rest and one for MI, with the most recent features of these classes. The mean and standard deviation of these two buffers, concatenated together, were used as the normalization coefficients in each iteration before passing the feature vector to the classifier.

Median filtering for ts-MS contamination removal

Using electromagnetic currents for stimulating the nervous system can introduce undesirable noise to the neural activity. As characterized in (Insausti-Delgado et al., 2017), the ts-MS distorts the EEG recordings, introducing peaks of short duration (~10

ms) and large magnitude. A median filter is a suitable method for minimizing the influence of the ts-MS contamination in the EEG signal (Insausti-Delgado et al., 2017, 2021). We applied the median filter as a sliding window of 20 ms in one-sample steps, calculating the median value for each window. This filter attenuates these large peaks preserving the sensorimotor oscillatory activity. A detailed characterization of how this filter can be used to remove similar peaks due to electrical stimulation can be found in (Insausti-Delgado et al., 2021).

6.3.6 Decoding accuracy

The performance of the classifier for each participant was estimated in terms of average decoding accuracy, calculated as the mean of the true positive rate (TPR) and the true negative rate (TNR). The TPR quantifies the success of the classifier during the MI period, defined as the time interval [1, 4] s. The TNR measures the classifier success during the rest period, which was defined as the time interval [-4, -1] s.

6.3.7 Neurophysiological measurements

Our BSI has been devised to be used as a rehabilitative tool for patients that have motor impairments. For future interventions based on BSIs, the potential of these systems to interact with cortico-spinal and spino-muscular circuitry is a relevant aspect. With the data recorded during the closed-loop blocks, we conducted some neurophysiological measures to assess the interactions of the BSI with the nervous system.

Trans-spinal motor evoked potentials (ts-MEP)

Ts-MS can activate the peripheral nervous system, exciting the spinal nerves at their exit through the intervertebral foramina towards the muscles, resulting in ts-MEPs (Ugawa et al., 1989; Matsumoto et al., 2013). The recruitment of peripheral motor nerves was demonstrated by measuring the ts-MEPs at the tibialis anterior (TA) muscle during spinal stimulation. EMG signals were high-pass filtered at 10 Hz with a 4^{th} order Butterworth filter and trimmed down to 45-ms epochs (from -5 to 40 ms with respect to the stimulation pulse). Epochs corresponding to the same ts-MS intensity were pooled together and averaged for each subject. The peak-to-peak amplitude of the ts-MEPs for

each intensity was determined as the difference between the maximum and the minimum values of the averaged potential.

Trans-spinal somatosensory evoked potentials (ts-SEP)

Spinal stimulation can activate the sensory cortex via the ascending pathways from the spine, which can be quantified as ts-SEPs (Kunesch et al., 1993). The EEG activity of the CPz channel during closed-loop was high-pass filtered using a 4th order Butterworth filter at 3 Hz. Signals were aligned to the stimulation artifact and epoched to 45-ms periods (from -5 to 40 ms with respect to the ts-MS pulse). Epochs were grouped according to their intensity and averaged for each subject. The peak-to-peak amplitude of the averaged ts-SEP was calculated as the difference between the maximum and the minimum values for each ts-MS intensity.

6.3.8 Usability assessments

The participants were asked to evaluate the degree of pain, discomfort and concentration at the end of each closed-loop block. They had to grade between 0 (very low) and 10 (very high): *(i)* how painful the stimulation was, *(ii)* how uncomfortable the stimulation was, and *(iii)* how easy it was to perform the motor imagery while being stimulated.

6.3.9 Statistical analysis

We studied the effect of stimulation condition on the BSI performance and on the neurophysiological measurements. The Shapiro-Wilk test was used to determine the Gaussianity of the data. To assess the effect of stimulation on MI decoding accuracy, we used a repeated measures analysis of variance (ANOVA), with stimulation condition as factor (4 levels: ts-MS at 20% of the MSO, ts-MS at 30% of the MSO, ts-MS at 40% of the MSO, and sham stimulation) and decoding accuracy as dependent variable. Post-hoc comparisons were conducted using paired t-tests with Bonferroni correction. To evaluate the influence of the median filter on the BSI performance, we ran paired t-tests with filtering as factor (with and without median filter) and decoding accuracy as dependent variable for each stimulation condition. To study the influence of stimulation intensity on

the peak-to-peak amplitude of ts-MEPs and ts-SEPs we used Friedman's test (3 levels: ts-MS at 20% of the MSO, ts-MS at 30% of the MSO, ts-MS at 40% of the MSO). Paired post-hoc comparisons were performed using the Wilcoxon signed-rank test to analyze significant amplitude differences between intensity pairs. All the statistical tests were conducted in IBM SPSS 25.0 Statistics software (SPSS Inc., Chicago, IL, USA).

6.4 Results

6.4.1 Brain-spine interface control

Seven out of the ten subjects showed strong cortical activation patterns during MI in the screening data, revealed as a significant event-related desynchronization (ERD) in alpha and beta bands (Figure 6.2).

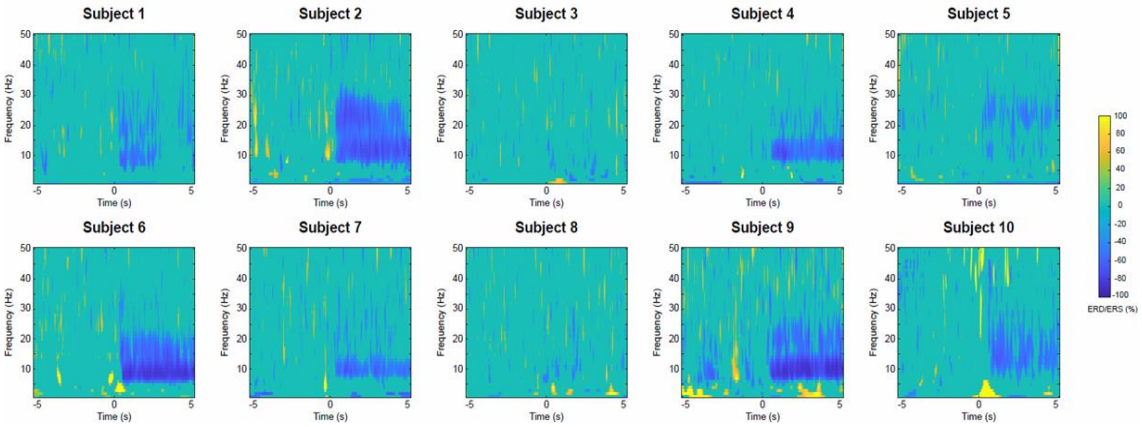

Figure 6.2: Cortical activation during motor imagery (computed from the screening blocks). Time-frequency maps for each individual, representing the event-related (de)synchronization ERD/ERS (Pfurtscheller and Lopes da Silva, 1999) of the optimized spatial filter (OSF) channel. Time 0 s represents the auditory cue to start the motor imagery.

Video 1 (Supplementary material in Insausti-Delgado et al., 2020a) shows one representative participant controlling the BSI. The participant was asked to rest or to perform MI of the right ankle dorsiflexion, guided by auditory cues. The EEG activity was processed (median filtered, band-pass filtered and OSF filtered) in real-time. To prove the efficacy of the system to remove online stimulation artifacts, the activity of the OSF channel with and without median filtering is displayed. The classifier triggered the ts-MS when the MI brain states were detected. Note that the stimulation was off during

resting periods. The experimenters in the video are the authors of the paper and give consent for publication of their video.

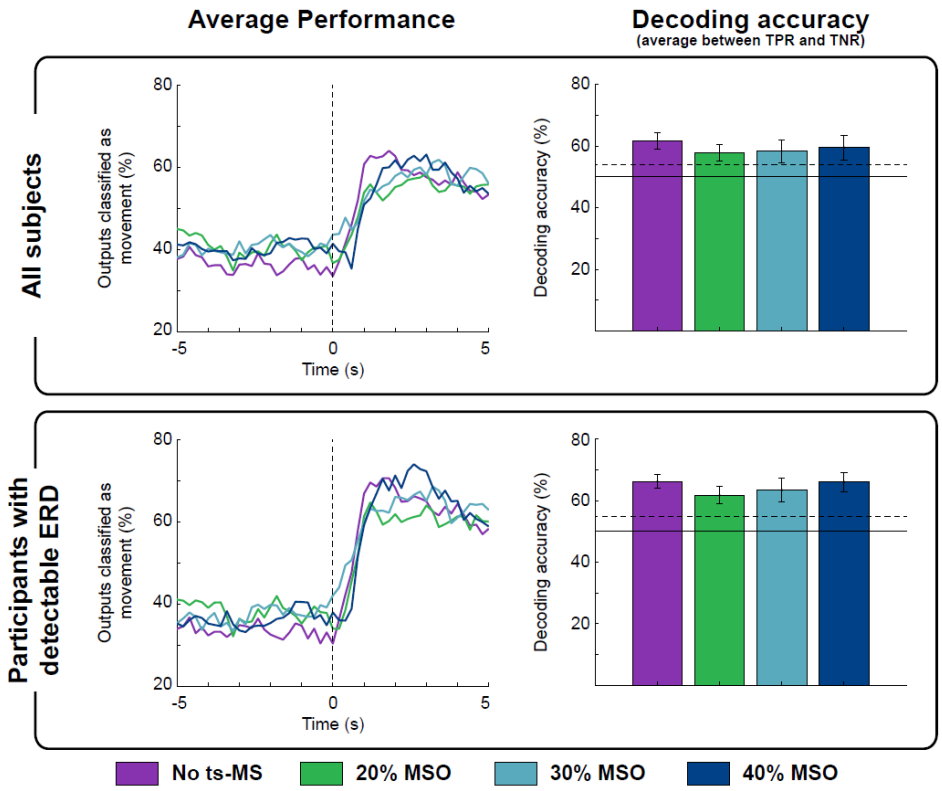

Figure 6.3: Average response of the classifier for all the stimulation conditions. (Left) Average time-response of the classifier for each stimulation condition. Each line represents the percentage of the outputs classified as motor imagery, averaged over all the participants. Notice that time 0 s is the beginning of the motor imagery period, and outputs prior to t=0 represent false positives, while outputs after t=0 mean true positives. (Right) Decoding accuracy, calculated as the mean between true negative rate (TNR) in the time interval [-1, -4] s and true positive rate (TPR) in the time interval [1, 4] s. The dashed line shows the confidence interval of the chance level (alpha = 0.05), calculated on the basis of all the test trials, according to (Müller-Putz et al., 2008). Panels show the values averaged for all the participants (top) and for the seven participants with detectable MI-related desynchronization in the alpha frequency band (bottom).

The average decoding accuracies for all the participants were 61.7%, 57.9%, 58.4% and 59.6% for sham stimulation, ts-MS at 20% of the MSO, ts-MS at 30% of the MSO and ts-MS at 40% of the MSO, respectively (Figure 6.3 top panel). There was no significant effect of stimulation condition on decoding accuracy, as revealed by the repeated measures ANOVA ($F(3, 27) = 1.912$, $p = 0.151$). As a post-hoc analysis, we discarded the data of the three participants who did not show a modulation of the sensorimotor alpha rhythm during MI in the screening phase (S3, S5 and S8). These three

participants had a decoding accuracy around chance level in the closed-loop phase for every stimulation condition. When we excluded them from the analysis, the average decoding accuracy increased up to 66.2%, 61.8%, 63.5% and 66.1%, respectively (Figure 6.3 bottom panel). These values were not significantly different between ts-MS intensities either (repeated measures ANOVA, $F(3, 18) = 2.008$, $p = 0.149$).

6.4.2 Effect of artifact removal

We also studied how ts-MS affects the cortical activity and the performance of the BSI. Stimulation artifacts distort the ongoing EEG activity, hindering its processing. The median filter effectively eliminated the high-amplitude peaks, allowing the quantification of sensorimotor modulation (Figure 6.4a). Figure 6.4b displays the estimated cortical activity of a representative participant during closed-loop ts-MS at 40% of the MSO (i.e., the highest stimulation intensity) with and without applying the median filtering. If the stimulation artifacts are not eliminated, they are observable in the EEG as a broadband event-related synchronization (ERS), or power increase, covering the frequencies of interest (Figure 6.4b left). Median filtering revealed the significant event-related desynchronization (ERD) of alpha and beta frequencies (Figure 6.4b right), which allowed the classifier to decode the MI (Figure 6.4c). We calculated the decoding accuracy of MI with and without median filter for each stimulation condition for those participants with detectable ERD. Paired t-tests revealed that applying the median filter led to significantly higher decoding accuracies in closed-loop ts-MS at 20% ($t(6) = -3.821$, $p = 0.009$), ts-MS at 30% ($t(6) = -5.215$, $p = 0.002$) and ts-MS at 40% of the MSO ($t(6) = -6.555$, $p = 0.001$) (Figure 6.4d).

6.4.3 Neurophysiological analysis

Trans-spinal motor evoked potentials (ts-MEP)

By analyzing the ts-MEPs, we assessed the neurophysiological effects of the stimulation on the peripheral nervous system (Figure 6.5a). We extracted the ts-MEPs from the closed-loop stimulation blocks (Figure 6.5b), and compared their amplitude according to the stimulation intensity (Figure 6.5c). The peak-to-peak amplitude of the

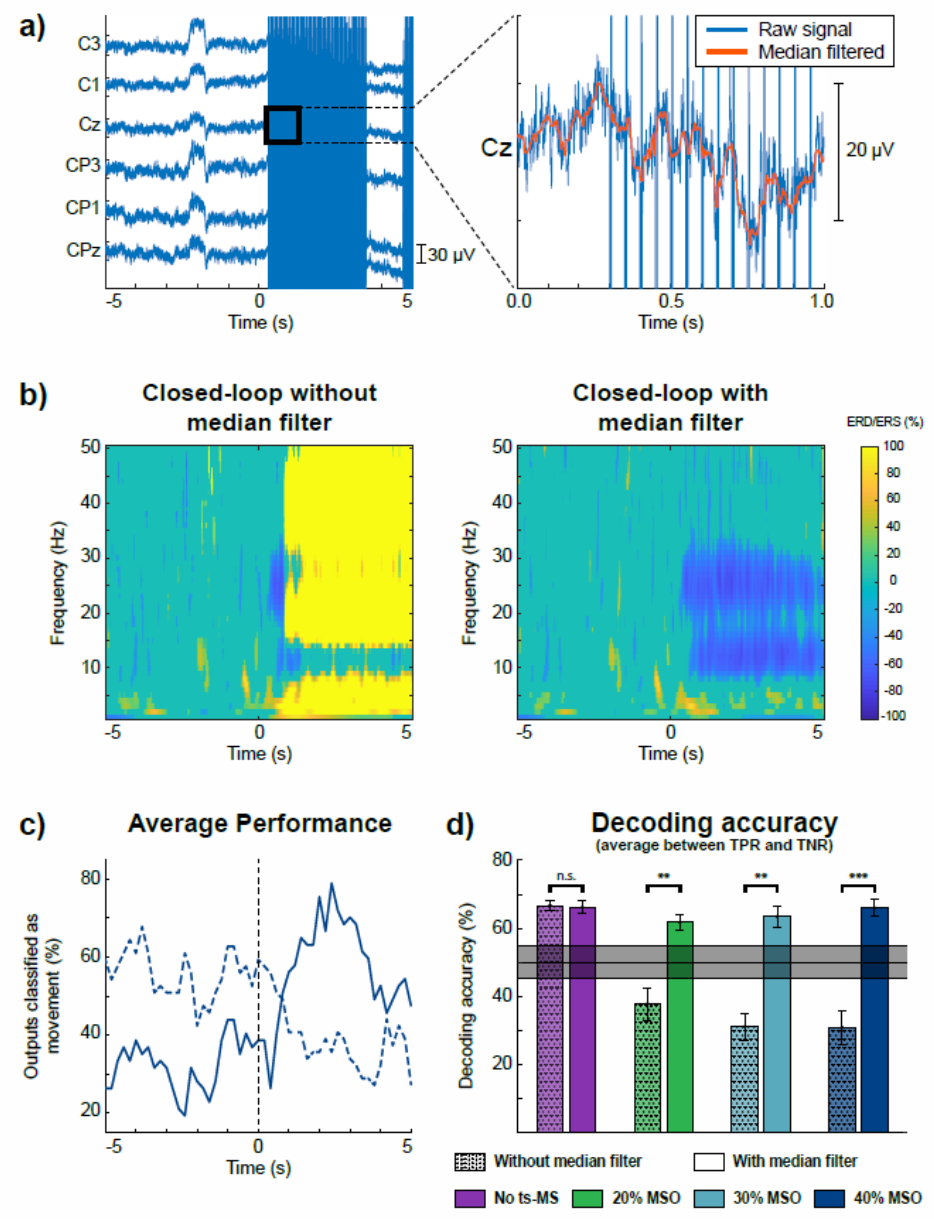

*Figure 6.4: Characterization of stimulation artifacts and their effects on cortical activity and decoding accuracy. The results for one representative participant are displayed in the most unfavorable scenario, with stimulation at 40% of the MSO. (a) EEG trace of one trial, showing the effect of the stimulation as high-amplitude artifacts. Zooming into a one-second segment, the details of the signal without (blue) or with (orange) median filtering can be appreciated. (b) Grand average time-frequency maps without (left) and with (right) median filter. Time 0 s corresponds to the onset of the motor imagery. (c) Average time-response of the classifier without (dashed) and with (solid) median filter. (d) Decoding accuracy calculated as the mean between TNR and TPR for each stimulation condition with and without median filter for the seven participants with detectable MI-related desynchronization in the alpha frequency band. The shaded gray area shows the confidence interval of the chance level (alpha = 0.05), calculated on the basis of all the test trials, according to (Müller-Putz et al., 2008). The asterisks indicate significant differences (** for p <0.01, *** for p <0.001) between decoding accuracies when median filtered is applied.*

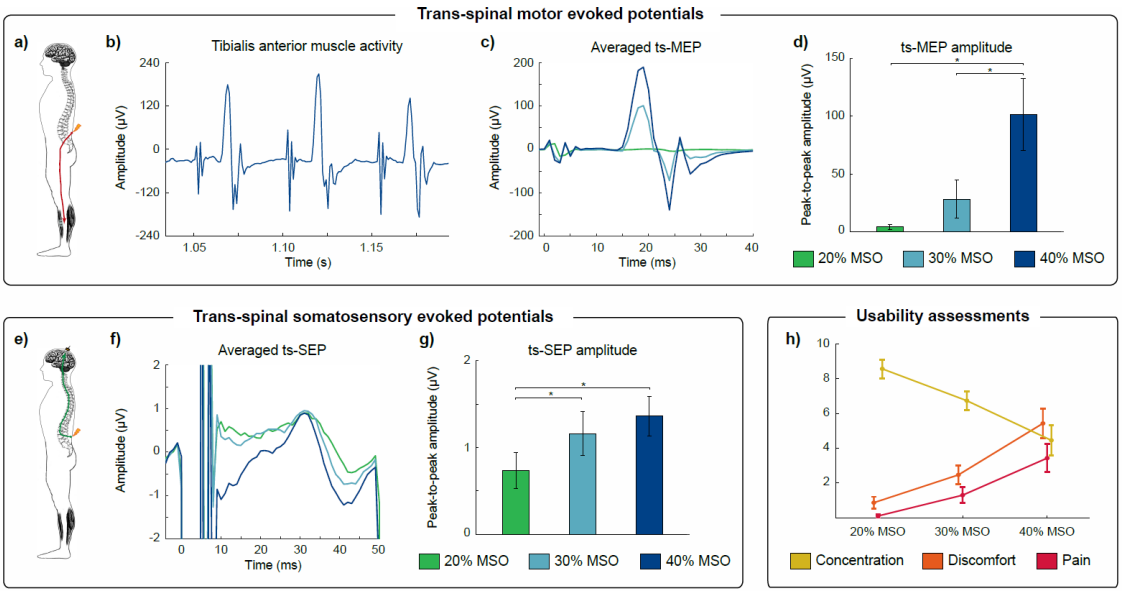

Figure 6.5: Neurophysiological and usability assessments. Upper panel, a) Recruitment of efferent pathways from the spine to the tibialis anterior (TA) muscle by ts-MS. b) EMG trace of the TA muscle of a representative participant during closed-loop stimulation at 40% ts-MS. The artifacts appear approximately at t = 1.05, 1.10 and 1.15 s (20 Hz stimulation), while the ts-MEPs are induced ~15 ms after the stimulation (peripheral motor conduction time from the spine to the TA). c) Average ts-MEPs of a representative participant for the three different stimulation intensities. d) Mean peak-to-peak amplitude of ts-MEPs and standard errors averaged over all participants for each stimulation intensity. The asterisks indicate significant (p < 0.05, Bonferroni corrected) differences in ts-MEP amplitude between ts-MS intensities. Bottom-left panel, e) Recruitment of afferent pathways from the spine to the cortex via ts-MS. f) Average ts-SEPs of a representative participant for the three different stimulation intensities. g) Mean peak-to-peak amplitude of ts-SEPs and standard errors averaged over all participants for each stimulation intensity. The asterisks indicate significant (p < 0.05, Bonferroni corrected) differences in ts-SEP amplitude between ts-MS intensities. Bottom-right panel, h) Usability scores for concentration, discomfort and pain, averaged over all participants

ts-MEPs was significantly affected by the intensity used (Friedman's $\chi^2(2) = 15.80$; $p < 0.001$). Post-hoc comparisons revealed significantly larger ts-MEPs amplitudes at 40% of the MSO compared to 20% ($Z = -2.803$, $p = 0.015$) and compared to 30% ($Z = -2.803$, $p = 0.015$) (Figure 6.5d).

Trans-spinal somatosensory evoked potentials (ts-SEP)

We computed the ts-SEPs to assess the neurophysiological effects of the stimulation on the central nervous system (Figure 6.5e). As for the ts-MEPs, we averaged the ts-SEPs for each subject, grouping by stimulation intensity. The ts-MS produced a positive peak with a latency of 30 ms and a negative peak at 40 ms (Figure 6.5f). The peak-to-peak amplitude of the ts-SEP was significantly affected by the stimulation

intensity (Friedman's $\chi^2(2) = 9.80$; $p = 0.007$). Post-hoc paired comparisons showed significantly smaller ts-SEPs when stimulating at 20% compared to 30% ($Z = -2.599$, $p = 0.027$) or 40% ($Z = -2.701$, $p = 0.021$) of the MSO (Figure 6.5g).

6.4.4 Usability assessments

Our descriptive analysis on usability shows that the participants perceived more discomfort and pain, and decreased concentration on the MI task, as the intensity of ts-MS increased (Figure 6.5h). All the participants described the stimulation at higher intensities as uncomfortable, rather than painful. No adverse effects due to ts-MS were reported by, or observed in, any of the participants.

6.5 Discussion

In this paper, we report on the first non-invasive brain-spine interface (BSI), based on the continuous control of trans-spinal magnetic stimulation (ts-MS) guided by EEG. Our BSI enables the direct association of cortical activity encoding motor intentions with the activation of afferent (from the spine to the somatosensory cortex) and efferent (from the spine to the lower-limb muscles) pathways. This natural approach to link brain activity with the peripheral nervous system could be used to exploit neuromodulatory mechanisms and might constitute a relevant tool for rehabilitation of patients with paralysis. The here presented findings provide sufficient basis towards designing, developing and further evaluating this innovative approach.

Brain-controlled spinal cord stimulation can potentially be employed for assistive or rehabilitative purposes by patients with lower-limb paralysis. Spinal cord stimulation has been used to neuromodulate the spinal circuitry, supporting motor recovery after lower-limb paralysis (Edgerton and Roy, 2012; Nardone et al., 2015b; Taccola et al., 2018). The first studies in animals evidenced the neuromodulatory properties of dorsal root stimulation of the spine (Budakova, 1972; Grillner and Zangger, 1979). Later investigations using epidural spinal stimulation supported previous findings and demonstrated the capacity of stimulation to enable standing and gait in paralyzed rodents and cats (Ichiyama et al., 2005; Gerasimenko et al., 2008; Wenger et al., 2016). In

humans, epidural stimulation of the spinal cord has been shown to facilitate locomotor-like patterns and produce long-lasting motor recovery after intensive training in spinal cord injury patients (Angeli et al., 2014; Grahn et al., 2017; Gill et al., 2018). However, controlling and modulating the stimulation based on brain activation is a more natural approach than continuously stimulating the spinal circuits (McPherson et al., 2015). In fact, the contingent association of cortical activity produced by the intention to move a paralyzed limb and the afferent volley generated by spinal stimulation can exploit Hebbian mechanisms and facilitate functional recovery (Ramos-Murguialday et al., 2013; Mrachacz-Kersting et al., 2016; Bonizzato et al., 2018). This association is the basic operating principle of brain-spine interfaces (Alam et al., 2016).

Brain-spine interfaces developed to date involve implantable technologies and have only been tested in animal models (Nishimura et al., 2013b; Alam et al., 2014; McPherson et al., 2015; Capogrosso et al., 2016; Bonizzato et al., 2018). Compared with continuous spinal stimulation, brain-controlled stimulation has been shown to enhance stepping quality and accelerate locomotor recovery (Capogrosso et al., 2016; Bonizzato et al., 2018). In humans, the only approaches presenting closed-loop volitional control of spinal stimulation proposed non-brain-commanded paradigms. On one hand, Nishimura and colleagues proposed the use of EMG of the arm to control non-invasive magnetic spinal stimulation in healthy subjects and SCI patients (Sasada et al., 2014; Nakao et al., 2015). On the other hand, Courtine and colleagues implanted epidural electrical stimulation electrodes in the lumbar spinal cord of SCI patients and used inertial measurement units (IMUs) located on the feet to control the stimulation (Wagner et al., 2018). Our approach relied on extracting motor commands non-invasively from brain activity by EEG to provide closed-loop control of transcutaneous magnetic stimulation of the spinal cord.

Non-invasive brain-machine interfaces (BMIs) allow the transmission of volitional cortical commands to control rehabilitative devices (Wolpaw et al., 2002a; Millán et al., 2010; López-Larraz et al., 2018d). For instance, there is ample evidence demonstrating contingent EEG control of robotic exoskeletons with patients (Ramos-Murguialday et al., 2013; Ang et al., 2015). Electric and magnetic neurostimulation can also be integrated with non-invasive BMIs. However, to date, contingent online control

of such neurostimulators has not been achieved, since the stimulation introduces currents to the body, causing strong artifacts that hinder extracting reliable information from the recordings of brain activity. Therefore, BMIs integrating neurostimulation have only been proposed triggering predefined stimulation patterns, not allowing a continuous control nor contingency (Pfurtscheller et al., 2005; Osuagwu et al., 2016; Trincado-Alonso et al., 2017; Biasiucci et al., 2018).

Dealing with stimulation artifacts is a challenge for closed-loop neural interfaces. Different approaches have been proposed for cleaning stimulation contamination from invasive and non-invasive neural recordings, such as blanking, interpolation or linear regression reference (LRR) (Walter et al., 2012a; Iturrate et al., 2018; Young et al., 2018). For invasive recordings, regression methods have been proven effective to eliminate the stimulation artifact (Young et al., 2018), mainly due to the low inter-electrode impedance variability and within-session stability, allowing closed-loop neurostimulation (Bouton et al., 2016; Ajiboye et al., 2017). However, none of these methods has been proven effective for EEG recordings, and the estimation of cortical activation during stimulation is biased even if blanking or interpolation of the artifacts is used (Walter et al., 2012a).

We proposed the use of a median filter, since it can eliminate high-amplitude peaks in a time-series without causing signal discontinuities (which is the main problem of blanking or interpolation). Its main limitation is that it attenuates the activity at higher frequencies (exponential attenuation between 0 Hz and the $1/w_s$ Hz, with w_s being the length of the window of the median filter) (Insausti-Delgado et al., 2021). However, this frequency-dependent attenuation does not have a big impact on the sensorimotor alpha oscillations (7-15 Hz) that we used to detect the motor imagery. To the best of our knowledge, this is the first time a non-invasive closed-loop system controls the stimulation in real-time and effectively deals with these artifacts.

Our adaptive decoder successfully dealt with the changes in brain activity due to ts-MS. The accuracy of the decoder was within the level of acceptance for closed-loop rehabilitative neuroprosthetics (Ramos-Murguialday et al., 2013). Remarkably, we demonstrated that the accuracy was not influenced by the stimulation intensity, which allows the implementation of different stimulation protocols, such as above or below

motor threshold (considering that the motor threshold of healthy subjects is between 25% and 40% of the MSO). All participants reported a decrease in usability of the system with higher stimulation intensities (i.e., more pain and discomfort, and less ability to concentrate on the task). However, their subjective perception of usability at high intensity did not affect the performance of the BSI.

The next natural step following this study would be to demonstrate the efficacy of the brain-controlled stimulation to promote Hebbian mechanisms that induce neuroplastic changes in human nervous system, as it has already been proven invasively in rodents and primates (McPherson et al., 2015; Capogrosso et al., 2016, 2018; Bonizzato et al., 2018). An exhaustive battery of assessments should be conducted, including the evaluation of motor and sensory pathways and spinal neural processes, to characterize in detail the neurophysiological effects of a BSI-based intervention. Although we did not conduct assessments of synaptic efficacy in this preliminary analysis, we studied the neuromodulatory effects during closed-loop stimulation. We demonstrated the capability of our platform to engage the central and peripheral nervous system as expected. The ts-MS activated efferent pathways, inducing ts-MEPs in lower-limb muscles, and afferent pathways, producing ts-SEPs. These findings prove that both afferent and efferent neuromodulation are intensity dependent, confirming previous results (Matsumoto et al., 2013; Rossini et al., 2015).

In conclusion, in this study we have proposed and validated the first non-invasive brain-spine interface. Further research should focus on studying the feasibility of this system as a rehabilitative tool in patient populations such as SCI or motor stroke. The role of ts-MS parameters (i.e., frequency, intensity, dose, etc.) on the excitability of spinal neural networks should also be disclosed in future investigations. Computational modelling might be a key tool to understand the ongoing mechanisms involved in spinal neuromodulation due to ts-MS in order to optimize interventions based on spinal cord stimulation that enhance functional recovery (Formento et al., 2018; Greiner et al., 2020; Khadka et al., 2020). Nevertheless, the here presented findings constitute the first steps towards the application of non-invasive BSIs as a novel neuroscientific and therapeutic tool.

6.6 Acknowledgments

This study was funded by the Bundesministerium für Bildung und Forschung BMBF MOTORBIC (FKZ 13GW0053) and AMORSA (FKZ 16SV7754), and the Fortüne-Program of the University of Tübingen (2422-0-1 and 2556-0-0 to ELL, and 2452-0-0 to ARM). The work of AID was funded by the Basque Government's scholarship for predoctoral students.

6.7 References

Ajiboye, A. B., Willett, F. R., Young, D. R., Memberg, W. D., Murphy, B. A., Miller, J. P., et al. (2017). Restoration of reaching and grasping movements through brain-controlled muscle stimulation in a person with tetraplegia: a proof-of-concept demonstration. *Lancet* 389, 1821–1830. doi:10.1016/S0140-6736(17)30601-3.

Alam, M., Chen, X., Zhang, Z., Li, Y., and He, J. (2014). A brain-machine-muscle interface for restoring hindlimb locomotion after complete spinal transection in rats. *PLoS One* 9. doi:10.1371/journal.pone.0103764.

Alam, M., Garcia-alias, G., Jin, B., Keyes, J., Zhong, H., Roy, R. R., et al. (2017). Electrical neuromodulation of the cervical spinal cord facilitates forelimb skilled function recovery in spinal cord injured rats. *Exp. Neurol.* 291, 141–150. doi:10.1016/j.expneurol.2017.02.006.

Alam, M., Rodrigues, W., Ngoc, B., and Thakor, N. V (2016). Brain-machine interface facilitated neurorehabilitation via spinal stimulation after spinal cord injury : Recent progress and future perspectives. *Brain Res.* 1646, 25–33. doi:10.1016/j.brainres.2016.05.039.

Ang, K. K., Chua, K. S. G., Phua, K. S., Wang, C., Chin, Z. Y., Kuah, C. W. K., et al. (2015). A randomized controlled trial of EEG-based motor imagery brain-computer interface robotic rehabilitation for stroke. *Clin. EEG Neurosci.* 46, 310–320. doi:10.1177/1550059414522229.

Angeli, C. A., Edgerton, V. R., Gerasimenko, Y. P., and Harkema, S. J. (2014). Altering spinal cord excitability enables voluntary movements after chronic complete paralysis in humans. *Brain* 137, 1394–1409. doi:10.1093/brain/awu038.

Biasiucci, A., Leeb, R., Iturrate, I., Perdikis, S., Al-Khodairy, A., Corbet, T., et al. (2018). Brain-actuated functional electrical stimulation elicits lasting arm motor recovery after stroke. *Nat. Commun.* 9, 2421. doi:10.1038/s41467-018-04673-z.

Bonizzato, M., Pidpruzhnykova, G., DiGiovanna, J., Shkorbatova, P., Pavlova, N., Micera, S., et al. (2018). Brain-controlled modulation of spinal circuits improves recovery from spinal cord injury. *Nat. Commun.* 9, 1–14. doi:10.1038/s41467-018-05282-6.

Borton, D., Bonizzato, M., Beauparlant, J., Digiovanna, J., Moraud, E. M., Wenger, N., et al. (2014). Corticospinal neuroprostheses to restore locomotion after spinal cord injury. *Neurosci. Res.* 78, 21–29. doi:10.1016/j.neures.2013.10.001.

Bouton, C. E., Shaikhouni, A., Annetta, N. V., Bockbrader, M. A., Friedenberg, D. A., Nielson, D. M., et al. (2016). Restoring cortical control of functional movement in a human with quadriplegia. *Nature* 533, 247–250. doi:10.1038/nature17435.

Budakova, N. N. (1972). Stepping movements evoked by repetitive dorsal root stimulation in a mesencephalic cat. *Neurosci. Behav. Physiol.* 5, 355–363. doi:10.1007/BF01183110.

Burg, J. P. (1967). Maximum Entropy Spectral Analysis. in *37th Annual International Meeting, Soc. of Explor. Geophys.*

Capogrosso, M., Milekovic, T., Borton, D., Wagner, F., Martin Moraud, E., Mignardot, J.-B., et al. (2016). A brain–spine interface alleviating gait deficits after spinal cord injury in primates. *Nature* 539, 284–288. doi:10.1038/nature20118.

Capogrosso, M., Wagner, F. B., Gandar, J., Moraud, E. M., Wenger, N., Milekovic, T., et al. (2018). Configuration of electrical spinal cord stimulation through real-time processing of gait kinematics. *Nat. Protoc.* 13, 2031–2061. doi:10.1038/s41596-

018-0030-9.

Dimitrijevic, M. R., Gerasimenko, Y., and Pinter, M. . (1998). Evidence for a Spinal Central Pattern Generator in Humans. *J. Chem. Inf. Model.* 53, 160. doi:10.1017/CBO9781107415324.004.

Edgerton, V. R., and Roy, R. R. (2012). A new age for rehabilitation. *Eur. J. Phys. Rehabil. Med.* 48, 99–109.

Formento, E., Minassian, K., Wagner, F., Mignardot, J. B., Camille G. Le Goff-Mignardot, A. R., Bloch, J., et al. (2018). Electrical spinal cord stimulation must preserve proprioception to enable locomotion in humans with spinal cord injury. *Nat. Neurosci.* 6, 153–158. doi:10.1038/s41593-018-0262-6.

Gerasimenko, Y., Gorodnichev, R., Machueva, E., Pivovarova, E., Semyenov, D., Savochin, A., et al. (2010). Novel and direct access to the human locomotor spinal circuitry. *J. Neurosci.* 30, 3700–3708. doi:10.1523/JNEUROSCI.4751-09.2010.

Gerasimenko, Y., Roy, R. R., and Edgerton, V. R. (2008). Epidural stimulation : Comparison of the spinal circuits that generate and control locomotion in rats , cats and humans. 209, 417–425. doi:10.1016/j.expneurol.2007.07.015.

Gerasimenko, Y., Sayenko, D., Gad, P., Kozesnik, J., Moshonkina, T., Grishin, A., et al. (2018). Electrical spinal stimulation, and imagining of lower limb movements to modulate brain-spinal connectomes that control locomotor-like behavior. *Front. Physiol.* 9, 1–13. doi:10.3389/fphys.2018.01196.

Gill, M. L., Grahn, P. J., Calvert, J. S., Linde, M. B., Lavrov, I. A., Strommen, J. A., et al. (2018). Neuromodulation of lumbosacral spinal networks enables independent stepping after complete paraplegia. *Nat. Med.* 24, 1677–1682. doi:10.1038/s41591-018-0175-7.

Grahn, P. J., Lavrov, I. A., Sayenko, D. G., Straaten, M. G. Van, Gill, M. L., Strommen, J. A., et al. (2017). Enabling Task-Specific Volitional Motor Functions via Spinal Cord Neuromodulation in a Human With Paraplegia. *Mayo Clin. Proc.* 92, 544–554.

doi:10.1016/j.mayocp.2017.02.014.

Graimann, B., and Pfurtscheller, G. (2006). Quantification and visualization of event-related changes in oscillatory brain activity in the time – frequency domain. *Prog. Brain Res.* 159, 79–97. doi:10.1016/S0079-6123(06)59006-5.

Greiner, N., Barra, B., Schiavone, G., James, N., Falleger, F., Borgognon, S., et al. (2020). Recruitment of Upper-Limb Motoneurons With Epidural Electrical Stimulation of the Primate Cervical Spinal Cord. *bioRxiv*, 2020.02.17.952796. doi:10.1101/2020.02.17.952796.

Grillner, S., and Zangger, P. (1979). On the central generation of locomotion in the low spinal cat. *Exp. brain Res.* 34, 241–261. doi:10.1007/BF00235671.

Groppa, S., Oliviero, A., Eisen, A., Quartarone, A., Cohen, L. G., Mall, V., et al. (2012). A practical guide to diagnostic transcranial magnetic stimulation: Report of an IFCN committee. *Clin. Neurophysiol.* 123, 858–882. doi:10.1016/j.clinph.2012.01.010.

Harkema, S., Gerasimenko, Y., Hodes, J., Burdick, J., Angeli, C., Chen, Y., et al. (2011). Effect of epidural stimulation of the lumbosacral spinal cord on voluntary movement, standing, and assisted stepping after motor complete paraplegia: a case study. *Lancet* 377, 1938–1947. doi:10.1016/S0140-6736(11)60547-3.

Hofstoetter, U. S., Freundl, B., Binder, H., and Minassian, K. (2018). Common neural structures activated by epidural and transcutaneous lumbar spinal cord stimulation: Elicitation of posterior root-muscle reflexes. *PLoS One* 13, 1–22. doi:10.1371/journal.pone.0192013.

Hubli, M., Dietz, V., Bolliger, M., Schrafl-Altermatt, M., and Bolliger, M. (2013). Modulation of spinal neuronal excitability by spinal direct currents and locomotion after spinal cord injury. *Clin. Neurophysiol.* 124, 1187–1195. doi:10.1016/j.clinph.2012.11.021.

Hultborn, H., and Nielsen, J. B. (2007). Spinal control of locomotion - From cat to man. *Acta Physiol.* 189, 111–121. doi:10.1111/j.1748-1716.2006.01651.x.

Ichiyama, R. M., Gerasimenko, Y. P., Zhong, H., Roy, R. R., and Edgerton, V. R. (2005). Hindlimb stepping movements in complete spinal rats induced by epidural spinal cord stimulation. 383, 339–344. doi:10.1016/j.neulet.2005.04.049.

Insausti-Delgado, A., López-Larraz, E., Bibián, C., Nishimura, Y., Birbaumer, N., and Ramos-Murguialday, A. (2017). Influence of trans-spinal magnetic stimulation in electrophysiological recordings for closed-loop rehabilitative systems. in *39th Annual International Conference of the IEEE Engineering in Medicine and Biology Society (EMBC)*, 2518–2521. doi:10.1109/EMBC.2017.8037369.

Insausti-Delgado, A., López-Larraz, E., Nishimura, Y., Birbaumer, N., Ziemann, U., and Ramos-Murguialday, A. (2019). Quantifying the effect of trans-spinal magnetic stimulation on spinal excitability. *9th Int. IEEE EMBS Conf. Neural Eng.* doi:10.1109/NER.2019.8717016.

Insausti-Delgado, A., López-Larraz, E., Nishimura, Y., Ziemann, U., and Ramos-Murguialday, A. (2020). Non-invasive brain-spine interface: continuous brain control of trans-spinal magnetic stimulation using EEG. *bioRxiv*.

Insausti-Delgado, A., López-Larraz, E., Omedes, J., and Ramos-Murguialday, A. (2021). Intensity and dose of neuromuscular electrical stimulation influence sensorimotor cortical excitability. *Front. Neurosci.* 14, 1359. doi:10.3389/fnins.2020.593360.

Insausti-Delgado, A., López-Larraz, E., Birbaumer, N., and Ramos-Murguialday, A. (2018). An exhaustive assessment to quantify changes in spinal excitability after spinal-cord stimulation. in *11th FENS Forum of Neuroscience*.

Iturrate, I., Pereira, M., and Millán, J. del R. (2018). Closed-loop electrical neurostimulation: challenges and opportunities. *Curr. Opin. Biomed. Eng.* 8, 28–37. doi:10.1016/j.cobme.2018.09.007.

Jackson, A., and Zimmermann, J. B. (2012). Neural interfaces for the brain and spinal cord—restoring motor function. *Nat. Rev. Neurol.* 8, 690–699. doi:10.1038/nrneurol.2012.219.

Kato, K., Sawada, M., and Nishimura, Y. (2019). Bypassing stroke-damaged neural pathways via a neural interface induces targeted cortical adaptation. *Nat. Commun.* 10, 1–13. doi:10.1038/s41467-019-12647-y.

Khadka, N., Liu, X., Zander, H., Swami, J., Rogers, E., Lempka, S., et al. (2020). Realistic anatomically detailed open-source spinal cord stimulation (RADO-SCS) model. *J. Neural Eng.* doi:10.1088/1741-2552/ab8344.

Knikou, M. (2013). Neurophysiological characteristics of human leg muscle action potentials evoked by transcutaneous magnetic stimulation of the spine. *Bioelectromagnetics* 34, 200–210. doi:10.1002/bem.21768.

Kunesch, E., Knecht, S., Classen, J., Roick, H., Tyercha, C., and Benecke, R. (1993). Somatosensory evoked potentials (SEPs) elicited by magnetic nerve stimulation. *Electroencephalogr. Clin. Neurophysiol. Evoked Potentials* 88, 459–467. doi:10.1016/0168-5597(93)90035-N.

López-Larraz, E., Figueiredo, T. C., Insausti-Delgado, A., Ziemann, U., Birbaumer, N., and Ramos-Murguialday, A. (2018a). Event-related desynchronization during movement attempt and execution in severely paralyzed stroke patients: an artifact removal relevance analysis. *NeuroImage Clin.* 20, 972–986. doi:10.1016/j.nicl.2018.09.035.

López-Larraz, E., Montesano, L., Gil-Agudo, Á., and Minguez, J. (2014). Continuous decoding of movement intention of upper limb self-initiated analytic movements from pre-movement EEG correlates. *J. Neuroeng. Rehabil.* 11, 153. doi:10.1186/1743-0003-11-153.

López-Larraz, E., Montesano, L., Gil-Agudo, Á., Minguez, J., and Oliviero, A. (2015). Evolution of EEG motor rhythms after spinal cord injury: A longitudinal study. *PLoS One* 10, e0131759. doi:10.1371/journal.pone.0131759.

López-Larraz, E., Sarasola-Sanz, A., Irastorza-Landa, N., Birbaumer, N., and Ramos-Murguialday, A. (2018b). Brain-machine interfaces for rehabilitation in stroke: A review. *NeuroRehabilitation* 43, 77–97. doi:10.3233/NRE-172394.

Matsumoto, H., Hanajima, R., Terao, Y., and Ugawa, Y. (2013). Magnetic-motor-root stimulation: Review. *Clin. Neurophysiol.* 124, 1055–1067. doi:10.1016/j.clinph.2012.12.049.

McPherson, J. G., Miller, R. R., Perlmutter, S. I., and Jacob G. McPherson, Robert R. Miller, and S. I. P. (2015). Targeted, activity-dependent spinal stimulation produces long-lasting motor recovery in chronic cervical spinal cord injury. *Neurosurgery* 78, N18–N19. doi:10.1073/pnas.1505383112.

Millán, J. D. R., Rupp, R., Müller-Putz, G. R., Murray-Smith, R., Giugliemma, C., Tangermann, M., et al. (2010). Combining brain-computer interfaces and assistive technologies: State-of-the-art and challenges. *Front. Neurosci.* 4, 1–15. doi:10.3389/fnins.2010.00161.

Minassian, K., Hofstoetter, U. S., Dzeladini, F., Guertin, P. A., and Ijspeert, A. (2017). The Human Central Pattern Generator for Locomotion: Does It Exist and Contribute to Walking? *Neurosci.* 3, 107385841769979. doi:10.1177/1073858417699790.

Mrachacz-Kersting, N., Jiang, N., Stevenson, A. J. T., Niazi, I. K., Kostic, V., Pavlovic, A., et al. (2016). Efficient neuroplasticity induction in chronic stroke patients by an associative brain-computer interface. *J. Neurophysiol.* 115, 1410–1421. doi:10.1152/jn.00918.2015.

Müller-Putz, G., Scherer, R., Brunner, C., Leeb, R., and Pfurtscheller, G. (2008). Better than random: A closer look on BCI results. *Int. J. Bioelectromagn.* 10, 52–55.

Nakao, Y., Sasada, S., Kato, K., Murayama, T., Kadowaki, S., S, Y., et al. (2015). Restoring walking ability in individuals with severe spinal cord injury using a closed-loop spinal magnetic stimulation. in *Proceedings of the 45th Annual Meeting of Society for Neuroscience* Available at: https://www.abstractsonline.com/Plan/ViewAbstract.aspx?sKey=70d620e9-53bf-4bef-858d-e79452be5b51&cKey=5f31c5f3-9c0c-4873-8cd1-2fab3b718c7d&mKey=d0ff4555-8574-4fbb-b9d4-04eec8ba0c84.

Nardone, R., Höller, Y., Brigo, F., Orioli, A., Tezzon, F., Schwenker, K., et al. (2015a).

Descending motor pathways and cortical physiology after spinal cord injury assessed by transcranial magnetic stimulation: a systematic review. *Brain Res.* 1619, 139–154. doi:10.1016/j.brainres.2014.09.036.

Nardone, R., Höller, Y., Taylor, A., Thomschewski, A., Orioli, A., Frey, V., et al. (2015b). Noninvasive Spinal Cord Stimulation: Technical Aspects and Therapeutic Applications. *Neuromodulation Technol. Neural Interface* 2015, 580–591. doi:10.1111/ner.12332.

Neuper, C., Scherer, R., Reiner, M., and Pfurtscheller, G. (2005). Imagery of motor actions : Differential effects of kinesthetic and visual – motor mode of imagery in single-trial EEG. 25, 668–677. doi:10.1016/j.cogbrainres.2005.08.014.

Nishimura, Y., Perlmutter, S. I., Eaton, R. W., and Fetz, E. E. (2013a). Spike-timing-dependent plasticity in primate corticospinal connections induced during free behavior. *Neuron* 80, 1301–1309. doi:10.1016/j.neuron.2013.08.028.

Nishimura, Y., Perlmutter, S. I., and Fetz, E. E. (2013b). Restoration of upper limb movement via artificial corticospinal and musculospinal connections in a monkey with spinal cord injury. *Front. Neural Circuits* 7, 57. doi:10.3389/fncir.2013.00057.

Osuagwu, B. C. A., Wallace, L., Fraser, M., and Vuckovic, A. (2016). Rehabilitation of hand in subacute tetraplegic patients based on brain computer interface and functional electrical stimulation: A randomised pilot study. *J. Neural Eng.* 13, 065002. doi:10.1088/1741-2560/13/6/065002.

Pfurtscheller, G., and Lopes da Silva, F. H. (1999). Event-related EEG/MEG synchronization and desynchronization: basic principles. *Clin. Neurophysiol.* 110, 1842–1857. doi:10.1016/S1388-2457(99)00141-8.

Pfurtscheller, G., Müller-Putz, G. R., Pfurtscheller, J., and Rupp, R. (2005). EEG-based asynchronous BCI controls functional electrical stimulation in a tetraplegic patient. *EURASIP J. Appl. Signal Processing* 2005, 3152–3155. doi:10.1155/ASP.2005.3152.

Ramos-Murguialday, A., Broetz, D., Rea, M., Läer, L., Yilmaz, Ö., Brasil, F. L., et al. (2013). Brain-machine interface in chronic stroke rehabilitation: A controlled study. *Ann. Neurol.* 74, 100–108. doi:10.1002/ana.23879.

Rossini, P. M., Burke, D., Chen, R., Cohen, L. G., Daskalakis, Z., Di Iorio, R., et al. (2015). Non-invasive electrical and magnetic stimulation of the brain, spinal cord, roots and peripheral nerves: Basic principles and procedures for routine clinical and research application. An updated report from an I.F.C.N. Committee. *Clin. Neurophysiol.* 126, 1071–1107. doi:10.1016/j.clinph.2015.02.001.

Sasada, S., Kato, K., Kadowaki, S., Groiss, S. J., Ugawa, Y., Komiyama, T., et al. (2014). Volitional walking via upper limb muscle-controlled stimulation of the lumbar locomotor center in man. *J. Neurosci.* 34, 11131–11142. doi:10.1523/JNEUROSCI.4674-13.2014.

Seeck, M., Koessler, L., Bast, T., Leijten, F., Michel, C., Baumgartner, C., et al. (2017). The standardized EEG electrode array of the IFCN. *Clin. Neurophysiol.* 128, 2070–2077. doi:10.1016/j.clinph.2017.06.254.

Taccola, G., Sayenko, D., Gad, P., Gerasimenko, Y., and Edgerton, V. R. (2018). And yet it moves: Recovery of volitional control after spinal cord injury. *Prog. Neurobiol.* 160, 64–81. doi:10.1016/j.pneurobio.2017.10.004.

Trincado-Alonso, F., López-Larraz, E., Resquín, F., Ardanza, A., Pérez-Nombela, S., Pons, J. L., et al. (2017). A Pilot Study of Brain-Triggered Electrical Stimulation with Visual Feedback in Patients with Incomplete Spinal Cord Injury. *J. Med. Biol. Eng.* 38, 790–803. doi:10.1007/s40846-017-0343-0.

Ugawa, Y., Rothwell, J. C., Day, B. L., Thompson, P. D., and Marsden, C. D. (1989). Magnetic stimulation over the spinal enlargements. *J. Neurol. Neurosurg. Psychiatry* 52, 1025–1032. doi:10.1136/jnnp.52.9.1025.

Wagner, F. B., Mignardot, J. B., Le Goff-Mignardot, C. G., Demesmaeker, R., Komi, S., Capogrosso, M., et al. (2018). Targeted neurotechnology restores walking in humans with spinal cord injury. *Nature* 563, 65–71. doi:10.1038/s41586-018-0649.

Walter, A., Ramos-Murguialday, A., Rosenstiel, W., Birbaumer, N., and Bogdan, M. (2012). Coupling BCI and cortical stimulation for brain-state-dependent stimulation: methods for spectral estimation in the presence of stimulation after-effects. *Front. Neural Circuits* 6, 87. doi:10.3389/fncir.2012.00087.

Wenger, N., Moraud, E. M., Gandar, J., Musienko, P., Capogrosso, M., Baud, L., et al. (2016). Spatiotemporal neuromodulation therapies engaging muscle synergies improve motor control after spinal cord injury. *Nat. Med.* 22, 5–7. doi:10.1038/nm.4025.

Wolpaw, J. R., Birbaumer, N., Mcfarland, D. J., Pfurtscheller, G., and Vaughan, T. M. (2002). Brain – computer interfaces for communication and control. 113, 767–791.

Yadav, A. P., Li, D., and Nicolelis, M. A. L. (2020). A Brain to Spine Interface for Transferring Artificial Sensory Information. *Sci. Rep.* 10, 1–15. doi:10.1038/s41598-020-57617-3.

Young, D., Willett, F., Memberg, W. D., Murphy, B., Walter, B., Sweet, J., et al. (2018). Signal processing methods for reducing artifacts in microelectrode brain recordings caused by functional electrical stimulation. *J. Neural Eng.* 15, 026014. doi:10.1088/1741-2552/aa9ee8.

Zimmermann, J. B., and Jackson, A. (2014). Closed-loop control of spinal cord stimulation to restore hand function after paralysis. *Front. Neurosci.* 8, 1–8. doi:10.3389/fnins.2014.00087.

7. Chapter 7: Brain-controlled trans-spinal magnetic stimulation to restore lower-limb paralysis: a proof-of-concept in stroke patients

7.1 Abstract

Brain-controlled neurotechnology has emerged as a powerful tool to interact with the nervous system and to repair neural damage in patients with motor diseases, such as stroke. In this context, brain-spine interfaces (BSI) rely on a timely-linked activation between brain and spinal networks via spinal cord stimulation and have demonstrated efficacy to recover lower-limb motor function. Recently, we devised the first non-invasive BSI based on continuous control of trans-spinal (ts-MS) stimulation with electroencephalographic (EEG) activity. However, the validation of this system with paralyzed patients is yet to be done and, more importantly, how this system can induce synaptic efficacy changes in the human nervous system and its effects on sensorimotor recovery remain unclear. With the objective of evaluating and characterizing the neurophysiological impact of a BSI intervention, we firstly recruited twenty-one healthy participants, who underwent a single-session experiment and in which we measure synaptic efficacy changes using an exhaustive battery of assessments. Secondly, seven stroke patients validated the system and were evaluated neurophysiological and clinically after an 8-session intervention. Our results showed that using the BSI system enhanced the excitability of corticomuscular pathways of healthy participants and that this enhancement was maintained 30 minutes after finishing the session. In addition, the increased responsiveness of corticomuscular tracts was positively correlated with the BSI performance. We also found that some stroke patients presented daily and over-session improvement in synaptic efficacy of corticomuscular projections. Moreover, stroke patients increased their motor function and experienced a decrease of spasticity after 8-day BSI intervention. Overall, our findings evidenced the capacity of the BSI to interact positively with the nervous system generating functional changes and shed light on the applicability of this technology as a rehabilitative tool for lower-limb paralysis.

7.2 Introduction

Neurological diseases, such as stroke or spinal cord injury (SCI), are characterized by a damage in the communication between the brain and the peripheral nervous system, leading to a deficit of movement control. Brain-machine interfaces (BMI) aim at bypassing the neurological impairment to repair this neural connection (Jackson and Zimmermann, 2012). Within this framework, brain-spine interfaces (BSI) have prompted as an efficient tool for gait rehabilitation that rely on brain-controlled spinal cord stimulation to generate locomotor rhythms or activation of lower-limb muscles (Alam et al., 2016; Capogrosso et al., 2016; Bonizzato et al., 2018).

Targeted neuromodulation of spinal cord circuitries through invasive electrical stimulation to regain motor function of lower limb, including standing and walking, has been widely investigated in animals (Gerasimenko et al., 2008; Capogrosso et al., 2016; Alam et al., 2017) and SCI individuals (Angeli et al., 2014; Grahn et al., 2017; Formento et al., 2018; Gill et al., 2018). All these studies evidenced the potential of epidural stimulation to be used for rehabilitative applications. However, the possibility of neuromodulating similar spinal neural networks using non-invasive approaches opens an alternative frame for the treatment of motor disabilities. A series of studies demonstrated that transcutaneous electrical stimulation induced locomotor-like activity in paralyzed legs and provided some volitional control of the movements (Gerasimenko et al., 2015; Hofstoetter et al., 2015; Minassian et al., 2016a; Gad et al., 2017). Similarly, there is evidence showing that trans-spinal magnetic stimulation (ts-MS) generates stepping-like rhythms using open-loop (Gerasimenko et al., 2010; Gorodnichev et al., 2010) or EMG-triggered protocols (Sasada et al., 2014; Nakao et al., 2015). However, all these stimulation strategies lacked volitional brain control of the stimulation.

The BSIs allow extracting brain activity encoding motor intentions and transforming it into commands to volitionally control spinal cord stimulation that activates leg muscles (Alam et al., 2016; Capogrosso et al., 2016, 2018). The BSIs boost functional recovery of lower limb and alleviate gait deficits in comparison to open-loop or pre-programmed stimulation protocols (McPherson et al., 2015; Bonizzato et al., 2018). The potential of BSIs to induce neuroplastic changes relies on timely linking the

cortical activation reflecting a motor task with the peripheral afference derived from modulating spinal circuits and activating muscles (Nishimura et al., 2013a; Ramos-Murguialday et al., 2013; Mrachacz-Kersting et al., 2016; López-Larraz et al., 2018d; Kato et al., 2019). However, to date implantable BSIs have mostly been developed and tested in animal models (McPherson et al., 2015; Capogrosso et al., 2016, 2018; Yadav et al., 2020), and the non-invasive approach of this technology would open a new frame of possibilities for its application in humans. Recently, we proposed the first non-invasive BSI, based on the continuous acquisition of brain activity with electroencephalography (EEG) for the direct and continuous control of ts-MS (Insausti-Delgado et al., 2020). Our non-invasive BSI contingently connected motor cortical activation with activation of lower-limb muscles and we demonstrated the capability of the system to engage central and peripheral nervous system through brain-controlled spinal stimulation.

Despite the number of investigations that have examined the effects of transcutaneous electrical spinal stimulation (Cogiamanian et al., 2012; Priori et al., 2014; Megía García et al., 2019) and ts-MS (Nielsen and Sinkjaer, 1997; Krause et al., 2004; Knikou, 2013; Insausti-Delgado et al., 2019) on neural excitability, how brain-controlled stimulation interacts with the human nervous system inducing modifications in synaptic efficacy remains unclear. Furthermore, the validation of our non-invasive BSI in patients with neurological disorders, such as stroke, and its corresponding evaluation of neurophysiological effects are yet to be done. Determining the neuromodulatory mechanisms activated by non-invasive BSIs is of great need for promoting functional recovery and would lead us to improve rehabilitative treatments for lower-limb motor disorders.

This study aims at assessing and characterizing the neurophysiological effects induced by a BSI-based intervention. Because the spinal cord is a complex structure where descending, ascending and propriospinal neural pathways are integrated, we hypothesized that the BSI intervention would lead to an increase of excitability in the entire neural system, including both motor and sensory pathways, and that the assessments would reflect this change. To test this hypothesis, we firstly propose a study with twenty-one healthy participants in which we measure neurophysiological changes with an exhaustive battery of assessments. Secondly, we conduct preliminary tests with

seven stroke patients, in which we validate the BSI, and evaluate neurophysiological changes and clinical scales before and after the intervention.

7.3 Materials and methods

7.3.1 Participants

Twenty-one healthy subjects (7 females, mean age 27.36 ± 4.56 years) with no neurological disorders and 7 stroke patients with lower-limb paralysis (see details in Table1) were recruited in the study. The inclusion criteria for stroke participants were: (1) lower-limb paralysis; (2) age between 18 and 80 years; (3) minimum time since stroke 6 months; (4) no cerebellar lesion; (5) no psychiatric or neurological condition other than stroke; (6) intracranial implant or any other metal object within the head; (7) no cardiac implants or unstable cardiac disease; (8) no epilepsy or medication for epilepsy during the last 6 months; (9) no Botox treatment during the last 3 months; (10) no pregnancy; (11) be able to understand and follow instructions. The ethical approval for the experimental procedure was provided by the committee of the Faculty of Medicine of the University of Tübingen (Germany). All participants were informed and gave written consent before participating in the study.

7.3.2 Data acquisition

Electroencephalographic (EEG) activity was registered using a commercial Acticap system (BrainProducts GmbH, Germany), with 32 electrodes placed on FP1, FP2, F7, F3, F4, F8, FC3, FC1, FCz, FC2, FC4, C5, C3, C1, Cz, C2, C4, C6, CP3, CP1, CPz, CP2, CP4, T7, T8, P7, P3, Pz, P4, P8, O1, and O2 (according to the international 10/20 system). The ground and reference electrodes were placed on FPz and Fz, respectively. The recording electrodes were connected to a monopolar BrainAmp amplifier (BrainProducts GmbH, Germany).

Electromyographic (EMG) activity of both legs was recorded using Ag/AgCl bipolar electrodes (Myotronics-Noromed, Tukwila, Wa, USA), with an inter-electrode space of 4 cm, connected to an MR-compatible BrainAmp amplifier (BrainProducts

GmbH, Germany). Four muscles (*tibialis anterior, soleus, gastrocnemius medialis and vastus medialis*) were recorded from each leg. In healthy participants, the ground electrode was placed on the patella of the right leg, while the patella of the paretic leg was used in patients.

	Age	Gender	Lesion side	Months since stroke
P1	67	M	L	126
P2	52	M	L	17
P3	79	M	R	65
P4	63	M	L	24
P5	58	M	L+R	31
P6	76	M	L	33
P7	67	M	R	106

Table 7.1: Demographic data of the patients at the time of enrollment in the study

7.3.3 Experimental design and procedure

Experiment 1: Quantifying the effect of BSI on synaptic efficacy of healthy participants

To study the effects of the closed-loop intervention on the synaptic efficacy, 21 healthy participants were involved in one experimental session. The participants were seated on a chair, while keeping their back straight, and their knee and ankle around 120° and 90°, respectively. To maintain the posture of the leg constant during the entire session, the participants placed their foot on a moveable wedge-shaped structure (Figure 7.1a).

The experiment consisted of a screening phase, a closed-loop stimulation phase and synaptic efficacy assessments (Figure 7.1b). The screening phase included 40 trials, while the closed-loop phase included as many trials as each participant needed to receive a total amount of 2000 pulses (more details about these 2 phases are described in section 7.3.4). The ts-MS intensity was set to the motor threshold of each participants, as described in section 7.3.5. To precisely characterize the changes in neural excitability between the cortex and muscles, we defined a comprehensive set of assessments

(explained in section 7.3.7). These assessments were conducted 4 times during the session, one at the beginning (Pre), one immediately after the screening (PostScreening), one right after concluding the closed-loop stimulation (Post0) and one 30 min afterwards (Post30). Running each set of assessments did not exceed 10 min.

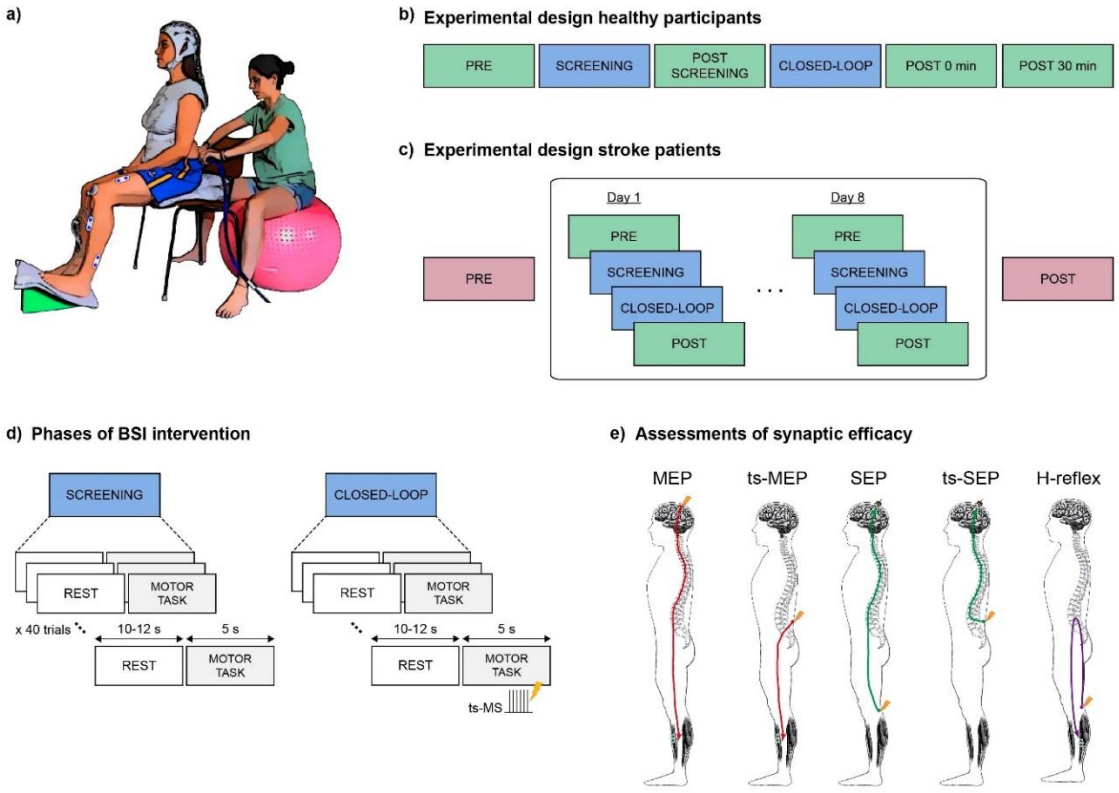

Figure 7.1: Experimental procedure and design. (a) Participant sitting on a chair while wearing EEG and EMG recoding systems, and experimenter applying trans-spinal magnetic stimulation (ts-MS). (b) Experimental design for healthy participants including 4 assessment blocks of synaptic efficacy measures (Pre, PostScreening, Post0 and Post30) and two BSI phases. (c) Experimental design for stroke patients consisting of BSI-intervention and assessments. The BSI-intervention included 8 daily sessions with measurements of motor evoked potentials before and after the two BSI phases. One day before and one day after the intervention a more exhaustive battery of measurements was carried out including synaptic efficacy, clinical and behavioral assessments. (d) Phases of the BSI intervention: screening and closed-loop stimulation. Each phase is composed by period of rest and motor task (motor imagery and attempt for healthy and stroke participants, respectively). In the closed-loop phase, participants used their brain activity to control the repetitive ts-MS at 20Hz applied at individuals' motor threshold. (e) Diagram of propagation of different impulses along the nervous pathways and recording sensors during assessments for synaptic efficacy. This battery of assessments includes motor evoked potentials (MEP), trans-spinal motor evoked potentials (ts-MEP), somatosensory evoked potentials (SEP), trans-spinal somatosensory evoked potentials (ts-SEP) and H-reflexes.

Experiment 2: Proof of concept with chronic stroke patients

To provide the first proof of concept that this platform can be used to rehabilitate lower-limb paralysis, seven stroke chronic patients were invited to an 8-session intervention (except for P6 and P7, who carried out 6 and 9 sessions, respectively) (Figure 7.1c). Every session consisted of a screening phase including 40 trials and a closed-loop stimulation phase. The intensity of the ts-MS was set to the motor threshold. Occasionally, due to chronic pain or other problems derived from the stroke, the intensity was decreased for patients' comfort. The number of closed-loop blocks, consisting in 20 trials per block, depended on the experimental fatigue of the patients and the temperature of the stimulating coil, which automatically blocked for safety measures when certain temperature was exceeded after repetitive use.

To measure the excitability changes in the nervous system, an exhaustive battery of assessments was conducted one day before beginning the intervention (Pre) and one day after finishing the intervention (Post). In addition to the measurements of synaptic efficacy, this experiment also included clinical and behavioral assessments (explained in section 7.3.8). Furthermore, to quantify synaptic efficacy changes within session, motor evoked potentials (MEPs) were daily measured before and after the BSI intervention. Brain oscillatory activity during rest was also recorded every day prior to the intervention.

To evaluate how practical and functional our BSI was, after every block of closed-loop stimulation, the patients were asked to report different usability indicators. They had to score each block between 0 (low) and 10 (high), describing how uncomfortable and painful the stimulation was, how exhausting the task was, and how easy it was to concentrate in the motor attempt task while being stimulated.

7.3.4 BSI intervention

The BSI intervention was divided into a screening phase and closed-loop stimulation phase. The screening consisted of 40 trials, which included periods of rest (10-12 s) and periods to perform a motor task (5 s). "Rest" and "Move" auditory cues announced the beginning of each period (Figure 7.1d). During rest, participants were instructed to stay relaxed without imagining or attempting any movement. During the

motor task, the healthy participants were asked to perform kinesthetic motor imagery (MI) of the right plantar dorsiflexion (Neuper et al. 2005), while the stroke patients were required to attempt plantar dorsiflexion of their paretic leg. The data acquired during the screening were used to build a classifier that discriminated between "rest" and "motor imagery/motor attempt" brain states.

The trials of the closed-loop stimulation phase were identically defined to the screening trials in timing. In this phase, the cortical signatures decoded during the motor attempt or MI triggered the ts-MS. Note that to avoid false positives, the stimulation was off during resting periods.

7.3.5 Trans-spinal magnetic stimulation (ts-MS)

Due to the unpleasant feeling that ts-MS can produce, and to ensure that all the participants could tolerate the stimulation, we performed a familiarization session with each participant on a separate day prior to the experiment. We used a magnetic stimulator (Magstim Rapid2, Magstim Ltd, UK) with a circular coil (Magstim 90 mm Coil, Magstim Ltd, UK) to apply the ts-MS (biphasic single cosine cycle pulses of 400 μs).

Before starting the session, the vertebrae from T12 to L5 were localized and marked following anatomical landmarks. The experimenter centered the coil over the midline of the vertebra T12 and advanced caudally, shifting one vertebra in each step (coil currents directed clockwise). Single pulses above the motor threshold were delivered to identify the hot-spot (i.e., spot inducing largest motor evoked potentials in the right or paretic tibialis anterior muscle). Using a skin-marker we drew the shape of the coil over the hot-spot in the back of the participants to minimize the variability when placing the coil during the assessments and closed-loop stimulation phase. Once the hot-spot was localized, we defined the motor threshold (Mth) as the minimum stimulator output intensity required to elicit at least 5 evoked potentials with an amplitude larger than 50 μV out of 10 successive stimulation pulses while the right or paretic tibialis anterior (TA) in rest. During the closed-loop stimulation phase, the frequency of the ts-MS was set to 20 Hz (Sasada et al., 2014).

7.3.6 Detection of movement intention

After the screening phase, the acquired brain activity was used to train a classifier to discriminate between rest and motor imagery/attempt brain states.

Data preprocessing

The recorded EEG data were band-pass [1-50 Hz] filtered with a 4th order Butterworth filter. The signals were arranged into 15-second trials (from -10 s to +5 s, being 0 the beginning of the motor task), and subsampled to 100 Hz. To maximize the estimation of the cortical motor activation, an optimized spatial filtering (OSF) was applied to the electrodes FC3, FC1, FCz, FC2, FC4, C5, C3, C1, Cz, C2, C4, C6, CP3, CP1, CPz, CP2 and, CP4 (17 electrodes from the 32 recorded). We band-pass filtered [7-15] Hz (4th order Butterworth) the signal of these electrodes to isolate the activity in the alpha frequency range (López-Larraz et al., 2014). The OSF calibration uses a gradient-descent optimization to calculate weights for the linear combination of electrodes that minimizes power in alpha during motor imagination/attempt and maximizes it during rest. This automated method enhances the estimation of event-related desynchronization (ERD) of sensorimotor modulation during motor tasks (Graimann and Pfurtscheller, 2006b) and results in a surrogate channel that merges the activation over the motor cortex. The OSF weights were calculated using only the trials of the screening phase and were fixed for the closed-loop phase.

Feature extraction

A one-second window was slid every 200 ms to each 15-second trial of the OSF channel between the interval [-3, -1] s for the rest class and [1, 3] s (which could be adapted for each participant) for motor task class, resulting in 6 windows per trial and class. From each of these windows, the power spectrum from 1 to 50 Hz was computed using a 20th-order autoregressive (AR) model with 1-Hz bin resolution, based on the Burg algorithm (Burg, 1967). We calculated the R-squared values (point-biserial correlation coefficients) to visually identify those frequencies of the sensorimotor rhythm that increased the separability between cortical activity during rest or motor task. Although alpha ([7-13] Hz) and beta ([14-30] Hz) oscillatory activities of the motor cortex are the

most responsive frequency bands during a motor task, the feature selection was constrained only to the alpha band, to prevent the influence of ts-MS at 20 Hz on our ongoing EEG activity. The power outputs of the selected frequency range were averaged and synthesized into one unique feature. Therefore, we extracted the power feature from each window and z-score normalized. These values were used to create a linear discriminant analysis (LDA) classifier to discriminate between rest and motor task classes.

Classification

During the closed-loop phase, the classifier constantly decoded the brain activity and activated the ts-MS providing contingent feedback when signatures related to the motor task were identified. EEG activity was acquired in real-time at 1000 Hz sampling rate and every 200 ms a package of new data arrived. This package was median filtered (see details in subsection *Median filtering for ts-MS contamination removal*), band-pass filtered between 1 and 50 Hz, OSF filtered (using the weights calculated from the screening data) and appended to a one-second ring-buffer. The power of the ring-buffer was calculated, and the classifier determined which class the estimated power corresponded to, either rest class or motor task class. When motor imagery/attempt was decoded, the classifier triggered the ts-MS providing associative feedback. Note that the stimulation was turned off during rest periods to prevent false positives.

The normalization coefficients of the features (initialized with the mean and standard deviation of the screening dataset) were continuously updated in order to adapt to EEG-nonstationarities and to possible modifications in the cortical activity derived from ts-MS. Each class had one 48-second buffer containing the newest power features corresponding to these classes. For every new power output of the ring-buffer, and before sending it to the classifier, both buffers were concatenated together, and the mean and standard deviation were used as the normalization coefficients.

Median filtering for ts-MS contamination removal

The interaction of electromagnetic currents with the nervous system results in noisy neurophysiological recordings. As described in (Insausti-Delgado et al., 2017),

applying ts-MS contaminates the EEG signals, inducing peaks of short duration (~10 ms) and large amplitude. The median filter has been shown to be an effective method to remove ts-MS artifacts from EEG recordings (Insausti-Delgado et al., 2020, 2021). Our median filtering relied on a 20-ms sliding window applied in one-sample steps to estimate the median value for each window. This filter removed the artifact peaks from the EEG signals without affecting the oscillatory alpha band activity.

Decoding accuracy

The performance of the classifier used to identify movement imagery/attempt was quantified by means of average decoding accuracy, defined as the mean of true positive rate (TPR) and true negative rate (TNR). TPR estimates the success of the classifier during the periods corresponding to the motor task within the interval [1, 4] s, while TNR estimates the success of the classifier during resting within the interval [-4, -1] s.

7.3.7 Assessments for synaptic efficacy

To address our hypothesis on whether brain-spin interfaces induce excitability changes in the nervous system, an exhaustive battery of neurophysiological assessments was performed. These assessments included the evaluation of different efferent and afferent neural segments that comprise the sensory-motor pathways. Note that we conducted the assessments on the right leg in healthy participants and on the paretic leg in stroke patients. During the assessment blocks, both EEG and EMG signals were synchronously acquired at a sampling rate of 5 kHz. The EEG and EMG activities were band-pass filtered (2^{nd} order Butterworth), [3-1000] Hz and [10-1000] Hz respectively.

Motor evoked potentials (MEP)

The efficacy of corticomuscular pathways can be assessed through MEPs. Since this measurement encompasses the entire motor neural network, eliciting descending volleys from the cortex to the target muscle, we defined the MEPs as our primary outcome measure (Figure 7.1e). We used the Rapid2 magnetic stimulator with a double-cone coil (Magstim 110 mm Coil, Magstim Ltd, UK) to apply single pulse stimuli over the primary motor cortex of the TA. To ensure consistency with the stimulation location

over the scalp, a neuronavigation system (Localite, GmbH, Germany) was employed to register participants' head in a 3D-model, where the optimal stimulation spot for TA MEPs was saved and tracked over sessions (due to technical problems, in patients 1, 3 ,4, 5 and 7 the neuronavigation system was not). Following the standardized proceedings defined by (Groppa et al., 2012), we set the cortical motor threshold (Mth) as the minimal stimulator output intensity required to generate at least 5 evoked potentials larger than 50 μV out of 10 consecutive stimuli. In every block of measurements, 20 repetitions were elicited at 120% of the daily cortical Mth every 5 to 5.5 seconds. The peak-to-peak amplitudes of the potentials belonging to the same assessment block were calculated and averaged for each participant.

Trans-spinal motor evoked potentials (ts-MEP)

Magnetic stimulation can be used to assess the peripheral nervous system, activating the spinal roots at their exit from the spine to the muscles through the intervertebral foramen, resulting in ts-MEPs (Figure 7.1e) (Matsumoto et al., 2013; Ugawa et al., 1989). The magnetic stimulator with a 90mm-circular coil was used to elicit ts-MEPs at the TA. The stimulation spot at the lumbar level and the estimation of the Mth were defined as previously explained in the section 7.3.5. Every block of measurements included 30 stimuli of ts-MEPs applied every 5 to 5.5 seconds at 120% of the spinal Mth. The peak-to-peak amplitudes of ts-MEPs were computed and averaged for each participant.

Somatosensory evoked potentials (SEP)

Stimulating peripheral nerves to produce cortical responses is a measure that reflects the integrity of the ascending pathways, which can be quantified as SEPs (Figure 7.1e) (Mauguiere et al., 1999). A programmable electrical stimulator Bonestim (Tecnalia, Serbia) stimulated the tibial nerve through self-adhesive electrodes. The cathode electrode was placed over the popliteal fossa and the anode electrode over the patella. The stimulation intensity was set slightly above the Mth, being the threshold defined as the minimum intensity needed to produce visible muscle twitches and muscular potentials ~100 μV in soleus muscle. The SEPs were recorded in the CPz channel and the

stimulation was delivered at 3 Hz in 500 μs square pulses. A total amount of 60 sweeps were baseline corrected and averaged for each block of measurements. The size of the cortical peak was measured as the amplitude difference between P30 and N40.

Trans-spinal somatosensory evoked potentials (ts-SEP)

Spinal stimulation can generate ascending volleys, from the spine to the brain, resulting in cortical potentials that can be estimated as ts-SEPs (Figure 7.1e) (Kunesch1993). We used the same stimulation setup, spot and parameters used for eliciting ts-MEPs (subsection *Trans-spinal motor evoked potentials* (ts-MEP)). Each assessment block consisted of 30 repetitions of ts-SEPs applied every 5 to 5.5 seconds. The cortical responses recorded in the CPz channel were baseline corrected and averaged to calculate the amplitude between the potential P25 and N35.

Hoffmann reflex (H-reflex)

The Hoffmann reflex reflects the efficacy of monosynaptic transmission from the afferent fibers to the motoneurons at spinal cord level (Figure 7.1e). The robustness of this assessment relies on the leg posture; hence the participants were required to keep their knee and ankle at 120° and 90°, respectively. We used the same electrical stimulator, self-adhesive electrodes and stimulation spot used for eliciting peripheral SEPs. The stimulation was delivered with a square pulse of 1 ms duration. To define the intensity required for this measurement, a recruitment curve of the H- and M-waves for the soleus muscle was performed for each participant (Pierrot-Deseilligny and Burke, 2005). This recruitment curve consisted in a scan of currents delivered in single pulses, starting at 5 mA and progressively increasing in steps of 1 mA until the M-wave stabilized in its maximum amplitude. For the assessments, we selected the intensity that elicited an H-reflex with 30% of the M-wave maximum amplitude, being this intensity in the ascending slope of the recruitment curve of the H-wave. During the assessment blocks, a pulse eliciting a maximum M-wave (Mmax) was followed by 20 H-reflex repetitions (10 repetitions in the case of healthy subjects). To ameliorate the effect of post-activation depression, but without compromising the experimental time, the interstimulus interval

lasted between 5 and 6 s. The peak-to-peak amplitude of the H-reflexes was averaged and referenced to the Mmax.

Brain oscillatory activity during rest

To evaluate the changes in neural excitability at cortical level, 2 minutes of brain activity were recorded in every assessment block while participants were resting. The power spectrum of the OSF channel for healthy subjects was computed using a periodogram with 1-second hamming windows, 50% of overlapping, and 0.25 Hz of frequency resolution. The peak power outputs corresponding to the frequencies selected for the classifier (i.e., alpha band) were averaged for each subject. For the descriptive analysis in stroke patients, the power spectral density was calculated averaging C3-Cz-C4.

7.3.8 Clinical and behavioral assessments

The clinical and behavioral assessments were only performed in stroke patients. The Fugl-Meyer assessment (FMA) (maximal score = 86 points), which was defined as primary behavioral outcome measure, was used to measure functional impairment of lower limb. The spasticity was evaluated by the modified Ashworth scale for spasticity (MAS) (maximal score = 30 points, including extensor and flexor muscles at the ankle, knee and hip joints). The ambulatory capacity and speed were evaluated by the 10-meter walk test (10MWT), the 2-minute walk test (2mWT) and the timed up and go (TUG) test (Bolliger et al., 2018). In the 10MWT, the participants walked straight for 14 m and the time used to cover the middle 10 m was measured. The goal of the 2mWT was to cover the longest distance within 2-minute period. The TUG consisted in standing up, walking straight for 3 m, walking back to the chair and sitting down. The time started as soon as their buttock lifted from the chair and finished when their buttock touched again the chair.

7.3.9 Statistical analysis

Firstly, we studied the effects of the BSI-based intervention on neural excitability changes in healthy participants. We determined the normality of the data using the Shapiro-Wilk test. To measure the influence of our intervention on the assessments of

synaptic efficacy over time, we used Friedman's test (4 levels: Pre, PostScreening, Post0 and Post30) for the six outcome measures: peak-to-peak amplitude of MEPs and ts-MEPs, P30-N40 amplitude of SEPs, P25-N35 amplitude of ts-SEPs, ratio of H-reflex amplitude to Mmax and power of brain oscillatory activity in the alpha band. Paired post-hoc comparisons with Bonferroni correction were done using the Wilcoxon signed-rank test to find significant differences between assessment blocks. In order to analyze whether the performance of the closed-loop intervention can induce modifications in the entire motor neural system, we studied the relationship between average decoding accuracy and the change in corticomuscular excitability after closed-loop phase (i.e., Post0 and Post30 with respect to the baseline, Pre) using linear regressions. Correlations between decoding accuracy and changes in MEP amplitude were calculated using Pearson's correlation.

Secondly, statistical analyses were performed to evaluate the changes in corticomuscular excitability of stroke participants, who underwent an 8-day BSI-based intervention. To study the effect of the intervention over sessions, we compared the initial MEP amplitude of the first session with the MEP amplitude right after finishing every daily intervention for each patient. We conducted paired comparisons for non-Gaussian variables using the Wilcoxon signed-rank test and Bonferroni correction. Moreover, the within session effect of the intervention on the corticomuscular excitability was also investigated. A one-sample t-test was performed to statistically evaluate significant changes in MEP size, estimated as the daily difference between Pre and Post, for each patient.

7.4 Results

7.4.1 Quantifying the effect of the BSI intervention on synaptic efficacy of healthy participants

Outcome measures of synaptic efficacy

Figure 7.2 shows the effects of the BSI intervention on the synaptic efficacy assessments conducted in healthy participants. We firstly studied the effects of the closed-loop intervention on the excitability of the corticomuscular pathways over time,

quantified as MEPs (i.e., primary outcome measure). The peak-to-peak amplitude of the TA MEPs increased 17.28% for PostScreening, 33.87% for Post0 and 32.39% for Post30 with respect to the baseline (Pre). We found a significant difference in the amplitude between the assessment blocks, (n = 17) $\chi^2(3) = 9.494$; p = 0.023. Post-hoc analysis revealed significantly larger TA MEP amplitudes in the Post0 (Z = -2.675; p = 0.042) and in the Post30 (Z = -2.817; p = 0.03) compared to the baseline (Pre). Similarly, the soleus muscle also presented significant changes in MEP amplitude between assessment blocks, (n = 17) $\chi^2(3) = 10.482$; p = 0.015. We found a significant increase of 56.48% in the size of the soleus motor potentials right after the finishing the BSI intervention at Post0 compared to Pre (Z = -3.006, p = 0.003).

The efficacy of the motor pathways connecting the spine with the TA muscle, quantified as ts-MEP, changed in the opposite direction compared to the MEPs. We found a decrease of ts-MEP amplitude following the closed-loop phase, although the changes between blocks were not significant ($\chi^2(3) = 3.743$; p = 0.291; n = 21). The differences in the size of H-reflexes between the assessment blocks were not statistically significant ($\chi^2(3) = 1.114$; p = 0.774; n = 14). Regarding the efficacy of sensory pathways, there were no significant changes in the amplitude of the SEPs ($\chi^2(3) = 0.720$; p = 0.868; n = 20) and ts-SEPs ($\chi^2(3) = 1.800$; p = 0.615; n = 15). We did not find any significant changes in the activation of the motor cortex, calculated as the peak power in the alpha band ($\chi^2(3) = 4.705$; p = 0.195; n = 19).

BSI control and correlation with MEP amplitude change

The average response of the decoder was based on the linear classifier (LDA) that optimized the cortical features for the detection of MI. Figure 7.3a depicts the average performance of the classifier indicating the percentage of outputs classified as movement on each time point. The average decoding accuracy, calculated as the mean between TPR and TNR, was 57.65% for healthy participants.

To study the effect of the closed-loop intervention on the significant changes observed in our primary outcome measurement, we ran linear regressions between the decoding accuracy and the changes in the TA MEP amplitudes in Post0 and Post30,

calculated as a percentage of the baseline (Pre). The linear models show that higher decoding accuracies resulted in significantly larger TA MEPs right after finishing the intervention at Post0 ($p = 0.018$) (Figure 7.3b left). However, this significant positive relationship between MEP amplitude change and decoding accuracy was not maintained 30min after the closed-loop intervention ($p = 0.84$) (Figure 7.3b right).

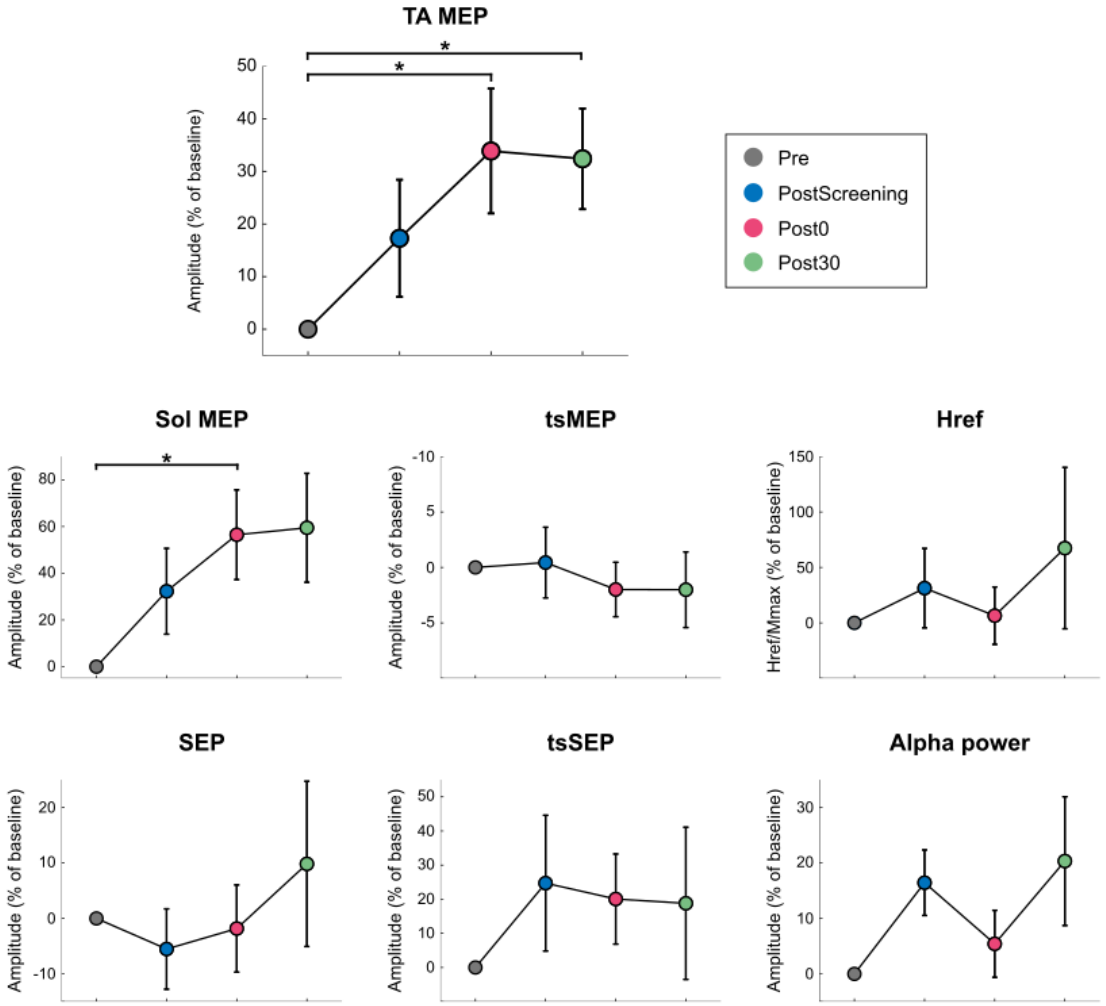

Figure 7.2: Effects of the BSI intervention on synaptic efficacy assessments of healthy participants. We evaluated different efferent and afferent neural segments that comprise the sensory-motor pathways by means of motor evoked potentials (MEPs) in tibialis anterior and soleus, trans-spinal motor evoked potentials (tsMEPs), H-reflexes, somatosensory evoked potentials (SEPs), trans-spinal somatosensory evoked potentials (tsSEPs) and activation of the motor cortex in the alpha band. Each plot shows the average, expressed as a percentage of the baseline (Pre), and standard error of the mean for the different assessment blocks. The statistically significant differences between assessment blocks are expressed with horizontal lines and stars.

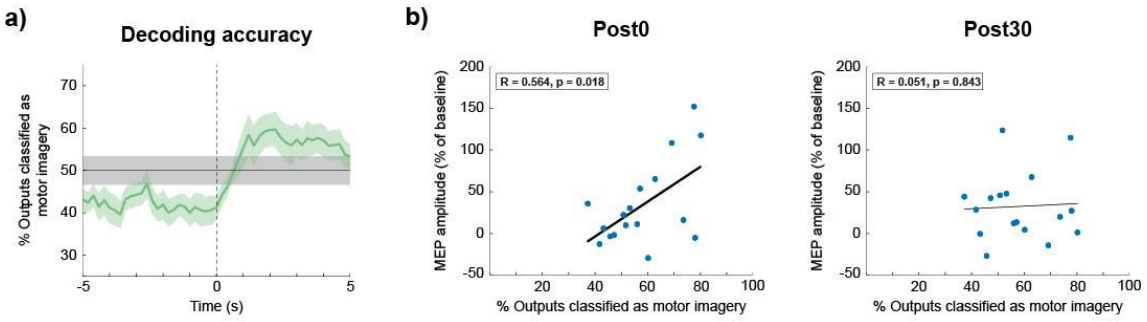

Figure 7.3: Average response of the BSI classifier and linear correlations of the amplitude change of tibialis anterior motor evoked potentials (MEP) with the BSI classifier response. (a) Averaged time-response of the classifier quantified as the percentage of the outputs classified as motor imagery, averaged over all the healthy participants. Notice that time 0 s represents the beginning of the motor imagery period, and outputs before to t = 0 correspond to false positives, while outputs after t = 0 mean true positives. The shaded gray areas show the confidence interval of the chance level (alpha = 0.05), calculated on the basis of all the test trials, according to (Müller-Putz et al., 2008). (b) Linear correlation between the change in MEP size after the BSI intervention and the decoding accuracy. The differences in MEP amplitude were estimated as percentage of the baseline (Pre-assessment). The decoding accuracies were calculated as the mean between true negative rate (TNR) in the time interval [-1, -4] s and true positive rate (TPR) in the time interval [1, 4] s. Significant correlations between MEP amplitude and decoding accuracy are represented with black solid linear regressions.

7.4.2 Proof of concept with chronic stroke patients

Outcome measures of synaptic efficacy

We evaluated the effects of the BSI-intervention on the corticomuscular excitability quantified as MEP amplitude. Results for the daily MEPs and final post-assessment MEP are summarized in boxplots in Figure 7.4. To study an over time effect of the therapy, every post-assessment was compared to the Pre-assessment of the first session. We found a significant increase of MEP amplitudes, especially in the last sessions, for some participants (Patients 2, 4, 5 and 7). However, this increasing trend of the MEP size was not maintained in the final assessment for all the aforementioned cases. Moreover, MEP amplitudes of the final assessment were significantly smaller for Patient 1. We also studied whether the daily intervention had a short-term effect on the excitability of corticomuscular tracts in stroke patients (Figure 7.5). We found that the BSI-intervention had a within session effect inducing significantly larger MEPs in 3 patients (one sample t-test, Patient 4: $t(7) = 2.521$, $p = 0.04$; Patient 6: $t(5) = 3.410$, $p = 0.019$; Patient 7: $t(8) = 3.939$, $p = 0.019$).

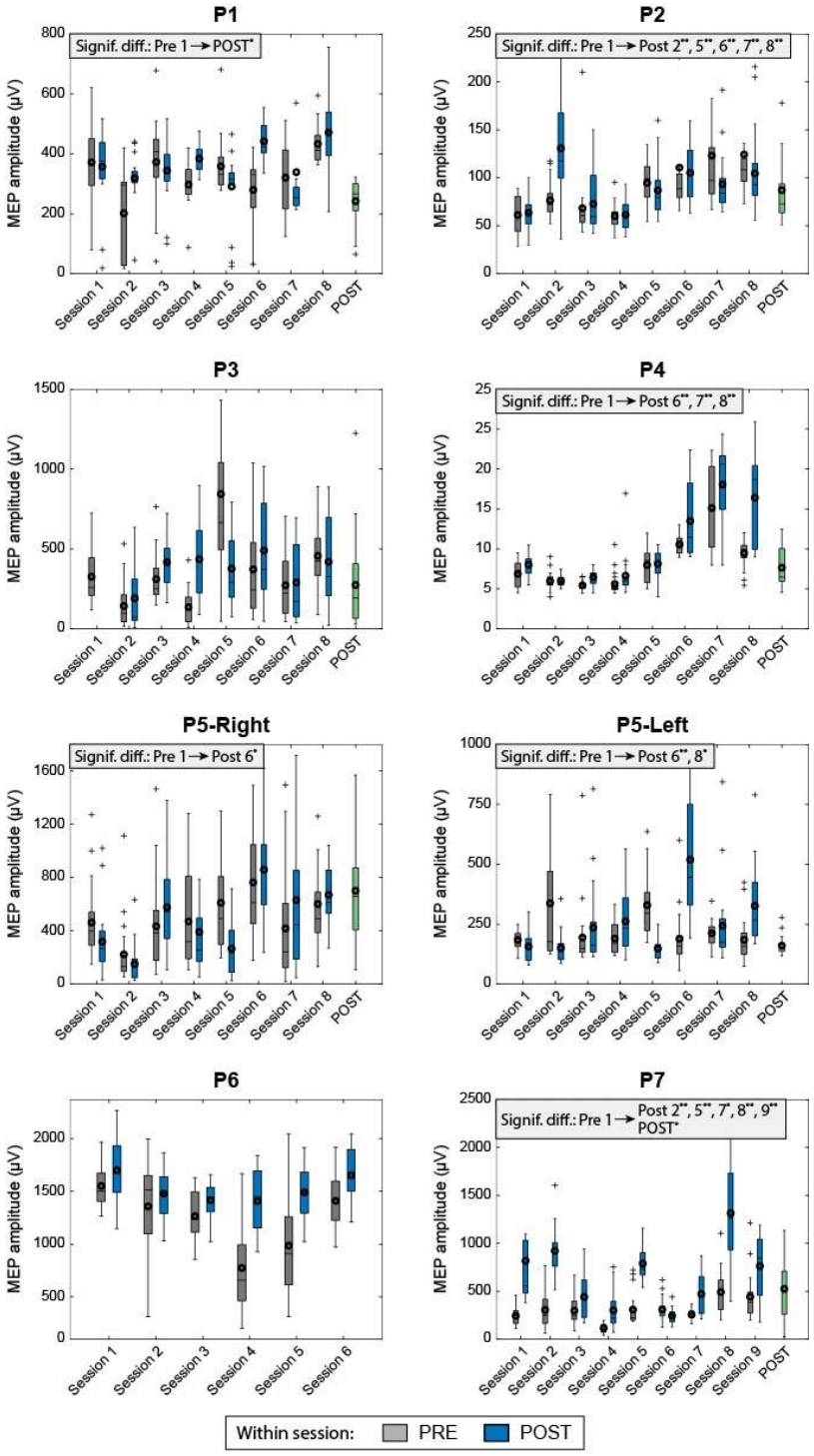

*Figure 7.4: Comparison of corticomuscular excitability over sessions in stroke patients. Boxplots display the amplitudes of motor evoked potentials (MEP) over sessions before and after the BSI intervention, and the final assessment for all the stroke patients. The median values are represented as solid black lines, 25-75th percentile as boxes, outliers as whiskers and mean values as black circles. The presence of the "Signif. Diff." panel indicates a significant change of MEP amplitude between Pre-assessment of the first session and post-assessment of following days, being **p < 0.01 and *p < 0.05. Note that all patients performed 8 sessions, with the exception of P6 and P7; and that the final assessment was not conducted in P6.*

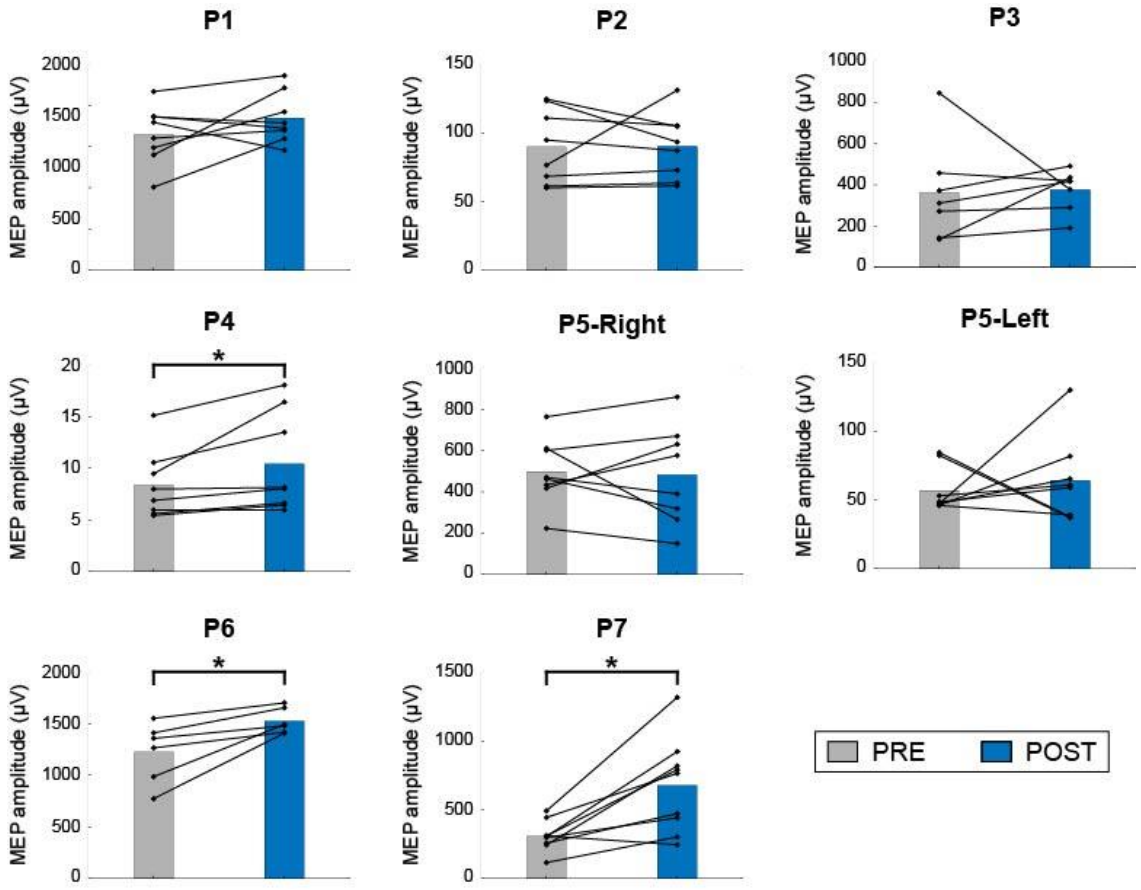

Figure 7.5: Comparison of the size of motor evoked potentials (MEP) within session. Bar plots reporting mean values averaged over sessions and solid lines reporting single session values of the MEP amplitudes for each patient before and after the daily BSI-intervention (all patients performed 8 sessions, except P6 with 6 sessions and P7 with 9 sessions). The within session significant differences are expressed with horizontal lines and stars.

We analyzed the changes in the other neurophysiological outcome measures before and after the whole therapy (Figure 7.6a). The descriptive analysis of these assessments showed no clear trend in the changes observed in the amplitude of H-reflexes, tsMEPs and tsSEPs. However, all patients presented a decrease of the SEP amplitude after the BSI intervention.

The cortical activity during rest was monitored over sessions and displayed in plots of power spectral density (Supplementary Figure 7.1). There was not a clear trend over time in the modulation of the brain activity. Notice that not all the patients presented prominent activity in the alpha band (7-15) Hz and the control of the BSI (i.e., performance) was conditioned by this neural correlate.

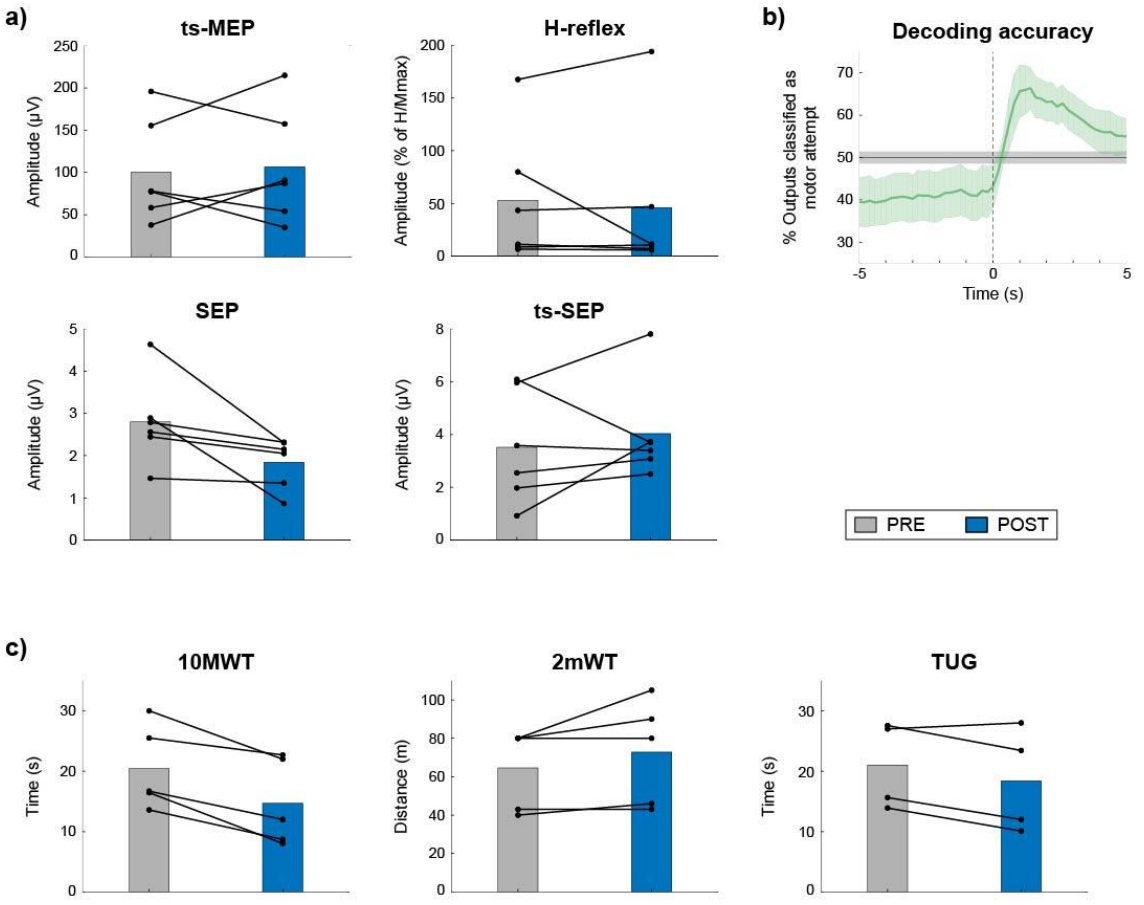

Figure 7.6: Comparison of synaptic efficacy and behavioral assessments and average response of the BSI classifier in stroke patients. (a) Bar plots representing the mean values of the synaptic efficacy assessments and solid lines reporting individual values of each patient. These assessments included the measurement of trans-spinal motor evoked potentials (ts-MEP), H-reflexes, somatosensory evoked potentials (SEP) and trans-spinal somatosensory evoked potentials (ts-SEP) before and after the BSI-intervention. (b) Averaged time-response of the classifier quantified as the percentage of the outputs classified as motor attempt, averaged over all the stroke patients. Notice that time 0 s represents the beginning of the motor attempt period, and outputs before to t = 0 correspond to false positives, while outputs after t = 0 mean true positives. The shaded gray areas show the confidence interval of the chance level (alpha = 0.05), calculated on the basis of all the test trials, according to (Müller-Putz et al., 2008). (c) Bar plots representing the mean values of the 10-meter walking test (10MWT) (left), the 2-minute walking test (2mWT) (middle) and the timed up and go test (TUG) (right), measured before and after the BSI-intervention. The solid black lines depict the evolution of each patient. Note that P2 did not perform the TUG; P5 was unable to stand up without assistance and could not perform the behavioral tests (10MWT, 2mWT and TUG) on his own; and none of the post-assessments were not conducted in P6.

BSI control and clinical and behavioral outcome measures

Figure 7.6b shows the average response over time of the BSI decoder that optimized the detection of cortical features reflecting motor attempt. The figure depicts

the average performance of the classifier over time reporting the percentage of outputs classified as motor attempt. The average decoding accuracy, computed as the mean between TPR and TNR, was 60.35% for stroke patients.

	Fugl-Meyer (max. 86)		Modified Ashworth scale (max. 30)	
	PRE	POST	PRE	POST
P1	74	79	4	2*
P2	71	76	1	0
P3	73	75	3	0
P4	65	75	1	0
P7	60	66	3	4
Mean values	68.6	74.2	2.4	1.2

Table 7.2 Comparison of clinical scales. Scores of the Fugl-Meyer assessment (FMA) and the modified Ashworth scale (MAS) for spasticity measured before and after the BSI intervention. The star indicates disappearance of clonus in the ankle. Note P5 was excluded from the clinical assessments because he could perform all movements in the FMA and had no spasticity; and none of the post-assessments were not conducted in P6.

Table 7.2 shows the comparison of clinical scales before and after the BSI intervention. The descriptive analysis of our primary clinical outcome measure showed that all the patients increased in the FMA, 5.6 points in average, indicating a reduction in sensorimotor impairment after the treatment. The secondary clinical outcome measure revealed an average decrease of 1.2 points in the MAS, which implies a decrease in spasticity after concluding the BSI intervention. Moreover, the BSI intervention led to the disappearance of ankle clonus in one patient. Regarding the other behavioral assessments, the descriptive analysis showed that at the conclusion of the study the patients were better at performing exercises that involved ambulatory capacity and walking speed. Compared to pre-assessments, all the participants reduced the time required to walk 10 meters (Figure 7.6c left), being this 5.76 s shorter in average after the BSI-intervention. Pre- and post-assessment comparison of the walking distance covered in the 2mWT displayed an averaged increment of 8.2 m (Figure 7.6c middle). Similarly, the participants were 2.64 s faster performing the TUG (Figure 7.6c right).

Usability assessments

Figure 7.7 illustrates the usability scores reported by each patient after every block of closed-loop stimulation. Our descriptive analysis on usability of the system revealed that the scores for discomfort, pain and fatigue were very low and within a tolerable range. The scores for concentration on the task of attempting the movement were high. All participants reported consistent usability values over sessions. During and after experimental period, no adverse consequences were addressed by any of the patients.

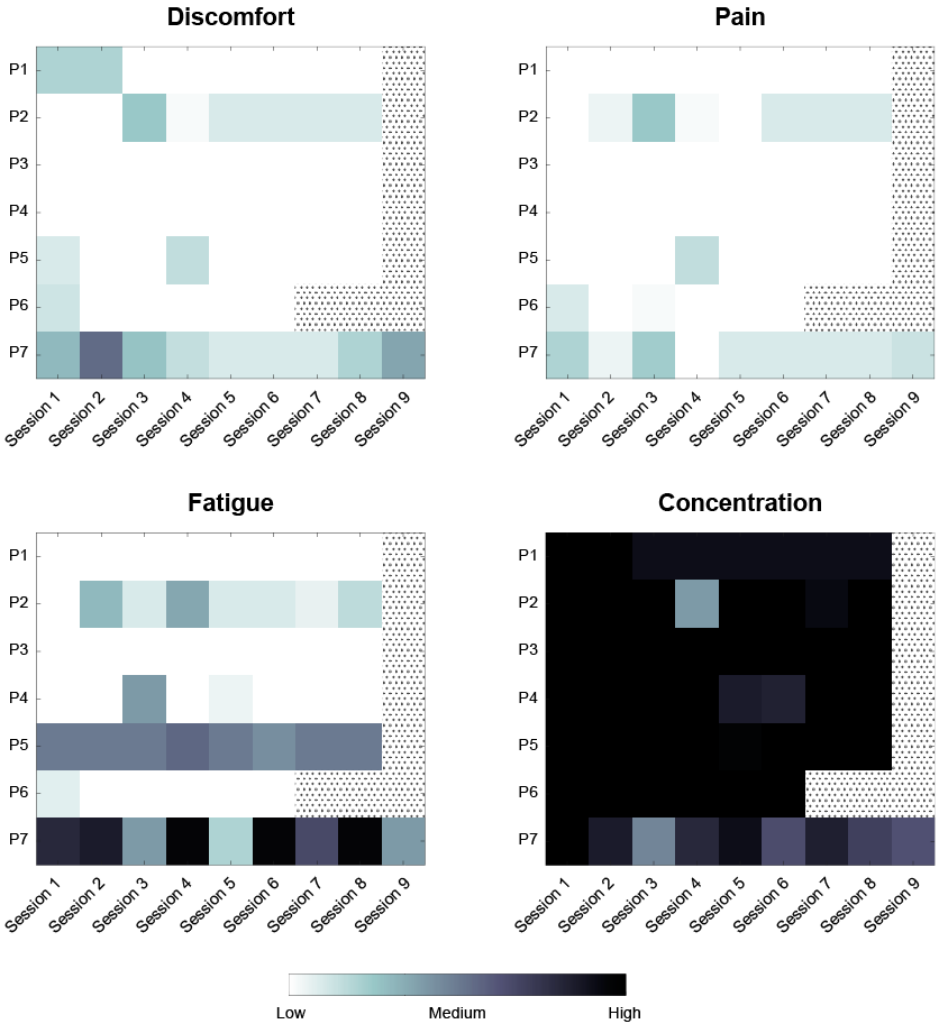

Figure 7.7 Usability scores of the BSI platform reported by stroke patients. Averaged usability scores over sessions describing how uncomfortable and painful the stimulation was, how exhausting the task was, and how easy it was to concentrate in the motor attempt task while being stimulated. Note that dotted areas indicate that some participants patients did not perform those sessions (all patients performed 8 sessions, with the exception of P6 and P7).

7.5 Discussion

The current study demonstrates for the first time that an intervention based on a non-invasive brain-spine interface (BSI), which relies on continuous EEG-guided trans-spinal magnetic stimulation (ts-MS), increases the responsiveness of corticomuscular pathways in healthy individuals. Furthermore, we validate the BSI system in stroke patients and report on the positive changes in corticomuscular excitability and improvement of behavioral and clinical scales after an 8-day intervention. The here presented results contribute to the development and design of BSI technology as a rehabilitative tool for lower-limb paralysis.

7.5.1 Healthy subjects

We found that a single-session BSI intervention, which included a screening and a closed-loop stimulation phase, resulted in a significant increase of the excitability of the cortical projections to the leg muscles. This increase of MEP amplitudes in the TA and Soleus muscles was observed right after finishing the closed-loop phase and, in the case of TA, remained for up to 30 min after. These findings indicate that our BSI intervention could induce long-term potentiation of the motor cortex and corticomuscular tracts. It should be considered that the absence of a control group for healthy participants limits the results of the current study. In spite of the improvements in corticomuscular efficacy shown after the intervention, we cannot conclude whether the increase in MEP amplitudes derives from the neural excitatory effects induced by the brain-controlled ts-MS or is a result of other factors, such as performing the MI task over time or the ts-MS itself. Nevertheless, in a previous study, Takahashi and colleagues instructed their participants to perform MI of their ankle dorsiflexion for 20 min and demonstrated that this was not sufficient to significantly enhance corticomuscular excitability (Takahashi et al., 2019). Indeed, they demonstrated that the MEP amplitude of TA was significantly increased when combining the MI task with peripheral stimulation, like demonstrated in previous literature (Kaneko et al., 2014; Yasui et al., 2019). Regarding the possible excitatory effects of the ts-MS itself, there is evidence supporting that the brain-controlled spinal stimulation boosts motor recovery of locomotion in contrast to open-loop

stimulation (Capogrosso et al., 2016; Bonizzato et al., 2018). In line with these findings, we found a significant relationship between the decoding accuracy and the changes induced in the corticomuscular pathways. Our results revealed that those subjects who controlled better the BSI system, achieved a more precise link between brain activity and spinal stimulation and, in turn, experienced larger increase of MEP amplitude. Although this positive relationship was not maintained 30 min after finishing the closed-loop phase, this finding supports the key role of associative connections enabled by the BSI platform. Altogether, one could surmise that the excitation of the corticomuscular connections might be reinforced by the combination of MI task and ts-MS.

The ts-MEP amplitudes barely changed through the session, meaning that the excitability of alpha motoneurons was maintained. This result differed from what we initially hypothesized, that was, a higher responsiveness of the spino-muscular pathways that could be caused by a shift in the triggering threshold of alpha motoneurons, making them more efficiently depolarized for a certain input (Murray and Knikou, 2019). Conversely, the BSI intervention did not produce the expected effect. Subsequently, if the output response of neurons from the spine to the muscle did not change over time, we could speculate that the excitability differences observed in the projections from the cortex to the target muscle rely on an increased efficacy of the cortico-spine connections and/or supraspinal neural structures.

We did not find any significant influence of the BSI intervention on H-reflexes. While some studies using open-loop trans-spinal direct current stimulation in healthy subjects reported decreased excitability of H-reflexes (Murray et al., 2018), others described increased amplitude of H-reflexes (Lamy et al., 2012) or moderate effects on the Hmax/Mmax ratio (Winkler et al., 2010). Due to the large variability among study protocols (e.g., posture, electrodes location and polarity, stimulation currents, duration, etc.), every assumption needs to be carefully considered. Nielsen and colleagues carried out a protocol comparable to ours (Nielsen and Sinkjaer, 1997), although it must be taken into account that they applied repetitive open-loop magnetic stimulation. After 5min of consecutive sequences of 5 s of rest and 5 s of ts-MS at 25 Hz, they found that healthy participants presented an initial increase of the H-reflexes followed by a depression of H-reflex amplitude that lasted for 30min, even though the changes were not significant. In

contrast, our results show the opposite effect (increase of H-reflex amplitudes) 30 min after finishing the closed-loop phase. However, we did not find any significant differences and cannot conclude whether the brain-controlled ts-MS modulates the responsiveness of group Ia afferents and spinal motor axons.

The BSI intervention did not significantly interfere with ascending somatosensory pathways, neither when SEPs were elicited peripherally nor spinally. Earlier evidence showed that anodal trans-spinal direct current stimulation reduced the SEP amplitudes up to 20 min following the stimulation offset (Cogiamanian et al., 2008). However, our results are not in line with this decrease in the excitability of the somatosensory cortex. While the peripherally evoked SEPs hardly changed over assessment blocks, the spinally evoked SEPs increased (not significantly) over time. Yet, we cannot conclude whether the BSI intervention generated an enhanced excitatory input from the spinal segment to the somatosensory cortex.

Amplitude changes of sensorimotor rhythms reflect modulation of the excitatory response of a population of neurons. Cortical activation and top-down control processes have been related to the power suppression of sensorimotor oscillatory activity in the alpha band (Klimesch et al., 2007). Therefore, after the BSI intervention, we expected to observe a reduction of this rhythmic band. However, the results were mixed and could not find any tendency. The duration of the session could have interfere by fatiguing the participants and, in turn, inhibiting the facilitatory effects of the intervention (Klimesch, 2012).

7.5.2 Stroke patients

This is the first study on stroke patients that validates a non-invasive BSI system, based on the continuous control of ts-MS, and explores the neurophysiological and clinical effects of it. The measurements of corticomuscular excitability revealed that the BSI intervention produced significant effects over experimental days and within session in some patients. The MEP amplitudes increased in comparison to the first session and this change was more likely to be significant in the last sessions. Interestingly, we observed that some patients presented a progressive increase of MEP amplitude over

time. Furthermore, we found that a single session could induce enlargement of MEP size, as we observed in healthy participants. Altogether, this implies that the BSI intervention might have immediate effects on the improvement of corticomuscular connection efficacy within a session, but it might not be sufficient and might require several sessions to produce long-term effects.

When observing the progressive increase of MEP amplitudes in some patients, one could expect the ts-MEP amplitudes to respond accordingly after the BSI intervention. However, we did not find significant changes in the response of spinal motor neurons and we cannot draw conclusions about the effect of the intervention on them. Indeed, given the lack of changes observed in the ts-MEP amplitudes of healthy subjects, one could speculate that the excitability modulation of this neural network might not be influenced by our intervention and that facilitatory changes may be more likely to occur in supraspinal and/or cortico-spine pathways.

Following the brain damage, the loss of supraspinal control and the imbalance between excitatory and inhibitory processes arise resulting in exaggerated spinal reflexes. In light of previous studies that described the correlation between motor recovery and H-reflex amplitude (Kawashima et al., 2013; Kawaishi et al., 2017), we expected to induce a reduction of the abnormal behavior of spinal reflexes. However, the changes in H-reflex amplitude were mixed and these results were not conclusive. Thus, we could not determine whether the BSI intervention had an effect on spinal reflexes. With regard to afferent pathways, it has been evidenced that stroke patients present low SEP amplitude compared with healthy subjects (Al-Rawi et al., 2009). Strengthening the integrity of sensory pathways has been correlated with functional recovery after stroke (Lee et al., 2010). While peripherally elicited SEP amplitudes decreased after the BSI intervention, the changes in ts-SEP amplitude did not show a clear trend. Our results suggested that there could be a reduced input from the periphery to the somatosensory cortex, although this descriptive analysis did not lead to definitive conclusions. Regarding the activation of the motor cortex over, despite the brain oscillatory activity has been proposed as a biomarker of motor recovery in stroke patients (Ray et al., 2020), we could not observe a strengthening of the sensorimotor rhythm in the alpha band over time.

The increased responsiveness of corticomuscular pathways over and within sessions observed in some patients might have potentiated the improvements in clinical and behavioral assessments. This potentiation might have positively affected the volitional motor control, balance and walking speed of stroke patients. Overall, they performed better the 10MWT, the 2mWT and the TUG tests after the BSI intervention. The FMA scores also improved indicating a decrease of the sensorimotor impairment in all the patients. These findings coincide with the beneficial effects regaining motor control reported on spinal cord injury patients who underwent transcutaneous spinal stimulation (Inanici et al., 2018; Alam et al., 2020). Additionally, the transcutaneous spinal cord stimulation has been proposed as a potential tool to attenuate the impact of spasticity in paralyzed patients (Hofstoetter et al., 2014, 2020; Minassian et al., 2016b). Within the approaches using magnetic stimulation, previous publications reported that this modality of stimulation applied over the lumbar nerve roots decreased the spastic tone in patients with different spinal lesions (Nielsen et al., 1996; Krause et al., 2004). They hypothesized that the stimulation provided proprioceptive input to the spinal and supraspinal neural networks diminishing the spasticity. Our experiment slightly differs from these studies, since the magnetic stimulation was not passively delivered, and the involvement of brain activation was necessary. However, our descriptive analysis also indicated that almost all the patients experienced a reduction of the spastic tone after the 8-day intervention. We even observed the disappearance of ankle clonus in one patient. Collectively, the EEG-guided ts-MS may be an optimal therapeutic neuromodulation tool to enhance motor control and decrease spasticity.

Stroke produces a wide heterogeneity of brain lesions that, in addition to the particularity of individual cortical activity, results in various cortical activations even in patients performing the same motor task (Stępień et al., 2011; Park et al., 2016). Thus, when evaluating the performance of the system it should be considered that the abnormal brain activation derived from the disease hinders the identification of neural correlates. Nevertheless, all the patients satisfactorily controlled the BSI system and the decoding accuracy was within the acceptable range for closed-loop neurorehabilitative systems (Ramos-Murguialday et al., 2013). Moreover, to validate the feasibility and applicability of the non-invasive BSI, we studied several usability scores. In general, there was a good

tolerability (e.g., low discomfort and pain) to the stimulation among the patients and none of them reported adverse effects. Most of the patients agreed on the low fatigability and constant concentration over the session.

7.5.3 Limitations

The main limitation of the current work is that it describes an exploratory study as no control group has been included in any of the experiments. Consequently, the here presented results have to be carefully considered. There is not enough evidence to support the conjecture that the contingent activation of relevant brain areas and spinal pools and muscles leads to beneficial effects. However, we believe that time-linked motor volition and sensory feedback is a key feature of our system that could promote Hebbian mechanisms contributing to functional recovery. Moreover, the comparisons between healthy participants and stroke patients has to be done with caution since the pathological condition is completely different between them.

The duration of the BSI intervention in stroke patients could have been a conditioning factor, since we could not see significant changes in all the neurophysiological assessments or in all subjects. Future research should investigate the rehabilitative benefits of treatments based on this technology in a larger population of stroke patients during a longer interventional period. Additionally, the framework of our BSI should be expanded beyond the treatment of lower-limb paralysis in stroke patients. The brain-controlled modulation of the spinal networks could also be used to rehabilitate hand and arm functional deficits and/or support the recovery from other neurological disorders, such as SCI.

As we previously evidenced (Insausti-Delgado et al., 2020), the EEG is a non-invasive recording system with good temporal resolution, but with proneness to become easily contaminated by undesired noise hindering the quantification of brain activity. Moreover, due to the low spatial resolution of this neuroimaging tool, identifying activation of the foot cortex located in the mesial wall is more complicated compared to hand movements, which activate larger and more superficial cortical regions which are easily discriminated (Pfurtscheller et al., 2006). These facts could have affected the

quality and stability of the signals hampering the estimation of brain activation and, in turn, reducing the accuracy and control of brain-controlled systems. Despite the room for improvement of this kind of technologies, the decoding accuracies were within the acceptable level of closed-loop driven neuroprosthetics (Ramos-Murguialday et al., 2013).

The posture of the participants during closed-loop stimulation might also have influenced the effectiveness of the intervention. Depending on the posture, the nerves in the spinal cord are more accessible and, in turn, the spinal motor threshold can be slightly modified. Thus, special care should be taken in keeping the back of the participants straight during the intervention. Moreover, the body constitution also plays a critical role when defining the motor threshold, since the amount of fat tissue located under the skin limits the diffusion of the magnetic field. In addition, stroke patients usually present chronic pain and other kind of disorders caused by the disease and experimental protocols, such as stimulation intensity, should be adapted to these situations.

The here presented findings provide a proof-of-concept towards the development of BSIs as a relevant tool for recovering from neurological disorders. Given the wide variety of spinal stimulation protocols in literature (e.g., stimulation parameters, type of stimulation: electrical vs. magnetic, open vs. closed-loop stimulation), results from previous studies can be hardly compared with our findings. In fact, our results are limited to the stimulation parameters selected and further studies should consider investigating the influence of other protocol parameters (e.g., intensity, frequency, dose, etc.) on spinal excitability in order to optimize BSI-based treatments. Apart from that, the spinal cord is a complex structure that presents a less clear spatial organization compared to the brain, which hampers the characterization of the components embedded in these neural circuits (Rybak et al., 2015). We defined a set of synaptic efficacy assessments to describe the neurophysiological changes that could be induced after a BSI intervention. However, additional assessments might be required to characterize in a more exhaustive manner how the brain-controlled spinal stimulation interacts with the nervous system. It is undeniable that computational neuroscience and bioelectromagnetic modeling, together with experimental findings, will provide paramount insights to the field of neurostimulation. Finally, the scientific progress and technological advances of the last

years will lead to new generation devices, which encourage us to be optimistic about this promising future of our research field.

7.6 Acknowledgments

This study was funded by the Bundesministerium für Bildung und Forschung BMBF MOTORBIC (FKZ 13GW0053) and AMORSA (FKZ 16SV7754), and the Fortüne-Program of the University of Tübingen (2422-0-1 and 2556-0-0 to ELL, and 2452-0-0 to ARM). The work of AID was funded by the Basque Government's scholarship for predoctoral students.

7.7 Supplementary material

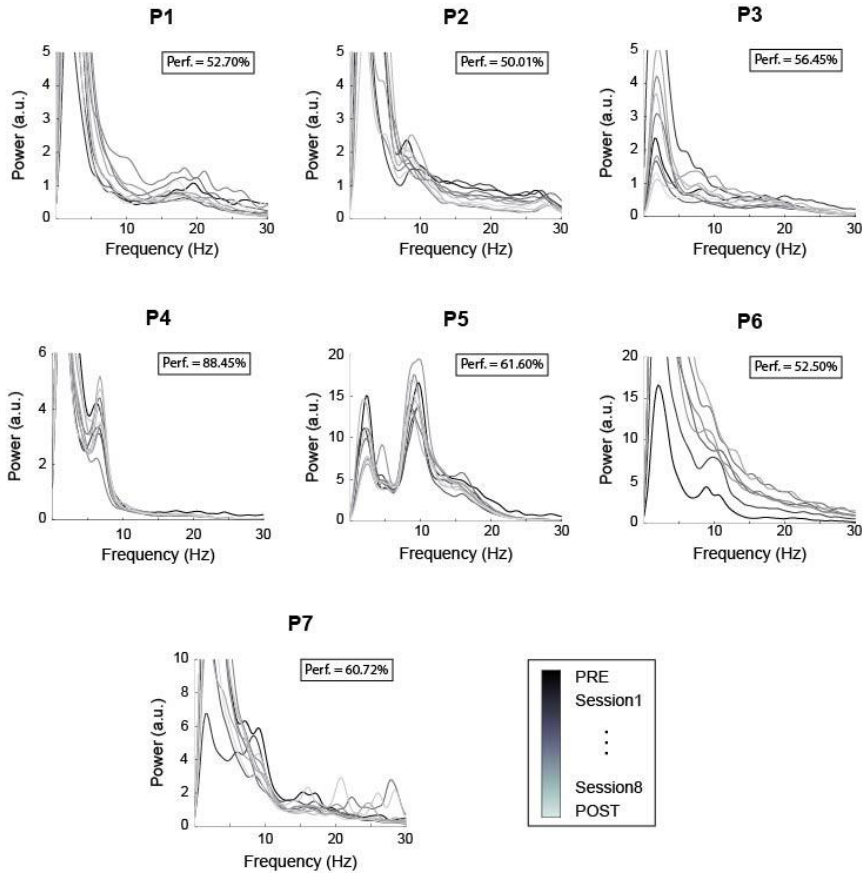

Supplementary Figure 7.1 Power spectral density of EEG activity during rest. The average power activity of channels C3, Cz and C4 (channels over the motor cortex) was computed for both assessment days and every interventional day. The color scale turns from dark to bright over time. The panels indicate the control of the BSI (i.e., decoding accuracy) averaged over sessions of each patient.

7.8 References

Al-Rawi, M. A. W., Hamdan, F. B., and Abdul-Muttalib, A. K. (2009). Somatosensory Evoked Potentials as a Predictor for Functional Recovery of the Upper Limb in Patients with Stroke. *J. Stroke Cerebrovasc. Dis.* 18, 262–268. doi:10.1016/j.jstrokecerebrovasdis.2008.11.002.

Alam, M., Garcia-alias, G., Jin, B., Keyes, J., Zhong, H., Roy, R. R., et al. (2017). Electrical neuromodulation of the cervical spinal cord facilitates forelimb skilled function recovery in spinal cord injured rats. *Exp. Neurol.* 291, 141–150. doi:10.1016/j.expneurol.2017.02.006.

Alam, M., Ling, Y. T., Wong, A. Y. L., Zhong, H., Edgerton, V. R., and Zheng, Y. P. (2020). Reversing 21 years of chronic paralysis via non-invasive spinal cord neuromodulation: a case study. *Ann. Clin. Transl. Neurol.* 7, 829–838. doi:10.1002/acn3.51051.

Alam, M., Rodrigues, W., Ngoc, B., and Thakor, N. V (2016). Brain-machine interface facilitated neurorehabilitation via spinal stimulation after spinal cord injury : Recent progress and future perspectives. *Brain Res.* 1646, 25–33. doi:10.1016/j.brainres.2016.05.039.

Angeli, C. A., Edgerton, V. R., Gerasimenko, Y. P., and Harkema, S. J. (2014). Altering spinal cord excitability enables voluntary movements after chronic complete paralysis in humans. *Brain* 137, 1394–1409. doi:10.1093/brain/awu038.

Bolliger, M., Blight, A. R., Field-Fote, E. C., Musselman, K., Rossignol, S., Barthélemy, D., et al. (2018). Lower extremity outcome measures: Considerations for clinical trials in spinal cord injury. *Spinal Cord* 56, 628–642. doi:10.1038/s41393-018-0097-8.

Bonizzato, M., Pidpruzhnykova, G., DiGiovanna, J., Shkorbatova, P., Pavlova, N., Micera, S., et al. (2018). Brain-controlled modulation of spinal circuits improves recovery from spinal cord injury. *Nat. Commun.* 9, 1–14. doi:10.1038/s41467-018-

05282-6.

Burg, J. P. (1967). Maximum Entropy Spectral Analysis. in *37th Annual International Meeting, Soc. of Explor. Geophys.*

Capogrosso, M., Milekovic, T., Borton, D., Wagner, F., Martin Moraud, E., Mignardot, J.-B., et al. (2016). A brain–spine interface alleviating gait deficits after spinal cord injury in primates. *Nature* 539, 284–288. doi:10.1038/nature20118.

Capogrosso, M., Wagner, F. B., Gandar, J., Moraud, E. M., Wenger, N., Milekovic, T., et al. (2018). Configuration of electrical spinal cord stimulation through real-time processing of gait kinematics. *Nat. Protoc.* 13, 2031–2061. doi:10.1038/s41596-018-0030-9.

Cogiamanian, F., Ardolino, G., Vergari, M., Ferrucci, R., Ciocca, M., Scelzo, E., et al. (2012). Transcutaneous spinal direct current stimulation. *Front. psychiatry* 3, 63. doi:10.3389/fpsyt.2012.00063.

Cogiamanian, F., Vergari, M., Pulecchi, F., Marceglia, S., and Priori, A. (2008). Effect of spinal transcutaneous direct current stimulation on somatosensory evoked potentials in humans. *Clin. Neurophysiol.* 119, 2636–2640. doi:10.1016/j.clinph.2008.07.249.

Formento, E., Minassian, K., Wagner, F., Mignardot, J. B., Camille G. Le Goff-Mignardot, A. R., Bloch, J., et al. (2018). Electrical spinal cord stimulation must preserve proprioception to enable locomotion in humans with spinal cord injury. *Nat. Neurosci.* 6, 153–158. doi:10.1038/s41593-018-0262-6.

Gad, P., Gerasimenko, Y., Zdunowski, S., Turner, A., Sayenko, D., Lu, D. C., et al. (2017). Weight bearing over-ground stepping in an exoskeleton with non-invasive spinal cord neuromodulation after motor complete paraplegia. *Front. Neurosci.* 11, 1–8. doi:10.3389/fnins.2017.00333.

Gerasimenko, Y., Gorodnichev, R., Machueva, E., Pivovarova, E., Semyenov, D., Savochin, A., et al. (2010). Novel and direct access to the human locomotor spinal

circuitry. *J. Neurosci.* 30, 3700–3708. doi:10.1523/JNEUROSCI.4751-09.2010.

Gerasimenko, Y., Gorodnichev, R., Moshonkina, T., Sayenko, D., Gad, P., and Edgerton, V. R. (2015). Transcutaneous electrical spinal-cord stimulation in humans. *Ann. Phys. Rehabil. Med.* 58, 225–231. doi:10.1016/j.rehab.2015.05.003.

Gerasimenko, Y., Roy, R. R., and Edgerton, V. R. (2008). Epidural stimulation : Comparison of the spinal circuits that generate and control locomotion in rats , cats and humans. 209, 417–425. doi:10.1016/j.expneurol.2007.07.015.

Gill, M. L., Grahn, P. J., Calvert, J. S., Linde, M. B., Lavrov, I. A., Strommen, J. A., et al. (2018). Neuromodulation of lumbosacral spinal networks enables independent stepping after complete paraplegia. *Nat. Med.* 24, 1677–1682. doi:10.1038/s41591-018-0175-7.

Gorodnichev, R. M., Machueva, E. N., Pivovarova, E. A., Semenov, D. V, Ivanov, S. M., Savokhin, A. A., et al. (2010). A New Method for the Activation of the Locomotor Circuitry in Humans. *Fiziol. Cheloveka* 36, 95–103. doi:10.1134/S0362119710060113.

Grahn, P. J., Lavrov, I. A., Sayenko, D. G., Straaten, M. G. Van, Gill, M. L., Strommen, J. A., et al. (2017). Enabling Task-Specific Volitional Motor Functions via Spinal Cord Neuromodulation in a Human With Paraplegia. *Mayo Clin. Proc.* 92, 544–554. doi:10.1016/j.mayocp.2017.02.014.

Graimann, B., and Pfurtscheller, G. (2006). Quantification and visualization of event-related changes in oscillatory brain activity in the time – frequency domain. *Prog. Brain Res.* 159, 79–97. doi:10.1016/S0079-6123(06)59006-5.

Groppa, S., Oliviero, A., Eisen, A., Quartarone, A., Cohen, L. G., Mall, V., et al. (2012). A practical guide to diagnostic transcranial magnetic stimulation: Report of an IFCN committee. *Clin. Neurophysiol.* 123, 858–882. doi:10.1016/j.clinph.2012.01.010.

Hofstoetter, U., Freundl, B., Danner, S., Krenn, M., Mayr, W., Binder, H., et al. (2020). Transcutaneous spinal cord stimulation induces temporary attenuation of spasticity

in individuals with spinal cord injury. *J. Neurotrauma* 37, 481–493. doi:10.1089/neu.2019.6588.

Hofstoetter, U. S., Krenn, M., Danner, S. M., Hofer, C., Kern, H., Mckay, W. B., et al. (2015). Augmentation of Voluntary Locomotor Activity by Transcutaneous Spinal Cord Stimulation in Motor-Incomplete Spinal Cord-Injured Individuals. doi:10.1111/aor.12615.

Hofstoetter, U. S., McKay, W. B., Tansey, K. E., Mayr, W., Kern, H., and Minassian, K. (2014). Modification of spasticity by transcutaneous spinal cord stimulation in individuals with incomplete spinal cord injury. *J. Spinal Cord Med.* 37, 202–11. doi:10.1179/2045772313Y.0000000149.

Inanici, F., Samejima, S., Gad, P., Edgerton, V. R., Hofstetter, C. P., and Moritz, C. T. (2018). Transcutaneous electrical spinal stimulation promotes long-term recovery of upper extremity function in chronic tetraplegia. *IEEE Trans. Neural Syst. Rehabil. Eng.* 26, 1272–1278. doi:10.1109/TNSRE.2018.2834339.

Insausti-Delgado, A., López-Larraz, E., Bibián, C., Nishimura, Y., Birbaumer, N., and Ramos-Murguialday, A. (2017). Influence of trans-spinal magnetic stimulation in electrophysiological recordings for closed-loop rehabilitative systems. in *39th Annual International Conference of the IEEE Engineering in Medicine and Biology Society (EMBC)*, 2518–2521. doi:10.1109/EMBC.2017.8037369.

Insausti-Delgado, A., López-Larraz, E., Nishimura, Y., Birbaumer, N., Ziemann, U., and Ramos-Murguialday, A. (2019). Quantifying the effect of trans-spinal magnetic stimulation on spinal excitability. *9th Int. IEEE EMBS Conf. Neural Eng.* doi:10.1109/NER.2019.8717016.

Insausti-Delgado, A., López-Larraz, E., Nishimura, Y., Ziemann, U., and Ramos-Murguialday, A. (2020). Non-invasive brain-spine interface: continuous brain control of trans-spinal magnetic stimulation using EEG. *bioRxiv*.

Insausti-Delgado, A., López-Larraz, E., Omedes, J., and Ramos-Murguialday, A. (2021). Intensity and dose of neuromuscular electrical stimulation influence sensorimotor

cortical excitability. *Front. Neurosci.* 14, 1359. doi:10.3389/fnins.2020.593360.

Jackson, A., and Zimmermann, J. B. (2012). Neural interfaces for the brain and spinal cord—restoring motor function. *Nat. Rev. Neurol.* 8, 690–699. doi:10.1038/nrneurol.2012.219.

Kaneko, F., Hayami, T., Aoyama, T., and Kizuka, T. (2014). Motor imagery and electrical stimulation reproduce corticospinal excitability at levels similar to voluntary muscle contraction. *J. Neuroeng. Rehabil.* 11, 1–7. doi:10.1186/1743-0003-11-94.

Kato, K., Sawada, M., and Nishimura, Y. (2019). Bypassing stroke-damaged neural pathways via a neural interface induces targeted cortical adaptation. *Nat. Commun.* 10, 1–13. doi:10.1038/s41467-019-12647-y.

Kawaishi, Y., Matsumoto, N., Nishiwaki, T., and Hirano, T. (2017). Postactivation depression of soleus H-reflex increase with recovery of lower extremities motor functions in patients with subacute stroke. *J. Phys. Ther. Sci.* 29, 1539–1542. doi:10.1589/jpts.29.1539.

Kawashima, N., Popovic, M. R., and Zivanovic, V. (2013). Effect of intensive functional electrical stimulation therapy on upper-limb motor recovery after stroke: Case study of a patient with chronic stroke. *Physiother. Canada* 65, 20–28. doi:10.3138/ptc.2011-36.

Klimesch, W. (2012). Alpha-band oscillations, attention, and controlled access to stored information. *Trends Cogn. Sci.* 16, 606–617. doi:10.1016/j.tics.2012.10.007.

Klimesch, W., Sauseng, P., and Hanslmayr, S. (2007). EEG alpha oscillations: The inhibition-timing hypothesis. *Brain Res. Rev.* 53, 63–88. doi:10.1016/j.brainresrev.2006.06.003.

Knikou, M. (2013). Neurophysiological characteristics of human leg muscle action potentials evoked by transcutaneous magnetic stimulation of the spine. *Bioelectromagnetics* 34, 200–210. doi:10.1002/bem.21768.

Krause, P., Edrich, T., and Straube, A. (2004). Lumbar repetitive magnetic stimulation reduces spastic tone increase of the lower limbs. *Spinal Cord* 42, 67–72. doi:10.1038/sj.sc.3101564.

Lamy, J.-C., Ho, C., Badel, A., Arrigo, R. T., and Boakye, M. (2012). Modulation of soleus H reflex by spinal DC stimulation in humans. *J. Neurophysiol.* 108, 906–914. doi:10.1152/jn.10898.2011.

Lee, S. Y., Lim, J. Y., Kang, E. K., Han, M. K., Bae, H. J., and Paik, N. J. (2010). Prediction of good functional recovery after stroke based on combined motor and somatosensory evoked potential findings. *J. Rehabil. Med.* 42, 16–20. doi:10.2340/16501977-0475.

López-Larraz, E., Montesano, L., Gil-Agudo, Á., and Minguez, J. (2014). Continuous decoding of movement intention of upper limb self-initiated analytic movements from pre-movement EEG correlates. *J. Neuroeng. Rehabil.* 11, 153. doi:10.1186/1743-0003-11-153.

López-Larraz, E., Sarasola-Sanz, A., Irastorza-Landa, N., Birbaumer, N., and Ramos-Murguialday, A. (2018). Brain-machine interfaces for rehabilitation in stroke: A review. *NeuroRehabilitation* 43, 77–97. doi:10.3233/NRE-172394.

Mauguiere, F., Allison, T., Babiloni, C., Buchner, H., Eisen, A., Goodin, D., et al. (1999). Somatosensory evoked potentials.

McPherson, J. G., Miller, R. R., Perlmutter, S. I., and Jacob G. McPherson, Robert R. Miller, and S. I. P. (2015). Targeted, activity-dependent spinal stimulation produces long-lasting motor recovery in chronic cervical spinal cord injury. *Neurosurgery* 78, N18–N19. doi:10.1073/pnas.1505383112.

Megía García, A., Serrano-Muñoz, D., Taylor, J., Avendaño-Coy, J., and Gómez-Soriano, J. (2019). Transcutaneous Spinal Cord Stimulation and Motor Rehabilitation in Spinal Cord Injury: A Systematic Review. *Neurorehabil. Neural Repair*, 1545968319893298. doi:10.1177/1545968319893298.

Minassian, K., Hofstoetter, U. S., Danner, S. M., Mayr, W., Bruce, J. A., Mckay, W. B., et al. (2016a). Spinal Rhythm Generation by Step-Induced Feedback and Transcutaneous Posterior Root Stimulation in Complete Spinal Cord – Injured Individuals. *Neurorehabil. Neural Repair* 30, 233–243. doi:10.1177/1545968315591706.

Minassian, K., Mckay, W. B., Binder, H., and Hofstoetter, U. S. (2016b). Targeting Lumbar Spinal Neural Circuitry by Epidural Stimulation to Restore Motor Function After Spinal Cord Injury. *Neurotherapeutics* 13, 284–294. doi:10.1007/s13311-016-0421-y.

Mrachacz-Kersting, N., Jiang, N., Stevenson, A. J. T., Niazi, I. K., Kostic, V., Pavlovic, A., et al. (2016). Efficient neuroplasticity induction in chronic stroke patients by an associative brain-computer interface. *J. Neurophysiol.* 115, 1410–1421. doi:10.1152/jn.00918.2015.

Müller-Putz, G., Scherer, R., Brunner, C., Leeb, R., and Pfurtscheller, G. (2008). Better than random: A closer look on BCI results. *Int. J. Bioelectromagn.* 10, 52–55.

Murray, L. M., and Knikou, M. (2019). Transspinal stimulation increases motoneuron output of multiple segments in human spinal cord injury. *PLoS One* 14.

Murray, L. M., Tahayori, B., and Knikou, M. (2018). Transspinal Direct Current Stimulation Produces Persistent Plasticity in Human Motor Pathways. *Sci. Rep.* 8, 717. doi:10.1038/s41598-017-18872-z.

Nakao, Y., Sasada, S., Kato, K., Murayama, T., Kadowaki, S., S, Y., et al. (2015). Restoring walking ability in individuals with severe spinal cord injury using a closed-loop spinal magnetic stimulation. in *Proceedings of the 45th Annual Meeting of Society for Neuroscience* Available at: https://www.abstractsonline.com/Plan/ViewAbstract.aspx?sKey=70d620e9-53bf-4bef-858d-e79452be5b51&cKey=5f31c5f3-9c0c-4873-8cd1-2fab3b718c7d&mKey=d0ff4555-8574-4fbb-b9d4-04eec8ba0c84.

Nielsen, J. F., and Sinkjaer, T. (1997). Long-lasting depression of soleus motoneurons

excitability following repetitive magnetic stimuli of the spinal cord in multiple sclerosis patients. *Mult. Scler. J.* 3, 18–30. doi:10.1177/135245859700300103.

Nielsen, J. F., Sinkjaer, T., and Jakobsen, J. (1996). Treatment of spasticity with repetitive magnetic stimulation; a double-blind placebo-controlled study. *Mult. Scler. J.* 2, 227–232.

Nishimura, Y., Perlmutter, S. I., Eaton, R. W., and Fetz, E. E. (2013). Spike-timing-dependent plasticity in primate corticospinal connections induced during free behavior. *Neuron* 80, 1301–1309. doi:10.1016/j.neuron.2013.08.028.

Park, W., Kwon, G. H., Kim, Y., Lee, J., and Kim, L. (2016). EEG response varies with lesion location in patients with chronic stroke. *J. Neuroeng. Rehabil.* 13, 21. doi:10.1186/s12984-016-0120-2.

Pfurtscheller, G., Brunner, C., Schlögl, A., and Lopes da Silva, F. H. (2006). Mu rhythm (de)synchronization and EEG single-trial classification of different motor imagery tasks. *Neuroimage* 31, 153–159. doi:10.1016/j.neuroimage.2005.12.003.

Pierrot-Deseilligny, E., and Burke, D. (2005). *The circuitry of the human spinal cord: its role in motor control and movement disorders*. doi:10.1017/CBO9781139026727.

Priori, A., Ciocca, M., Parazzini, M., Vergari, M., and Ferrucci, R. (2014). Transcranial cerebellar direct current stimulation and transcutaneous spinal cord direct current stimulation as innovative tools for neuroscientists. *J. Physiol.* 592, 3345–3369. doi:10.1113/jphysiol.2013.270280.

Ramos-Murguialday, A., Broetz, D., Rea, M., Läer, L., Yilmaz, Ö., Brasil, F. L., et al. (2013). Brain-machine interface in chronic stroke rehabilitation: A controlled study. *Ann. Neurol.* 74, 100–108. doi:10.1002/ana.23879.

Ray, A. M., Figueiredo, T. D., López-Larraz, E., Birbaumer, N., and Ramos-Murguialday, A. (2020). Brain oscillatory activity as a biomarker of motor recovery in chronic stroke. *Hum. Brain Mapp.* 41, 1296–1308. doi:doi:10.1002/hbm.24876.

Rybak, I. A., Dougherty, K. J., and Shevtsova, N. A. (2015). Organization of the

Mammalian Locomotor CPG: Review of Computational Model and Circuit Architectures Based on Genetically Identified Spinal Interneurons. *eNeuro* 2. doi:10.1523/ENEURO.0069-15.2015.

Sasada, S., Kato, K., Kadowaki, S., Groiss, S. J., Ugawa, Y., Komiyama, T., et al. (2014). Volitional walking via upper limb muscle-controlled stimulation of the lumbar locomotor center in man. *J. Neurosci.* 34, 11131–11142. doi:10.1523/JNEUROSCI.4674-13.2014.

Stępień, M., Conradi, J., Waterstraat, G., Hohlefeld, F. U., Curio, G., and Nikulin, V. V (2011). Event-related desynchronization of sensorimotor EEG rhythms in hemiparetic patients with acute stroke. *Neurosci. Lett.* 488, 17–21.

Takahashi, Y., Kawakami, M., Yamaguchi, T., Idogawa, Y., Tanabe, S., Kondo, K., et al. (2019). Effects of leg motor imagery combined with electrical stimulation on plasticity of corticospinal excitability and spinal reciprocal inhibition. *Front. Neurosci.* 13. doi:10.3389/fnins.2019.00149.

Winkler, T., Hering, P., and Straube, A. (2010). Spinal DC stimulation in humans modulates post-activation depression of the H-reflex depending on current polarity. *Clin. Neurophysiol.* 121, 957–961. doi:10.1016/j.clinph.2010.01.014.

Yadav, A. P., Li, D., and Nicolelis, M. A. L. (2020). A Brain to Spine Interface for Transferring Artificial Sensory Information. *Sci. Rep.* 10, 1–15. doi:10.1038/s41598-020-57617-3.

Yasui, T., Yamaguchi, T., Tanabe, S., Tatemoto, T., Takahashi, Y., Kondo, K., et al. (2019). Time course of changes in corticospinal excitability induced by motor imagery during action observation combined with peripheral nerve electrical stimulation. *Exp. Brain Res.* 237, 637–645. doi:10.1007/s00221-018-5454-5.